VOGTLE ELECTRIC GENERATING PLANT

GEORGIA POWER COMPANY

CONTAINMENT BUILDING

DESIGN REPORT

Prepared

by

Bechtel Power Corporation, Los Angeles, California

October 1984

VEGP-CONTAINMENT BUILDING
DESIGN REPORT

TABLE OF CONTENTS

TABLE OF CONTENTS (cont)

LIST OF TABLES

LIST OF FIGURES

VEGP-CONTAINMENT BUILDING
DESIGN REPORT

1.0 INTRODUCTION

The Nuclear Regulatory Commission Standard Review Plan, NUREG-0800, requires the preparation of design reports for Category 1 structures.

This design report represents one of a series of 11 design reports and one seismic analysis report prepared for the Vogtle Electric Generating Plant (VEGP). These reports are listed below:

- Containment Building Design Report
- Containment Internal Structure Design Report
- Auxiliary Building Design Report
- Control Building Design Report
- Fuel Handling Building Design Report
- NSCW Tower and Valve House Design Report
- Diesel Generator Building Design Report
- Auxiliary Feedwater Pumphouse Design Report
- Category 1 Tanks Design Report
- Diesel Fuel Oil Storage Tank Pumphouse Design Report
- Category 1 Tunnels Design Report
- Seismic Analysis Report

The Seismic Analysis Report describes the seismic analysis methodology used to obtain the acceleration responses of Category 1 structures and forms the basis of the seismic loads in all 11 design reports.

The purpose of this design report is to provide the Nuclear Regulatory Commission with specific design and construction information for the containment building, in order to assist in planning and conducting a structural audit. Quantitative information is provided regarding the scope of the actual design computations and the final design results.

The report includes a description of the structure and its function, design criteria, loads, materials, analysis and design methodology, and a design summary of representative key structural elements including the governing design forces.

2.0 DESCRIPTION OF STRUCTURE

The containment building is a pressure vessel consisting of a prestressed, reinforced concrete cylinder and hemispherical dome supported on a conventionally reinforced concrete basemat (see figures 1 and 2). The basemat has a central cavity (reactor cavity) to house the reactor pressure vessel (RPV). The inside face of the containment building is lined with steel plates welded together to form a leaktight barrier. The liner plate is typically 1/4-inch thick and is thickened locally around penetrations, basemat anchorages, and large brackets. The liner plate system (see figure 3) is anchored to the concrete, and leak chase channels are provided at seam welds which are inaccessible after construction.

Other pressure-retaining components of the containment building covered by this design report include the equipment hatch, personnel lock, escape lock, and the fuel transfer tube housing expansion bellows.

Several nonpressure-retaining components are considered integral parts of the containment building and are covered by this design report. These include the polar crane brackets, tendon gallery, access shaft number one, and equipment hatch missile shield.

All other structures inside of the containment building pressure boundary are covered in the Containment Internal Structure Design Report.

2.1 GENERAL DESCRIPTION

The containment building encloses the reactor and the reactor coolant system as well as portions of the reactor auxiliary systems and engineered safeguard systems. The containment building ensures that leakage of radioactive material to the environment, following a postulated accident, will not exceed 10 CFR 100 guidelines.

The containment building is required to sustain, without loss of essential functions, the effects of natural phenomena in addition to the effects of normal operating and postulated accident conditions.

The concrete shell, in conjunction with other safety systems, is required to provide radiation shielding to preclude a post-accident site dose greater than 10 CFR 100 guidelines and to preclude normal operating doses from exceeding 10 CFR 20 limits.

2.2 LOCATION AND FOUNDATION SUPPORT

All Category 1 structures are founded within the area of the power block excavation. The excavation removed in-situ soils to elevation 130'± where the marl bearing stratum was encountered. All Category 1 structures are located either directly on the marl bearing stratum or on Category 1 backfill placed above the marl bearing stratum. The backfill consists of densely compacted select sand and silty sand. The nominal finished grade elevation is 219'-6". The high groundwater table is at elevation 165'-0".

The two containment building units are located 340 feet apart in the power block area. As shown in figure 4, adjacent structures for each containment unit include the auxiliary, fuel handling, and control buildings. Access shaft No. 1 is integral with the containment building (see section 2.4.2) below the top of the basemat.

The bottom of the containment basemat is at elevation 158'-6"; however, there are two portions of the containment building basemat which extend below the main basemat (see figure 2). The tendon gallery and the associated access shaft No. 1 have a bottom of concrete elevation of 143'-6". The reactor cavity has a lowest point bottom of concrete elevation of 130'-6".

The high groundwater table level (elevation 165'-0") coincides approximately with the mid-thickness of the basemat.

2.3 GEOMETRY AND DIMENSIONS

The containment building cylinder and hemispherical dome each have a nominal inside radius of 70 feet. The apex of the dome is 182 feet above the finished grade (elevation 219'-6") and the low point of the basemat is 89 feet below the finished grade. All figures shown in this report are for Unit 1. Unit 2 is opposite hand about the north-south centerline of the power block.

A more detailed description of the individual portions of the containment building is provided in the following section.

2.4 KEY STRUCTURAL ELEMENTS

2.4.1 Containment Foundation

The foundation consists of a circular basemat which is 154 feet 6 inches in diameter and 10 feet 6 inches thick. The basemat has a central cavity (reactor cavity) which extends 28 feet lower than the main portion of the foundation as shown in figure 2. The entire interior surface of the basemat and reactor cavity are lined with steel plate (see section 2.4.5 for a more detailed description) to serve as a portion of the leaktight barrier. The basemat is conventionally reinforced concrete as shown in figures 5 and 6.

Anchorage of the containment internal structures through the floor liner plate into the basemat is discussed in the Containment Internal Structures Design Report.

2.4.2 Tendon Gallery and Access Shaft No. 1

The tendon gallery is a corridor attached to the underside of the basemat that circles its periphery. The gallery is 10 feet wide by approximately 9 feet 6 inches high and provides access for installation and inspection of the inverted U-shaped tendons (see figures 1 and 2). The gallery walls are 3 feet to 4 feet thick and the slab varies in thickness from 4 feet 6 inches to 5 feet due to the sloping floor (for drainage purposes).

Access shaft No. 1 is a vertical shaft attached to the basemat and tendon gallery as shown in figures 1 and 2. This access shaft provides access from the finished grade to the tendon gallery, and is structurally isolated from the containment shell above the basemat, with a gap of 5-1/2 inches.

Access shaft No. 2 and 3 are integral portions of adjacent buildings, which are structurally isolated from the containment with a gap of 5-1/2 inches. All three access shafts are located around the shell buttresses to provide access for the installation and inspection of the horizontal hoop prestressing tendons.

The tendon gallery and access shaft No. 1 are conventional reinforced concrete structures.

2.4.3 Containment Shell

The shell is comprised of a cylinder portion which extends from the basemat at elevation 169'-0" up to the springline at elevation 327'-9" where it transitions into the hemispherical dome (see figures 1 and 2). The cylinder and dome are both 3 feet 9 inches thick with a nominal inside radius of 70 feet. The entire interior surface of the cylinder and dome are lined with steel plate to serve as a portion of the leaktight barrier.

A haunch, linearly varying in thickness from 3 feet 9 inches to 4 feet 9 inches, is provided at the junction of the cylinder and basemat (see figure 2). Above the haunch, various penetrations exist as described later in this report. At the largest penetration, the equipment hatch, the cylinder is thickened locally on the inside face as shown in figures 1 and 7.

Typical reinforcing for the prestressed reinforced concrete shell is shown in figure 8. Sheets 1 and 2 of figure 8 show typical outside and inside face horizontal and vertical reinforcing. Sheet 3 of figure 8 shows the reinforcing provided at the equipment hatch thickened area. Sheets 4 and 5 show typical buttress reinforcing. The prestressing system is described in detail in the next section.

2.4.4 Prestressing System

The prestressing of the containment is achieved by a two-way, ungrouted, post-tensioned system consisting of circumferential hoop tendons and two groups of vertical inverted U-shaped tendons (see figures 9 and 10). The U-shaped tendons extend over the dome (see figure 9, sheet 1) and are anchored at the bottom of the basemat in the tendon gallery. Buttresses are provided at 120-degree increments around the shell (see figure 1) for hoop tendon anchorage locations. The hoop tendons are anchored at buttresses 240 degrees apart, bypassing the intermediate buttress (see figure 9, sheet 2). Hoop tendons are provided in the dome up to 45 degrees above the springline.

The prestressing tendons are fabricated from 1/2-inch-diameter, 7-wire strands. Each tendon consists of 55 strands with end anchor components consisting of anchor heads, wedges, and retainer plates utilizing the VSL Corporation anchorage and post-tensioning techniques. The tendons are installed in metal sheaths which form ducts through the concrete. At the tendon anchorage points, the sheaths are attached to the trumpet assemblies shown in figure 10.

After tensioning of tendons, an anticorrosion material is pumped into the sheathing to fill the remaining voids in order to protect the tendons.

2.4.5 Liner Plate System

The liner plate is a steel membrane anchored to the inside face of the containment building to provide a leaktight barrier (see figure 3). The stiffened liner plate system also serves as a form for the cylinder and dome concrete placement. A leak chase system is provided consisting of steel shapes welded at inaccessible liner plate seams (such as the basemat liner plate due to its associated fill slab).

Penetrations are provided in the liner plate and containment concrete to provide for access/egress, and to permit passage of electrical or mechanical systems. These penetrations are described later in this design report.

The liner is typically 1/4-inch thick with American Society of Mechanical Engineers (ASME) ASME SA-285, Grade A, plate and is thickened locally around penetrations, nozzles, large brackets, and at embed plates with ASME SA-516, Grade 70, plate material. The liner is anchored to the concrete with 3 inch by 2 inch angle stiffeners spaced at approximately 15 inches.

2.4.6 Polar Crane Bracket

The containment building is designed to support a polar crane (located near the springline) which can be positioned over and lift items during construction, refueling, and maintenance.

A series of 37 equally spaced brackets is provided near the springline to support the polar crane runway girders (see figure 2). The polar crane brackets are anchored into the cylinder concrete. The brackets consist of built-up steel sections as shown in figure 11.

2.4.7 Equipment Hatch and Missile Shield Door

A 20-foot-diameter equipment hatch (see figures 1 and 7) is provided immediately above the operating floor to permit removal and replacement of equipment during construction or plant shutdown. The dished head of the equipment hatch is 1-1/2-inch-thick steel plate. A reinforced concrete missile shield door (see figure 4) is provided to protect the hatch from postulated tornado missiles and to provide radiation shielding.

2.4.8 Personnel and Escape Locks

Two personnel locks are provided for containment access/egress as shown in figure 1. A 9-foot-10-inch-diameter personnel lock exists immediately above the operating floor and serves as the main access/egress route for the containment. A smaller personnel lock (escape lock) is 5 feet 9 inches in diameter and serves as an emergency escape route.

The personnel lock and escape lock each have two doors which are interlocked during plant operation to prevent both being opened simultaneously. The personnel lock and escape lock details are shown in figure 7.

2.4.9 Other Containment Penetrations

In addition to the equipment hatch, personnel lock, and escape lock, many small containment penetrations exist. Electrical penetrations are provided on the north half of the containment to permit control, instrumentation, and power systems to pass into the containment from the control building. Mechanical penetrations are provided (mostly on the south half of the containment) to permit process piping, fuel transfer, and heating, ventilating, and air-conditioning (HVAC) systems to pass into the containment building from the auxiliary, control, and fuel handling buildings. Four pipes, terminating at the containment basemat sumps, penetrate the containment basemat.

2.5 MAJOR EQUIPMENT

All major equipment in the containment building is discussed in the Containment Internal Structure Design Report.

3.0 DESIGN BASES

3.1 CRITERIA

The following documents are applicable to the design of the containment building.

3.1.1 Codes and Standards

- American Society of Mechanical Engineers (ASME) Boiler and Pressure Vessel Code (hereinafter called the ASME Code), Section III, Division 2, 1975 Edition through the Winter 1975 Addenda, Article CC-3000 only. -
  - Applicable to the containment shell and basemat which form part of the pressure boundary.

- American Concrete Institute (ACI), Building Code Requirements for Reinforced Concrete, ACI 318-71, including the 1974 supplement.
  - Applicable to the tendon gallery and access shaft No. 1.

- American Institute of Steel Construction (AISC), Specification for the Design, Fabrication, and Erection of Structural Steel for Buildings, adopted February 12, 1969, and Supplements No. 1, 2, and 3.
  - Applicable to all structural steel.

3.1.2 Regulations

- 10 CFR 50, Domestic Licensing of Production and Utilization Facilities

3.1.3 General Design Criteria (GDC)

- GDC 1, 2, 4, 16, and 50 of Appendix A to 10 CFR 50.

3.1.4 Industry Standards

Nationally recognized industry standards, such as American Society of Testing Materials (ASTM), American Concrete Institute (ACI), and American Iron and Steel Institute (AISI), are used to specify material properties, testing procedures, fabrication, and construction methods.

3.2 LOADS

The containment building is designed for all credible loading conditions. The loads are listed and defined in Appendix A and supplemented as follows. Probable maximum precipitation loads (N) are not applicable to the design of the containment building due to the dome configuration.

The nomenclature in Appendix A is consistent with the ASME Code, Article CC-3000, since the major structural elements covered by this design report are designed in accordance with this Code.

The load nomenclature for the structural elements designed in accordance with ACI or AISC varies from the ASME nomenclature as described below.

ASME	AISC or ACI
P_v	NA
P_t	NA
T_t	NA
E_o	E
E_{ss}	E'
R_{rj}	Y_j
R_{rr}	Y_r
R_{rm}	Y_m

3.2.1 Normal Loads

3.2.1.1 Dead Loads (D)

Dead loads include the weight of the structure itself, permanent equipment, and hydrostatic loads (excluding groundwater hydrostatic loads which are considered live loads).

The only piece of permanent equipment directly related to the containment shell design is the polar crane and trolley. The dead load used for the polar crane and trolley is in accordance with the manufacturer's data. The worst case trolley position is used to maximize shell stresses.

No hydrostatic loads act on the containment building.

3.2.1.2 Live Loads (L)

Live loads on the containment building include dome snow loads, polar crane lifted loads, soil pressure loads, and groundwater hydrostatic loads.

Due to the dome configuration, precipitation loads are not applicable to the containment building. However, a 30 psf snow load is applied to the upper portions of the dome.

The 225-ton service lift of the polar crane and the associated impact loads are considered as live loads. The worst case live load position (trolley position) is used to maximize shell stresses. Polar crane lifts other than the 225-ton service lift are discussed in the construction load section.

The containment building is mostly encircled by other buildings, but there is a portion of the shell near the equipment hatch which has Category 1 compacted backfill against it. The static lateral earth pressure due to this backfill and the lateral earth pressure due to a 250 psf surcharge (to account for incidental surface loads) are considered as live loads. Shell wall surcharges from adjacent structures are not applicable since all adjacent structures have their basemats or extensions of their basemats at or lower than the top of the containment basemat.

The tendon gallery on the bottom of the containment basemat is designed for the static lateral earth pressure due to the Category 1 compacted backfill against it plus a surcharge from the control building of 8.8 ksf.

The high water table elevation occurs at elevation 165'-0". The lateral hydrostatic loading due to this groundwater is not applicable for the shell design since the top of basemat is elevation 169'-0". However, this hydrostatic load is applicable in the design of the reactor cavity, tendon gallery, and access shaft No. 1.

3.2.1.3 Prestress Loads (F)

The end-of-lifetime (after prestressing losses due to strand relaxation, concrete creep, and concrete shrinkage) and beginning-of-lifetime (before these losses) prestress forces are both investigated for all load combinations listed in Appendix B. Angular and wobble friction losses as well as elastic shortening effects are taken into consideration in determining the amount of effective prestress. The increase in effective prestress under internal pressure loads is investigated where applicable.

3.2.1.4 Operating/Shutdown Thermal Loads (T_o)

The containment building will be subjected to different thermal profiles depending on the ambient conditions outside. During normal operating conditions, the containment inside face temperature is 120°F and does not vary significantly due to the outside temperature.

3.2.1.5 Operating/Shutdown Pipe Reactions (R_o)

The most significant R_o loads on the containment shell are the loads at the anchor points (6-way restraints) where process piping penetrates the containment cylinder. These loads are based on the anchor point reactions obtained from the pipe stress analyses (the anchor point reactions for the inside containment pipe analysis and the outside containment pipe analysis are superimposed since they act concurrently). These loads affect only localized areas of the cylinder and are investigated individually.

3.2.1.6 Pressure Variations During Normal Operating Conditions (P_v)

The containment design pressure, P_v, due to pressure variations during normal plant operation is -3 psig.

3.2.2 <u>Construction Loads</u>

The most significant conditions that occur only during the construction phase are as follows.

3.2.2.1 Live Load (L)

The polar crane is positioned and tested before the dome is erected. An investigation was performed to check the structural integrity of the domeless shell during the polar crane preoperational test lift (225-ton rated capacity) and static load test (125 percent of the rated capacity). Vertical, lateral, and longitudinal impact factors are included in this load.

3.2.2.2 Prestress Load (F)

During tensioning of each tendon, there is a short-term load increase due to the jacking procedure. This short-term load increase affects localized areas only and continues only during jacking until the tendon being stressed is anchored.

3.2.3 Test Loads

These loads are applicable only during the structural integrity and leak rate tests.

3.2.3.1 Test Pressure (P_t)

The containment test pressure (60 psi) is 1.15 times the containment design accident pressure (P_a) described in section 3.2.6.

3.2.3.2 Test Temperature Loads (T_t)

The thermal loads during the tests are conservatively taken as being equal to the operating temperature loads (T_o).

3.2.4 Severe Environmental Loads

3.2.4.1 Operating Basis Earthquake, OBE (E_o)

Based on the plant site geologic and seismologic investigations, the peak ground acceleration for OBE is established as 0.12g. The free-field response spectra and the development of horizontal and vertical floor accelerations and in-structure response spectra at the basemat and selected elevations of the shell are discussed in the Seismic Analysis Report. Table 1 provides the OBE horizontal and vertical floor accelerations.

OBE damping values, as percentages of critical, applicable to the containment building design are as follows.

Prestressed Concrete Structures	2
Reinforced Concrete Structures	4
Welded Steel Structures	2
Bolted Steel Structures	4

The dynamic lateral earth pressures (active) due to the OBE are based upon the Mononobe-Okabe analysis of dynamic pressures in dry cohesionless materials as shown in figure 12.

The OBE polar crane loads are in accordance with the crane manufacturer's seismic report.

3.2.4.2 Design Wind (W)

The containment building is designed for a wind velocity of 110 mph based on the speed 30 feet above the ground. The wind effective velocity pressure profile (see figure 13) for height above ground level is in accordance with reference 1. This pressure profile is based on an Exposure C (flat open country) and the pressure values take into account the dynamic response to gusts. No reduction in pressures is made for the effects of direct shielding provided by the auxiliary, fuel handling, and control buildings.

The wind load acting on the shell is the wind velocity pressure times the effective external pressure coefficient. The pressure coefficients (C_p) are dependent on the external shape of the building and orientation of the wind. The effective internal pressure coefficient is zero since the containment building is a sealed structure. The effective external pressure coefficients for the dome and cylinder are given in figure 14 and define the shell areas subjected to positive or negative pressures.

3.2.5 <u>Extreme Environmental Loads</u>

3.2.5.1 Safe Shutdown Earthquake, SSE (E_{ss})

Based on the plant site geologic and seismologic investigations, the peak ground acceleration for SSE is established as 0.20g. The free-field response spectra and the development of horizontal and vertical floor accelerations and in-structure response spectra at the basemat and selected elevations of the shell are discussed in the Seismic Analysis Report. Table 1 provides the SSE horizontal and vertical floor accelerations.

SSE damping values, as percentages of critical, applicable to the containment building design are as follows.

Prestressed concrete structures	5
Reinforced concrete structures	7
Welded steel structures	4
Bolted steel structures	7

The dynamic lateral earth pressures (active) due to the SSE are based upon the Mononobe-Okabe analysis of dynamic pressures in dry cohesionless materials as shown in figure 12.

The SSE polar crane loads are in accordance with the crane manufacturer's seismic report.

3.2.5.2 Tornado Loads (W_t)

Loads due to the design tornado include wind pressures, atmospheric pressure differentials, and tornado missile strikes. The design tornado parameters, which are in conformance with the Region I parameters defined in Regulatory Guide 1.76, are as follows:

• Rotational tornado speed	290 mph
• Translational tornado speed	70 mph maximum 5 mph minimum
• Maximum wind speed	360 mph
• Radius of tornado at maximum rotational speed	150 feet
• Atmospheric pressure differential	-3 psi
• Rate of pressure differential change	2 psi/sec

The resultant tornado effective velocity pressure profile for the above parameters is given in figure 13. The effective velocity pressure includes the size coefficient and is used in conjunction with the external pressure coefficients for the dome and shell (figure 14) to determine the net positive and negative pressures. No reduction in pressures is made for the effects of direct shielding provided by the auxiliary, fuel handling, and control buildings.

The containment building is a completely sealed structure and is subjected to the maximum atmospheric pressure drop of 3 psi.

The containment building is also designed to withstand tornado missile impact effects from airborne objects transported by the tornado. The tornado missile design parameters are listed in table 2. Missile trajectories up to and including 45 degrees off the horizontal use the listed horizontal velocities. Those trajectories greater than 45 degrees use the listed vertical velocities.

Tornado loading (W_t) is defined as the worst case of the following combinations of tornado load effects.

$W_t = W_{tq}$ (Velocity pressure effects)
$W_t = W_{tp}$ (Atmospheric pressure drop effects)
$W_t = W_{tm}$ (Missile impact effects)
$W_t = W_{tq} + 0.5\ W_{tp}$
$W_t = W_{tq} + W_{tm}$
$W_t = W_{tq} + 0.5\ W_{tp} + W_{tm}$

3.2.5.3 Blast Load (B)

The blast load accounts for a postulated site-proximity explosion. The blast load is conservatively taken as a peak positive incident overpressure of 2 psi (acting inward or outward) applied as a static load.

3.2.6 Abnormal Loads

3.2.6.1 Accident Pressure (P_a)

The containment building is designed for a design accident pressure of 52 psig.

3.2.6.2 Thermal Loads under Accident Conditions (T_a)

Figure 15 provides representative temperature gradients through the containment shell for the loss-of-coolant accident (LOCA) and main steam line break (MSLB) conditions. Figure 15 shows the temperature profiles of the liner plate and shell concrete at various periods after the postulated break.

3.2.6.3 Pipe/Equipment Reactions under Accident Conditions (R_a)

The most significant R_a loads on the containment shell are the loads at the anchor points (6-way restraints) where process piping penetrates the containment cylinder. These loads are based on the anchor point reactions obtained from the pipe stress analyses (the anchor point reactions for the inside containment pipe analysis and outside containment pipe analysis are superimposed since they act concurrently). These loads affect only localized areas of the cylinder and are investigated individually.

3.2.6.4 Pipe Rupture Loads (R_{rj}, R_{rr}, and R_{rm})

Localized areas of the containment cylinder are subjected to pipe rupture loads (R_{rj} and R_{rr}) due to postulated high-energy line breaks. These loads are obtained from pipe break analyses and are applied to the shell on a break-by-break basis since only one pipe break is postulated to occur at a time.

There are no pipe whip restraints attached to the containment shell, and pipes are not allowed to whip against the liner plate; therefore, R_{rm} is equal to zero for the shell.

3.3 LOAD COMBINATIONS AND STRESS/STRENGTH LIMITS

The load combinations and allowable stress limits for steel and strength limits for concrete are as listed in Appendix B.

The load combinations listed in Table B.1 are in conformance with the requirements of ASME Code, Section III, Division 2, Subarticle CC-3200, except as discussed below.

- The word "or" has been inserted between E_o and W in the third abnormal/severe environmental combination to correct an error in the ASME Code. This error has also been recognized in section 3.8.1 of the Standard Review Plan (July 1981).

- W loads have been included in the construction combination.
- R_o loads have been included in the extreme environmental load combinations.
- An additional combination accounting for the effects of the blast load has been included in the extreme environmental factored load combination.

The allowable stresses and strains are in accordance with the requirements of the ASME code, Article CC-3000 with the following modifications.

- In subparagraph CC-3421.4.1(b), the second sentence is taken to read "If M' is negative, use equation (4).". (This conforms to an error correction made by the Winter 1976 Addenda.)
- In subparagraph CC-3421.4.2, the second sentence shall be taken to read "For $\rho \geqq 0.003$, $K = 1.75 - (0.036/n\rho) + 4.0n\rho$ but not less than 0.6." (This conforms to an error correction made by the Summer 1977 Addenda.)
- The increased allowable ($f_c = .40\ f'_c$) for membrane stress under primary service load combinations that include W or E is not utilized.

3.4 MATERIALS

The following materials and material properties are used in the design of the containment building.

3.4.1 Concrete

Cylinder and dome (high-strength, air-entrained concrete)

- Compressive strength $f'_c = 6$ ksi
- Modulus of elasticity $E_c = 4{,}234$ ksi
- Shear modulus $G = 1{,}694$ ksi
- Poisson's ratio $\nu = 0.17 - 0.25$

Basemat, tendon gallery, access shaft, and equipment hatch missile shield (high-strength, air-entrained concrete)

- Compressive strength $f'_c = 5$ ksi
- Modulus of elasticity $E_c = 3{,}865$ ksi
- Shear modulus $G = 1{,}546$ ksi
- Poisson's ratio $\nu = 0.17 - 0.25$

3.4.2 <u>Reinforcement - ASTM A615, Grade 60</u>

- Minimum yield stress $F_y = 60$ ksi
- Minimum tensile strength $F_{ult} = 90$ ksi
- Minimum elongation 7% to 9% in 8 inches

3.4.3 <u>Structural Steel</u>

3.4.3.1 ASTM A36 and ASME SA-36

- Minimum yield stress $F_y = 36$ ksi
- Minimum tensile strength $F_{ult} = 58$ ksi
- Modulus of elasticity $E_s = 29{,}000$ ksi

3.4.3.2 ASME SA-516, Grade 70

- Minimum yield stress $F_y = 38$ ksi
- Minimum tensile strength $F_{ult} = 70$ ksi
- Modulus of elasticity, $E_s = 29{,}000$ ksi

3.4.3.3 ASTM A500 Grade B, Structural Tubing

- Minimum yield stress $F_y = 46$ ksi
- Minimum tensile strength $F_{ult} = 58$ ksi
- Modulus of elasticity $E_s = 29{,}000$ ksi

3.4.4 <u>Structural Bolts</u>

3.4.4.1 ASTM A325 (1/2-inch to 1-inch diameter inclusive)

- Minimum yield stress $F_y = 92$ ksi
- Minimum tensile strength $F_{ult} = 120$ ksi

3.4.4.2 ASTM A325 (1-1/8-inch to 1-1/2-inch diameter inclusive)

- Minimum yield stress F_y = 81 ksi
- Minimum tensile strength F_{ult} = 105 ksi

3.4.5 Steel Liner Plate

3.4.5.1 ASME SA-285, Grade A

- Minimum yield stress F_y = 24 ksi
- Minimum tensile strength F_{ult} = 45 ksi
- Modulus of elasticity E_s = 29,000 ksi

3.4.5.2 ASME SA-516, Grade 70

- Minimum yield stress F_y = 38 ksi
- Minimum tensile strength F_{ult} = 70 ksi
- Modulus of elasticity E_s = 29,000 ksi

3.4.6 Anchor Bolts and Headed Anchor Studs

3.4.6.1 ASTM A36

- Minimum yield stress F_y = 36 ksi
- Minimum tensile strength F_{ult} = 58 ksi

3.4.6.2 ASTM A108

- Minimum yield stress F_y = 50 ksi
- Minimum tensile strength F_{ult} = 60 ksi

3.4.6.3 ASTM A307

- Minimum yield stress F_y is not applicable
- Minimum tensile strength F_{ult} = 60 ksi

3.4.7 Prestressing System

3.4.7.1 Tendons

ASTM A416, Grade 270

- Minimum yield stress $F_y \geq 0.85\ F_{ult}$
- Minimum tensile strength F_{ult} = 270 ksi

3.4.7.2 Tendon Anchor Head

AISI 1026, (Plain carbon steel)

3.4.7.3 Anchor Head Bearing Plate

ASTM A537, Class 1

- Minimum yield stress F_y = 45 ksi
- Minimum tensile strength F_{ult} = 65 ksi

3.4.7.4 Anchor Head Wedges

AISI 86L20, (Low-alloy, nickel-chromium-molybdenum steel)

3.4.8 Foundation Media

3.4.8.1 General Description

See section 2.2

3.4.8.2 Category 1 Backfill

- Moist unit weight γ_m = 126 pcf
- Saturated unit weight γ_t = 132 pcf
- Shear modulus

G	Depth (feet)
1530 ksf	0-10
2650 ksf	10-20
3740 ksf	20-40
5510 ksf	40-Marl bearing stratum

- Angle of internal friction Ø = 34°
- Cohesion C = 0

3.4.8.3 Modulus of Subgrade Reaction

- Static 60 kcf
- Dynamic 130 kcf

3.4.8.4 Net Bearing Capacities

- Ultimate 61.7 ksf
- Allowable static 20.6 ksf
- Allowable dynamic 30.9 ksf

4.0 STRUCTURAL ANALYSIS

This section describes the structural analysis methodologies employed to determine design forces at key locations of the containment building using the applicable loads and load combinations specified in section 3.0.

The structural analysis is performed either by manual or computer analysis. In the manual analysis, the building structure or substructure is considered as an assemblage of slabs, beams, walls, and columns and the analysis is performed using standard structural analysis techniques. In the computer analysis, the building structure or substructure is modeled as an assemblage of finite elements and the analysis is performed using the standard finite element method and the Bechtel Structural Analysis Program (BSAP), which is a general purpose computer program for linear type finite element analyses. This program uses the direct stiffness approach to perform linear elastic analyses of one-, two-, or three-dimensional structural models.

For manual analyses, the analysis techniques, boundary conditions, and application of loads are provided to illustrate the method of analysis. For computer analyses, the finite element modeling techniques, boundary conditions, application of loads, and computer plots of the finite element model are provided to illustrate the overall method of analysis.

For both manual and computer analyses, representative results are provided to illustrate the overall behavior of the structure and the magnitude of design forces acting at the key locations.

4.1 CONTAINMENT SHELL

4.1.1 Analysis Methodology and Computer Model

The containment shell is analyzed with the BSAP computer program using a three-dimensional finite element model which represents the shell (cylinder and dome), basemat, and internal structure (see figure 16). The mesh near the basemat/shell junction and near the cylinder/dome junction (springline) is finer than the mesh for the remainder of the structure for increased analysis accuracy at these locations of discontinuity (areas where rapid variation of stresses occur). Likewise, the mesh near the polar crane brackets is fine for increased analysis accuracy for the effect of polar crane loads.

The equipment hatch and all other smaller penetrations are not included in the shell analysis model because they do not affect the global response of the structure and because the finite element mesh would have to be significantly finer in the penetration areas to obtain accurate results. A separate finite element model is used to analyze the equipment hatch thickened shell area. The local areas around all other shell penetrations are evaluated by combining the shell analysis results (with the appropriate stress concentration factors) with the results from an additional penetration finite element analysis (which accounts for all localized penetration loads) as discussed in section 6.3.

The basemat and internal structure are included in the shell model to realistically represent their interaction effects at the basemat/shell junction (to ensure strain compatibility).

The model shown in figure 16 is comprised of plate elements. Sheet 1 of figure 16 shows one-third of the shell portion of the model. The other two-thirds are identical. The eccentric loads on the shell due to the polar crane brackets are accounted for by modeling each bracket with beam elements as shown in figure 16, sheet 4.

The soil flexibility is simulated with boundary elements attached to the basement nodes. These boundary elements are translational linear springs in three mutually orthogonal directions (one vertical and two horizontal) per node.

The containment model described above is analyzed under all applicable loads as described in section 4.1.2.

4.1.2 Application of Loads

Piping-related loads (R_o, R_a, and R_r) are insignificant with respect to the overall containment structural response and are not included in the BSAP finite element analysis. These loads are accounted for in the design of the local areas around penetrations.

Thermal loads (T_o, T_t, and T_a) are not included in the BSAP finite element analysis. These loads are accounted for by using the thermal capabilities of the OPTCON module of the BSAP-POST computer program as discussed in section 5.1.1.

4.1.2.1 Dead Loads (D)

The weight of each modeled structural element is accounted for by means of the element mass density input parameter. The dead load of the polar crane and trolley is applied to the modeled polar crane brackets (see figure 16, sheet 4) as nodal loads determined from the tributary wheel loads.

4.1.2.2 Live Loads (L)

The polar crane live load (lifted load) is applied to the modeled polar crane brackets (see figure 16, sheet 4) as nodal loads determined from the tributary wheel loads.

The snow load is applied to the applicable dome nodes based upon the tributary area of each node projected on a horizontal plane.

The lateral earth pressure loads are applied to the appropriate cylinder elements as average uniform pressure loads.

4.1.2.3 Prestress Loads (F)

Dome prestress loads are applied as nodal loads as determined by computer program TENDON. TENDON calculates dome prestress loads for three buttress, hemispherical dome containment buildings based upon the actual geometry of the dome hoop, and inverted U-shaped tendons (see figure 9). TENDON accounts for angular and wobble friction losses in determining the magnitudes of the nodal loads. The three mutually orthogonal loads are determined for nodes which correspond to the BSAP finite element model nodes shown in figure 16, sheet 2.

Cylinder prestress loads due to the vertical inverted U-shaped tendons are applied as nodal loads. Cylinder prestress loads due to the hoop tendons are represented by equivalent element pressure loads.

All prestress loads are with respect to the end-of-lifetime (after all losses). Beginning-of-lifetime loads are accounted for as discussed in section 5.1.1.2.

4.1.2.4 Pressure Variations during Normal Operating Conditions (P_v)

This load is not included as a primary load case in the BSAP finite element analysis, but is accounted for by using an appropriate scale factor on the results of the accident pressure load (P_a).

4.1.2.5 Test Pressure (P_t)

This load is applied as a pressure load to all shell and basemat elements.

4.1.2.6 Operating Basis Earthquake, OBE (E)

The accelerations for this three-directional seismic event are input as three separate primary load cases. Static equivalent accelerations for the vertical and two horizontal directions are applied to the mass of each individual element of the model.

The dynamic earth pressure loads are applied to the appropriate cylinder elements as average uniform pressure loads.

The three-directional OBE polar crane loads are applied as nodal loads to the modeled polar crane brackets (see figure 16, sheet 4).

4.1.2.7 Design Wind (W)

This load is applied to all shell elements above ground level as element pressure loads.

4.1.2.8 Safe Shutdown Earthquake, SSE (E')

Refer to section 4.1.2.6.

4.1.2.9 Tornado Load (W_t)

The load due to tornado wind pressure effects is applied to all shell elements above ground level as element pressure loads. The load due to the atmospheric pressure drop is applied as a uniform element pressure load to all shell elements. Local effects due to tornado missile impact are accounted for as described in Appendix C.

4.1.2.10 Blast Load (B)

This load is excluded as a primary load case in the BSAP finite element analysis because the load combination which includes this blast load was determined not to govern the design (see section 4.1.3).

4.1.2.11 Design Accident Pressure (P_a)

This load is applied as a pressure load to all shell and basemat elements.

4.1.3 Total Applied Load

BSAP output includes a table which lists the total applied load for each primary load case (see table 3). This table is used to aid in determining nongoverning load cases, and to verify (against manual calculations) the applied loads.

Load combinations which include wind (W) or tornado (W_t) are shown not to govern when the total applied loads (table 3) for W and W_t are compared against OBE(X) and SSE(X), respectively. This conclusion is supported by a review of the load factors and load combinations shown in Appendix B, Table B.1. Therefore, all load combinations which include W or W_t are excluded from consideration during design.

Similarly, the load combination which includes blast load (B) does not govern. This conclusion is based on a review of the load factors and load combinations for the extreme environmental factored load combinations listed in Appendix B, Table B.1. Since the total applied load for B is less than W_T or SSE(X), it is excluded from further consideration. Refer to section 3.2.5 for a description of the load parameters for B, W_T, and SSE(X) and to table 3 for a comparison of W_T versus SSE(X).

4.1.4 Analysis Results

Resultant forces are evaluated at every point in the containment shell, but analysis results are presented in this report for a selected number of points at key locations and other representative locations. A cross section of the containment is provided in figure 17. Table 4 provides the meridional moments and forces for 15 primary load cases.

Section 4.1.3 provides the grounds for concluding that load combinations which include wind (W) or tornado (W_t) do not govern. This conclusion is additionally supported by a review of the meridional forces and moments (see table 4) for W versus OBE(X) and W_t versus SSE(X).

4.2 CONTAINMENT FOUNDATION

4.2.1 Analysis Methodology and Computer Model

The containment basemat is analyzed with the BSAP computer program using a three-dimensional finite element model which represents the cylinder, dome, basemat, and internal structure (see figure 18). This model is not the same model used to analyze the shell (figure 16 versus figure 18) since the mesh is refined for the specific structural components under investigation for each model. The basemat and reactor cavity are modeled using eight node brick elements. The shell is modeled with three node triangular simple plate elements except at the basemat/shell junction where four node rectangular plate elements are used. The primary shield walls and the mass concrete supporting the refueling canal at its west end are modeled with brick elements. All other modeled portions of the internal structure utilize plate or beam elements.

The soil flexibility is simulated with boundary elements attached to the basemat and reactor cavity nodes which are adjacent to the soil. These boundary elements are translational linear springs in three mutually orthogonal directions (one vertical and two horizontal) per node.

4.2.2 Application of Loads

Piping-related loads (R_o, R_a, and R_r) are insignificant with respect to the overall structural response of the basemat and are not included in the BSAP finite element analysis. These loads are accounted for in the design of localized areas such as the anchorage of basemat embedments.

Thermal loads (T_o, T_t, and T_a) are not included in the BSAP finite element analysis. These loads are accounted for by using the thermal capabilities of the OPTCON module of the BSAP-POST computer program as discussed in section 5.1.1.

Wind (W), tornado (W_t), and blast (B) loads are not included in the BSAP finite element analysis. These loads are shown not to govern the shell design (see section 4.1.3), and this conclusion is equally applicable to the basemat design. W, W_t, and B are therefore omitted from further evaluation.

4.2.2.1 Dead Load (D)

The weight of each modeled structural element is accounted for by means of the element mass density input parameter. The dead load of the polar crane and trolley is applied to the appropriate cylinder nodes as concentrated forces and moments.

The dead loads of the major equipment (RPV, RCP, SG, pressurizer, accumulator tanks, pressurizer relief tank, etc.) are applied as nodal loads to the appropriate basemat or internal structure nodes.

4.2.2.2 Live Loads (L)

The polar crane live load (lifted load) is applied to the appropriate cylinder nodes as concentrated forces and moments.

The snow load is applied to the dome as nodal loads. For modeled concrete slab areas of the internal structure, floor live loads (or operating floor laydown loads when applicable) are applied to the plate elements as pressure loads.

4.2.2.3 Prestress Loads (F)

The prestress loads on the shell are represented as an equivalent inward (compressive type) pressure applied to all plate elements in the shell. The loads due to the anchor points of the vertical inverted U-shaped tendons are applied as upward nodal loads at the bottom of basemat (roof of the tendon gallery).

4.2.2.4 Pressure Variations during Normal Operating Conditions (P_v)

This load is not included as a primary load case in the BSAP finite element analysis, but is accounted for by using an appropriate scale factor on the results of the accident pressure load (P_a).

4.2.2.5 Test Pressure (P_t)

Refer to section 4.2.2.4.

4.2.2.6 Operating Basis Earthquake,OBE (E)

The effects for this three-directional seismic event are input as three separate primary load cases. Static equivalent accelerations for the vertical and two horizontal directions are applied to the mass of each individual basemat element of the model.

For the shell and internal structure, static equivalent forces for the vertical and two horizontal directions are applied to the appropriate model nodes.

Equipment seismic loads are applied to the appropriate model nodes as three-directional concentrated forces.

4.2.2.7 Safe Shutdown Earthquake, SSE (E')

Refer to section 4.2.2.6.

4.2.2.8 Design Accident Pressure (P_a)

This load is applied as a uniform element pressure load to all elements which define the pressure boundary. The pressure boundary includes all elements of the cylinder and dome and the interior faces of all applicable brick elements in the basemat and reactor cavity.

4.2.3 <u>Resultant Section Forces and Load Combinations</u>

The results from the BSAP finite element analysis are in terms of normal and shear stresses for individual brick elements. Since the basemat is modeled as four layers of brick elements, the results must be transformed into resultant section forces and moments. The RESULT module of computer program BSAP-POST is used to compute the resultant forces and moments based upon defining a grid element which represents a stack of brick elements. Figure 19 shows the grid elements for the basemat, reactor cavity walls, and reactor cavity slab.

Load combinations applicable to the basemat and reactor cavity design are shown in table 5.

Co-directional responses due to three component earthquake effects are combined as described in section 5.1.1.2.

4.2.4 Analysis Results

Analysis results are evaluated at every point in the basemat and reactor cavity, but results are presented in this report for a selected number of points at key locations and other representative locations (see figure 19).

Figure 20 shows the deflected shape of the basemat under two representative load cases. Maximum and minimum displacements for the dead load and test pressure load are provided.

As described in section 4.2.1, the soil flexibility is simulated with three mutually orthogonal translational linear springs. Table 6 provides the maximum soil bearing pressures for each of the applicable load combinations of table 5. Figure 21 shows the basemat nodes which correspond to the locations of the maximum foundation bearing pressures provided in table 6, sheet 1. Table 6, sheet 2, provides a summary of the actual and allowable foundation bearing pressures and the corresponding static and dynamic factors of safety.

Table 7 provides representative analysis results for the basemat.

4.3 THICKENED SHELL AT THE EQUIPMENT HATCH

4.3.1 Analysis Methodology and Computer Model

The thickened shell at the equipment hatch is analyzed with the BSAP computer program using two separate three-dimensional finite element models. The finite element mesh for this locally thickened shell area is established based upon the actual layout configurations (see figure 9, sheet 4) of the horizontal hoop and vertical inverted U-shaped tendons.

One model, hereafter called "half model," is used in conjunction with all axisymmetric loads. The other model, hereafter called "full model," is used in conjunction with all nonaxisymmetric loads. Each fixed-base model extends from the top of the basemat to a distance above the horizontal centerline of the opening of approximately four times the opening radius.

4.3.1.1 Half Model

This model represents a half segment of the thickened equipment hatch area as shown in figure 22, sheet 1. The half model is based on an axis of symmetry about the vertical centerline of the hatch. To allow flexibility in the method for considering thermal effects, this model is created with three layers of brick elements.

For the nonthickened portion of the model, the outside layer of brick elements is equal in thickness to one-half the total shell thickness (see figure 22, sheet 2 for a typical brick element layer). The thicknesses of the middle and inside layers of brick elements are equal to one-third and one-sixth the total shell thickness, respectively.

For the thickened portion of the model, the thickness of each layer is determined based upon the centroidal locations of the horizontal and vertical tendons.

The layering of the half model permits the insertion of truss elements to represent the actual tendon layout. As stated previously, the finite element mesh is established such that the node locations represent the actual intersections of the horizontal and vertical tendons or tendon group. Each truss element represents one, two, or four tendons. Figure 22, sheet 3, shows the modeled tendons as they splay around the equipment hatch opening.

Boundary conditions are established to represent the actual behavior of the structure under axisymmetric load conditions.

4.3.1.2 Full Model

This model represents a full 360-degree portion of the containment shell as shown in figure 22, sheet 4. The full model consists entirely of shell elements located at a radius corresponding to the distance between the cylinder wall centroid and the cylinder vertical centerline. Elements near the hatch opening are increased in thickness to correspond to the actual shell thickness.

The mesh of this model is created such that the nodes near the hatch opening coincide with those in the half model. The partial plot of the full model (figure 22, sheet 5) is identical to the brick elements shown in figure 22, sheet 2.

The method used to combine the results of the half and full models is discussed in section 5.1.1.

4.3.2 Application of Loads

As stated previously, the half and full models are used in conjunction with axisymmetric and nonaxisymmetric loads, respectively.

Piping-related loads (R_o, R_a, and R_r) are not applicable for the design of the thickened shell at the equipment hatch. Live loads (L) due to the polar crane lifted load and dome snow load cause insignificant forces at the elevation of the equipment hatch area and are neglected.

Wind (W), tornado (W_t), and blast effect (B) loads are shown not to govern in the analyses for the shell and basemat and are therefore neglected in this analysis.

Thermal loads (T_o, T_t, and T_a) on the liner plate are not included in the BSAP finite element analysis. These loads are accounted for by using the hot liner plate option of the OPTCON module of the BSAP-POST computer program as discussed in section 5.1.1.

Pressure loads on the containment due to P_v and P_t are not included in the BSAP finite element analysis, but the effects due to these loadings are considered by using the appropriate scale factor on the results of the design accident pressure (P_a).

4.3.2.1 Dead Loads (D) - Half Model

The weight of each modeled structural element is accounted for by means of the element mass density input parameter. The dead load of the shell above the modeled portion of the equipment hatch and the polar crane dead load are accounted for by applying a downward surface pressure load on the top surface of the uppermost layer of brick elements.

4.3.2.2 Live Loads (L) - Full Model

The lateral earth pressure loads (at rest condition) are applied to the appropriate shell elements as average pressure loads.

4.3.2.3 Prestress Loads (F) - Half Model

The effects of the horizontal and vertical prestressing tendons are simulated by applying a pseudo-thermal load to the half model truss elements. This pseudo-thermal load in conjunction with the thermal coefficient of expansion for the truss elements creates an axial force in the truss elements which equals the average tension in the tendons.

The end-of-lifetime prestress loads are used in the BSAP finite element analysis. The beginning-of-lifetime prestress loads are accounted for by means of the load scale factor feature of BSAP-POST.

4.3.2.4 Operating Basis Earthquake, OBE (E) - Full Model

The accelerations for this three-directional seismic event are input as three separate primary load cases. Static equivalent accelerations for the vertical and two horizontal directions are applied to the mass of each individual element of the model.

The effects of the seismic loads of the shell, above the modeled portion of the cylinder, are accounted for by applying concentrated forces to the row of nodes at the boundary of the top of the model. Polar crane seismic loads cause insignificant forces at the elevation of the equipment hatch area and are neglected.

The dynamic earth pressure loads are applied to the appropriate cylinder elements as average uniform pressure loads.

4.3.2.5 Safe Shutdown Earthquake, SSE (E') - Full Model

Refer to section 4.3.2.4.

4.3.2.6 Design Accident Pressure (P_a) - Half Model

This load is applied as a surface pressure to the interior face of the entire inner layer of brick elements. To account for the reaction of the hatch cover on the periphery of the opening, the total force due to pressure on the cover is distributed as concentrated forces applied to all nodes on the opening periphery. The effect of the upward pressure acting on the dome is accounted for by applying an upward surface pressure load on the top surface of the three layers of brick elements at the top boundary.

4.3.2.7 Thermal Loads (T_o, T_t and T_a)

The temperature gradients through the shell for the operating, test, and accident conditions (the test condition is conservatively assumed to be identical to the operating condition) are applied to the three layers of brick elements as uniform temperature differences from the initial unstressed temperature. Each layer has a unique temperature difference based upon the average temperature gradient through the thickness of the layer.

4.3.3 <u>Resultant Section Forces</u>

The results for the half model BSAP finite element analysis are in terms of normal and shear stresses for each individual brick element. Since the half model is composed of three layers of brick elements, the results must be transformed into resultant section forces and moments. The RESULT module of computer program BSAP-POST is used to compute the resultant forces and moments based upon defining a grid element which represents a stack of brick elements.

The grid element numbering system is identical to the full model numbering system shown in figure 22, sheet 5, in order to facilitate the correlation of section forces and moments for the two models.

4.3.4 Analysis Results

Analysis results are evaluated for every element (grid element for the half model and shell element for the full model) in the thickened portion of the equipment hatch models. Results are presented in this report for a selected number of elements at a representative key location. The key location is shown in figure 22, sheet 5. Table 8 provides representative analysis results (meridional moments and forces) for 15 primary load cases.

4.4 POST-TENSIONING SYSTEM

The post-tensioning system consists of the tendons, anchorages, and the buttresses. The buttresses and anchorage are discussed in section 5.4.

4.4.1 Analysis Methodology

The post-tensioning system is presented in figures 9 and 10. A manual calculation is performed using standard post-tensioning analysis techniques. Tendon forces are evaluated under all conditions; at jacking, at beginning-of-lifetime, at end-of-lifetime, and under design accident pressure conditions.

The analysis takes into consideration elastic losses (resulting from the tendon stressing sequence), strand relaxation (loss of tendon stress with time), concrete creep (deformation with time under sustained loads), and concrete shrinkage (volume decrease due to continual concrete curing).

Additional losses due to friction along the length of the tendon are accounted for in determining the effective tendon forces. Friction losses occur due to sheathing misalignment due to construction tolerances (wobble friction) and due to tendon curvature in the cylinder and dome (angular friction).

4.4.2 Application of Loads

The tendons are tensioned with stressing jacks from both ends of the tendon simultaneously and in accordance with the supplier-(VSL Corporation) supplied stressing sequence. Prestress losses due to slip at anchorage are accounted for in the VSL Corporation anchorage technique such that, after anchorage, the stress at the end of the tendon is equal to 0.70 F_{ult}.

4.4.3 Analysis Results

The analysis results are presented in table 9 and figures 23 and 24.

4.5 POLAR CRANE SUPPORT SYSTEM

The polar crane support system described in section 2.4.6 consists of the runway box girders (which directly support the polar crane) and the brackets (which support the runway box girders). The brackets are anchored into the containment shell and are discussed in this design report, whereas the runway box girders are entirely inside of the pressure boundary and are discussed in the Containment Internal Structure Design Report.

4.5.1 Analysis Methodology

A typical bracket (all 37 brackets are identical) is presented in figure 11. A manual calculation is performed using standard beam formulas for determining bracket moments and shears. The bracket is analyzed as a cantilever beam (horizontally and vertically), which is representative of the boundary conditions at its anchorage into the shell.

4.5.2 Application of Loads

The majority of the loads listed in section 3.2 are not applicable to the bracket due to its location, design features, etc. For example, pressure loads are not applicable since vents (see figure 11) are provided to equalize this loading. The load combinations listed in Appendix B, Table B.3 reduce to the following.

	Equation
D + L (construction lift with impact)	1
D + L (service lift) + E	2
D + L (service lift) + E'	7

All loads listed above (excluding construction lift with impact) are obtained from the supplier's "seismic report." The governing bracket design loads occur when the polar crane trolley is positioned at its "end-of-travel", (main hook is 12 feet from the runway rail centerline). The polar crane wheels are positioned such that the resultant shears, moments, and torsion on the bracket are maximized.

The dead load of the runway box girder and its associated three-component seismic inertia loads are additionally considered in the total applied load on the bracket.

An evaluation of load magnitudes, load factors, and applicable load combinations is performed to determine the governing load combination for the analysis and design of the bracket. It is determined that load combination equation 2 containing OBE governs, therefore, all other load combinations are excluded from further consideration.

4.5.3 Analysis Results

The analysis results for the governing load combination are presented in table 10.

5.0 STRUCTURAL DESIGN

This section provides the design methodology and a summary of design results for selected critical structural elements. The structural elements are designed either manually or by computer, in accordance with the applicable sections of the codes listed in section 3.1.1.

5.1 CONTAINMENT SHELL

5.1.1 Design Methodology

The shell (excluding out-of-plane shear reinforcement) is designed by computer in accordance with the service load and factored load criteria of the ASME Code, Article CC-3000. The design requirements considered in proportioning the containment shell are strength, tornado missile protection, and radiation shielding.

The computer design is accomplished using the OPTCON module of the BSAP-POST computer program. BSAP-POST (which consists of a collection of modules that perform specific independent tasks) is a general purpose, post-processor program for the BSAP finite element analysis program. BSAP-POST reads computed BSAP results into an internal common data storage base and optionally performs one or several additional operations (e.g., plotting) or calculations (e.g., creating load combinations or designing reinforced concrete members).

In general, the OPTCON processor is a reinforced concrete analysis and design program for doubly reinforced concrete sections which creates reinforced concrete interaction diagrams (IAD) based on the maximum allowable resistance of a section for given stress and strain limitations (Code allowables). Any load combination whose design axial force and corresponding moment (load set) fall within the IAD indicates all stress and strain Code criteria are satisfied.

OPTCON also has the capability of calculating the thermal moment, considering the concrete cracking and reinforcement yielding effects, due to a given linear thermal gradient (i.e., a difference in temperature between the two concrete faces). For each load combination, the state of stress and strain is determined before the thermal load is applied. Then the thermal moment is approximated based upon an iterative approach which considers equilibrium and compatibility conditions, and is based on the assumption that the section is free to expand axially without any constraints. The final force-moment set (which includes the cracked section final thermal moment) is checked to verify that it falls within the Code allowable IAD.

For sections with a liner plate, OPTCON has the capability to include the effects on the section due to a hot liner plate, and to include any applicable liner plate stress/strain criteria in the formulation of the IAD.

The term "utilization factor" (UF) refers to the amount of resistance of the IAD that has been used relative to the zero curvature line. The zero curvature line refers to a line defined by a series of points whose force-moment load set creates constant strain across the section, a neutral axis at infinity, and a strain diagram curvature of zero. A UF of 100 indicates that the section is 100 percent utilized by the design load. UF refers to the utilization factor for ASME primary stress allowables, and "UFS" refers to the utilization factor for ASME primary plus secondary stress allowables.

5.1.1.1 Tangential Shear

The ASME Code has no provisions for allowable stresses for tangential shear (i.e., membrane or "in-plane" shear) in prestressed containment buildings. The shell design procedure provides a conservative and viable technique for accounting for the effects of tangential shear. Reinforcement for tangential shear is provided by defining "equivalent" membrane forces:

For seismic loads:

$$N_{ht} = (N_h^2 + V_u^2)^{1/2}$$

$$N_{vt} = (N_v^2 + V_u^2)^{1/2}$$

For wind, tornado, or blast loads:

$$N_{ht} = N_h + V_u$$
$$N_{vt} = N_v + V_u$$

where:

N_{ht}, N_{vt} = "equivalent" membrane forces in the horizontal and vertical directions, respectively.

N_h, N_v = membrane forces, due to the same loading causing the tangential shear, in the horizontal and vertical directions, respectively.

V_u = tangential shear force due to seismic, wind, tornado, or blast loads.

5.1.1.2 Load Combinations

The design of the shell is based on the results of the shell finite element analysis as described in section 4.1. The analysis results for the primary load cases are multiplied by the appropriate load factors and combined into the required load combinations (see Appendix B, Table B.1) during the reinforcing design phase.

As previously discussed in section 4.1.3, all load combinations listed in Appendix B, Table B.1 which include wind (W), tornado (W_t), or blast (B) do not govern and are excluded from further consideration. See table 5 for the load combinations applicable to the overall containment shell design.

The combination of co-directional responses due to three component earthquake effects are performed using the Square Root of the Sum of the Squares (SRSS) method, i.e., $R = \left(R_i^2 + R_j^2 + R_k^2\right)^{1/2}$ or the component factor method, i.e.,

$$R = \pm R_i \pm 0.4\ R_j \pm 0.4\ R_k$$
$$R = \pm 0.4\ R_i \pm R_j \pm 0.4\ R_k$$
$$R = \pm 0.4\ R_i \pm 0.4\ R_j \pm R_k$$

wherein 100 percent of the design forces from any one of the three components of the earthquake is considered in combination with 40 percent of the design forces from each of the other two components of the earthquake.

As discussed in section 4.1.2, the prestress primary load case is for end-of-lifetime forces. To account for the beginning-of-lifetime forces, the primary load case results are multiplied by scale factors of 1.176 and 1.14 for shell elements in the cylinder and dome, respectively. These two scale factors account for the larger tendon forces existing before the prestress losses occur (see section 4.4) and are determined by dividing the average beginning-of-lifetime tendon stresses by the average end-of-lifetime tendon stresses.

Thermal effects on the shell concrete and liner plate are accounted for in OPTCON by applying a thermal gradient to the concrete and a temperature increase to the liner plate as discussed in section 5.1.1.

5.1.1.3 Preliminary Design Without Thermal Effects

Shell elements in the finite element model are evaluated by OPTCON for all applicable load combinations (excluding thermal effects) listed in table 5. This permits the selection of critical elements without requiring OPTCON to perform an iterative cracked section analysis on every individual shell element. A minimum of one critical element per element group (see figure 17 for element group locations) is selected. For both the horizontal and vertical reinforcement, the selection process takes into consideration the area of steel required for the inside face and outside face.

Table 11 lists the critical elements for each of the key locations shown in figure 17. The table additionally provides the governing load combinations as defined in table 5, area of steel required ("optimum" steel), and area of steel provided. Critical elements are selected for both end-of-lifetime and beginning-of-lifetime prestress conditions.

For table 11, sheet 1 (critical elements selected by vertical steel requirements) and sheet 2 (critical elements selected by horizontal steel requirements), A_s and A_s' represent the outside face and inside face reinforcement, respectively.

5.1.2 Final Design Results with Thermal Effects Included

Critical elements are analyzed by the OPTCON iterative cracked section method to account for the thermal effects on the shell. The cracked section analyses are based on the area of steel provided (see table 11 for the area of steel provided for the key locations shown in figure 17). The final force-moment load sets, which include the cracked section final thermal moment, for each critical element are checked to verify that they fall within the Code allowable IAD.

Figure 25 provides representative IADs for vertical and horizontal reinforcement for service load and factored load criteria. Each sheet of figure 25 lists the area of steel provided for the section, all pertinent section dimensions, material properties, and the final section forces and moments for the applicable load combinations.

Sheets 1 through 4 of figure 25 show IADs applicable only at the cylinder/basemat junction. This area of gross structural discontinuity is designed to satisfy primary plus secondary stress allowables in accordance with the ASME Code listed in section 3.1.1.

Sheets 5 through 8 of figure 25 show IADs applicable only at key location 8 (see figure 17). The elements at this location are designed to satisfy primary stress allowables (when thermal effects are excluded) or primary plus secondary stress allowables (when thermal effects are included).

Sheets 9 through 12 of figure 25 show IADs applicable to all locations of the shell from the top of the haunch (elevation 179'-0") to the springline (dome/cylinder junction) inclusive. The elements at these locations are designed to satisfy primary or primary plus secondary stress allowables as applicable.

An identical design approach is used for all critical elements in the dome. Dome elements are designed to satisfy primary or primary plus secondary stress allowables as applicable.

5.1.3 Buttress Design

The design of the buttresses is discussed in conjunction with the post-tensioning system (section 5.4).

5.1.4 Radial Shear and Radial Tension Design

Radial (i.e., transverse or out-of-plane) shear is produced by the design loads and the presence of structural discontinuities (i.e., the basemat/cylinder junction and the cylinder/dome junction). Radial tension is caused by the curvature of the post-tensioning tendons in the wall and dome. Shear reinforcement is designed manually to satisfy the requirements of radial shear or radial tension, whichever is greater.

Radial tension is determined based upon the worst case post-tensioning stresses (at-transfer). Radial tension reinforcement is provided based upon BC-TOP-5-A (reference 2) which satisfies the requirements of the ASME Code, Article CC-3000.

Radial shear is determined based upon the BSAP finite element analysis results. Longitudinal moments along various meridional lines are evaluated to determine which meridional line has the most rapid variation of longitudinal moments (M_{yy}). This case is plotted and the radial shear at any point is determined based upon the moment gradient. Radial shear reinforcement is provided in accordance with the ASME Code listed in section 3.1.1.

5.1.5 Design Details

Representative design details are provided in figure 8, sheets 1, 2, and 3.

5.2 CONTAINMENT FOUNDATION

5.2.1 Design Methodology

The foundation (excluding out-of-plane shear reinforcement) is designed by computer in accordance with the service load and factored load criteria of the ASME Code, Article CC-3000. The computer design is accomplished using the OPTCON module of the BSAP-POST computer program as described in section 5.1.1.

The finite element analysis results for the basemat and reactor cavity are in terms of resultant section forces and moments as described in section 4.2.3.

Thermal effects on the basemat and reactor cavity concrete and liner plate are accounted for in OPTCON (as described in section 5.1.1) by applying a thermal gradient and uniform temperature increase to the critical sections.

The design requirement considered in proportioning the basemat and reactor cavity is strength.

5.2.2 Final Design Results

Grid elements representing the basemat, reactor cavity wall, and reactor cavity slab are evaluated to determine the controlling sections based upon the worst case moment and membrane force combinations (excluding thermal effects).

Controlling elements are analyzed by the OPTCON iterative cracked section method to account for the thermal effects. The cracked section analyses are based on the area of steel provided. The initial (before thermal effects) and final (which includes the cracked section thermal moment) force-moment load sets for each controlling element are checked to verify that they fall within the Code allowable IAD.

Figure 26 provides representative IADs for controlling elements for service load and factored load criteria. Each sheet of figure 26 lists the area of steel provided for the section, all pertinent section dimensions, material properties, and section forces and moments for the applicable load combinations.

Sheets 1 through 4 of figure 26 show IADs applicable to key location 1 (N-S and E-W grid reinforcement). Sheets 5 through 8 show IADs applicable to key location 2 (radial and circumferential reinforcement pattern). Sheets 9 through 12 show IADs applicable to key location 3 (reactor cavity wall reinforcement). Sheets 13 through 16 show IADs applicable to key location 4 (reactor cavity slab reinforcement). See figure 19 for identification of key locations.

All controlling sections shown in figure 26 are designed to satisfy primary stress allowables (when thermal effects are excluded) or primary plus secondary stress allowables (when thermal effects are included).

5.2.3 Transverse Shear

Transverse (or out-of-plane) shear is produced by the design loads and the presence of structural discontinuities. Transverse shear is determined based upon the results of the BSAP finite element analysis. Shear reinforcement in the basemat and reactor cavity is designed manually in accordance with the ASME Code, Article CC-3000.

5.2.4 Design Details

Representative design details are provided in figures 5 and 6.

5.3 THICKENED SHELL AT THE EQUIPMENT HATCH

5.3.1 Design Methodology

The thickened equipment hatch portion of the containment shell (excluding out-of-plane shear reinforcement) is designed by computer in accordance with the service load and factored load criteria of the ASME Code, Article CC-3000. The computer design is accomplished using the OPTCON module of the BSAP-POST computer program as described in section 5.1.1.

The design requirement considered in proportioning the equipment hatch portion of the containment shell is strength.

5.3.1.1 Tangential Shear

Tangential shear is accounted for as described in section 5.1.1.1.

5.3.1.2 Load Combinations

The design of the thickened shell at the equipment hatch is based on the results of the half and full model finite element analyses as described in section 4.3. As discussed in section 4.3.2, wind, tornado, blast, and piping do not govern. See table 5 for the load combinations applicable to the equipment hatch design.

Co-directional responses due to three component earthquake effects are combined as discussed in section 5.1.1.2.

5.3.2 Final Design Results

All thickened areas of the equipment hatch models are evaluated to determine the controlling sections. Controlling sections are analyzed by the OPTCON iterative cracked section method to account for the thermal effects. The cracked section analyses are based on the area of steel provided.

Table 12 provides representative design results for a controlling section for service and factored load criteria. The initial (before thermal effects) and final (which includes the cracked section thermal moment) force-moment load sets are checked to verify that they fall within the Code allowable IAD. All controlling sections are designed to satisfy primary stress allowables (when thermal effects are excluded) or primary plus secondary stress allowables (when thermal effects are included).

5.3.3 Radial Shear and Radial Tension Design

See the discussion in section 5.1.4.

5.3.4 Design Details

Representative design details are provided in figure 8, sheet 3.

5.4 POST-TENSIONING SYSTEM

5.4.1 Design Methodology

The post-tensioning system is designed in accordance with CC-3433 and CC-3540 of the ASME Code. Strength is the design requirement considered in proportioning the post-tensioning system.

The design of the tendon anchorage zone (buttress) is based on the results and recommendations of two test programs conducted by Bechtel to demonstrate the adequacy of several reinforcing patterns for use in anchorage zone concrete in the basemat and buttresses. The test results demonstrate satisfactory performance of the test anchorages. The description, results, and recommendations of the test programs are contained in BC-TOP-7 (reference 2).

The tendon anchorage system (see figure 10) is designed by VSL Corporation.

5.4.2 Design Results

The design results are provided in table 13.

5.4.3 Design Details

Representative design details are provided for tendon layout (see figure 9), buttress reinforcement (see figure 8, sheets 4 and 5), and anchorage (see figure 10).

5.5 POLAR CRANE SUPPORT SYSTEM

5.5.1 Design Methodology

The polar crane brackets (all 37 brackets are identical) are designed manually in accordance with the AISC Specification. The design requirements considered in proportioning the brackets are strength and stability.

The resultant design forces for the bracket are shown in table 10. Standard design techniques are used to determine tension, compression, shear, and bending stresses, section compactness, local buckling, and web crippling.

The bracket embedment into the shell is designed manually in accordance with the ASME Code, Article CC-3000. Standard design techniques are used to determine concrete bearing stress and shear stress.

5.5.2 Design Results

The design results for the governing load combination are presented in table 14.

5.5.3 Design Details

Representative design details are provided in figure 11.

6.0 MISCELLANEOUS ANALYSIS AND DESIGN

As described in section 4.1, the containment building is evaluated for the effects of abnormal loads and tornado loads, where applicable, on a local area basis. In addition, the overall stability of the containment building is evaluated. This section describes these analyses and significant special provisions employed in the containment building design.

6.1 STABILITY ANALYSIS

The overall stability of the containment building is evaluated by determining the factor of safety against overturning, sliding, and flotation.

6.1.1 Overturning

The factor of safety against overturning is determined using the equivalent static method and the energy balance method. The equivalent static method does not account for the dynamic characteristics of the loading and, therefore, results in a factor of safety significantly lower than the energy balance method. The factor of safety obtained from the energy balance method reflects the actual design conditions and, therefore, provides a more appropriate measure of the design margin.

The factor of safety against overturning using the equivalent static method is defined as the ratio of the resisting moment due to net gravity forces to the overturning moment caused by the maximum lateral forces acting on the structure. The gravity forces are reduced to account for the effects of buoyancy and the vertical component of earthquake.

The factor of safety against overturning using the energy balance method is defined as the ratio of the increase in the potential energy at the point of overturning about the critical edge of the structure to the maximum kinetic energy that could be imparted to the structure as a result of earthquake loading. The energy balance analysis methodology is described in BC-TOP-4-A (reference 2).

6.1.2 Sliding

The factor of safety against sliding is defined as the ratio of the foundation sliding resistance (due to combined frictional forces and at rest soil pressures) to the maximum calculated lateral force. Both the sliding resistance and the applied lateral force account for dynamic increment soil pressure effects.

6.1.3 Flotation

The factor of safety against flotation is defined as the ratio of the total weight of the structure and its foundation to the buoyant force, defined as the volume of the groundwater displaced by the submerged portion of the structure multiplied by the unit weight of water.

6.1.4 Analysis Results

The minimum required factors of safety and the calculated factors of safety for stability are provided in table 15.

6.2 TORNADO LOAD EFFECTS

Tornado load effects result from wind pressures, atmospheric pressure differentials, and tornado missile strikes. The magnitude and combinations of tornado load effects considered are described in section 3.2.5. The load combination involving tornado load effects is provided in Table B.1 in Appendix B.

The shell is evaluated for tornado load effects, and the localized response is combined with the analysis results of the overall structural response, as applicable, to confirm that design integrity is maintained. It is demonstrated that the required ductility is less than 2 compared to an allowable ductility of 10 for flexure with two-way reinforcing.

Similarly, the equipment hatch missile shield door is evaluated and designed in accordance with the ACI 318 Code. The computed ductility from that tornado missile analysis is 6.1, which is less than the allowable ductility of 10.

The methodology used to analyze and design the structural elements to withstand the tornado load effects is described in BC-TOP-3-A (reference 2). Specific procedures used for analysis of missile impact effects are described in Appendix C.

The containment building is provided with f'_c = 6000 psi minimum concrete strength and 3 feet 9 inches minimum shell thickness. The equipment hatch missile shield is provided with f'_c = 5000 psi minimum concrete strength and 2 feet 6 inches minimum thickness.

All other shell openings are protected by the roofs and walls of adjacent structures which have f'_c = 4000 psi minimum concrete strength, have a minimum thickness of 24 inches for walls and 21 inches for roofs, to preclude missile perforation and concrete scabbing.

6.3 SMALL PENETRATION ANALYSIS AND DESIGN

As discussed in sections 4.1.1 and 4.1.2, piping-related loads (R_o, R_a, and R_r) are not included in the shell BSAP finite element analysis because they are insignificant with respect to the overall containment structural response. This section describes the methodology used to account for these localized loads.

6.3.1 Analysis Methodology

The containment shell penetrations are analyzed with the BSAP computer program using a three-dimensional finite element model as shown in figure 27. The model represents the largest piping penetration and includes a portion of the shell large enough to ensure that effects due to the local penetration loads are negligible at the model boundary (fixed conditions). The results obtained from the analysis envelop the membrane forces and bending moments for smaller penetrations. Unit loads are applied to the model as five separate primary load cases (the effects due to torsion are negligible in the design of flexure and shear reinforcement, but are accounted for in the design of the penetration sleeve) as shown in figure 27.

The penetration model analysis results for the five primary unit load cases are provided in table 16. These values are multiplied by the actual penetration loads at the shell centerline to obtain the resultant design forces and moments due to the local piping-related loads.

Analysis results for the effects of local piping loads from the main steam line (largest key piping penetration) are provided in table 16.

6.3.2 Design Methodology

The flexural and shear reinforcement is designed by computer and manually designed, respectively, in accordance with the service load and factored load criteria of the ASME Code, Article CC-3000. The computer design is accomplished using the OPTCON module of the BSAP-POST computer program as described in section 5.1.1.

Thermal effects on the shell concrete and liner plate are accounted for in OPTCON by applying a thermal gradient to the concrete and a temperature increase to the liner plate as discussed in section 5.1.1.

The forces and moments obtained from the penetration analysis (of localized loads) are combined with the shell analysis (nonlocalized loads) forces and moments (described in section 4.1) in accordance with the load combinations shown in Appendix B, Table B.1. The shell analysis results (whose model did not include penetrations) are multiplied by stress concentration factors, determined by classical methods, to account for the existence of the penetration.

Representative design results are provided in table 17 for the design of meridional (vertical) flexural reinforcement adjacent to the main steam line penetrations.

6.4 CONTAINMENT ULTIMATE PRESSURE CAPACITY ANALYSIS

Refer to Appendix D for the analysis methodology and results.

7.0 CONCLUSION

The analysis and design of the containment building includes all credible loading conditions and complies with all applicable design requirements.

8.0 REFERENCES

1. "Building Code Requirements for Minimum Design Loads in Buildings and Other Structures," ANSI A58.1-1972, American National Standards Institute, New York, N.Y., 1972.

2. Bechtel Topical Reports

- BC-TOP-1, Revision 1, Containment Building Liner Plate Design Report, December 1972.
- BC-TOP-3-A, Revision 3, Tornado and Extreme Wind Design Criteria for Nuclear Power Plants, August 1974.
- BC-TOP-4-A, Revision 3, Seismic Analyses of Structures and Equipment for Nuclear Power Plants, November 1974.
- BC-TOP-5-A, Revision 3, Prestressed Concrete Nuclear Reactor Containment Structures, February 1975.
- BC-TOP-7, Revision 0, Full Scale Buttress Test for Prestressed Nuclear Containment Structures, September 1972.
- BC-TOP-8, Revision 0, Tendon End Anchor Reinforcement Test, September 1972.

TABLE 1

CONTAINMENT BUILDING SEISMIC ACCELERATION VALUES

		Floor Accelerations (g's)(1)					
		OBE			SSE		
		Horizontal		Vert.	Horizontal		Vert.
Elevation	Description	E-W	N-S		E-W	N-S	
163'-11"	Basemat	0.14	0.13	0.23	0.21	0.20	0.38
193'-10"		0.15	0.15	0.22	0.22	0.22	0.34
220'-0"	Finished Grade	0.17	0.17	0.23	0.25	0.25	0.35
258'-5"		0.22	0.22	0.27	0.31	0.31	0.41
290'-8"		0.26	0.26	0.28	0.38	0.38	0.42
323-0"	Polar Crane Level	0.30	0.30	0.30	0.45	0.45	0.43
361'-0"		0.36	0.36	0.30	0.54	0.54	0.44
399'-0"	Dome Apex	0.44	0.44	0.26	0.64	0.64	0.45

(1) The actual acceleration values used in the design of the structure may be higher than the values shown.

TABLE 2

TORNADO MISSILE DATA

Missile	Weight W (lb)	End-On Height Limit (ft)	End-On Horizontal Velocity (ft/sec)	Vertical Velocity (ft/sec)
4" x 12" x 12' Plank	200	216	200	160
3" Ø std x 10' Pipe	78.5	212	200	160
1" Ø x 3' Steel Rod	8	Unlimited	317	254
6" Ø std x 15' Pipe	285	101	160	128
12" Ø std x 15' Pipe	744	46	150	120
13-1/2" Ø x 35' Utility Pole	1490	30(1)	211	169
Automobile (20-ft^2 Projected Area)	4000	0	75	60

(1) To 30 feet above all grade levels within 1/2 mile of facility structures.

TABLE 3

TOTAL APPLIED LOADS FOR THE SHELL FINITE ELEMENT ANALYSIS

TOTAL[1] APPLIED LOADS (kips)

Primary Load Case Number	Description of Load	Direction of Load[2]		
		X	Y	Z
1	Dead Load	-	-	-154,392
2	Live Load	-	-	-827
3	Prestress	-	-	-
4	Test Pressure	-	-	-
5	Accident Pressure	-	-	-
6	OBE (X-Direction)	34,274	-	-
7	OBE (Y-Direction)	-	33,517	-
8	OBE (Z-Direction)	-	-	41,089
9	SSE (X-Direction)	49,856	-	-
10	SSE (Y-Direction)	-	48,655	-
11	SSE (Z-Direction)	-	-	64,134
12	Soil Pressure	4,676	-409	-
13	Extreme Wind	474	-	196
14	Tornado (Wind Velocity Effect)	2,060	-	714
15	Tornado (Pressure Drop Effect)	-	-	7,006

(1) The loads tabulated above are "unfactored" (i.e., the load factors shown in Appendix B, Table B.1 are not included).

(2) X and Y are the two orthogonal horizontal axes, and Z is the vertical axis (positive up).

TABLE 4

SHELL ANALYSIS RESULTS AT SELECTED KEY LOCATIONS (Sheet 1 of 3)

Key Location See Note (1)	Dead Load		Live Load		Prestress		Test Pressure		Accident Pressure	
	S_{yy} (k/ft)	M_{yy} (ft-k /ft)	S_{yy} (k/ft)	M_{yy} (ft-k /ft)	S_{yy} (k/ft)	M_{yy} (ft-k /ft)	S_{yy} (k/ft)	M_{yy} (ft-k /ft)	S_{yy} (k/ft)	M_{yy} (ft-k /ft)
1	-20	0	-1	0	-381	10	298	36	258	31
2	-24	3	-1	0	-551	26	308	-22	267	-19
3	-38	-7	0	1	-570	-64	316	39	274	34
4	-41	4	0	3	-549	94	317	-29	275	-25
5	-45	10	0	4	-538	133	318	-57	276	-49
6	-89	-1	-4	0	-471	48	325	5	281	4
7	-120	-66	-3	-2	-461	-12	301	221	261	191
8	-113	-86	-3	-2	-466	-186	286	587	247	509
9	-133	-83	-3	-2	-455	-275	304	906	263	785

S_{yy} is the meridional force. $+S_{yy}$ indicates membrane tension.

M_{yy} is the meridional moment. $+M_{yy}$ indicates compression on the outside face.

(1) Refer to figure 17 for key locations.

The results listed on sheets 1, 2, and 3 are with respect to the +X axis meridional line.

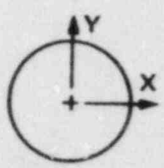

TABLE 4

SHELL ANALYSIS RESULTS AT SELECTED KEY LOCATIONS (Sheet 2 of 3)

Key Location See Note (1)	OBE (X)		OBE (Y)		OBE (Z)		SSE (X)		SSE (Y)	
	S_{yy} (k/ft)	M_{yy} (ft-k /ft)	S_{yy} (k/ft)	M_{yy} (ft-k /ft)	S_{yy} (k/ft)	M_{yy} (ft-k /ft)	S_{yy} (k/ft)	M_{yy} (ft-k /ft)	S_{yy} (k/ft)	M_{yy} (ft-k /ft)
1	-1	0	0	0	6	0	-2	0	0	0
2	-6	1	-1	0	7	-1	-8	1	-1	0
3	-20	35	-2	3	11	2	-31	50	-3	4
4	-19	115	-2	-1	12	-1	-30	167	-4	-1
5	-17	213	6	32	13	-3	-27	210	9	45
6	-63	-5	-6	0	26	0	-90	-6	-8	0
7	-139	-17	-6	0	34	19	-199	-25	-9	0
8	-140	27	-1	2	32	24	-200	38	-1	3
9	-154	94	-13	6	38	23	-221	135	-18	8

S_{yy} is the meridional force. $+S_{yy}$ indicates membrane tension.

M_{yy} is the meridional moment. $+M_{yy}$ indicates compression on the outside face.

The signs on the seismic results reflect the values for the seismic accelerations applied in the positive directions of the global coordinate system. The positive/negative nature of the seismic loads is accounted for in the formulation of the load combinations.

(1) Refer to figure 17 for key locations.

TABLE 4

SHELL ANALYSIS RESULTS AT SELECTED KEY LOCATIONS (Sheet 3 of 3)

Key Location See Note (1)	SSE (Z)(2)		Soil Pressure		Extreme Wind	Tornado(3)			Tornado(4)	
	S_{yy} (k/ft)	M_{yy} (ft-k /ft)	S_{yy} (k/ft)	M_{yy} (ft-k /ft)	S_{yy} (k-ft)	M_{yy} (ft-k /ft)	S_{yy} (k/ft)	M_{yy} (ft-k /ft)	S_{yy} (k/ft)	M_{yy} (ft-k /ft)
1	9	0	-1	0	-3	0	-13	-1	15	2
2	11	-2	-1	0	-3	0	-14	1	15	-1
3	17	3	-2	1	-4	1	-19	3	15	1
4	18	-1	-2	4	-5	3	-20	14	15	-3
5	20	-4	-2	7	-5	6	-20	27	15	-6
6	39	1	-3	-1	-5	0	-23	-2	15	0
7	51	27	-5	0	-3	-1	-13	-3	14	9
8	48	36	-5	2	-2	-1	-10	-4	13	26
9	57	34	-5	4	-3	-1	-11	-3	14	42

S_{yy} is the meridional force. $+S_{yy}$ indicates membrane tension.

M_{yy} is the meridional moment. $+M_{yy}$ indicates compression on the outside face.

(1) Refer to figure 17 for key locations.

(2) Refer to sheet 2 of this table for a discussion of the positive/negative nature of seismic loads.

(3) Wind velocity effect.

(4) Pressure drop effect.

TABLE 5

APPLICABLE LOAD COMBINATIONS FOR THE CONTAINMENT BUILDING[1] DESIGN

Category	D	L	F	P_t	P_a	T_t	T_o	T_a	E_o	E_{ss}	P_v	Load Combination Number
Service												
Test	1.0	1.0	1.0	1.0	-	1.0	-	-	-	-	-	1
Construction	1.0	1.0	1.0	-	-	-	1.0	-	-	-	-	2[2]
Normal	1.0	1.0	1.0	-	-	-	1.0	-	-	-	1.0	3
Severe environmental	1.0	1.0	1.0	-	-	-	1.0	-	1.0	-	1.0	4
Factored												
Severe environmental	1.0	1.3	1.0	-	-	-	1.0	-	1.5	-	1.0	5[3]
Extreme environmental	1.0	1.0	1.0	-	-	-	1.0	-	-	1.0	1.0	6
Abnormal	1.0	1.0	1.0	-	1.5	-	-	1.0	-	-	-	7
Abnormal/severe environmental	1.0	1.0	1.0	-	1.25	-	-	1.0	1.25	-	-	8
Abnormal/extreme environmental	1.0	1.0	1.0	-	1.0	-	-	1.0	-	1.0	-	9

These load combinations are the nine possible governing cases out of the original 16 listed in Appendix B, Table B.1. See section 4.1.3 for discussion of nongoverning cases for the shell.

(1) This table is applicable for the containment shell, foundation, and equipment hatch area designs.
(2) Nongoverning for the foundation and equipment hatch designs.
(3) Nongoverning for the foundation design.

TABLE 6

MAXIMUM FOUNDATION BEARING PRESSURES (Sheet 1 of 2)

Load Combination (See table 5)	Node Number	Element Force (k)	Tributary Area (ft^2)	Soil Pressure (ksf)	Type of Loading
1	454	-97	10.5	9.3	Static
3	222	-340	39.8	8.6	Static
4	226	-668	39.8	16.8	Dynamic
6	226	-832	39.8	20.9	Dynamic
7	454	-103	10.5	9.9	Static
8	230	-679	39.8	17.1	Dynamic
9	226	-769	39.8	19.3	Dynamic

This table provides the maximum gross foundation bearing pressure, obtained from the foundation finite element analysis discussed in section 4.2.4, for each applicable load combination. For the allowable foundation bearing pressures, see section 3.4.8.

TABLE 6

MAXIMUM FOUNDATION BEARING PRESSURES(1) (Sheet 2 of 2)

Gross Static (ksf)	Net Static (ksf)	Gross Dynamic (ksf)	Net Dynamic (ksf)	Allowable Net(2) Bearing Capacity		Computed(3) Factor of Safety	
				Static (ksf)	Dynamic (ksf)	Static	Dynamic
8.4	1.0	20.9	13.5	20.6	30.9	61.7	4.6

(1) Maximum foundation bearing pressures are defined as follows:

Gross Static = Total structure dead load plus operating live load divided by total basemat area.

Net Static = The static pressure in excess of the overburden pressure at the base of the structure.

Gross Dynamic = Maximum soil pressure under dynamic loading conditions (i.e., unfactored SSE).

Net Dynamic = The dynamic pressure in excess of the overburden pressure at the base of the structure.

(2) The allowable net static and dynamic bearing capacities are obtained by dividing the ultimate net bearing capacity by factors of 3 and 2 respectively. The ultimate net bearing capacity is the pressure in excess of the overburden pressure at the foundation level at which shear failure may occur in the foundation stratum.

(3) The computed factor of safety is the ultimate net bearing capacity divided by the net static or net dynamic pressure.

TABLE 7

REPRESENTATIVE BASEMAT FINITE ELEMENT ANALYSIS RESULTS (Sheet 1 of 2)

Load Combination (See table 5)	Grid Element Number	(1) XCG (ft)	F_y (k/ft)	F_z (k/ft)	V_y (k/ft)	V_z (k/ft)	M_y (ft-k/ft)	M_z (ft-k/ft)
4	223	21.4	-83	-102	135	-13	375	220
	194	27.7	-73	-89	54	4	873	467
	164	34.4	-65	-93	-4	-3	961	544
	134	41.1	-60	-119	-73	-10	619	437
	104	49.1	-52	-118	4	-5	406	393
	74	57.9	-39	-96	-85	-4	-25	266
	41	66.8	-31	-191	-183	-17	-1167	-197
	9	73.8	-13	-108	42	6	-120	71
6	223	21.4	-106	-112	167	-13	419	236
	194	27.7	-90	-99	72	7	1038	541
	164	34.4	-78	-106	4	0	1173	646
	134	41.1	-69	-140	-78	-9	800	538
	104	49.1	-57	-142	4	-3	544	488
	74	57.9	-39	-121	-105	-5	-14	326
	41	66.8	-28	-227	-226	-19	-1451	-266
	9	73.8	-15	-135	52	11	-145	67
8	223	21.4	48	168	3	24	-1035	-591
	194	27.7	58	137	14	28	-971	-621
	164	34.4	65	121	11	43	-937	-629
	134	41.1	70	100	19	37	-858	-606
	104	49.1	64	68	56	20	-768	-605
	74	57.9	67	62	76	9	-208	-454
	41	66.8	79	-3	87	28	473	-141
	9	73.8	-3	-47	21	36	3	-287

(1) XCG is the distance from the center of the containment to the cg of the grid element.

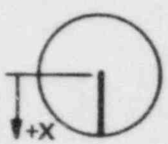

The representative results provided above are for grid elements along this N-S radial line. See figure 19 for location of grid elements.

TABLE 7

REPRESENTATIVE BASEMAT FINITE ELEMENT ANALYSIS RESULTS (Sheet 2 of 2)

Load Combination (See table 5)	Grid Element Number	(1) YCG (ft)	F_y (k/ft)	F_z (k/ft)	V_y (k/ft)	V_z (k/ft)	M_y (ft-k/ft)	M_z (ft-k/ft)
4	216	-15.4	-73	-97	20	-29	211	500
	186	-21.6	-46	-97	19	21	269	505
	156	-29.3	-55	-99	14	64	192	185
	126	-37.5	-54	-104	18	11	127	-12
	96	-45.5	-45	-114	18	35	91	-129
	66	-55.5	-28	-78	25	11	116	-61
	33	-66.3	-94	-36	19	97	92	-232
	1	-73.9	-66	2	25	-11	112	-36
8	216	-15.4	146	274	41	-29	-634	-1282
	186	-21.6	105	261	23	-50	-593	-938
	156	-29.3	140	241	49	-55	-461	-529
	126	-37.5	148	238	41	-1	-426	-369
	96	-45.5	175	258	19	-12	-401	-286
	66	-55.5	216	222	5	70	-891	-796
	33	-66.3	197	-20	78	-479	-803	-430
	1	-73.9	251	-12	24	-14	-575	-3
8	216	-15.4	175	318	23	6	-619	-1276
	186	-21.6	120	312	7	-30	-689	-1188
	156	-29.3	169	279	38	-63	-571	-755
	126	-37.5	183	270	27	8	-539	-549
	96	-45.5	207	286	4	-25	-508	-398
	66	-55.5	254	240	-18	83	-1034	-847
	33	-66.3	254	-41	65	-612	-817	-130
	1	-73.9	318	-16	-3	-4	-624	35

(1) YCG is the distance from the center of the containment to the cg of the grid element.

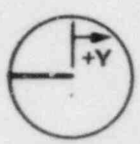

The representative results provided above are for grid elements along this E-W radial line. See figure 19 for location of grid elements.

TABLE 8

REPRESENTATIVE FINITE ELEMENT ANALYSIS RESULTS FOR THE THICKENED SHELL AT THE EQUIPMENT HATCH (Sheet 1 of 3)

Element Number See Note (1)	Half Model Dead Load		Full Model Live Load		Half Model Prestress		Half Model Test Pressure		Half Model Accident Pressure	
	S_{yy} (k/ft)	M_{yy} (ft-k /ft)	S_{yy} (k/ft)	M_{yy} (ft-k /ft)	S_{yy} (k/ft)	M_{yy} (ft-k /ft)	S_{yy} (k/ft)	M_{yy} (ft-k /ft)	S_{yy} (k/ft)	M_{yy} (ft-k /ft)
166	-454	24	-18	-14	-1191	184	(2)	(2)	319	746
175	-360	33	-15	-19	-1173	194	(2)	(2)	417	614
184	-293	26	-14	-20	-1078	146	(2)	(2)	454	497
185	-219	19	-11	-12	-898	117	(2)	(2)	447	319
186	-157	15	-8	-5	-654	85	(2)	(2)	405	141
187	-126	14	-6	1	-466	82	(2)	(2)	353	43
188	-117	13	-5	-1	-419	53	(2)	(2)	320	11
189	-112	13	-3	-2	-451	25	(2)	(2)	288	-12
190	-110	12	-1	-4	-497	14	(2)	(2)	267	-29
191	-109	12	1	-6	-512	12	(2)	(2)	260	-35

S_{yy} is the meridional force.

M_{yy} is the meridional moment.

(1) Refer to figure 22, sheet 5, for element locations.
(2) The results of the test pressure are equal to the accident pressure results times a scale factor of 1.15.

TABLE 8

REPRESENTATIVE FINITE ELEMENT ANALYSIS RESULTS FOR THE THICKENED SHELL AT THE EQUIPMENT HATCH (Sheet 2 of 3)

	Half Model		Half Model		Half Model		Full Model		Full Model	
	T_t		T_o		T_a		OBE (X)		OBE (Y)	
Element Number(1)	S_{yy} k/ft	M_{yy} ft-k/ft	(3) S_{yy} k/ft	(4) M_{yy} ft-k/ft	(3) S_{yy} k/ft	(4) M_{yy} ft-k/ft	S_{yy} k/ft	M_{yy} ft-k/ft	S_{yy} k/ft	M_{yy} ft-k/ft
166	(2)	(2)	-	1496	-	3891	-380	-8	15	12.5
175	(2)	(2)	-	1333	-	3411	-303	-10	-4	12.9
184	(2)	(2)	-	1183	-	3039	-252	-13	-19	12.1
185	(2)	(2)	-	935	-	2391	-180	-12	-27	7.6
186	(2)	(2)	-	715	-	1705	-127	-9	-31	4.9
187	(2)	(2)	-	532	-	1256	-98	-7	-30	3.0
188	(2)	(2)	-	472	-	1119	-92	-7	-35	2.5
189	(2)	(2)	-	468	-	1111	-86	-7	-41	1.4
190	(2)	(2)	-	468	-	1115	-80	-5	-49	1.2
191	(2)	(2)	-	469	-	1118	-76	-5	-55	1.1

S_{yy} is the meridional force.

M_{yy} is the meridional moment.

(1) Refer to figure 22, sheet 5, for element locations.
(2) The test temperature effects are conservatively assumed to equal the operating temperature effects.
(3) Thermal gradients produce bending moment/curvature only.
(4) These moments are elastically calculated. The final thermal moments are determined using the cracked section capabilities of OPTCON as discussed in section 5.1.1.

TABLE 8

REPRESENTATIVE FINITE ELEMENT ANALYSIS RESULTS FOR THE THICKENED SHELL AT THE EQUIPMENT HATCH (Sheet 3 of 3)

	Full Model		Full Model		Full Model		Full Model		Half Model	
	OBE (Z)		SSE (X)		SSE (Y)		SSE (Z)		P_v	
Element Number(1)	S_{yy} (k/ft)	M_{yy} (ft-k /ft)	S_{yy} (k/ft)	M_{yy} (ft-k /ft)	S_{yy} (k/ft)	M_{yy} (ft-k /ft)	S_{yy} (k/ft)	M_{yy} (ft-k /ft)	S_{yy} (k/ft)	M_{yy} (ft-k /ft)
166	111	5.0	-554	-9.0	22.8	18.2	166	7.5	(2)	(2)
175	90	5.1	-441	-12.4	-5.7	18.8	134	7.6	(2)	(2)
184	76	5.8	-367	-17.4	-26.8	17.7	113	8.6	(2)	(2)
185	55	4.4	-262	-15.8	-39.4	11.2	82	6.6	(2)	(2)
186	40	3.2	-186	-12.7	-45.0	7.2	59	4.8	(2)	(2)
187	31	2.4	-143	-9.0	-44.3	4.4	47	3.5	(2)	(2)
188	30	2.3	-135	-9.7	-51.1	3.7	45	3.4	(2)	(2)
189	29	2.0	-125	-9.4	-60.1	2.1	43	3.0	(2)	(2)
190	29	1.6	-117	-8.0	-71.3	1.7	43	2.3	(2)	(2)
191	29	1.2	-111	-7.4	-79.7	1.5	43	1.8	(2)	(2)

S_{yy} is the meridional force.

M_{yy} is the meridional moment.

(1) Refer to figure 22, sheet 5, for element locations.
(2) The results of pressure variation (P_v) are equal to the accident pressure results times a scale factor of 0.058.

TABLE 9

POST-TENSIONING SYSTEM ANALYSIS RESULTS

Tendon Stresses:

Jacking stress = 0.80 F_{ult} (refer to section 3.4.7 for F_{ult})
= 216 ksi

Anchorage stress(1) = 0.70 F_{ult}
= 189 ksi

Prestress Losses:

Concrete elastic shortening	=	5.7 ksi
Concrete creep and shrinkage	=	14.0 ksi(2)
Strand relaxation	=	7.6 ksi(3)
Total losses	=	27 ksi (excluding friction losses)

Effective Prestress (accounting for friction losses):

Refer to figures 23 and 24.

Tendon stress under LOCA conditions:

The cylinder hoop tendons are subjected to the largest stress increase due to the pressurization effect.

ΔF = 6.4 ksi (cylinder hoop tendons)

(1) After slip losses (refer to section 4.4.2).

(2) Based upon a total strain (creep plus shrinkage) of 500 by 10^{-6} in./in. at the end-of-plant life.

(3) Based upon a 4 percent, low relaxation tendon.

TABLE 10

POLAR CRANE BRACKET ANALYSIS RESULTS

GOVERNING LOAD COMBINATION EQUATION 2: (D + L + OBE)

Load Direction	Applied Loads: Horizontal Load(1) (Perpendicular to Runway Girder)	Horizontal Load(2) (Parallel to Runway Girder)	Vertical Load(3) Per Wheel
Point of Application	Centerline of Runway Girder Top Flange	Top of Runway Rail	Top of Runway Rail
Load Magnitude	208 kips	203 kips	222 kips

(1) There are two lateral stops (seismic restraints) per polar crane end.
(2) Applied by the drive/brake wheels (two per polar crane end).
(3) Eight wheels per polar crane end.

ANALYSIS RESULTS:

FORCES SHOWN OCCUR AT THE BRACKET/WALL INTERFACE.

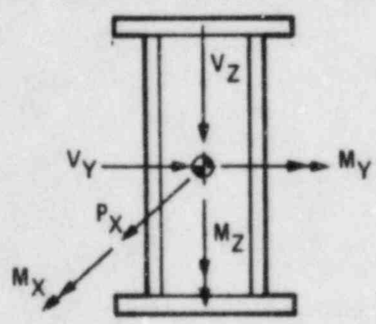

POLAR CRANE BRACKET CROSS-SECTION AT WALL INTERFACE

Polar Crane Position(6)	Resultant Design Forces(4): P_x(5)	V_y (k)	V_z (k)	M_x (in.-k)	M_y (in.-k)	M_z (in.-k)
A	0	241	556	5,800	21,100	9,200
B	0	241	427	8,000	16,200	9,200

(4) Construction tolerances are accounted for in the determination of the resultant forces.
(5) Brace loads are not shown since they decrease the bracket stresses.
(6) A and B represent two polar crane positions which maximize the bracket forces.

TABLE 11

CRITICAL ELEMENTS FOR SHELL REINFORCEMENT DESIGN (Sheet 1 of 4)

VERTICAL(2) REINFORCEMENT
Preliminary design without thermal effects.
PRESTRESS LOADS AT END-OF-LIFETIME

		Outside Face Reinforcement				Inside Face Reinforcement			
Key Location(1)	Element Group Number	Governing Load Comb. Equation(4)	Critical Element Number	A_s Rq'd	A_s Provided	Governing Load Comb. Equation(4)	Critical Element Number	A'_s Rq'd	A'_s Provided
1	30	7	2	.563(3)	1.27	7	2	.480(3)	0.79
2	26	7	3	.563(3)	3.87	7	3	.480(3)	1.00
3	18	8	58	.563(3)	3.87	8	58	.480(3)	2.25
4	17	8	21	.563(3)	3.86	8	21	.529(3)	3.99
5	16	8	22	.563(3)	3.86	8	22	1.279	3.99
6	8	8	17	.563(3)	3.86	8	17	.529(3)	3.99
7	2	8	45	.563(3)	3.86	8	45	2.029	3.99
8	1	8	136	.635	3.86	8	136	2.814	7.98
9	1	5	55	2.243	3.86	8	10	5.118	7.98

(1) Refer to figure 17 for key location.
(2) Corresponds to radial or cap reinforcement in the dome.
(3) Governed by minimum code reinforcement requirements.
(4) Refer to table 5 for load combination equations.

TABLE 11

CRITICAL ELEMENTS FOR SHELL REINFORCEMENT DESIGN (Sheet 2 of 4)

VERTICAL[2] REINFORCEMENT
Preliminary design without thermal effects.
PRESTRESS LOADS AT BEGINNING-OF-LIFETIME

		Outside Face Reinforcement				Inside Face Reinforcement			
Key Location[1]	Element Group Number	Governing Load Comb. Equation[4]	Critical Element Number	A_s Rq'd	A_s Provided	Governing Load Comb. Equation[4]	Critical Element Number	A'_s Rq'd	A'_s Provided
1	30	7	2	.563[3]	1.27	7	2	.480[3]	0.79
2	26	7	3	.563[3]	3.87	7	3	.480[3]	1.00
3	18	8	58	.563[3]	3.87	8	58	.480[3]	2.25
4	17	8	21	.563[3]	3.86	8	21	.529[3]	3.99
5	16	8	22	.563[3]	3.86	8	22	.779	3.99
6	8	8	17	.563[3]	3.86	8	17	.529[3]	3.99
7	2	8	45	.563[3]	3.86	8	45	2.029	3.99
8	1	8	136	.635	3.86	8	136	2.814	7.98
9	1	5	55	2.243	3.86	8	10	5.118	7.98

(1) Refer to figure 17 for key location.
(2) Corresponds to radial or cap reinforcement in the dome.
(3) Governed by minimum code reinforcement requirements.
(4) Refer to table 5 for load combination equations.

TABLE 11

CRITICAL ELEMENTS FOR SHELL REINFORCEMENT DESIGN (Sheet 3 of 4)

HORIZONTAL[4] (HOOP) REINFORCEMENT
Preliminary design without thermal effects.
PRESTRESS LOADS AT END-OF-LIFETIME

		Outside Face Reinforcement				Inside Face Reinforcement			
Key Location[1]	Element Group Number	Governing Load Comb. Equation[3]	Critical Element Number	A_s Rq'd	A_s Provided	Governing Load Comb. Equation[3]	Critical Element Number	A'_s Rq'd	A'_s Provided
1	30	7	8	.563[2]	1.27	2	8	.480[2]	0.79
2	26	7	8	.563[2]	1.78	7	8	.480[2]	2.17
3	18	7	34	.563[2]	2.10	7	34	1.730	3.02
4	17	7	34	.600[2]	3.69	7	34	1.491	3.69
5	16	7	34	.600[2]	3.69	7	34	1.491	3.69
6	8	7	27	.600[2]	3.69	7	27	.991	3.69
7	2	8	55	.600[2]	3.69	8	55	.491[2]	3.69
8	1	4	127	.672	3.69	4	127	.491[2]	3.69
9	1	4	56	2.780	3.69	4	63/65	2.171	3.69

(1) Refer to figure 17 for key location.
(2) Governed by minimum code reinforcement requirements.
(3) Refer to table 5 for load combination equations.
(4) Corresponds to cap reinforcement at the top of the dome.

TABLE 11

CRITICAL ELEMENTS FOR SHELL REINFORCEMENT DESIGN (Sheet 4 of 4)

HORIZONTAL[4] (HOOP) REINFORCEMENT
Preliminary design without thermal effects.
PRESTRESS LOADS AT BEGINNING-OF-LIFETIME

		Outside Face Reinforcement				Inside Face Reinforcement			
Key Location[1]	Element Group Number	Governing Load Comb. Equation[3]	Critical Element Number	A_s Rq'd	A_s Provided	Governing Load Comb. Equation[3]	Critical Element Number	A'_s Rq'd	A'_s Provided
1	30	2	6	.563[2]	1.27	2	6	.480[2]	0.79
2	26	7	8	.563[2]	1.78	7	8	.480[2]	2.17
3	18	7	34	.563[2]	2.10	7	34	.980	3.02
4	17	7	52	.600[2]	3.69	7	52	.491[2]	3.69
5	16	8	15	.600[2]	3.69	8	15	.491[2]	3.69
6	8	7	27	.600[2]	3.69	7	27	.491[2]	3.69
7	2	8	55	.600[2]	3.69	8	55	.491[2]	3.69
8	1	4	127	.672	3.69	4	127	.491[2]	3.69
9	1	4	56	2.780	3.69	4	30	2.171	3.69

(1) Refer to figure 17 for key location.
(2) Governed by minimum code reinforcement requirements.
(3) Refer to table 5 for load combination equations.
(4) Corresponds to cap reinforcement at the top of the dome.

TABLE 12

REPRESENTATIVE DESIGN RESULTS FOR THE THICKENED SHELL AT THE EQUIPMENT HATCH

Load Combination (See table 5)	Axial Force (1) (k/ft)	Without Thermal Effects		With Thermal Effects	
		Moment (2) (ft-k/ft)	Utilization Factor (3)	Moment (2) (ft-k/ft)	Utilization Factor (4)
1	-855	610	54.9	1541	77.2
3	-1362	161	23.0	1410	72.5
4	-1640	156	33.8	1376	80.5
5	-947	172	7.9	1408	37.7
6	-954	167	7.7	1408	37.5
7	-710	738	32.7	2130	67.4
8	-1163	639	29.1	2465	68.6
9	-1326	546	25.3	2530	71.6

A_s = 7.72 in.^{2} (outside face)

A_s' = 8.00 in.^{2} (inside face)

(1) Negative axial force indicates compression.
(2) Positive moment indicates compression on the inside face.
(3) With respect to ASME primary stress allowables.
(4) With respect to ASME primary plus secondary stress allowables.

The above table is applicable to the area adjacent to the opening for the key location shown in figure 22, sheet 5.

TABLE 13

POST-TENSIONING SYSTEM DESIGN RESULTS

1. Maximum concrete bursting stress in buttress

   Refer to reference 2, section 8, of this design report (BC-TOP-7, "Full Scale Buttress Test for Prestressed Nuclear Containment Structures").

2. Bearing stress at anchorage under hoop tendon anchor plate

   Actual stress = 3.6 ksi

   Allowable stress = 3.9 ksi

3. Bearing stress at anchorage under inverted U-shaped tendon anchorage

   Actual stress = 3.6 ksi

   Allowable stress = 5.8 ksi

TABLE 14

POLAR CRANE BRACKET DESIGN RESULTS

Stresses	Actual (ksi, UNO)	Allowable (ksi UNO)	Actual / Allowable
Top Flange			
Tension	1.0	22.8	.04
Bending, M_y	7.9	22.8	.35
Bending, M_z	14.8	28.5	.52
Combined stresses			.91 <1.0
Upper Anchor Plate			
Plate bending	16.2	28.5	.57
Plate shear	3.7	15.2	.24
Concrete bearing	1.2	2.5	.46
Concrete punching shear	101 psi	263 psi	.38
Lower Anchor Plate			
Plate bending	19.2	28.5	.67
Plate shear	3.4	15.2	.22
Concrete bearing	1.1	2.5	.42
Concrete punching shear	104 psi	263 psi	.40

Bracket material: ASME SA-516, Grade 70.
See figure 11 and figure 16, sheet 4, for location of the critical elements listed above.

Governing load combination: Equation 2 from Appendix B, Table B.3.

TABLE 15

FACTORS OF SAFETY FOR STRUCTURAL STABILITY

Load[1][3] Combination	Overturning Factor of Safety			Sliding Factor of Safety		Flotation Factor of Safety	
	Minimum Required	Calculated: Equivalent Static	Calculated: Energy Balance	Minimum Required	Calculated	Minimum Required	Calculated
D + H + E	1.5	1.7	(2)	1.5	1.9	-	-
D + H + E'	1.1	1.3	893	1.1	1.4	-	-
D + F'	-	-	-	-	-	1.1	5.9

(1) D = Dead weight of structure
H = Lateral earth pressure
E = OBE
E' = SSE
F' = Buoyant force under design basis flood

(2) The factor of safety for the SSE load case also satisfies the minimum required factor of safety for the OBE case.

(3) Lateral loads caused by design wind, tornado, and blast are less in magnitude than lateral loads caused by design OBE and SSE.

TABLE 16

SMALL PENETRATION ANALYSIS RESULTS (Sheet 1 of 2)

PENETRATION MODEL ANALYSIS RESULTS

Applied Load and Magnitude	Results for the Load Magnitude Given				Key Location (see figure 27)
	M_{xx} (ft-k/ft)	M_{yy} (ft-k/ft)	S_{xx} (k/ft)	S_{yy} (k/ft)	
Radial Force (1 kip)	±.149 ±.029	±.028 ±.150	±.067 ±.034	±.021 ±.019	1 2
Hoop Force (1 kip)	- ±.007	- ±.006	- ±.052	- ±.009	1 2
Longitudinal Force (1 kip)	- -	- -	±.009 -	±.053 -	1 2
Hoop Moment (1 ft-k/ft)	- ±.014	- ±.025	- ±.002	- ±.001	1 2
Longitudinal Moment (1 ft-k/ft)	±.024 -	±.014 -	±.003 -	- -	1 2

TABLE 16

SMALL PENETRATION ANALYSIS RESULTS (Sheet 2 of 2)

MAIN STEAM LINE PENETRATION ANALYSIS RESULTS

Load Combination (see Table B.1)	Type of Load	Applied Piping Loads			Resultant Forces and Moments			
		P_{max} (k)	V_{max} (k)	M_{max} (ft-k)	S_{xx} (k/ft)	S_{yy} (k/ft)	M_{xx} (ft-k/ft)	M_{yy} (ft-k/ft)
3 (S)	R_o	49	78	1523	8	3	44	46
4 (S)	R_o	201	252	4761	30	9	144	152
6 (F)	R_o	288	339	6352	41	12	195	205
8 (F)	R_o	277	321	6032	39	12	186	195
10 (F)	R_o	49	78	1523	8	3	44	46
11 (F)	R_a	61	98	1903	10	3	55	57
12 (F)	R_a	245	296	5549	35	11	169	178
15 (F)	R_a	135	120	2362	17	5	77	81
15 (F)	R_r	1459	0	0	98	27	217	219

(F) = Factored load combination
(S) = Service load combination

TABLE 17

SMALL PENETRATION DESIGN RESULTS (Sheet 1 of 2)

MERIDIONAL MEMBRANE FORCES AND BENDING MOMENTS

The results correspond to key location 2 shown in figure 27.
The forces and moments shown do not include any load, stress concentration, or scale factors.

Type of Load (see App. A)	Results Obtained From	Stress Concentration Factor	Scale Factor	Beginning-of-Lifetime (5)		End-of-Lifetime (6)		Remarks
				S_{yy} (k/ft)	M_{yy} (ft-k/ft)	S_{yy} (k/ft)	M_{yy} (ft-k/ft)	
D	(1)	1.41	NA	-104	0	-103	1	
L	(1)	1.41	NA	-2	0	-2	0	
L (soil)	(1)	1.41	NA	-1	-2	6	-2	
F	(1)	1.26	1.176(3)	-470	-43	-469(3)	-41	
P_t	(1)	1.26	NA	324	-8	323	-9	
P_a	(1)	1.26	NA	281	-7	280	-8	
E_o (X)	(1)	1.41	NA	75	-3	70	-2	
E_o (Y)	(1)	1.41	NA	86	1	89	-1	
E_o (Z)	(1)	1.41	NA	30	0	30	0	
E_{ss} (X)	(1)	1.41	NA	107	-5	101	-3	
E_{ss} (Y)	(1)	1.41	NA	123	1	128	-2	
E_{ss} (Z)	(1)	1.41	NA	45	0	45	0	
R_o	(2)	NA	NA	9	±152	9	±152	(7)
R_o/R_a	(2)	NA	NA	12	±205	12	±205	(8)
R_a	(2)	NA	NA	5	±81	5	±81	(9)
R_r	(2)	NA	NA	27	±219	27	±219	(9)
P_v	(1)	1.26	-0.058(4)	281	-7	280	-8	

(1) Containment shell analysis (see section 4.1).
(2) Penetration analysis (see section 6.3).
(3) This scale factor is used to account for the beginning-of-lifetime prestress forces as discussed in section 5.1.1.2.
(4) This scale factor is used on the P_a load results to obtain the P_v load results as discussed in section 4.1.2.
(5) Critical element number 17 in element group 7 (see figure 17).
(6) Critical element number 1 in element group 7 (see figure 17).
(7) Used with service load combinations 3 and 4 (Appendix B, Table B.1).
(8) Used with factored load combinations 6, 8, 10, 11, and 12 (Appendix B, Table B.1).
(9) Used with factored load combination 15 (Appendix B, Table B.1).

TABLE 17

SMALL PENETRATION DESIGN RESULTS (Sheet 2 of 2)

DESIGN RESULTS FOR MERIDIONAL REINFORCEMENT ADJACENT TO THE MAIN STEAM PENETRATION

Reinforcement Provided: A_s = 7.72 in.^{2}/ft A_s' = 7.98 in.^{2}/ft

Load Combination (Table E.1)	Without Thermal Effects			With Thermal Effects		
	S_{yy} (k/ft)	M_{yy} (ft-k/ft)	Utilization Factor	S_{yy} (k/ft)	M_{yy} (ft-k/ft)	Utilization Factor
1(1)	-437	-73	11	-437	357	9
2(1)	-845	-63	10	-845	374	5
3(1)	-857	-214	38	-857	526	21
4(1)	-1037	-213	47	-676	525	23
6(1)	-601	-220	17	-586	559	17
8(1)	-612	-220	17	-598	558	16
10(1)	-302	-281	22	-302	619	16
11(1)	-476	-328	26	-476	885	33
12(1)	-177	-284	22	-617	948	34
15(1)	-214	-377	30	-704	1031	37
1(2)	-331	-62	9	-331	347	10
2(2)	-739	-51	7	-739	386	8
3(2)	-750	-202	32	-750	538	23
4(2)	-933	-199	38	-568	535	25
6(2)	-501	-207	16	-477	563	19
8(2)	-511	-207	16	-488	565	19
10(2)	-197	-271	21	-197	525	10
11(2)	-371	-317	25	-371	789	28
12(2)	-57	-273	24	-514	891	32
15(2)	-92	-365	30	-616	992	37

S_{yy} is the meridional force. $+S_{yy}$ indicates membrane tension.
M_{yy} is the meridional moment. $+M_{yy}$ indicates tension on the outside face.

(1) The values shown are with beginning-of-lifetime prestress forces for critical element 17 in element group 7 (see figure 17).

(2) The values shown are with end-of-lifetime prestress forces for critical element 1 in element group 7 (see figure 17).

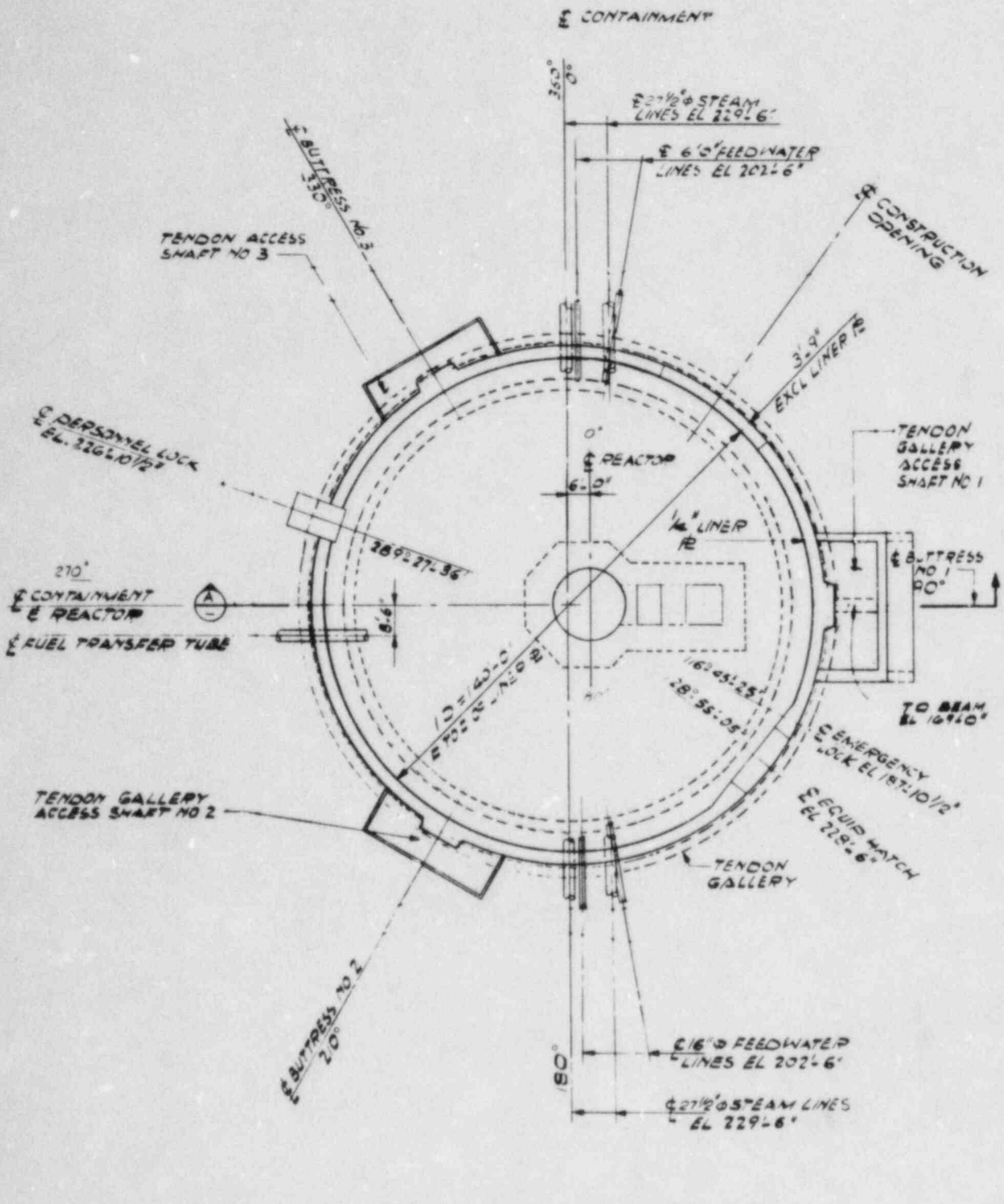

Figure 1
CONTAINMENT PLAN VIEW (UNIT 1)

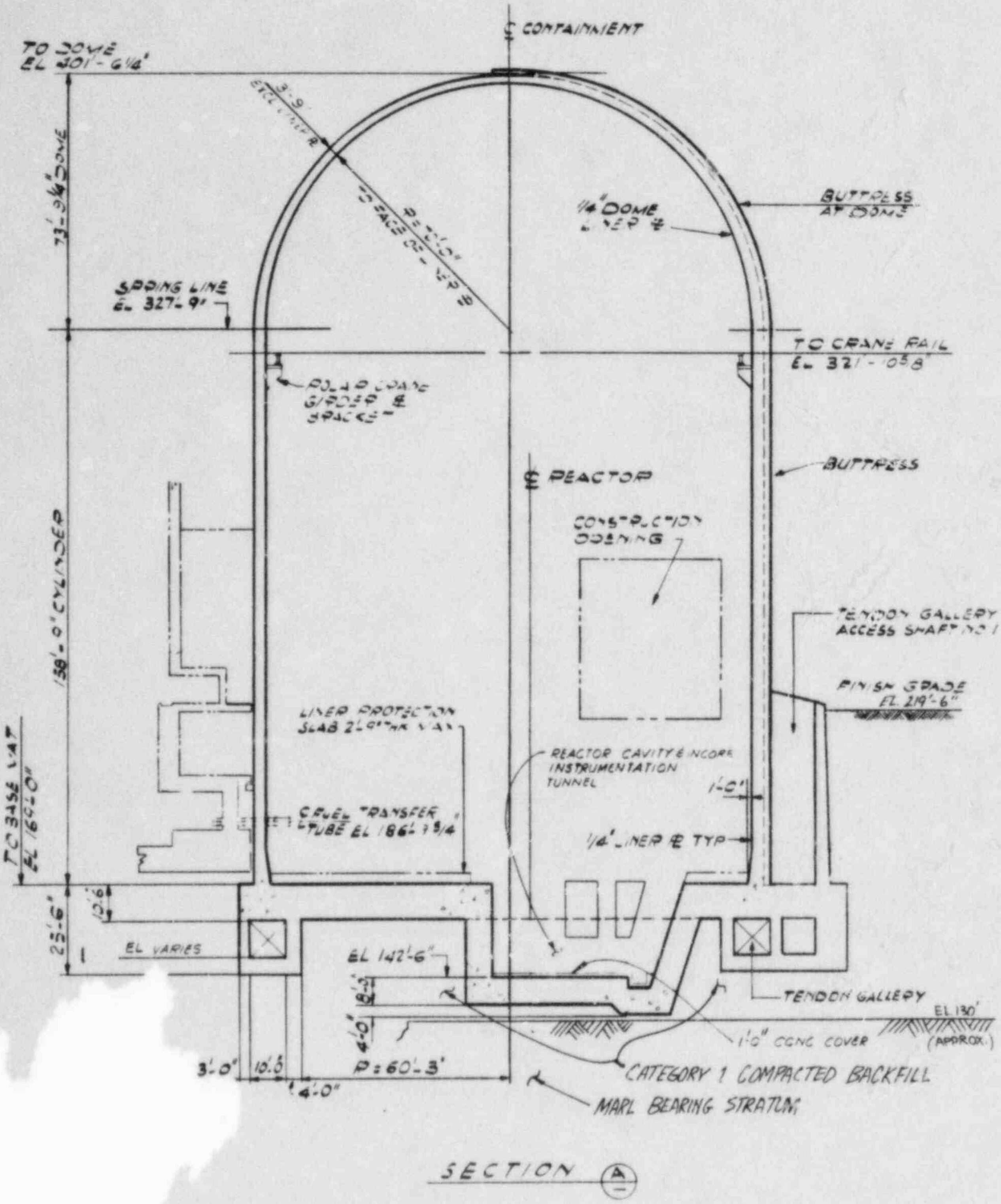

Figure 2
CONTAINMENT SECTION (UNIT 1)

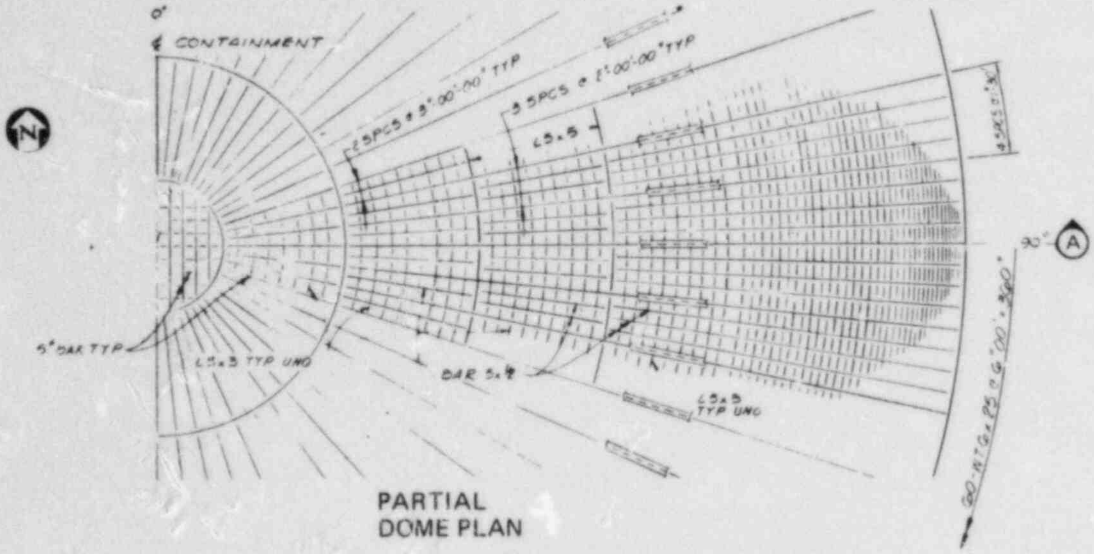

PARTIAL
DOME PLAN

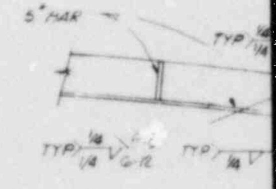

DET

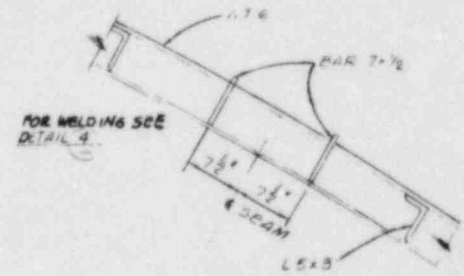

DETAIL 6
1½"=1'0"

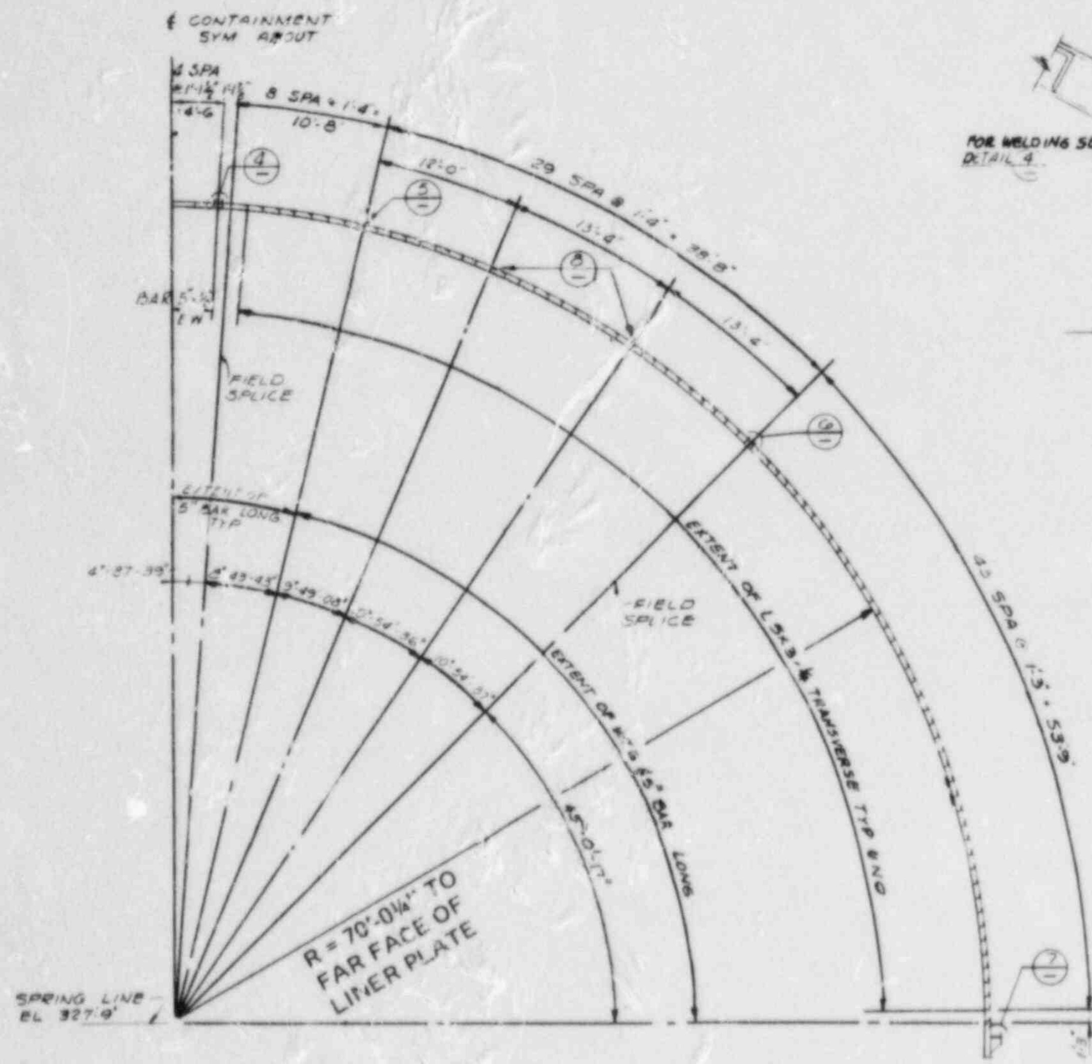

SECTION A

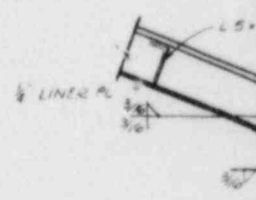

DETAIL
1½"=1'0"

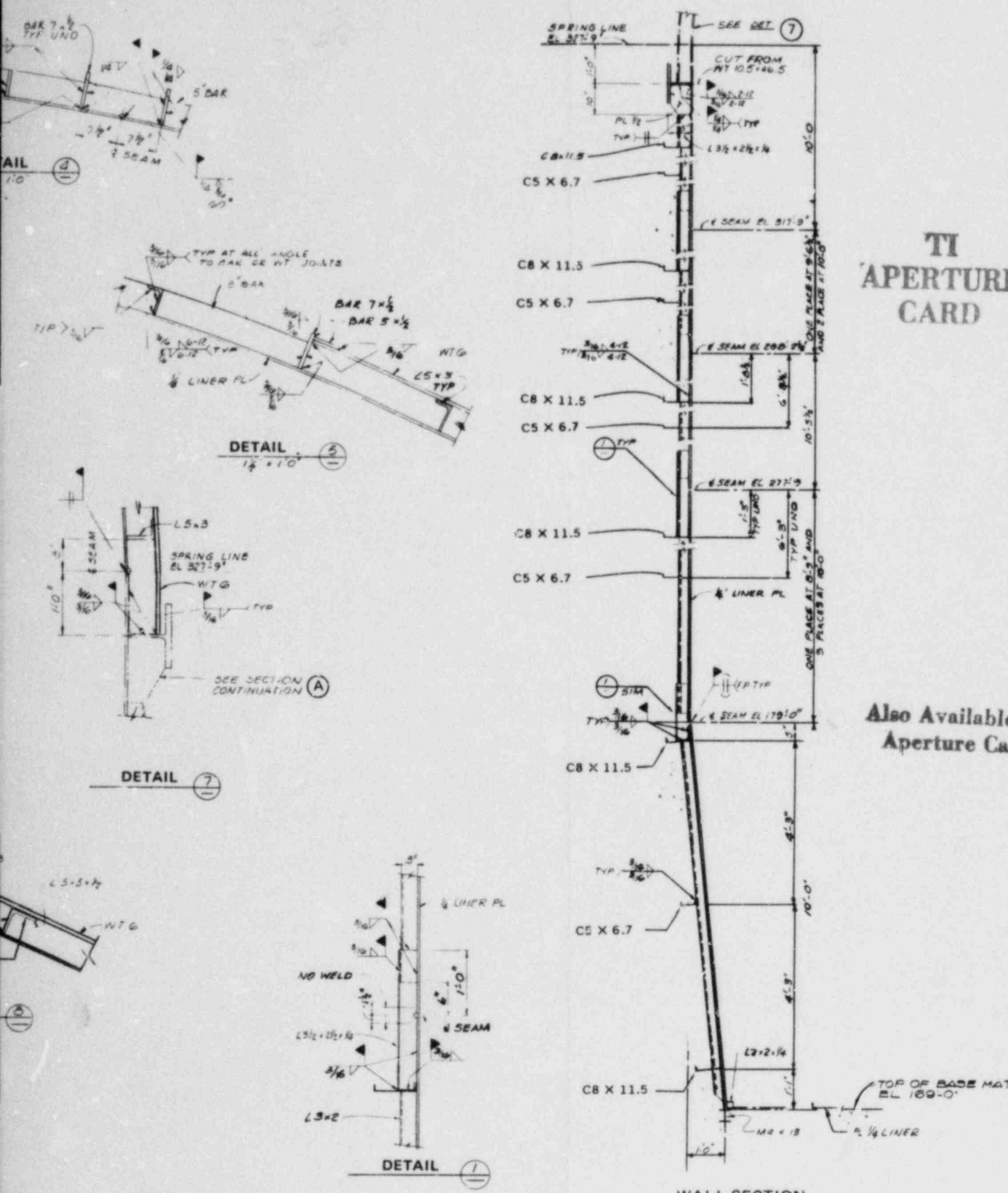

TI APERTURE CARD

Also Available On Aperture Card

Figure 3
CONTAINMENT LINER PLATE PLAN, SECTIONS, DETAILS (UNIT 1)

8411050161-01

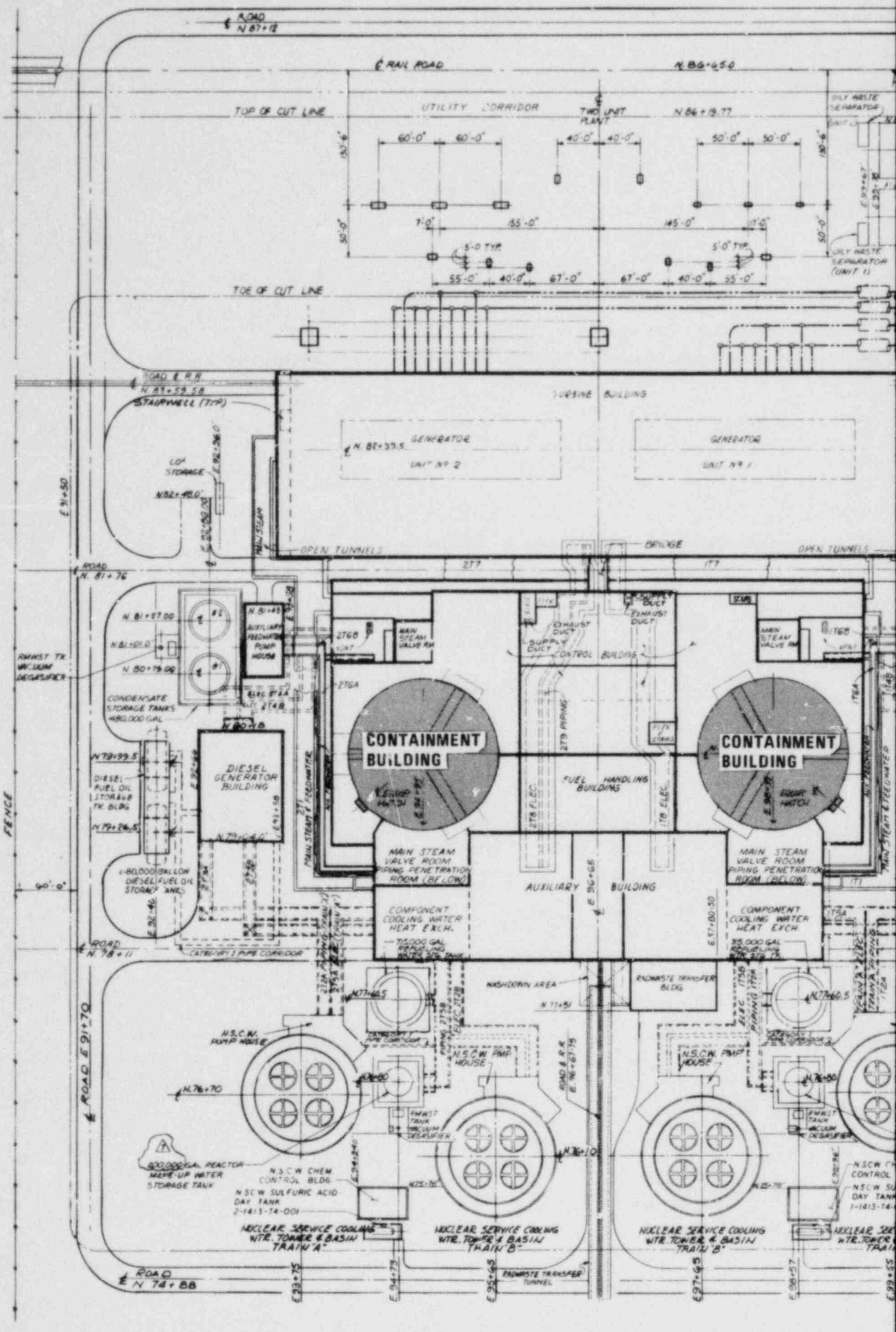

ROAD N 87+12
RAIL ROAD
N 86+65.0
TOP OF CUT LINE
UTILITY CORRIDOR
TWO UNIT PLANT
N 86+19.77
OILY WASTE SEPARATOR
TOE OF CUT LINE
ROAD & R.R. N 83+59.58
STAIRWELL (TYP)
TURBINE BUILDING
GENERATOR UNIT Nº 2
GENERATOR UNIT Nº 1
CO2 STORAGE
OPEN TUNNELS
BRIDGE
ROAD N. 81+76
RMWST TK VACUUM DEGASIFIER
CONDENSATE STORAGE TANKS 480,000 GAL
AUXILIARY FEEDWATER PUMP HOUSE
MAIN STEAM VALVE RM
CONTROL BUILDING
EXHAUST DUCT
SUPPLY DUCT
CONTAINMENT BUILDING
CONTAINMENT BUILDING
DIESEL GENERATOR BUILDING
DIESEL FUEL OIL STORAGE TK BLDG
FUEL HANDLING BUILDING
FENCE
MAIN STEAM VALVE ROOM PIPING PENETRATION ROOM (BELOW)
AUXILIARY BUILDING
COMPONENT COOLING WATER HEAT EXCH.
ROAD N 78+11
CATEGORY 1 PIPE CORRIDOR
WASHDOWN AREA
RADWASTE TRANSFER BLDG
N.S.C.W. PUMP HOUSE
N.S.C.W. PMP HOUSE
ROAD E 91+70
N 76+70
RMWST TANK VACUUM DEGASIFIER
500,000 GAL REACTOR MAKE-UP WATER STORAGE TANK
N.S.C.W. CHEM CONTROL BLDG
N.S.C.W. SULFURIC ACID DAY TANK 2-1413-T4-001
NUCLEAR SERVICE COOLING WTR. TOWER & BASIN TRAIN "A"
NUCLEAR SERVICE COOLING WTR. TOWER & BASIN TRAIN "B"
ROAD N 74+88
RADWASTE TRANSFER TUNNEL

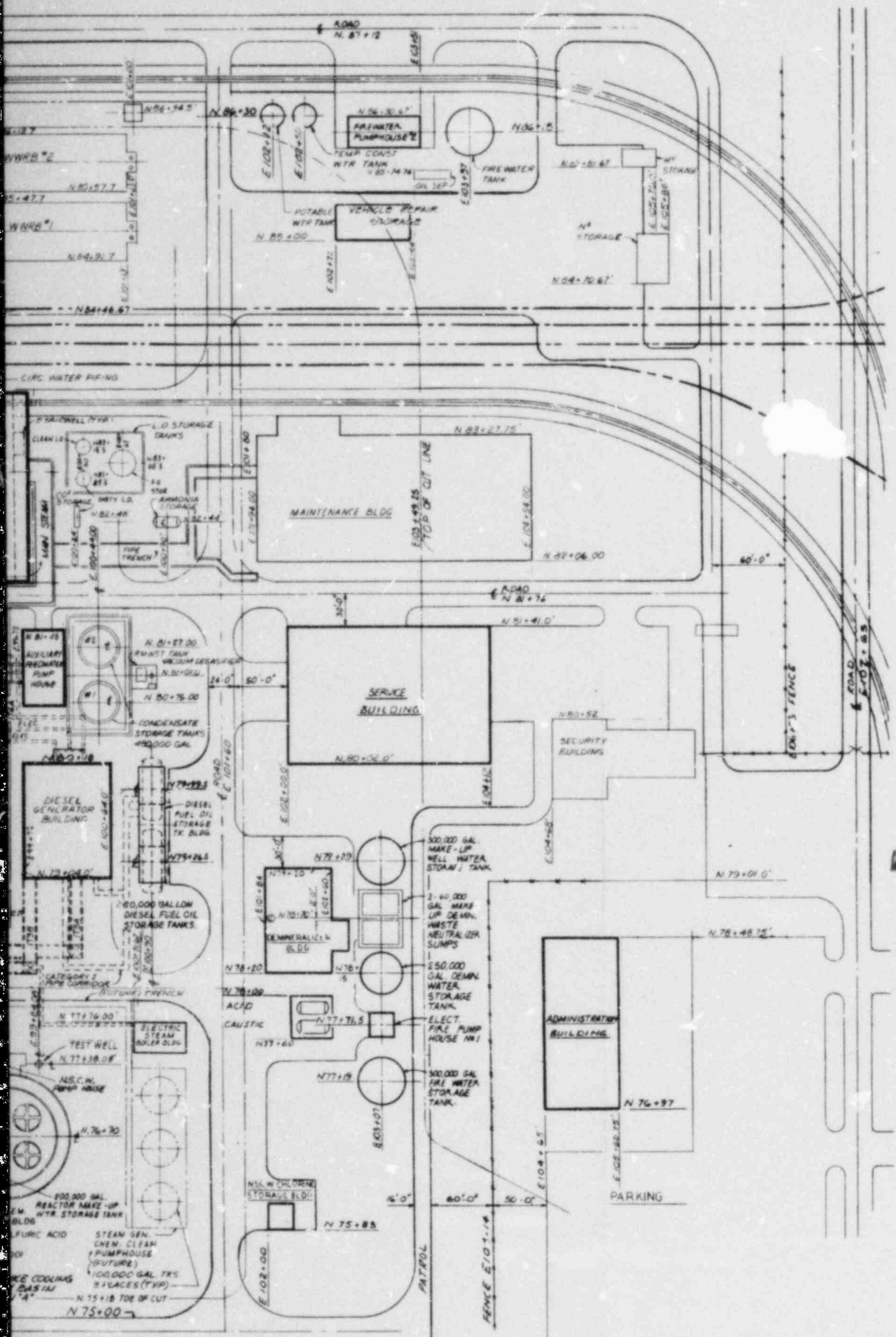

Figure 4
LOCATION OF CONTAINMENT BUILDING

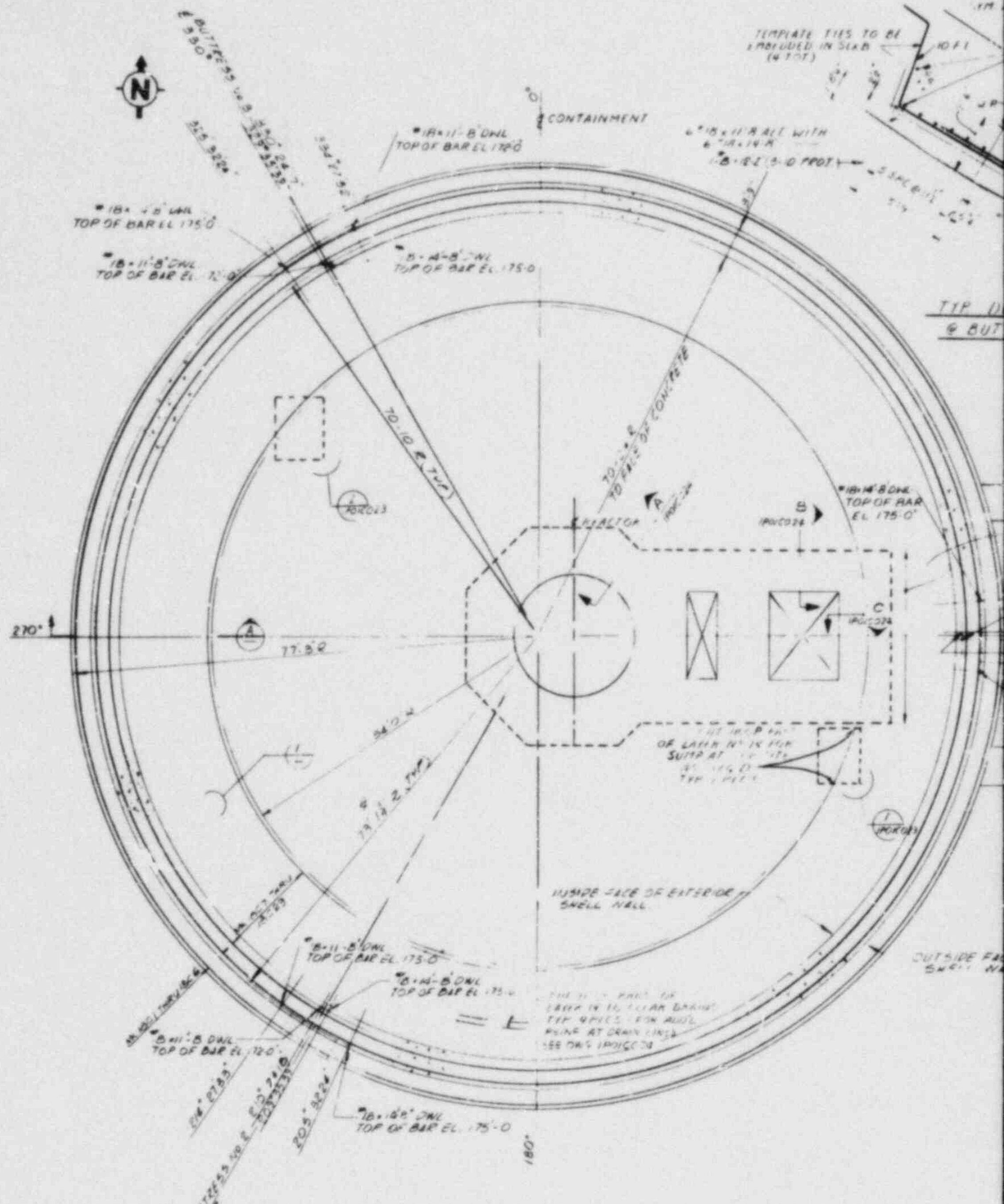

PLAN - BASE MAT HOOP REINF.

3/8" = 1'-0"

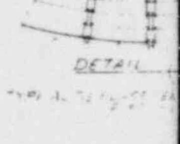

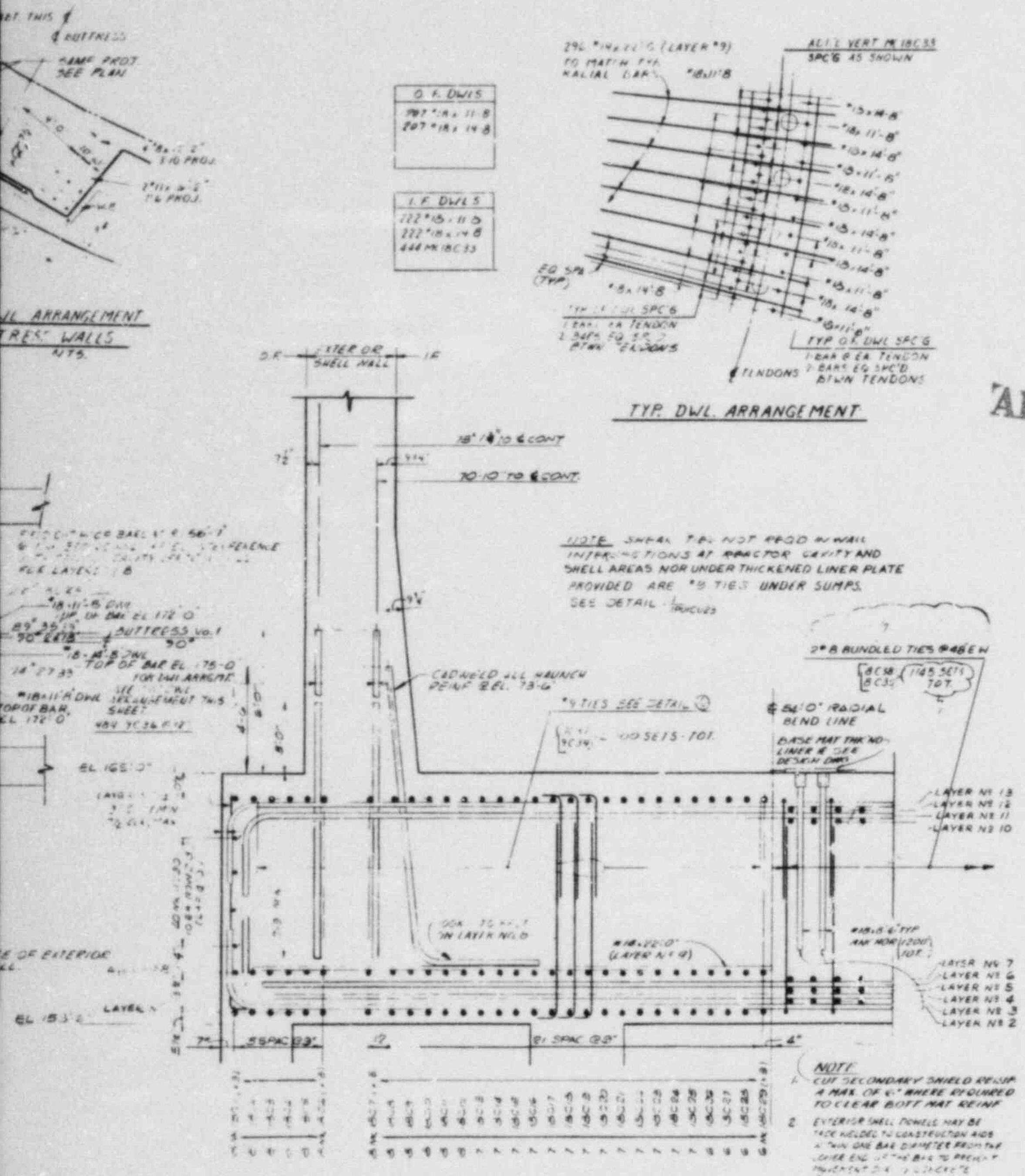

TI
APERTURE
CARD

Also Available On
Aperture Card

Figure 5
CONTAINMENT BASEMAT HOOP AND
DOWEL REINFORCEMENT (UNIT 1)

8411050161-03

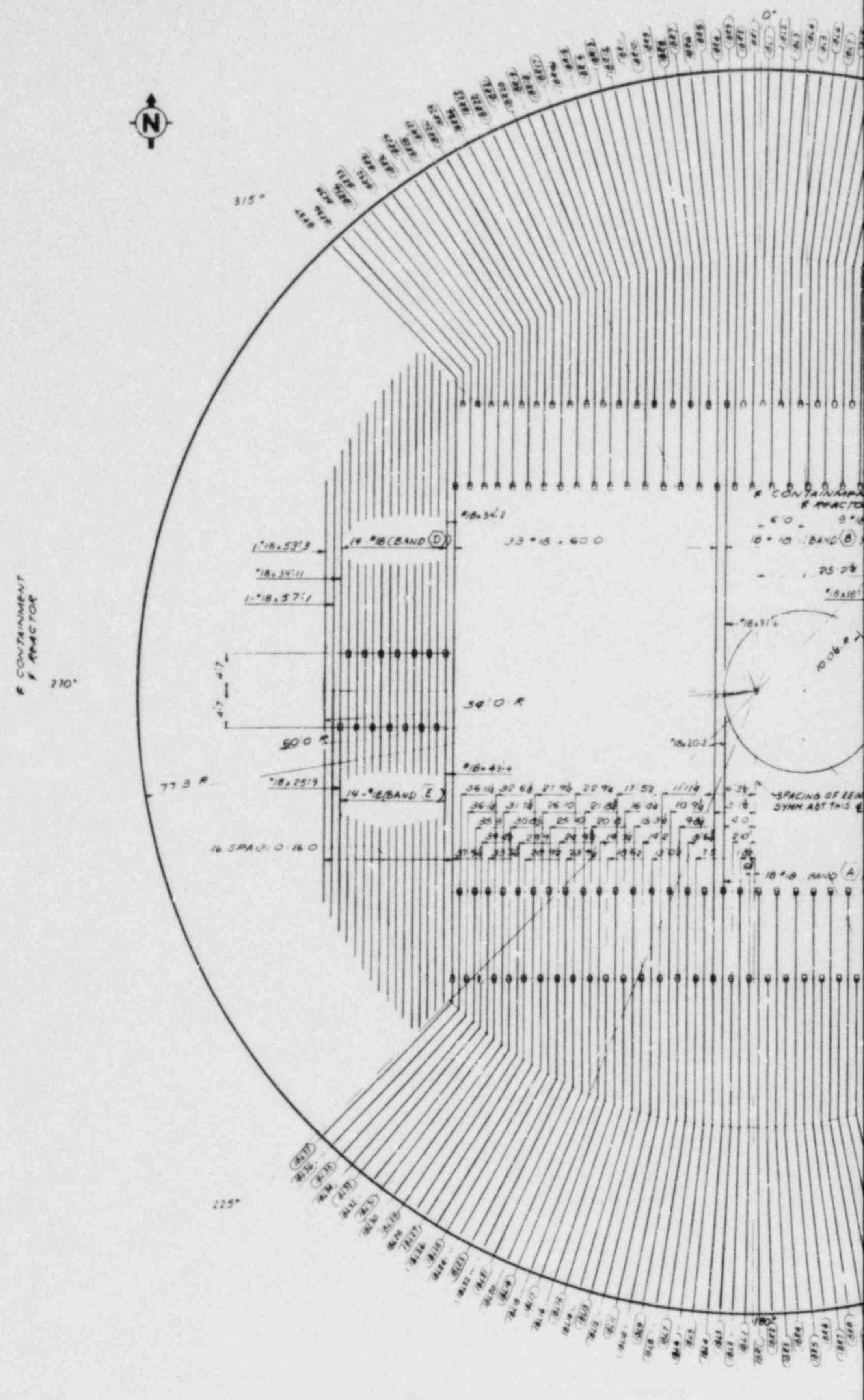

N
0°
315°
270°
225°
180°
CONTAINMENT
REACTOR
14-#18 (BAND D)
33 #18 + 60.0
34'0 R
50'0 R
77'3 R
14-#18 (BAND E)
BAND B
BAND A

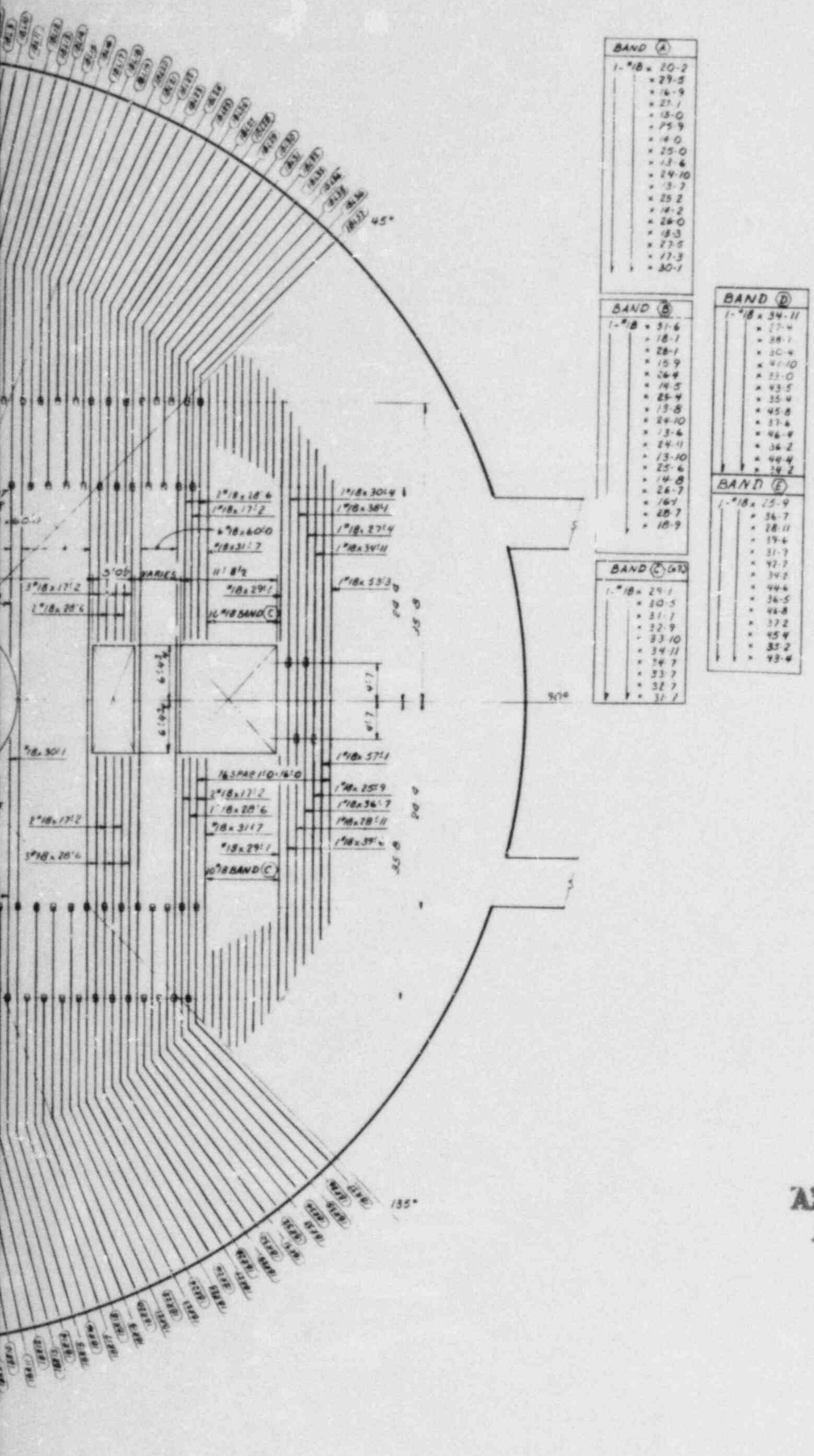

Figure 6
CONTAINMENT BASEMAT REINFORCEMENT
TYPICAL N-S LAYOUT (UNIT 1)
(Sheet 1 of 2)

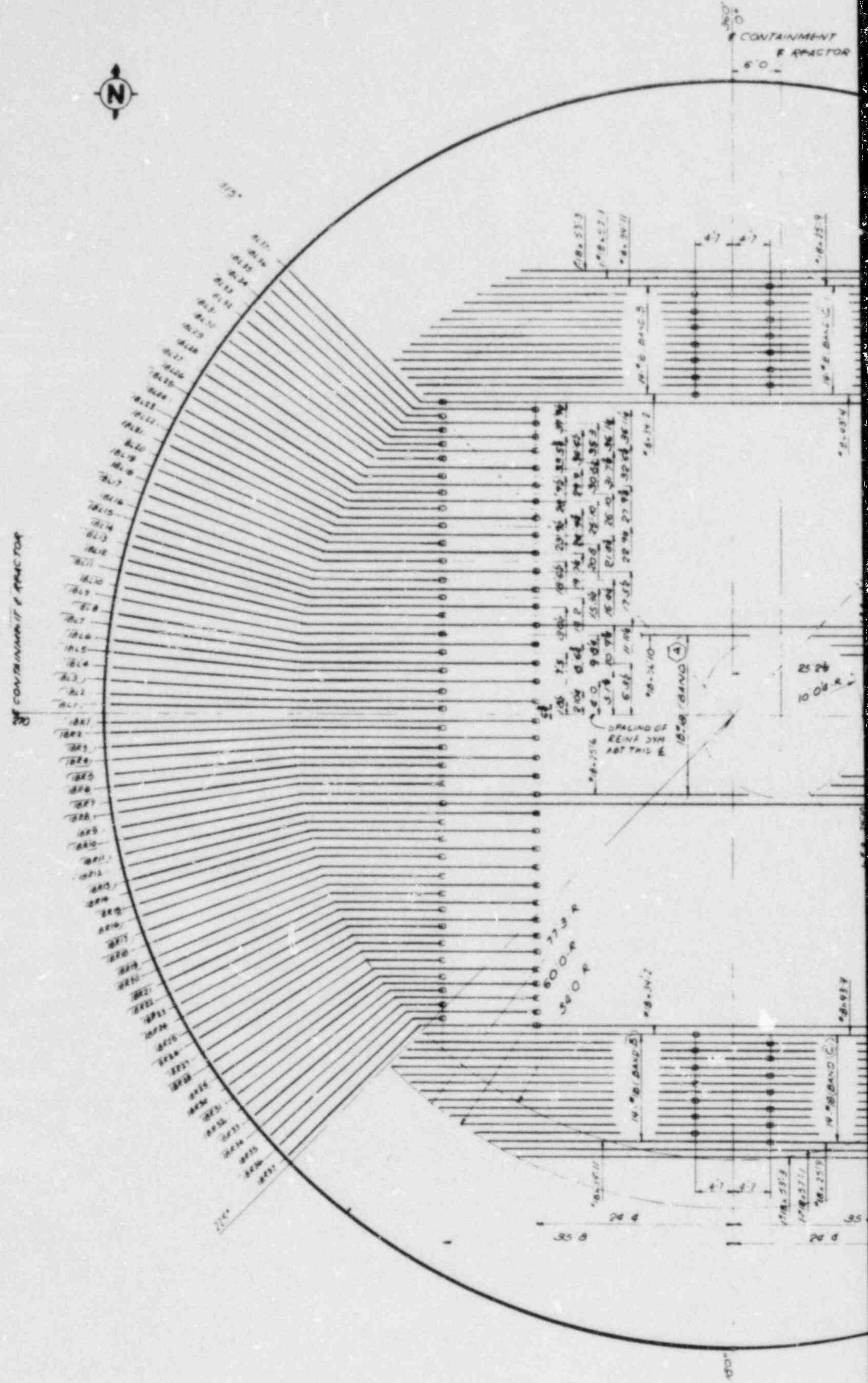

CONTAINMENT
REACTOR
N

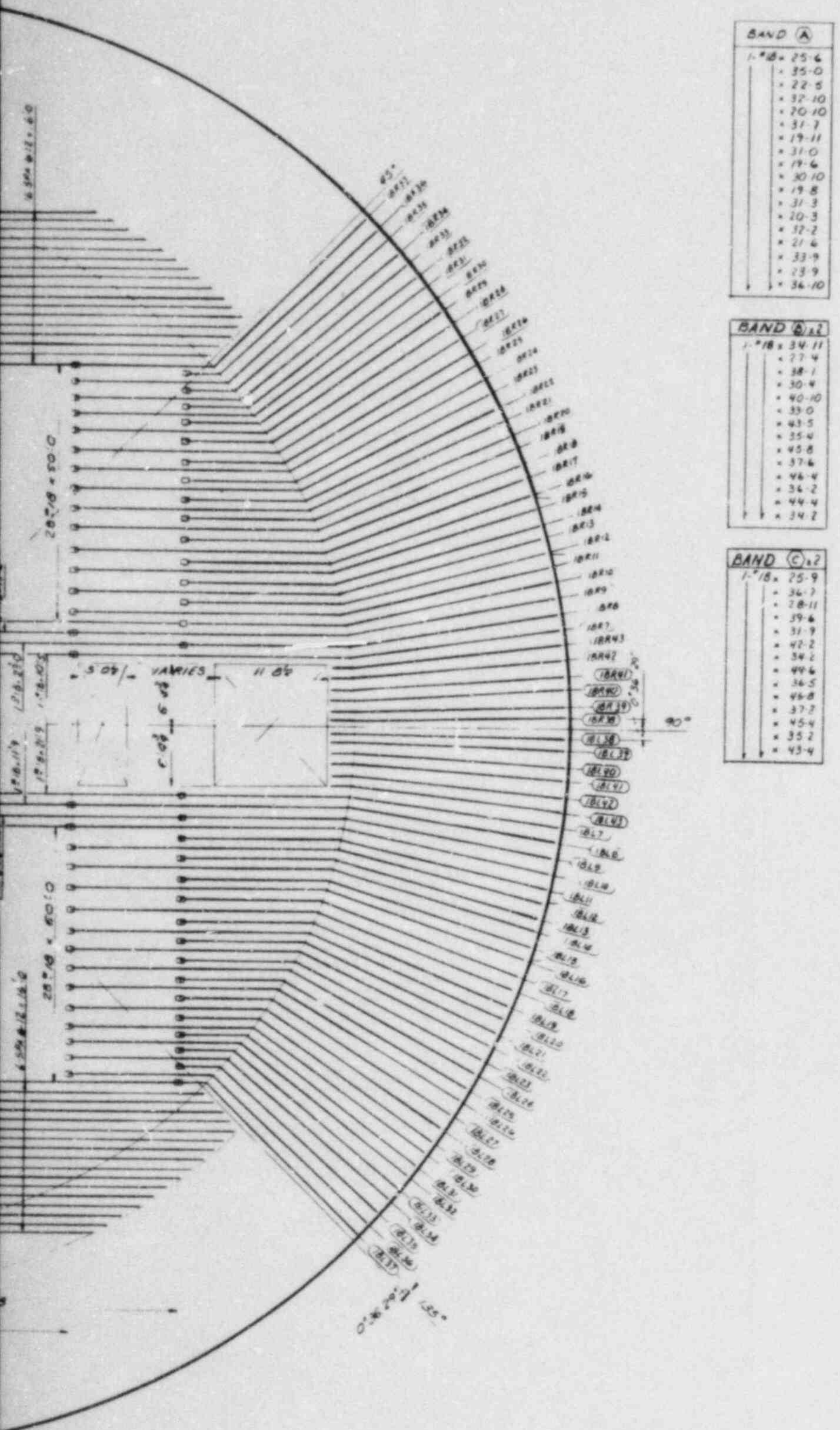

Also Available On
Aperture Card

Figure 6
CONTAINMENT BASEMAT REINFORCEMENT
TYPICAL E-W LAYOUT (UNIT 1)
(Sheet 2 of 2)

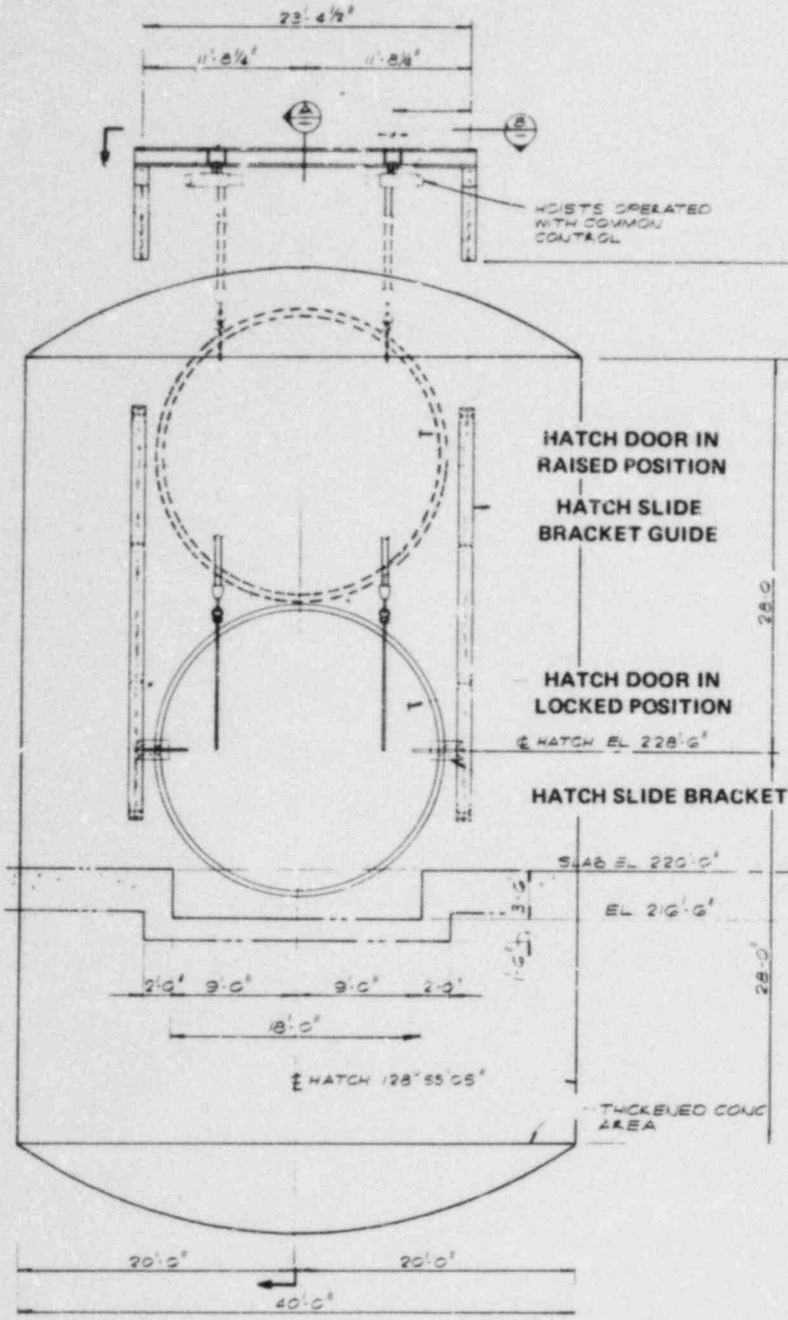

EQUIPMENT HA⸮⸮H INTERIOR ELEVATION

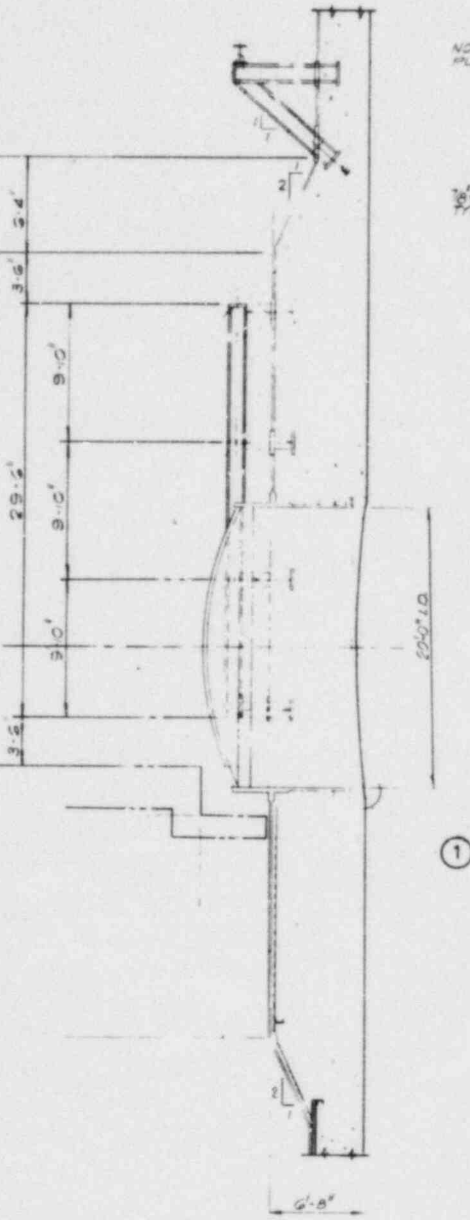

SECTION Ⓐ

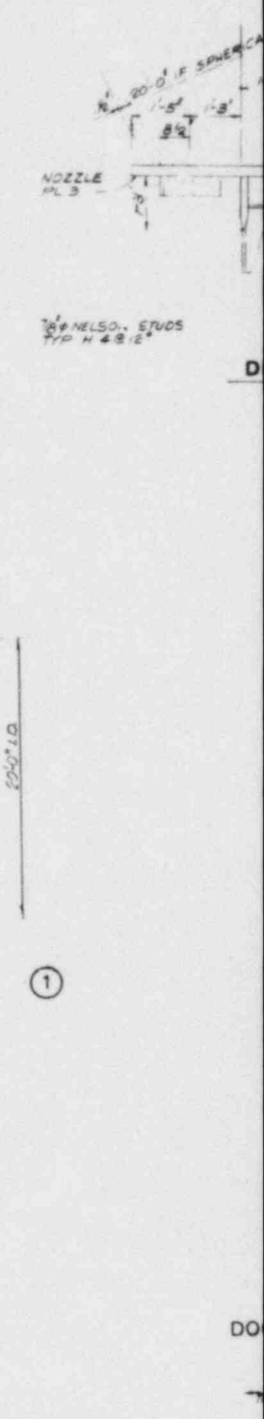

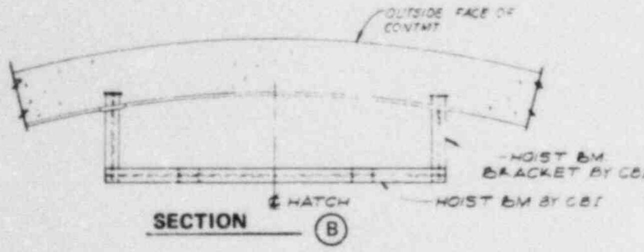

SECTION Ⓑ

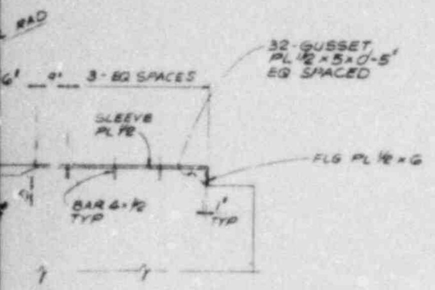

DETAIL ① (partial)

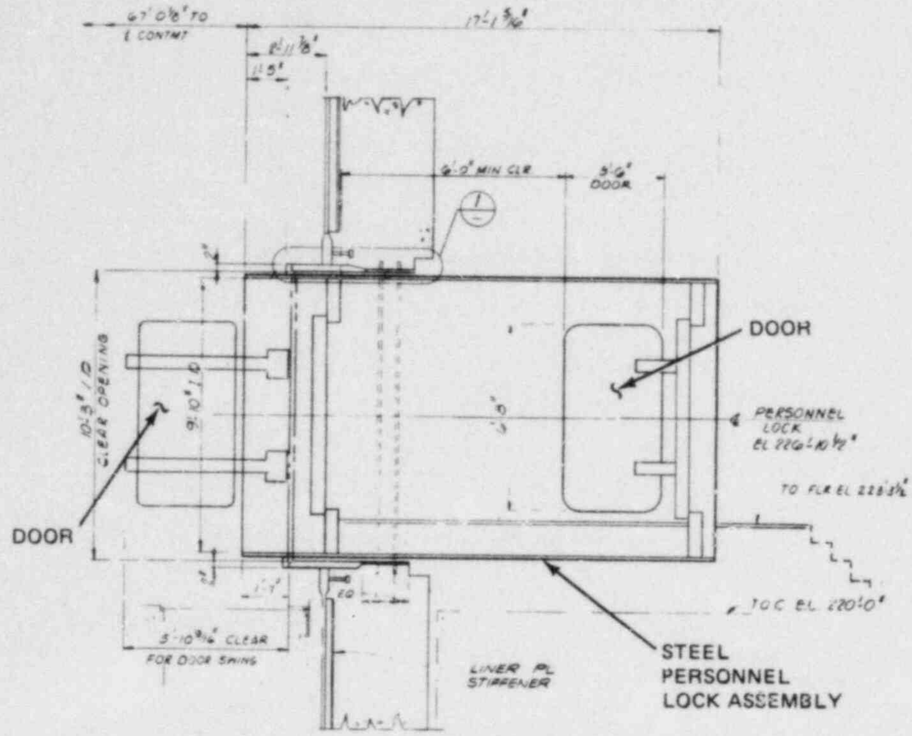

PERSONNEL LOCK VERTICAL SECTION

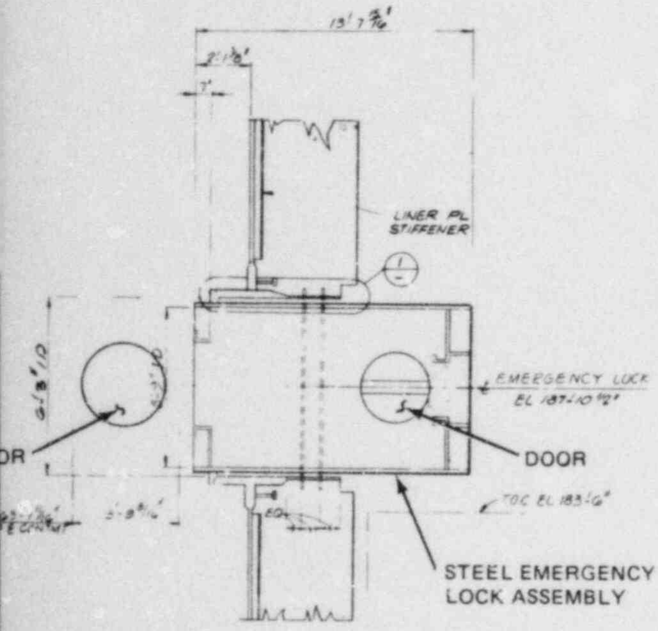

EMERGENCY LOCK VERTICAL SECTION

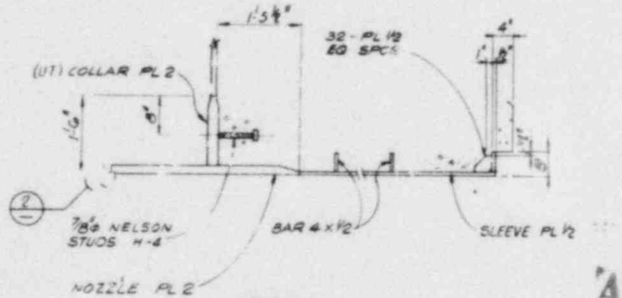

DETAIL ①

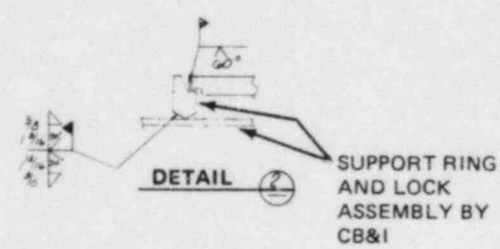

DETAIL ②

Figure 7
CONTAINMENT MAJOR OPENINGS
SECTIONS AND DETAILS

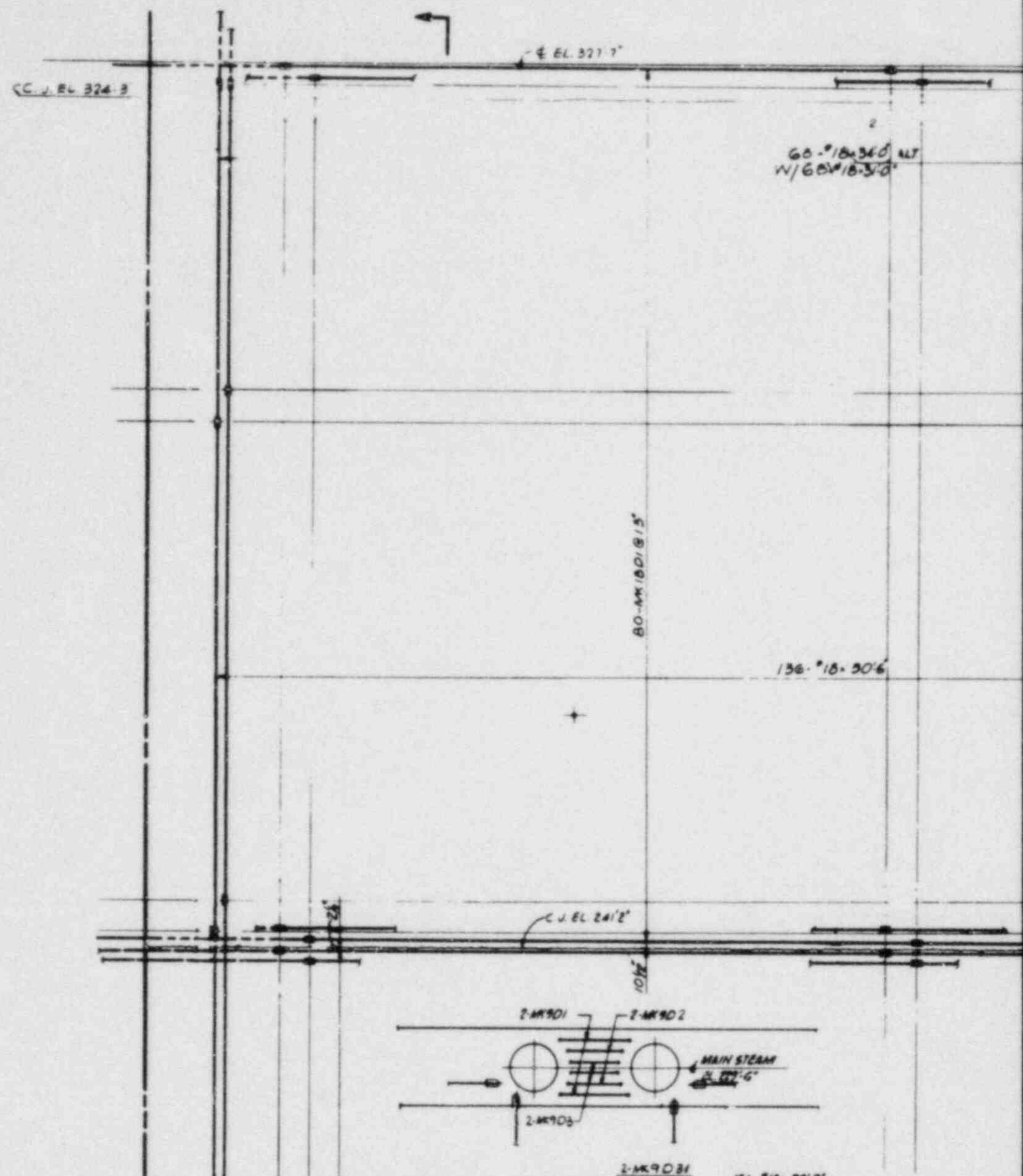

DEVELOPED WALL ELEVATION

OUTSIDE FACE VERT. & HORIZ. REINF.
℄ PLACING RADIUS 75'-1 3/8" FOR VERT BARS
℄ PLACING RADIUS 75'-4 1/2" FOR HORIZ. BARS

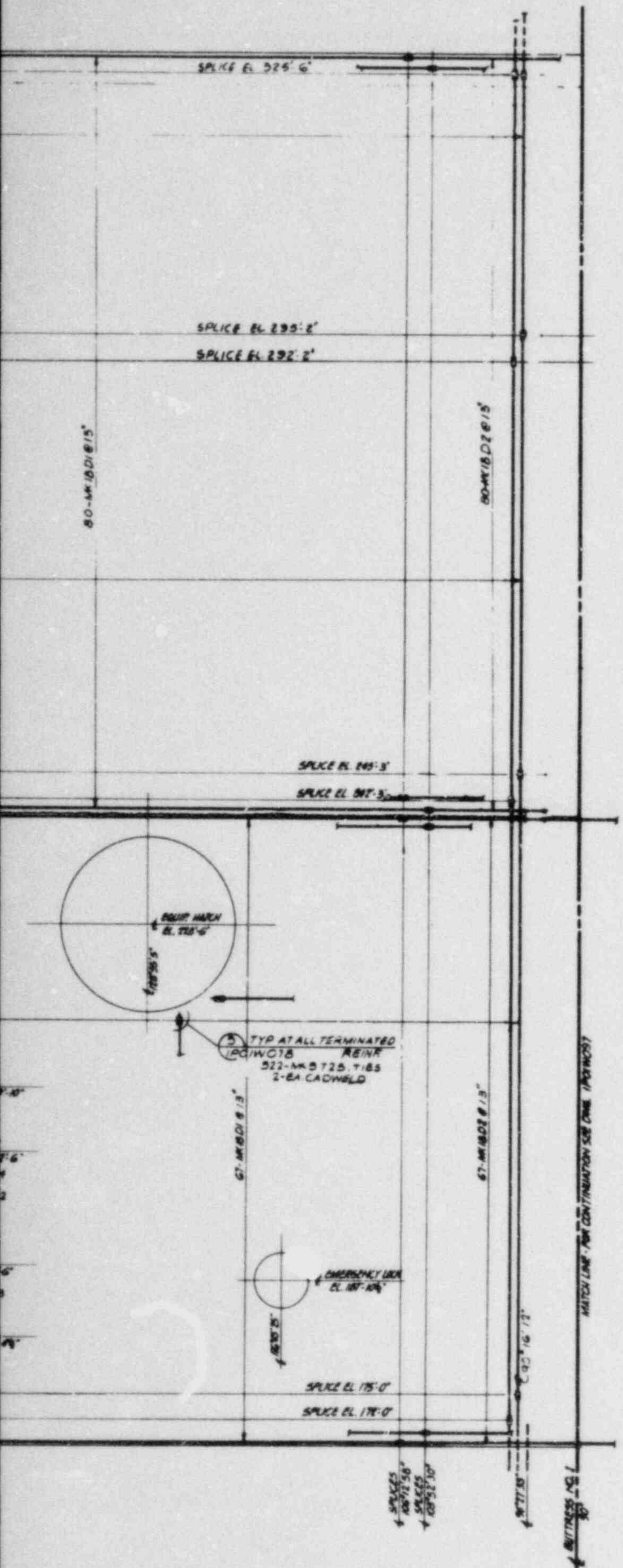

Figure 8
SHELL WALL REINFORCEMENT CONTAINMENT
BUILDING UNIT 1 OUTSIDE FACE VERTICAL
AND HORIZONTAL BUTTRESS 1 TO 2
(Sheet 1 of 5)

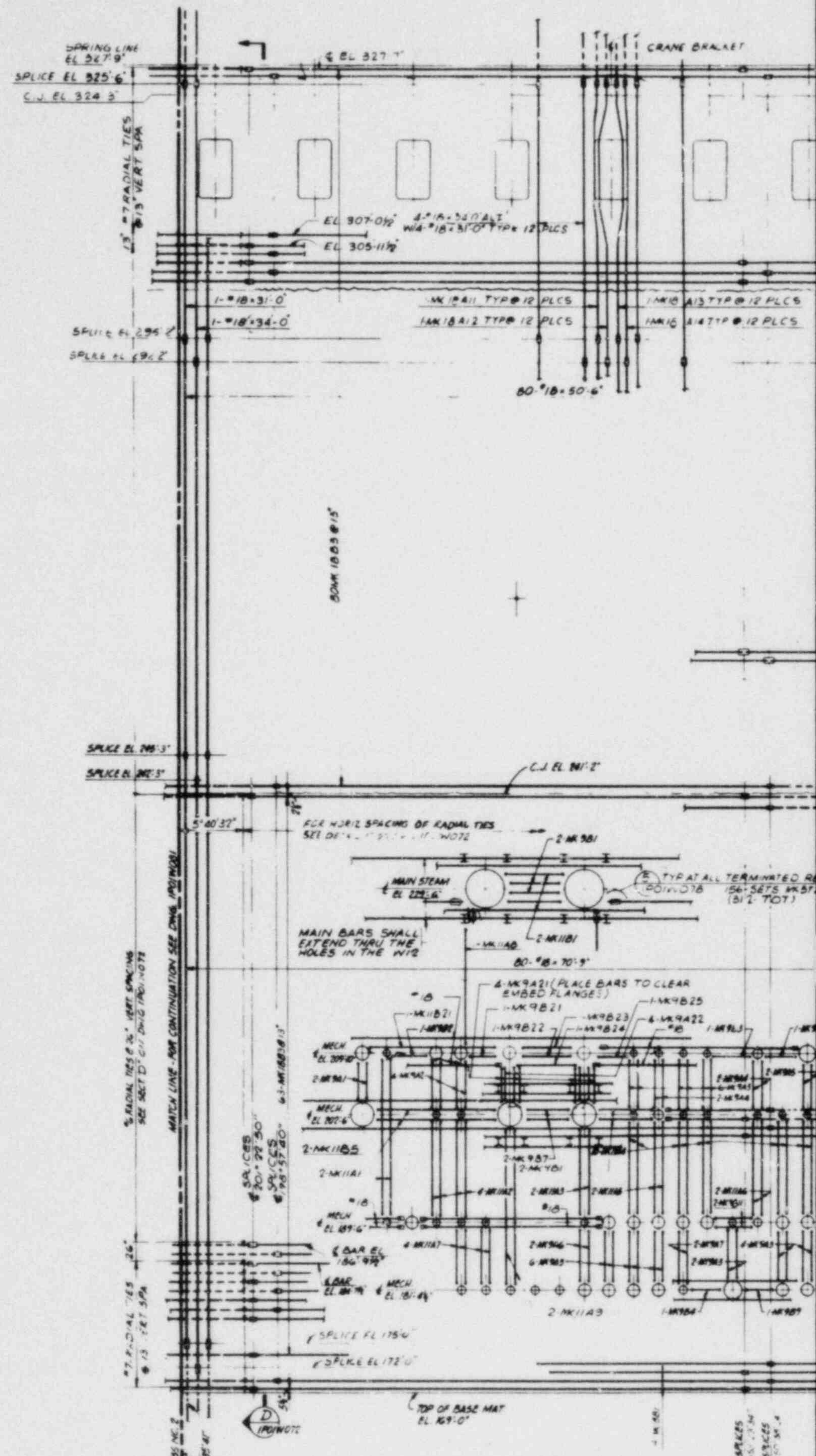

DEVELOPED WALL

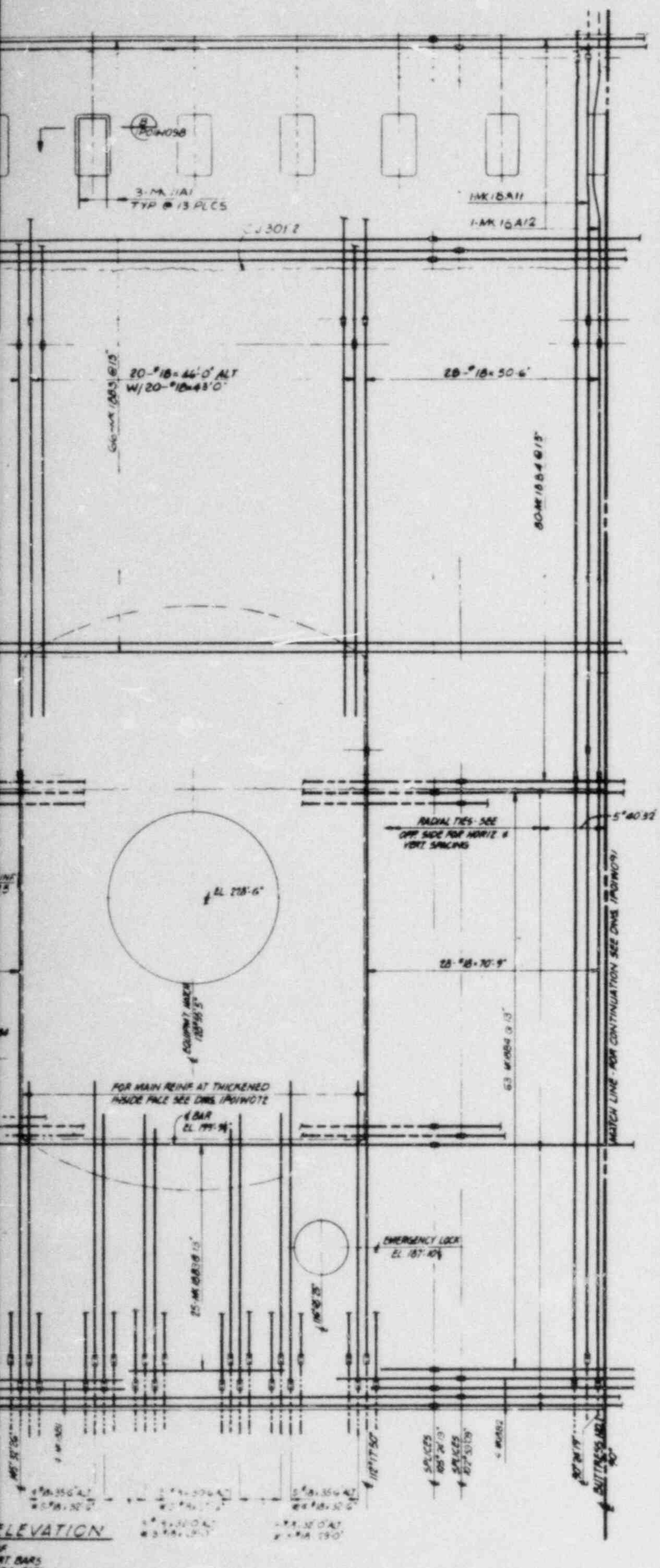

Figure 8
SHELL WALL REINFORCEMENT CONTAINMENT BUILDING UNIT 1 INSIDE FACE VERTICAL AND HORIZONTAL BUTTRESS 1 TO 2
(Sheet 2 of 5)

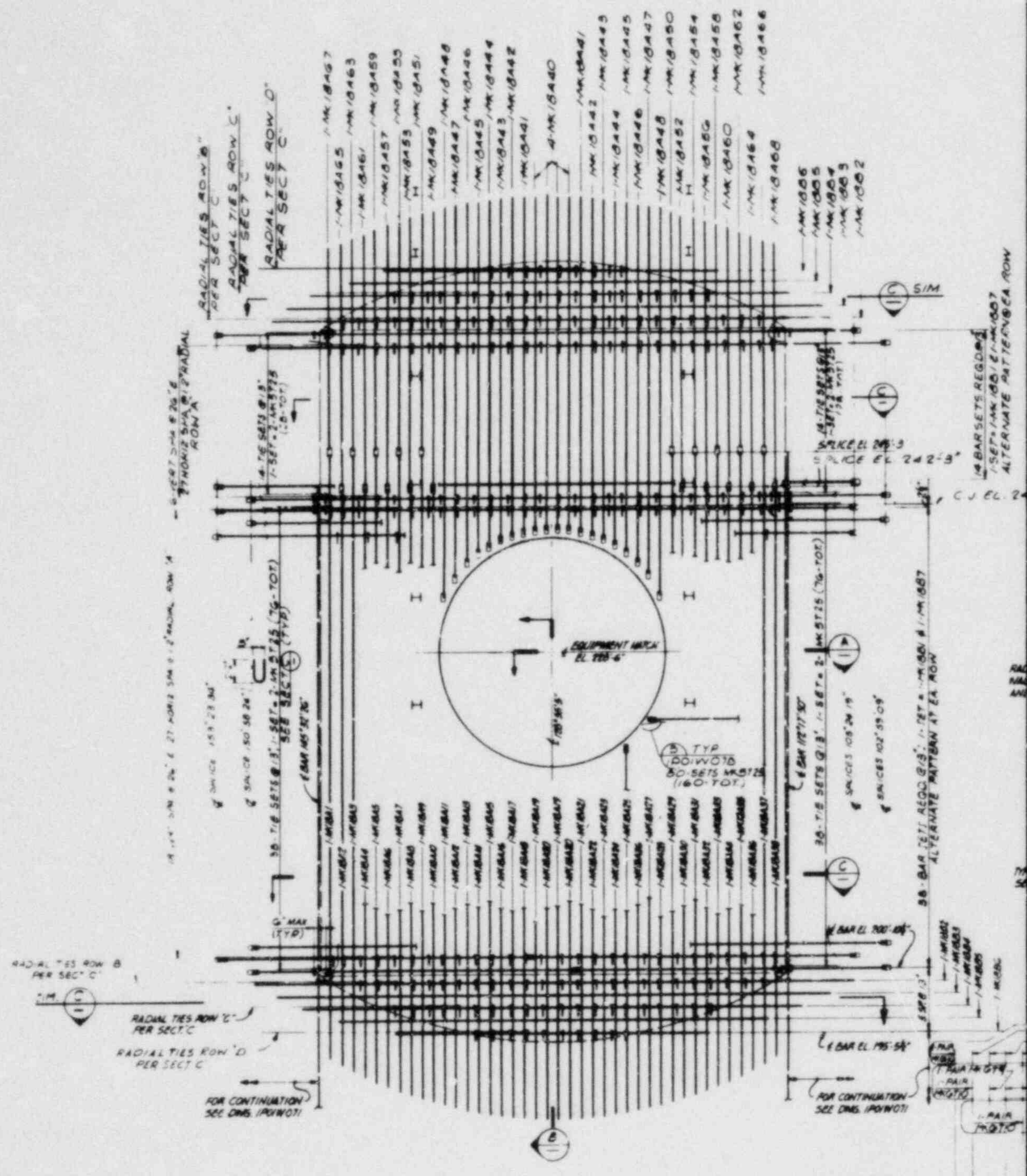

DEVELOPED ELEVATION AT EQUIPMENT HATCH

HORIZ AND VERT MAIN REINF. INSIDE FACE OF THICKENED WALL

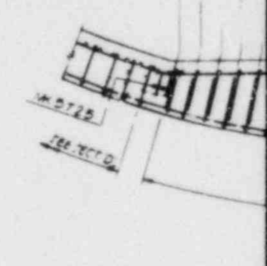

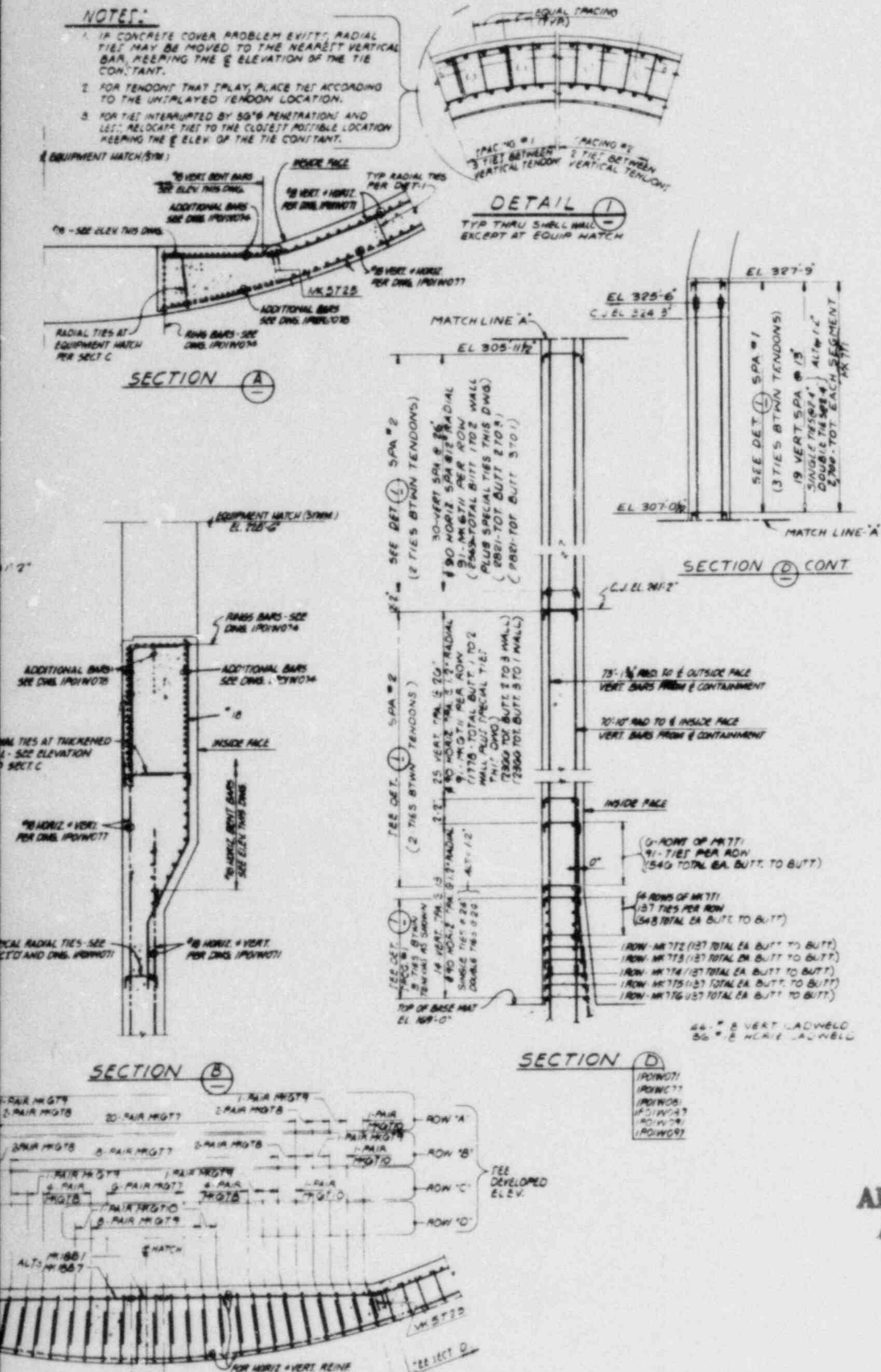

Figure 8
SHELL WALL REINFORCEMENT CONTAINMENT BUILDING UNIT 1 INSIDE FACE VERTICAL AND HORIZONTAL AT EQUIPMENT HATCH
(Sheet 3 of 5)

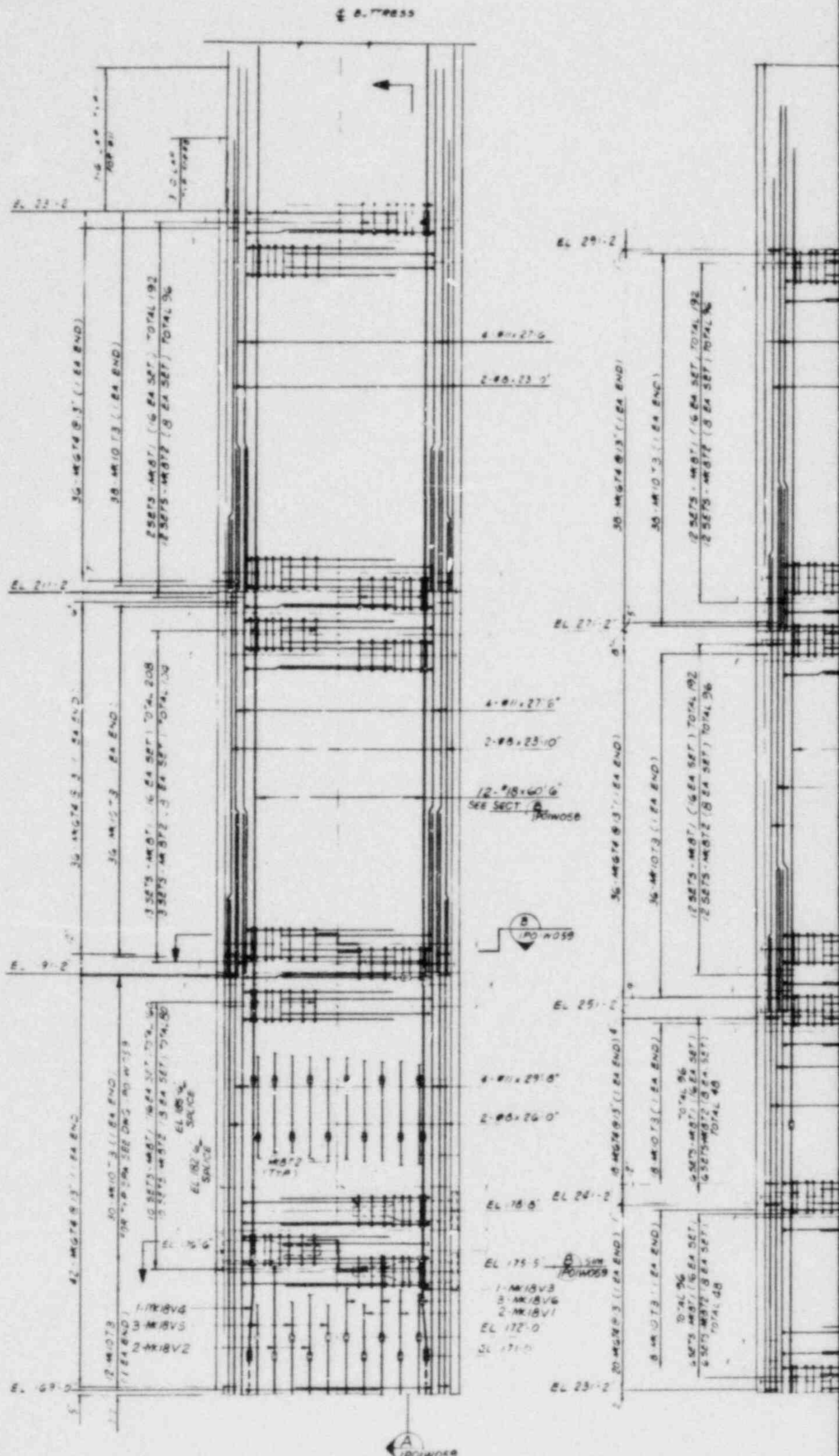

ELEVATION - BUTTRESS RE

BUTTRESS Nº1 (SHOWN) BUTTRESS Nº 2

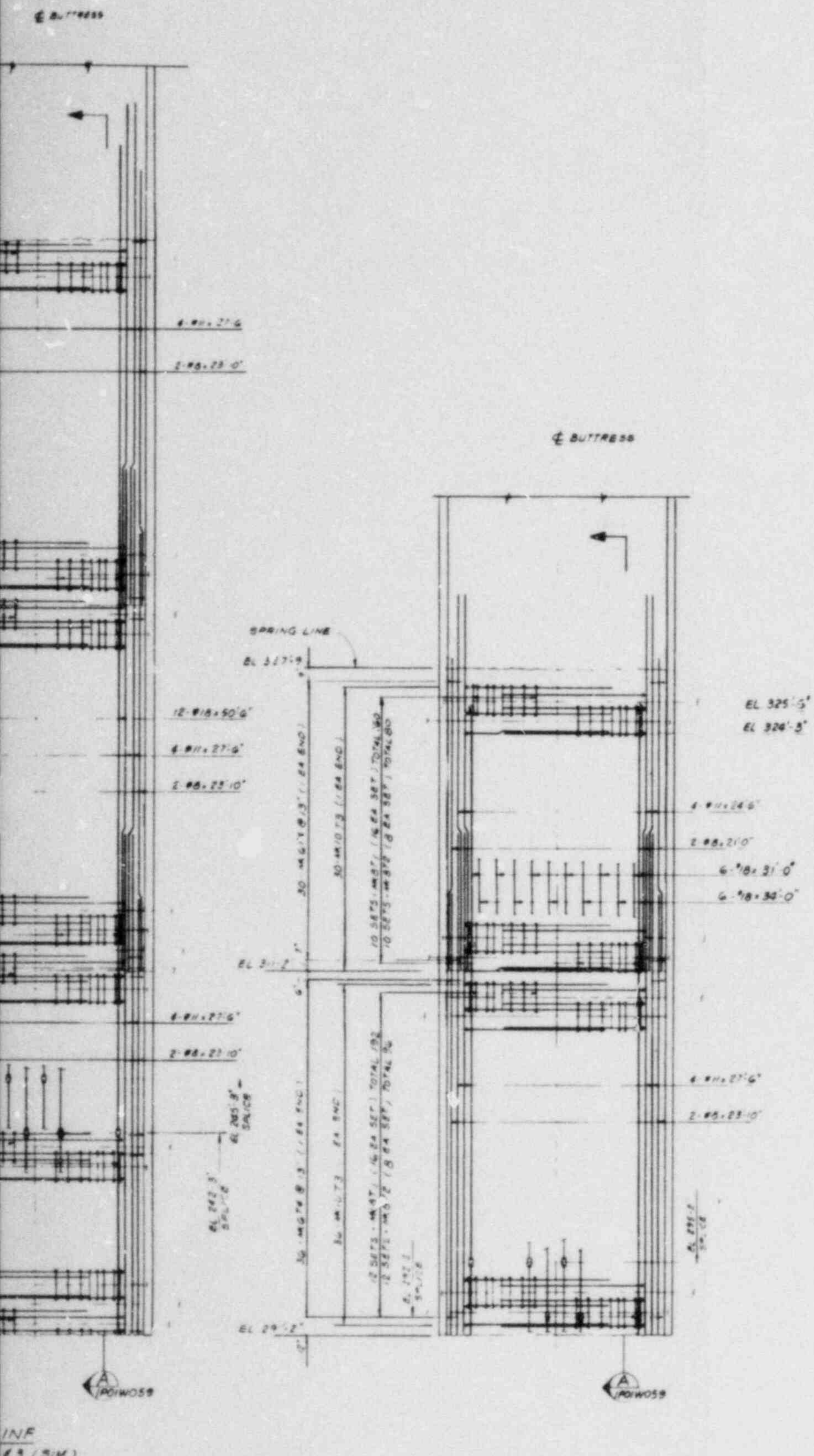

Figure 8
SHELL WALL REINFORCEMENT
CONTAINMENT BUILDING UNIT 1
OUTSIDE FACE AT BUTTRESS 1
(Sheet 4 of 5)

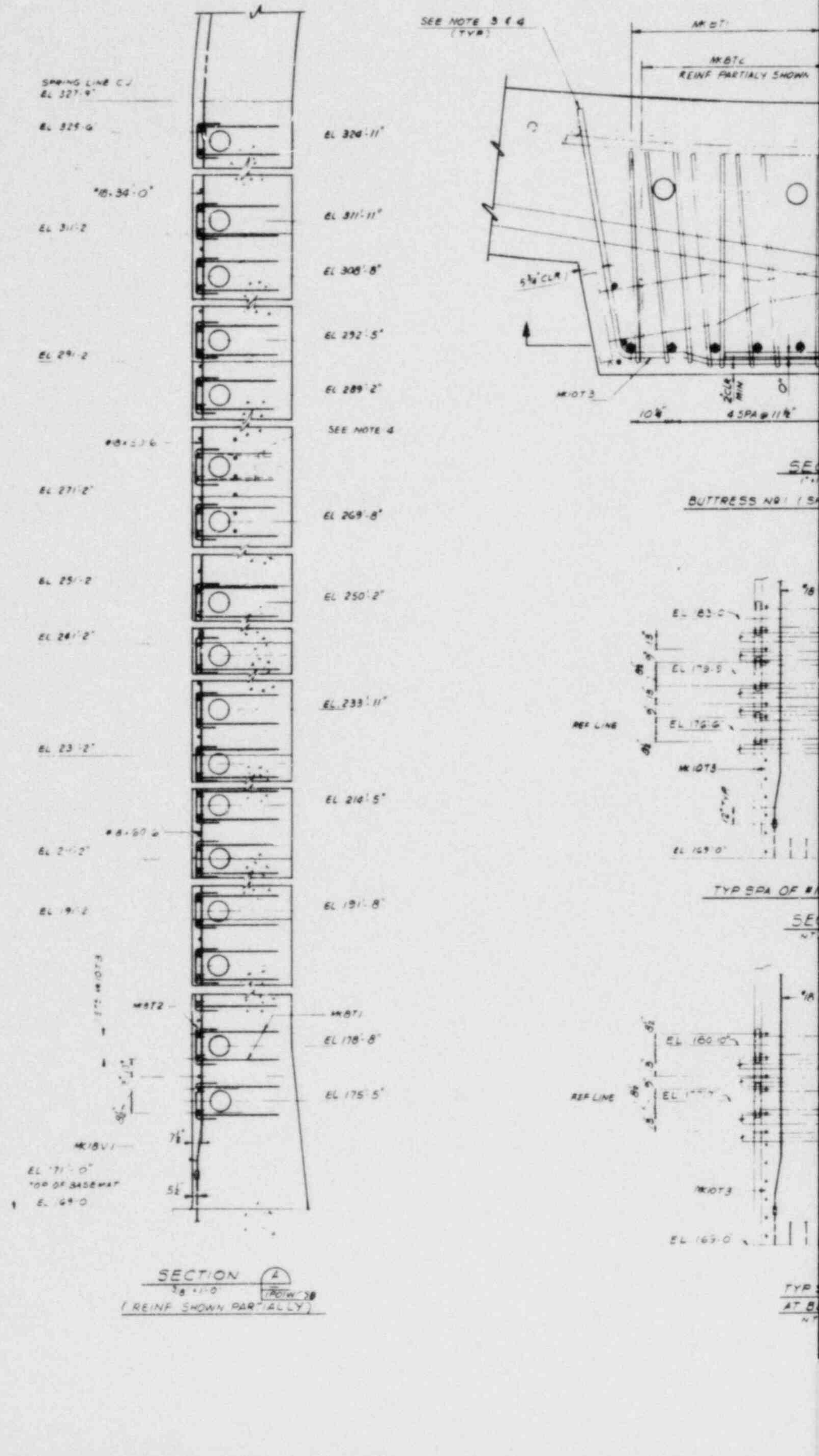
SPRING LINE CJ
EL 327'-9"
SEE NOTE 3 & 4 (TYP)
REINF PARTIALY SHOWN
SEE NOTE 4
BUTTRESS NO 1
REF LINE
TYP SPA OF
SECTION
(REINF SHOWN PARTIALLY)

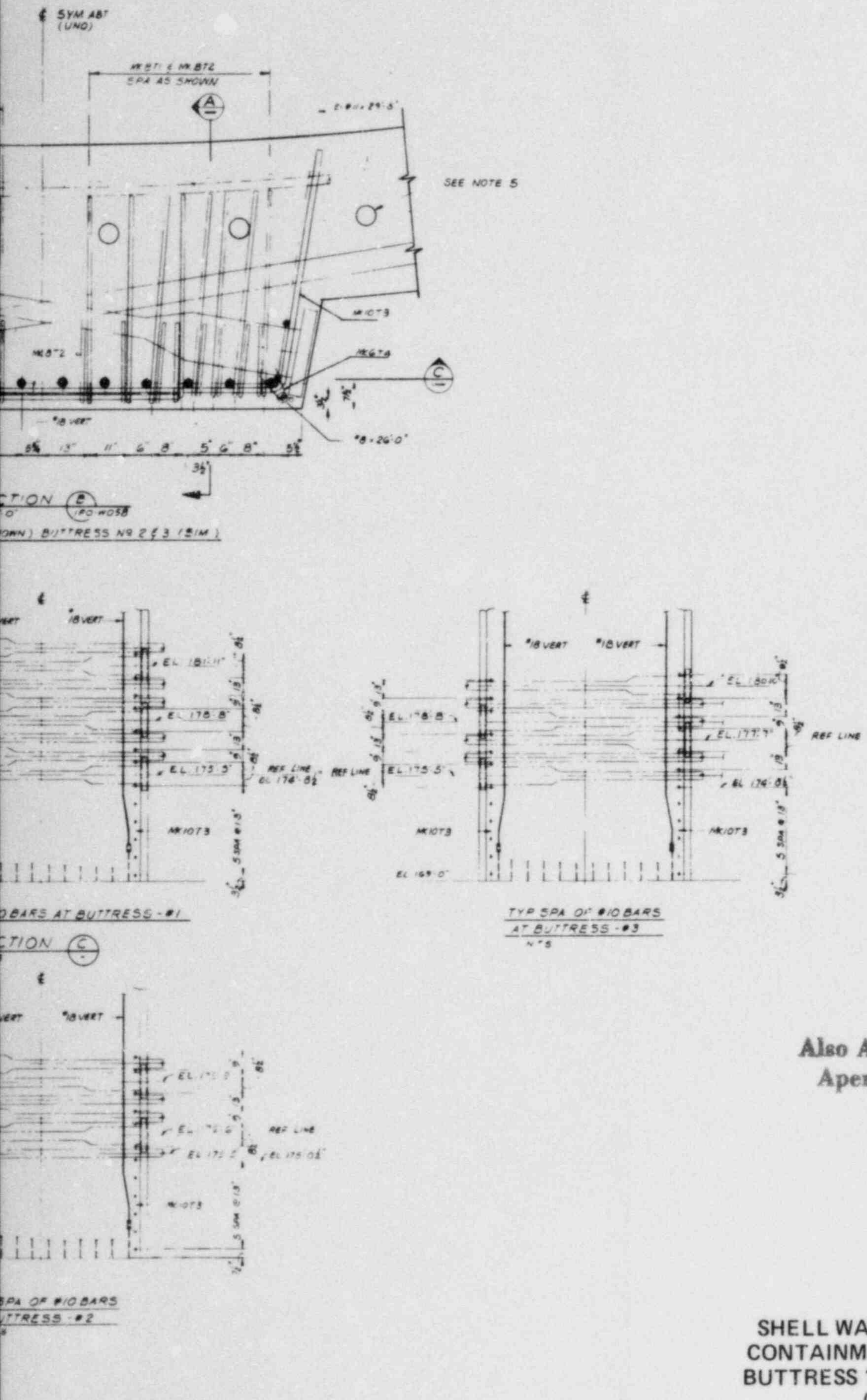

TI
APERTURE
CARD

Also Available On
Aperture Card

Figure 8
SHELL WALL REINFORCEMENT
CONTAINMENT BUILDING UNIT 1
BUTTRESS 1 PLAN AND SECTIONS
(Sheet 5 of 5)

8411050161 -11

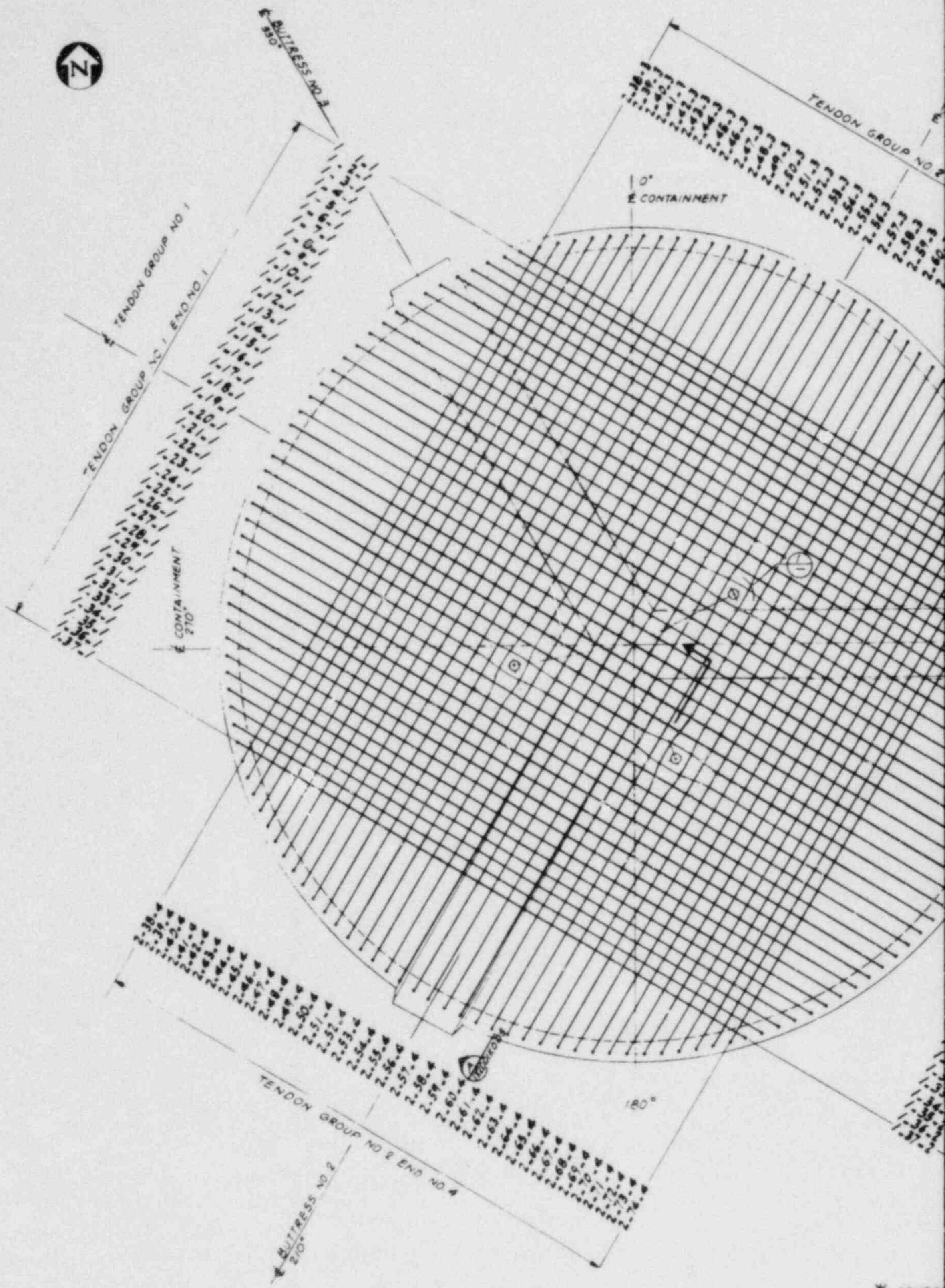
N
TENDON GROUP NO 1
TENDON GROUP NO 1 END NO 1
0°
℄ CONTAINMENT
℄ CONTAINMENT
270°
180°
TENDON GROUP NO 2
TENDON GROUP NO 2 END NO 4
℄ BUTTRESS NO 2
210°

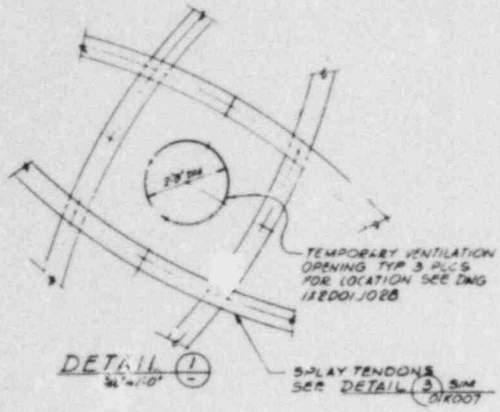

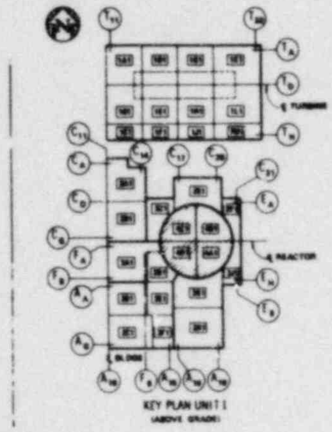

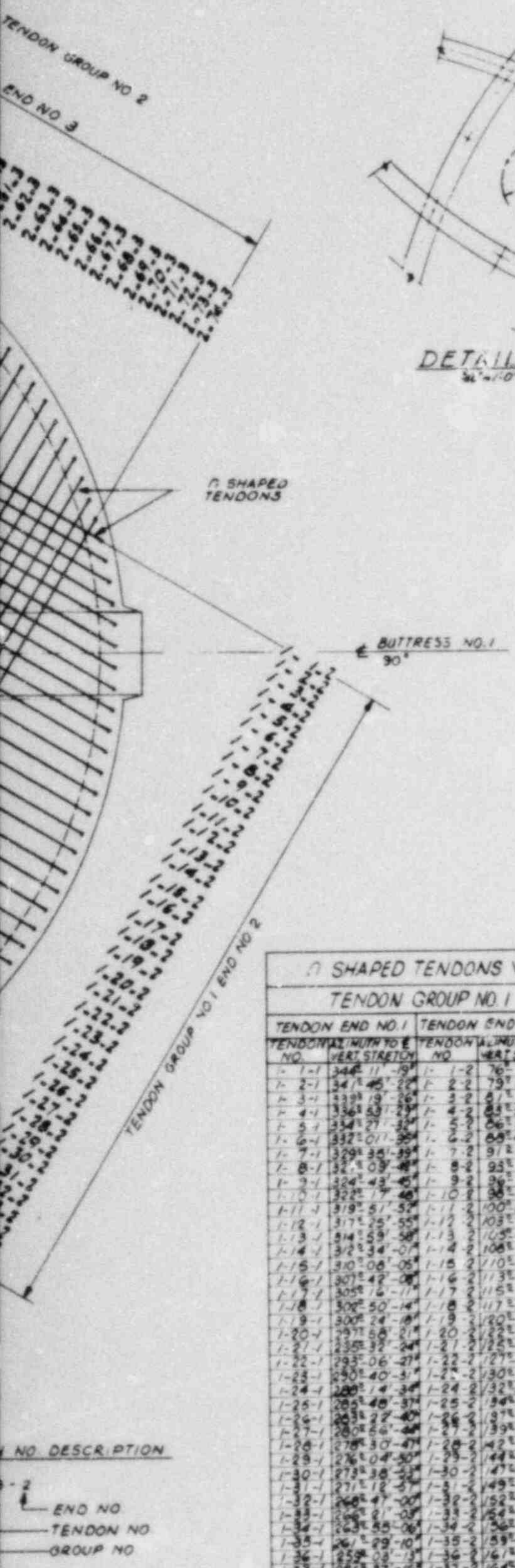

Ո SHAPED TENDONS VERTICAL STRETCH SCHEDULE *							
TENDON GROUP NO. 1				TENDON GROUP NO 2			
TENDON END NO. 1		TENDON END NO. 2		TENDON END NO. 3		TENDON END NO. 4	
TENDON NO.	AZIMUTH TO ℄ VERT. STRETCH	TENDON NO.	AZIMUTH TO ℄ VERT. STRETCH	TENDON NO.	AZIMUTH TO ℄ VERT. STRETCH	TENDON NO.	AZIMUTH TO ℄ VERT. STRETCH
1-1-1	344°-11'-19"	1-1-2	76°-37'-16"	2-38-3	346°-37'-16"	2-38-4	254°-11'-19"
1-2-1	341°-45'-22"	1-2-2	79°-03'-13"	2-39-3	349°-03'-13"	2-39-4	251°-46'-22"
1-3-1	339°-19'-26"	1-3-2	81°-29'-10"	2-40-3	351°-29'-10"	2-40-4	249°-19'-26"
1-4-1	336°-53'-29"	1-4-2	83°-55'-08"	2-41-3	353°-55'-06"	2-41-4	246°-53'-29"
1-5-1	334°-27'-32"	1-5-2	86°-21'-03"	2-42-3	356°-21'-03"	2-42-4	244°-27'-32"
1-6-1	332°-01'-35"	1-6-2	88°-47'-00"	2-43-3	358°-47'-00"	2-43-4	242°-01'-35"
1-7-1	329°-35'-39"	1-7-2	91°-12'-57"	2-44-3	1°-12'-57"	2-44-4	239°-35'-39"
1-8-1	327°-09'-42"	1-8-2	93°-38'-53"	2-45-3	3°-38'-53"	2-45-4	237°-09'-42"
1-9-1	324°-43'-45"	1-9-2	96°-04'-50"	2-46-3	6°-04'-50"	2-46-4	234°-43'-45"
1-10-1	322°-17'-48"	1-10-2	98°-30'-47"	2-47-3	8°-30'-47"	2-47-4	232°-17'-48"
1-11-1	319°-51'-52"	1-11-2	100°-56'-44"	2-48-3	10°-56'-44"	2-48-4	229°-51'-52"
1-12-1	317°-25'-55"	1-12-2	103°-22'-40"	2-49-3	13°-22'-40"	2-49-4	227°-25'-55"
1-13-1	314°-59'-58"	1-13-2	105°-48'-37"	2-50-3	15°-48'-37"	2-50-4	224°-59'-58"
1-14-1	312°-34'-01"	1-14-2	108°-14'-34"	2-51-3	18°-14'-34"	2-51-4	222°-34'-01"
1-15-1	310°-08'-05"	1-15-2	110°-40'-31"	2-52-3	20°-40'-31"	2-52-4	220°-08'-05"
1-16-1	307°-42'-08"	1-16-2	113°-06'-27"	2-53-3	23°-06'-27"	2-53-4	217°-42'-08"
1-17-1	305°-16'-11"	1-17-2	115°-32'-24"	2-54-3	25°-32'-24"	2-54-4	215°-16'-11"
1-18-1	302°-50'-14"	1-18-2	117°-58'-21"	2-55-3	27°-58'-21"	2-55-4	212°-50'-14"
1-19-1	300°-24'-18"	1-19-2	120°-24'-18"	2-56-3	30°-24'-18"	2-56-4	210°-24'-18"
1-20-1	297°-58'-21"	1-20-2	122°-53'-14"	2-57-3	32°-50'-14"	2-57-4	207°-58'-21"
1-21-1	295°-32'-24"	1-21-2	125°-16'-11"	2-58-3	35°-16'-11"	2-58-4	205°-32'-24"
1-22-1	293°-06'-27"	1-22-2	127°-42'-08"	2-59-3	37°-42'-08"	2-59-4	203°-06'-27"
1-23-1	290°-40'-31"	1-23-2	130°-08'-05"	2-60-3	40°-08'-05"	2-60-4	200°-40'-31"
1-24-1	288°-14'-34"	1-24-2	132°-34'-01"	2-61-3	42°-34'-01"	2-61-4	198°-14'-34"
1-25-1	285°-48'-37"	1-25-2	134°-59'-58"	2-62-3	44°-59'-58"	2-62-4	195°-48'-37"
1-26-1	283°-27'-40"	1-26-2	137°-25'-55"	2-63-3	47°-25'-55"	2-63-4	193°-22'-40"
1-27-1	280°-56'-44"	1-27-2	139°-51'-51"	2-64-3	49°-51'-51"	2-64-4	190°-56'-44"
1-28-1	278°-30'-47"	1-28-2	142°-17'-48"	2-65-3	52°-17'-48"	2-65-4	188°-30'-47"
1-29-1	276°-04'-50"	1-29-2	144°-43'-45"	2-66-3	54°-43'-45"	2-66-4	186°-04'-50"
1-30-1	273°-38'-53"	1-30-2	147°-09'-42"	2-67-3	57°-09'-42"	2-67-4	183°-38'-53"
1-31-1	271°-12'-57"	1-31-2	149°-35'-39"	2-68-3	59°-35'-39"	2-68-4	181°-12'-57"
1-32-1	268°-47'-00"	1-32-2	152°-01'-35"	2-69-3	62°-01'-35"	2-69-4	178°-47'-00"
1-33-1	266°-21'-03"	1-33-2	154°-27'-32"	2-70-3	64°-27'-32"	2-70-4	176°-21'-03"
1-34-1	263°-55'-06"	1-34-2	156°-53'-29"	2-71-3	66°-53'-29"	2-71-4	173°-55'-06"
1-35-1	261°-29'-10"	1-35-2	159°-19'-26"	2-72-3	69°-19'-26"	2-72-4	171°-29'-10"
1-36-1	258°-03'-13"	1-36-2	161°-45'-22"	2-73-3	71°-45'-22"	2-73-4	169°-03'-13"
1-37-1	256°-37'-16"	1-37-2	164°-11'-19"	2-74-3	74°-11'-19"	2-74-4	166°-37'-16"

NOTES

1. FOR GENERAL NOTES AND REFERENCE DRAWINGS SEE DRAWING 1X2D01K001.
2. FOR Ո SHAPED TENDONS GEOMETRY AT THE DOME SEE DRAWING 1X2D01K003.

Also Available On
Aperture Card

TI
APERTURE
CARD

Figure 9
CONTAINMENT TENDON ARRANGEMENT
(UNIT 1)
(Sheet 1 of 4)

8411050161 -/2

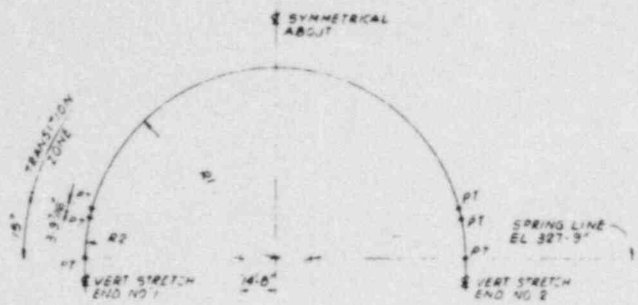

GEOMETRY OF ∩ SHAPED TENDONS
GROUP NO 1

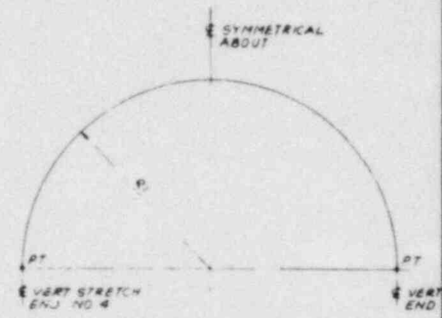

GEOMETRY OF ∩ SHAPED TENDONS
GROUP NO 2

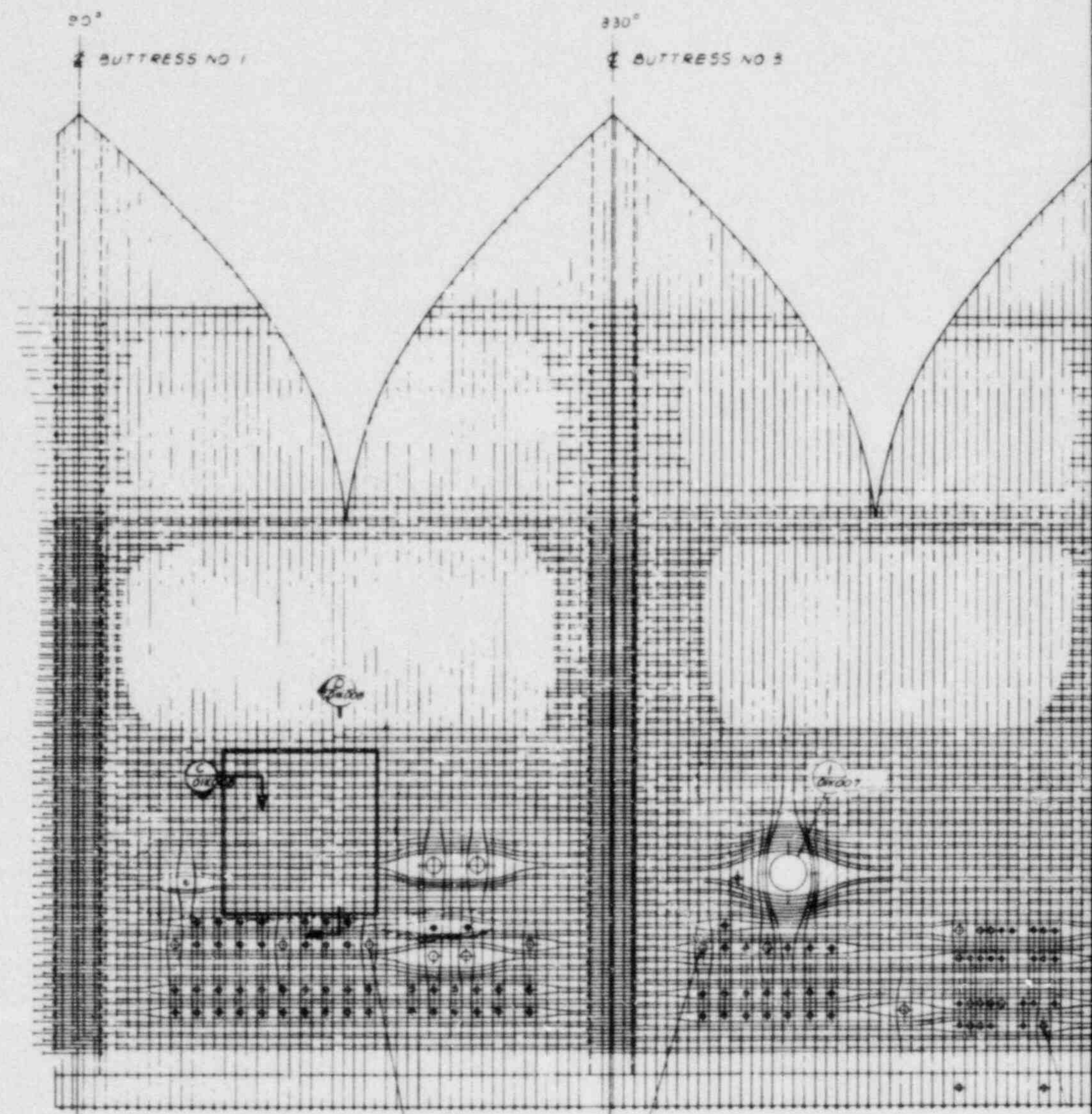

WALL DEVELOPED ELEVATION
1/16" = 1'-0"

∩ SHAPED TENDONS RADII AT THE DOME					
TENDON GROUP NO 1			TENDON GROUP NO 2		
TENDON NO	R1	R2	TENDON NO	R1	R2
1 & 37	51'-5 7/16	37'-9 [illegible]	38 & 74	51'-11 [illegible]	
2 & 36	53'-6 [illegible]	39'-4 [illegible]	39 & 73	54'-0 [illegible]	
3 & 35	55'-6 [illegible]	41'-4 [illegible]	40 & 72	56'-0 [illegible]	
4 & 34	57'-4 [illegible]	43'-2 [illegible]	41 & 71	57'-10 [illegible]	
5 & 33	59'-1 [illegible]	44'-11 [illegible]	42 & 70	59'-7 [illegible]	
6 & 32	60'-9 [illegible]	46'-7 [illegible]	43 & 69	61'-3 [illegible]	
7 & 31	62'-4 [illegible]	48'-2 [illegible]	44 & 68	62'-10 [illegible]	
8 & 30	63'-9 [illegible]	49'-7 [illegible]	45 & 67	64'-3 [illegible]	
9 & 29	65'-1 [illegible]	50'-11 [illegible]	46 & 66	65'-7 [illegible]	
10 & 28	66'-3 [illegible]	52'-1 [illegible]	47 & 65	66'-9 [illegible]	
11 & 27	67'-4 [illegible]	53'-2 [illegible]	48 & 64	67'-10 [illegible]	
12 & 26	68'-4 [illegible]	54'-2 [illegible]	49 & 63	68'-10 [illegible]	
13 & 25	69'-2 [illegible]	55'-0 [illegible]	50 & 62	69'-8 [illegible]	
14 & 24	69'-10 [illegible]	55'-8 [illegible]	51 & 61	70'-4 [illegible]	
15 & 23	70'-5 [illegible]	56'-3 [illegible]	52 & 60	70'-11 [illegible]	
16 & 22	70'-11"	56'-9"	53 & 59	71'-5"	
17 & 21	71'-2 [illegible]	57'-0 [illegible]	54 & 58	71'-8 [illegible]	
18 & 20	71'-5 [illegible]	57'-3 [illegible]	55 & 57	71'-11 [illegible]	
19	71'-6"	57'-4"	56 &	72'-0"	

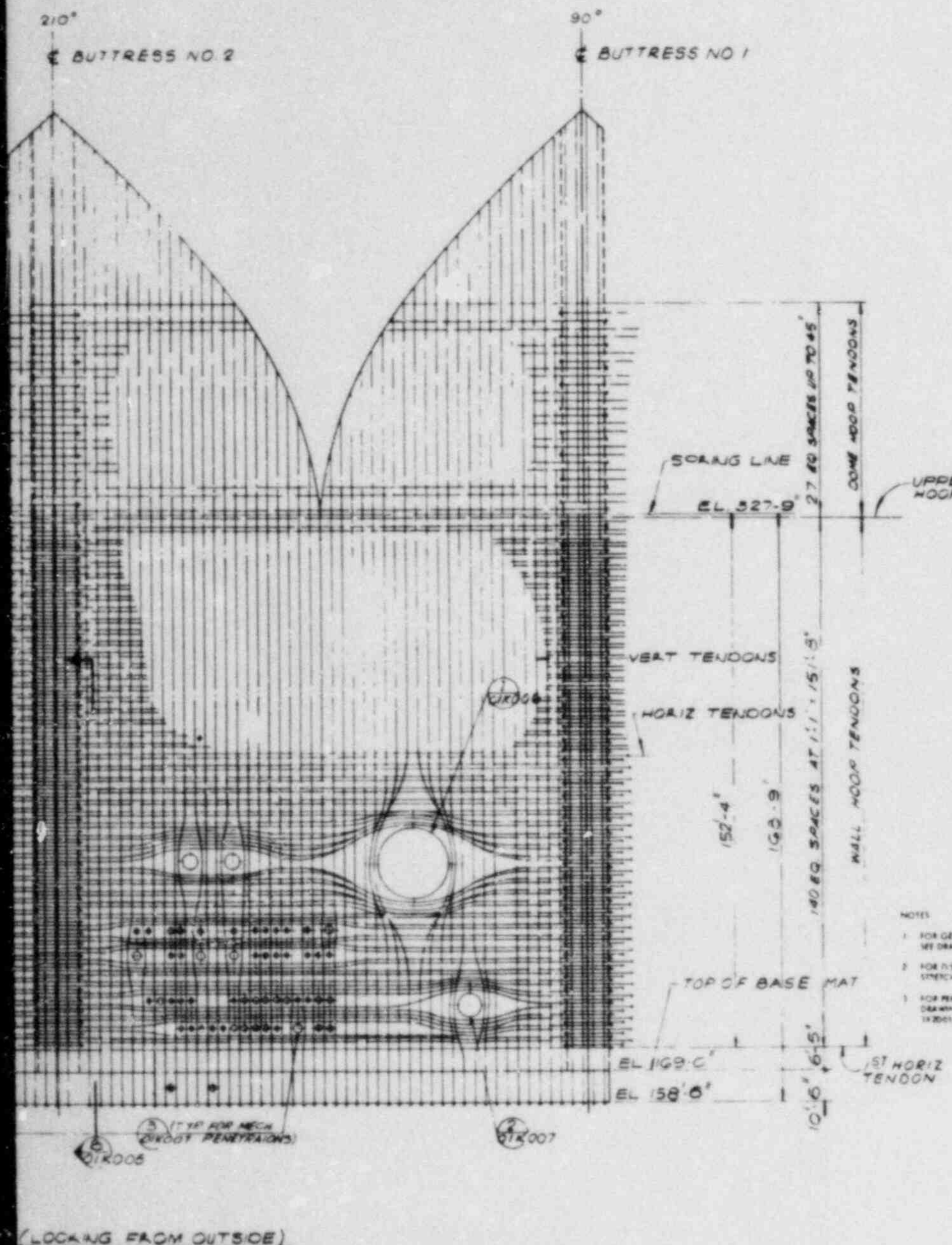

NOTES

1. FOR GENERAL NOTES AND REFERENCE DRAWINGS SEE DRAWING 1X2DO1K001
2. FOR ∩-SHAPED TENDON NUMBER AND VERTICAL STRETCH LOCATION SEE DRAWING 1X2DO1K002
3. FOR PENETRATION SIZE AND LOCATIONS SEE DRAWINGS 1X2D01J009, 1X2D01J010, 1X2D01J011, 1X2D01J012 AND 1X2D01J013

TI
APERTURE
CARD

Also Available On
Aperture Card

Figure 9
CONTAINMENT TENDON ARRANGEMENT
(UNIT 1)
(Sheet 2 of 4)

8411050161 -13

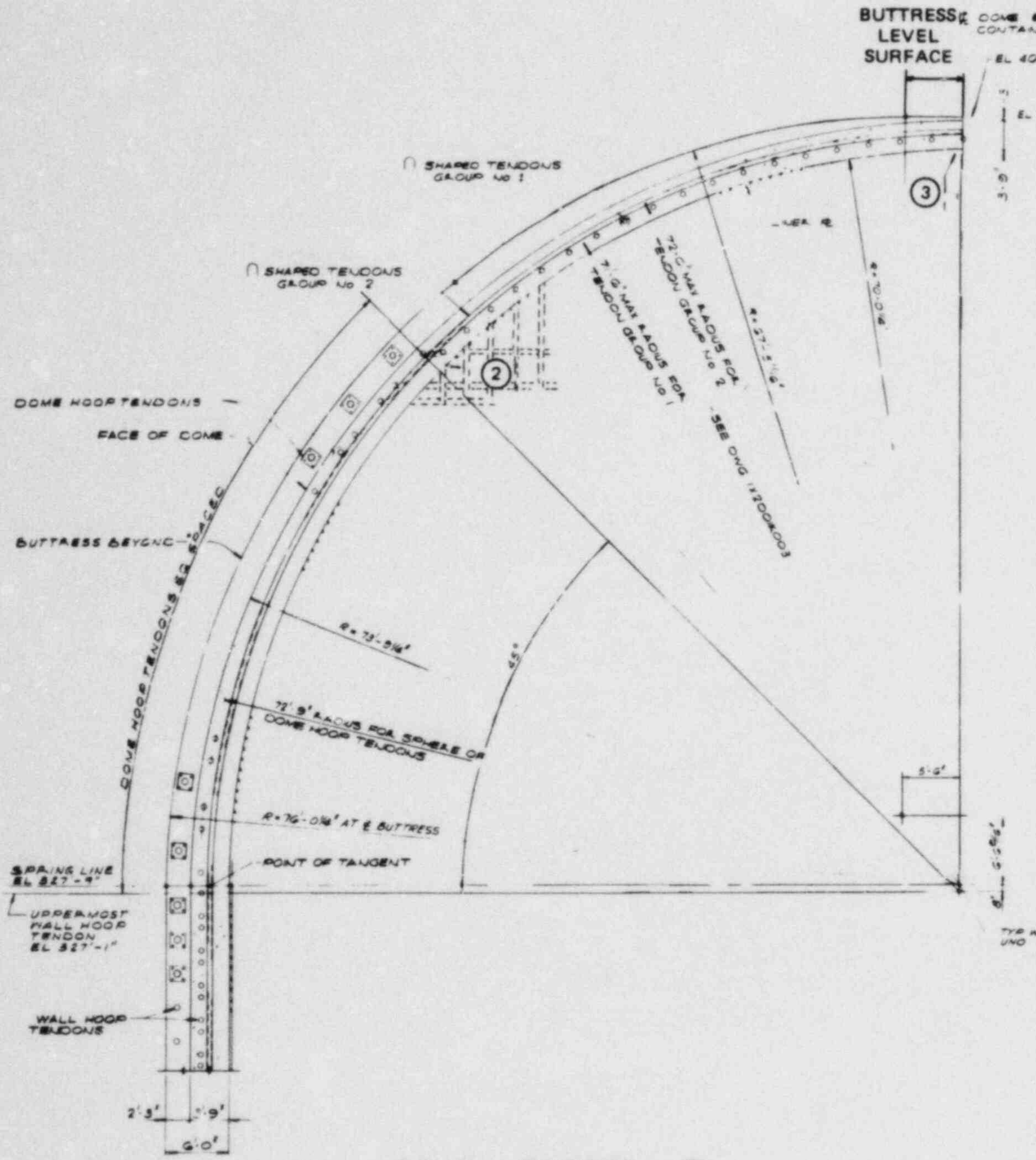

DOME SECTION (A)

FROM FIGURE 3.8.1-6, SHEET 1 OF 3

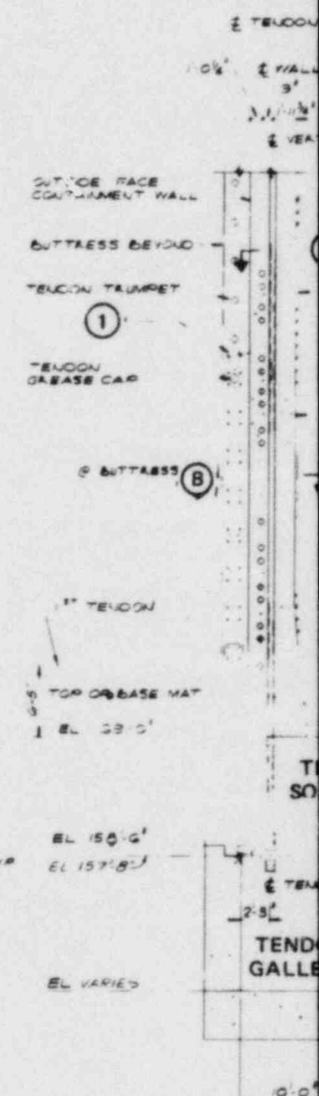

WALL SEC

FROM FIGURE 3.8.1

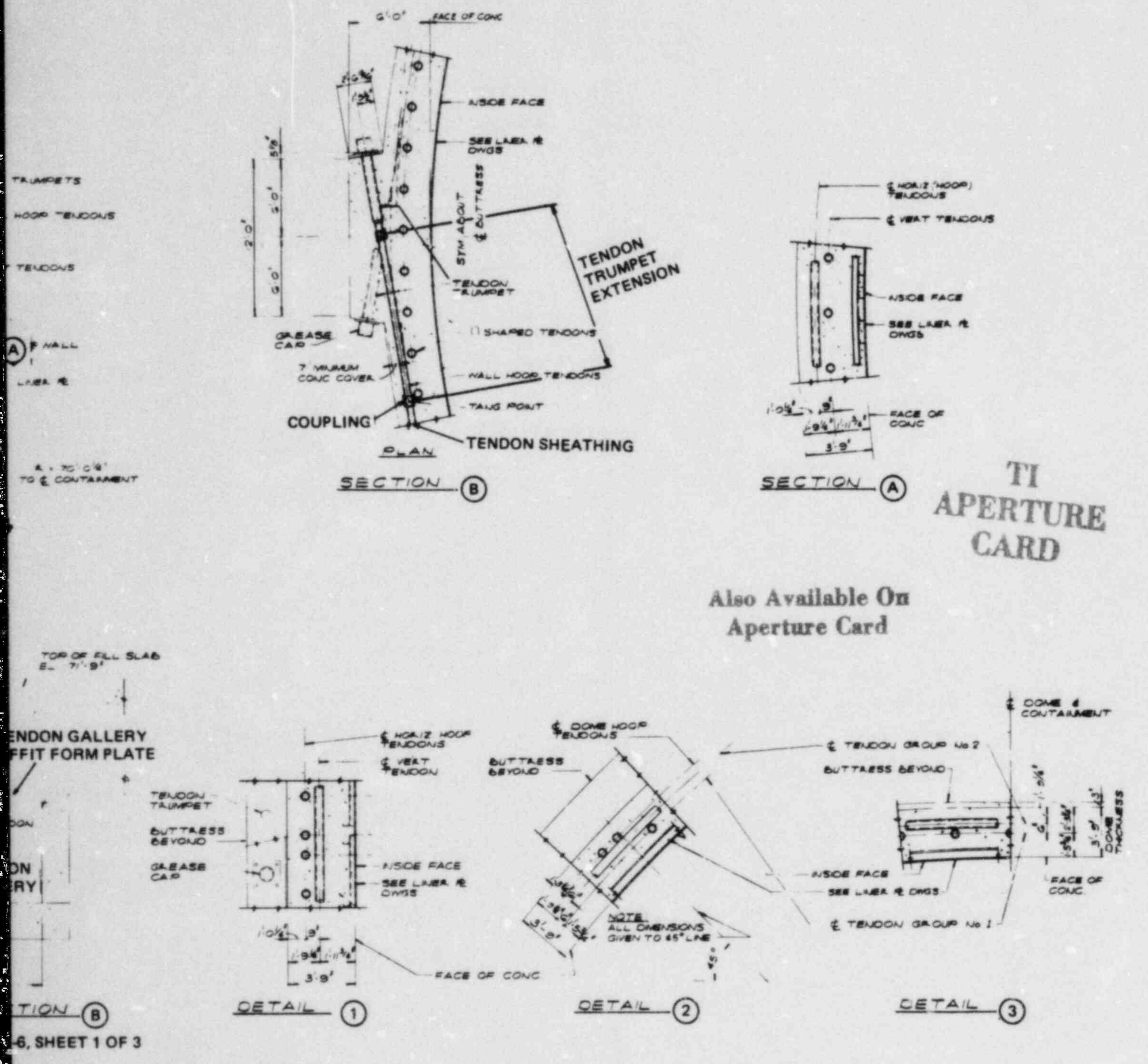

Figure 9
CONTAINMENT TENDON ARRANGEMENT
(UNIT 1)
(Sheet 3 of 4)

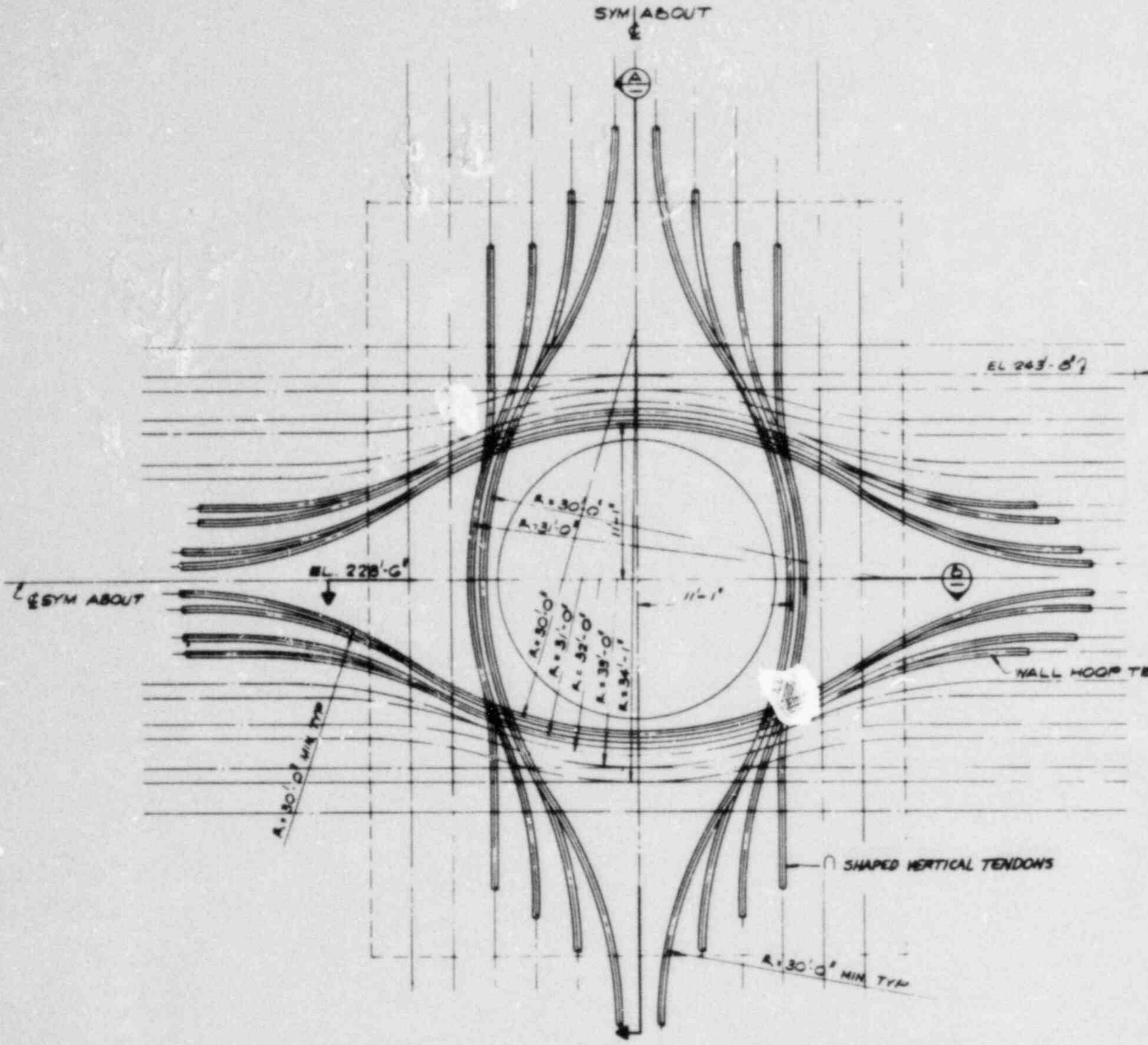

TENDON ELEV AT EQUIPMENT HATCH

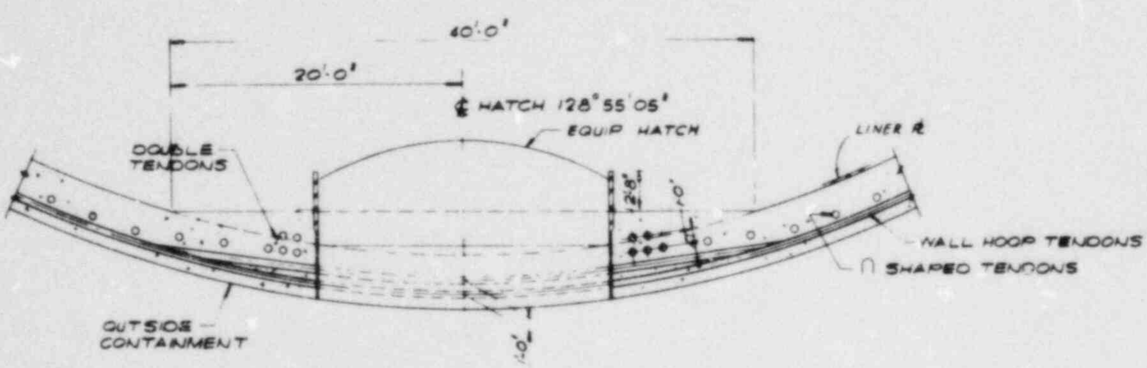

SECTION B

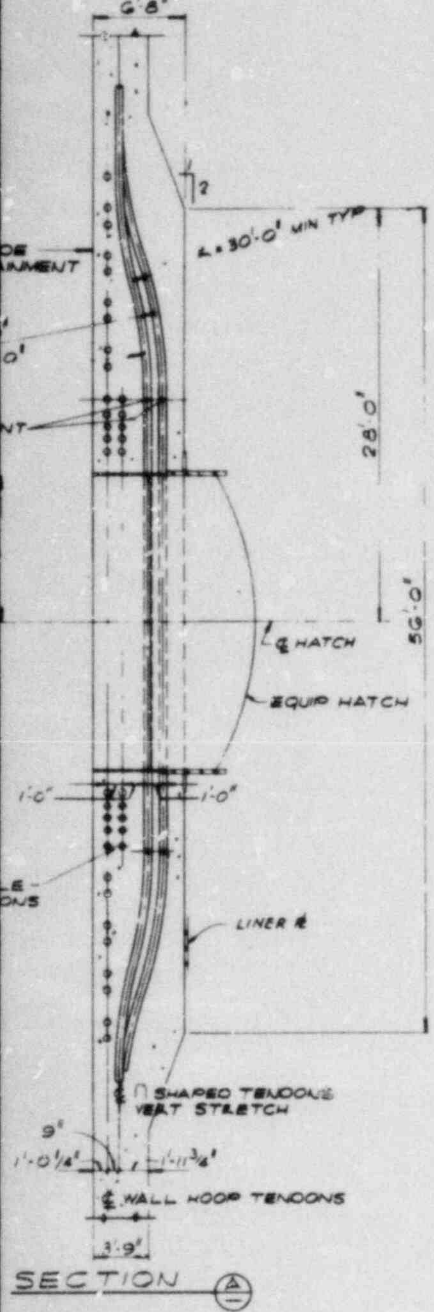

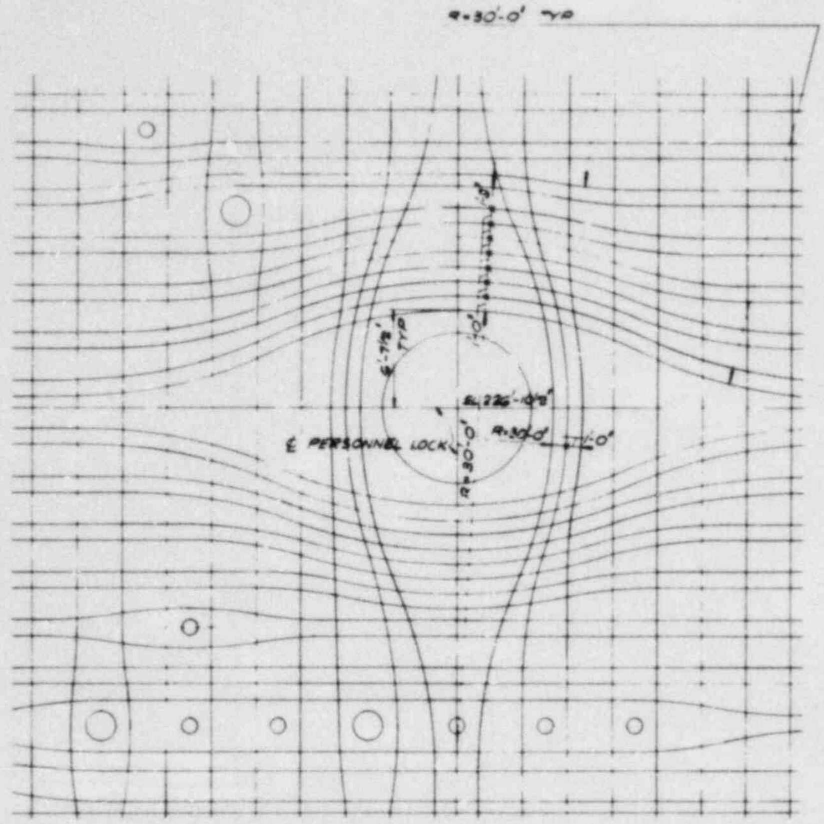

TENDON ELEVATION AT
PERSONNEL LOCK

TI
APERTURE
CARD

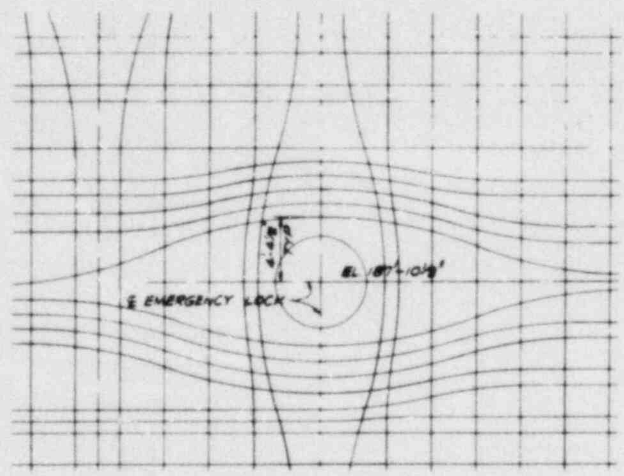

TENDON ELEVATION AT
EMERGENCY LOCK

Also Available On
Aperture Card

Figure 9
CONTAINMENT TENDON ARRANGEMENT
(UNIT 1)
(Sheet 4 of 4)

8411050161 -15

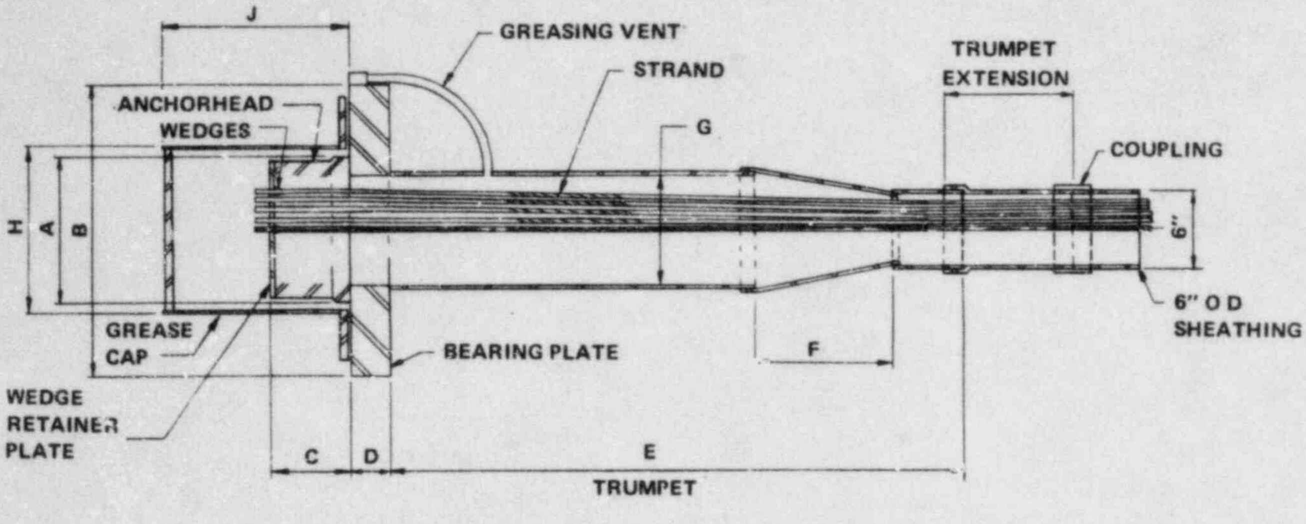

PERMANENT ANCHORAGE ASSEMBLY

TYPE		A	B	C	D	E	F	G	H	J
55 STRAND (VSL)	PERMANENT	12"	24"SQ.	6"	3½"	48"	8"	9"	14"	20"
	DETENSIONABLE	12"	24"SQ.	6"	3½"	48"	11"	13"	18"	22"

STRAND AREA = 0.155 SQ. IN.

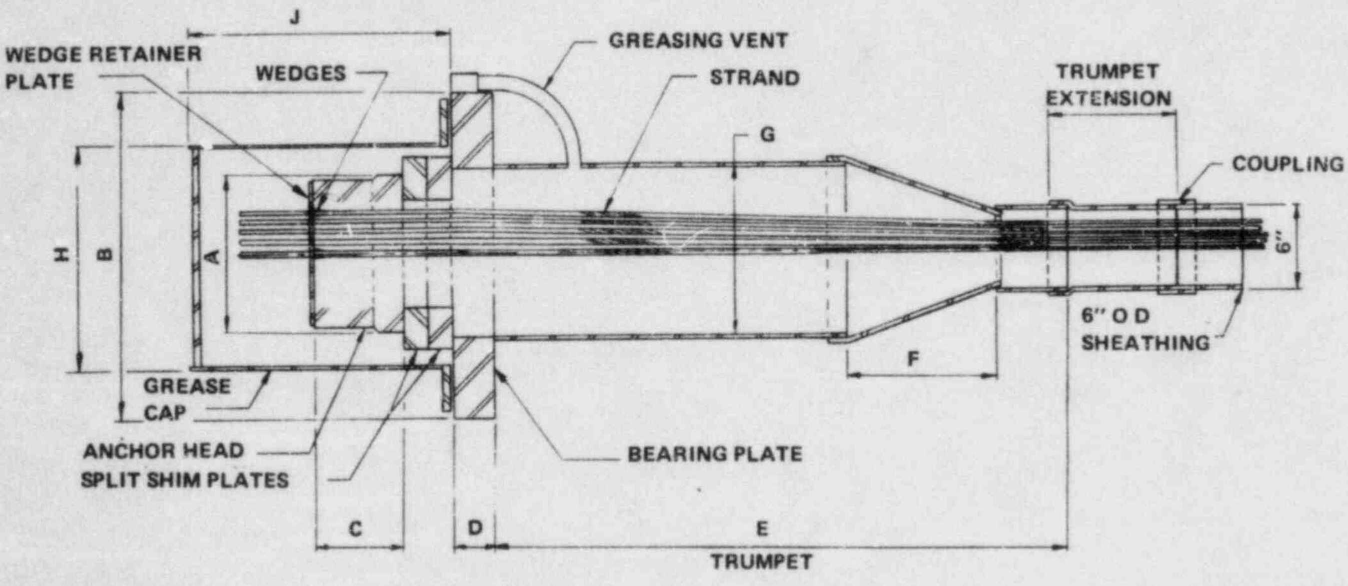

DETENSIONABLE ANCHORAGE ASSEMBLY

*SELECTED SURVEILLANCE TENDONS HAVE A GREATER QUANTITY OF SHIM PLATES AND A CORRESPONDING LONGER GREASE CAP.

Figure 10
CONTAINMENT TENDON END ANCHORAGE
ASSEMBLY

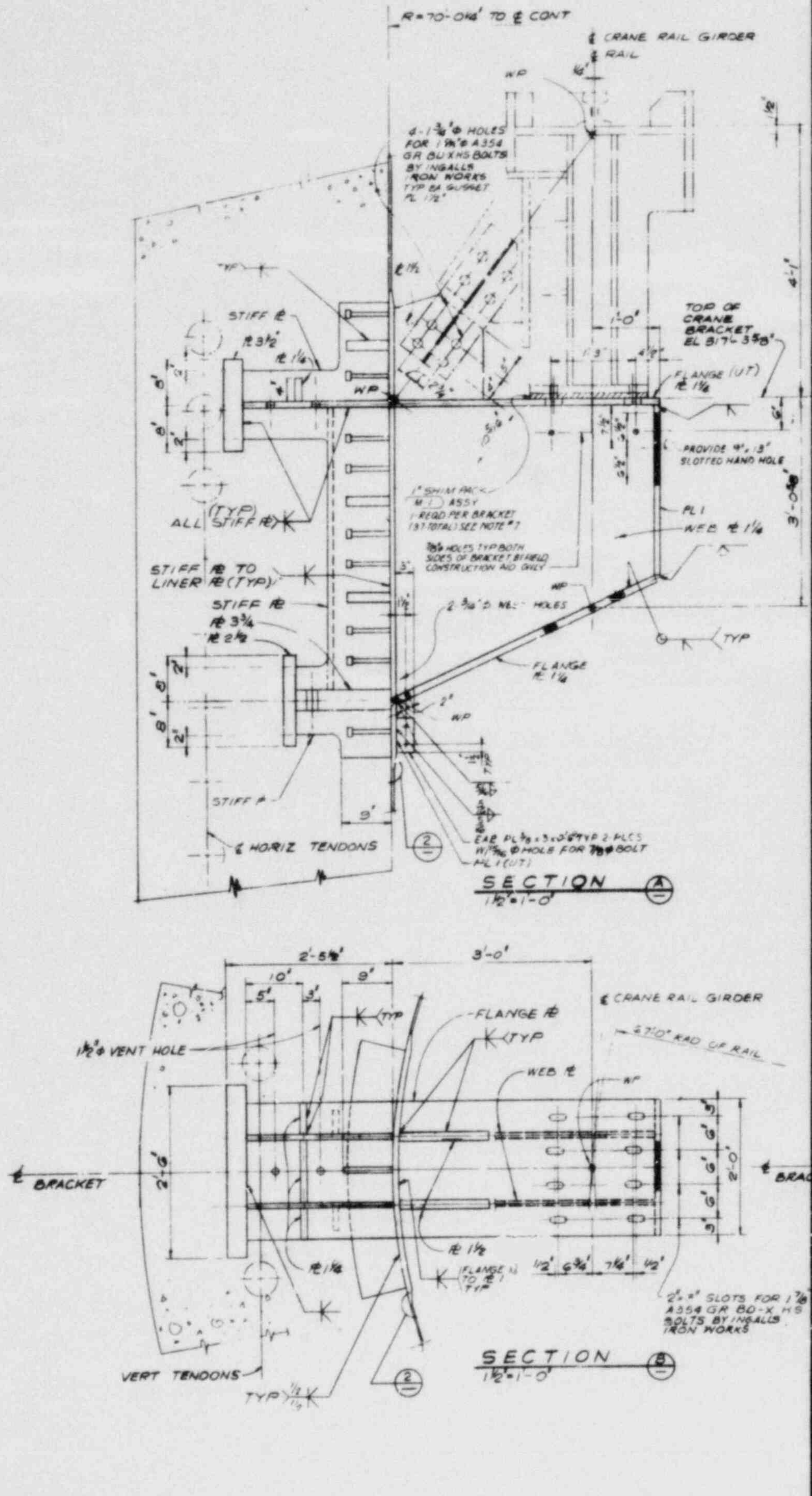

R=70'-0¼" TO ℄ CONT
℄ CRANE RAIL GIRDER
℄ RAIL
WP
TOP OF CRANE BRACKET EL 317'-3⅝"
STIFF ℞
ALL STIFF ℞ (TYP)
STIFF ℞ TO LINER ℞ (TYP)
STIFF ℞
FLANGE (UT)
PROVIDE 4"x13" SLOTTED HAND HOLE
PL 1
WEB ℞ 1¼
FLANGE ℞ 1¼
TYP
STIFF ℞
℄ HORIZ TENDONS
PL 1 (UT)
SECTION A
1½"=1'-0"
2'-5⅝"
3'-0"
℄ CRANE RAIL GIRDER
FLANGE ℞
WEB ℞
1½"φ VENT HOLE
℄ BRACKET
VERT TENDONS
SECTION B
1½"=1'-0"

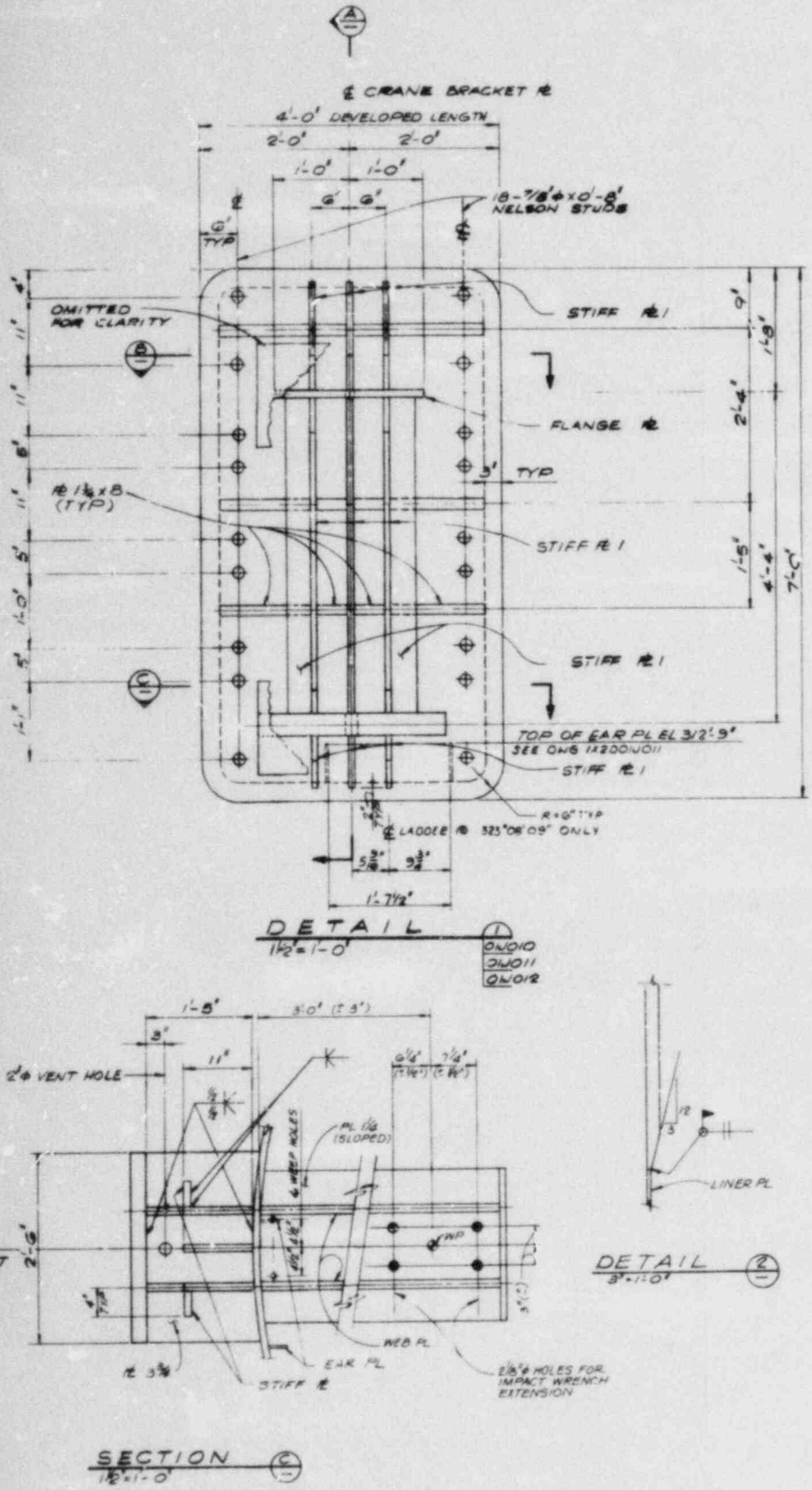

Figure 11
POLAR CRANE BRACKET DETAILS

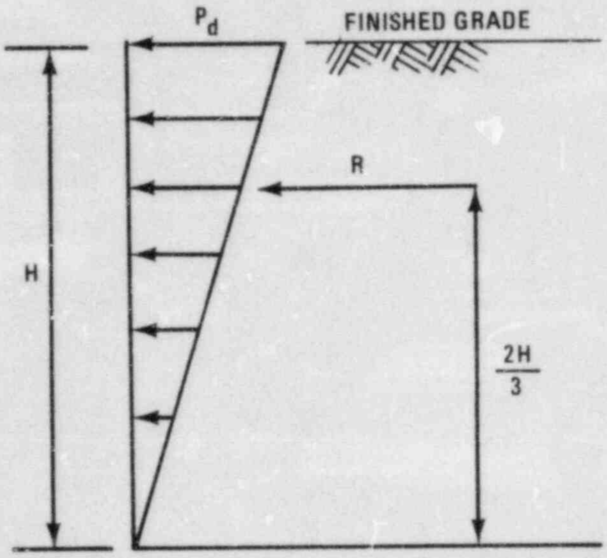

H = HEIGHT FROM BASE OF STRUCTURE TO SOIL SURFACE

R = RESULTANT FORCE*

$= .075\ \gamma_M H^2$ (FOR SSE)

$= .045\ \gamma_M H^2$ (FOR OBE)

$P_d = \frac{2R}{H}$

γ_M = SOIL MOIST UNIT WEIGHT, PCF

*DERIVED USING THE PEAK GROUND ACCELERATIONS OF 0.12g AND 0.20g FOR OBE AND SSE RESPECTIVELY.

Figure 12
DYNAMIC INCREMENTAL SOIL PRESSURE PROFILE

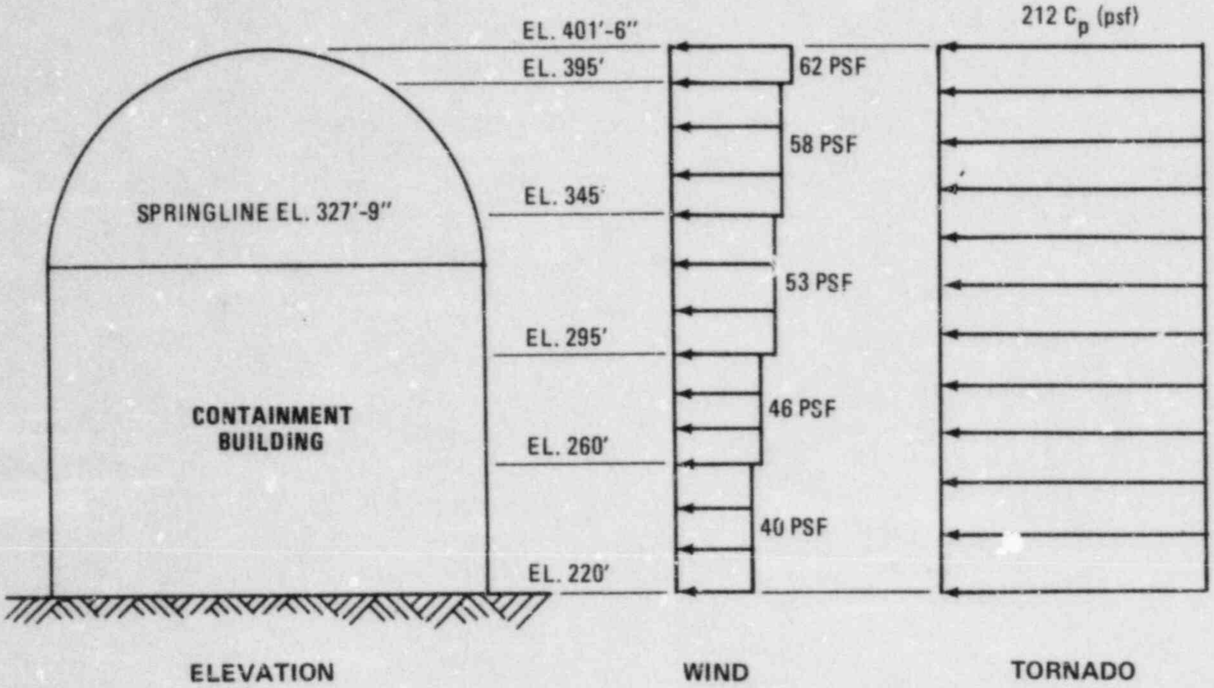

$P = C_s P_{max} C_p$

WHERE:

C_s = SIZE COEFFICIENT = .64

$P_{max} = 0.00256 (V_{max})^2$
$= 0.00256 (360 \text{ mph})^2$
$= 332$ Psf

C_p = EFFECTIVE EXTERNAL PRESSURE COEFFICIENT (SEE FIG. 14)

$P = (.64)(332 \text{ psf}) C_p$
$= 212 C_p$ (psf)

Figure 13
WIND AND TORNADO EFFECTIVE VELOCITY
PRESSURE PROFILES

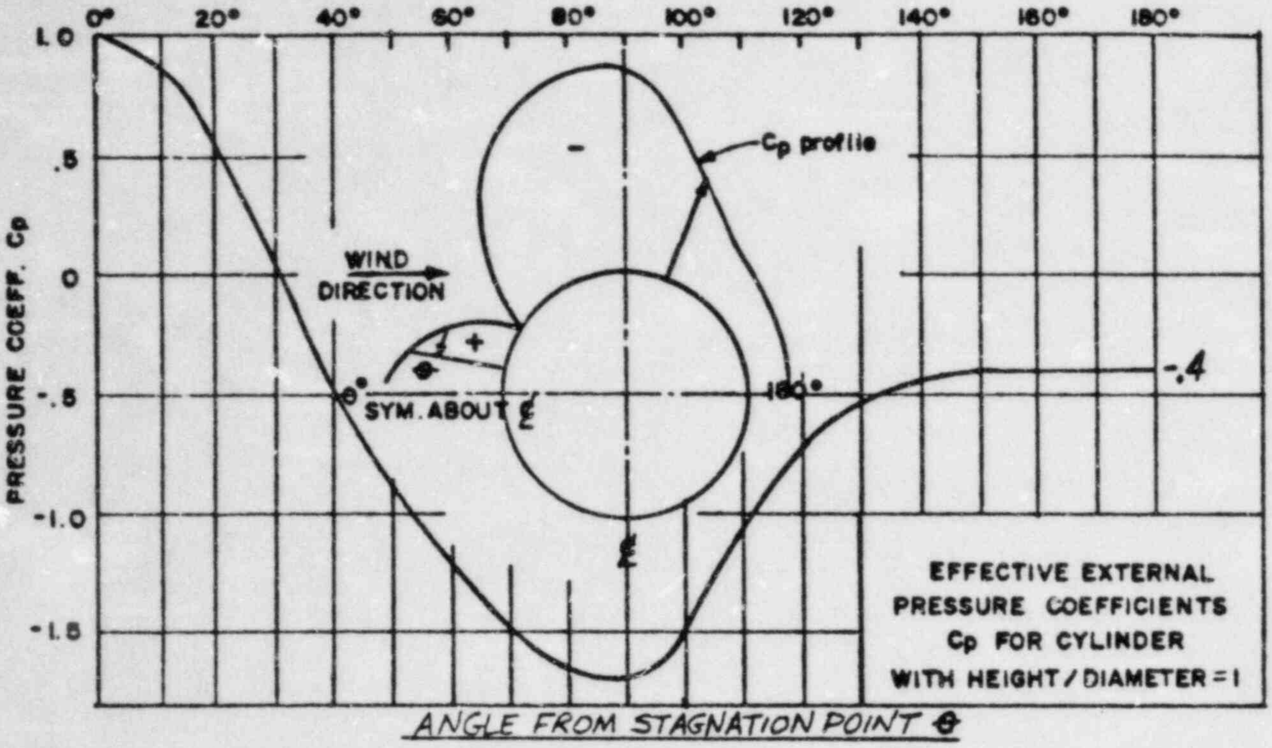

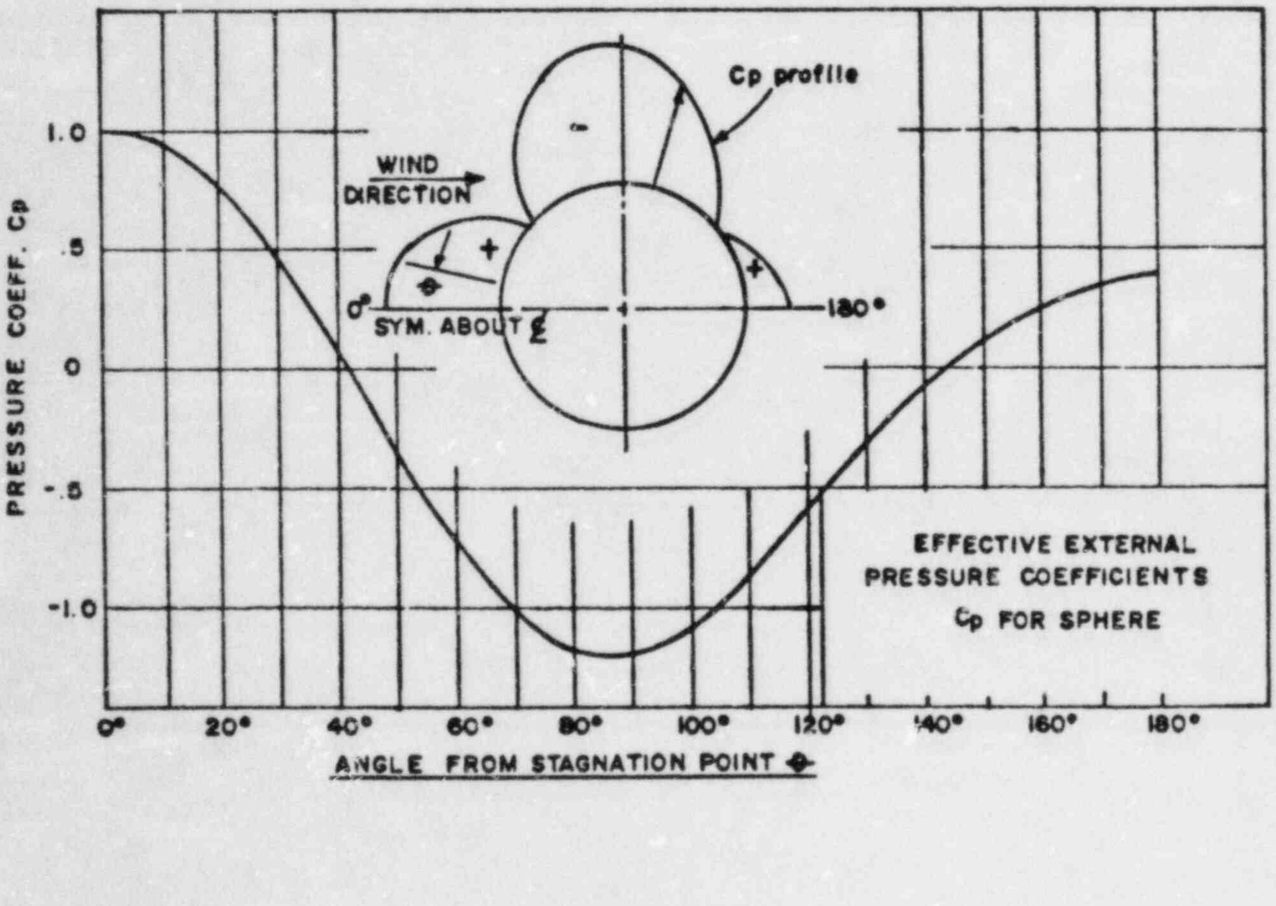

Figure 14
EFFECTIVE EXTERNAL
PRESSURE COEFFICIENTS

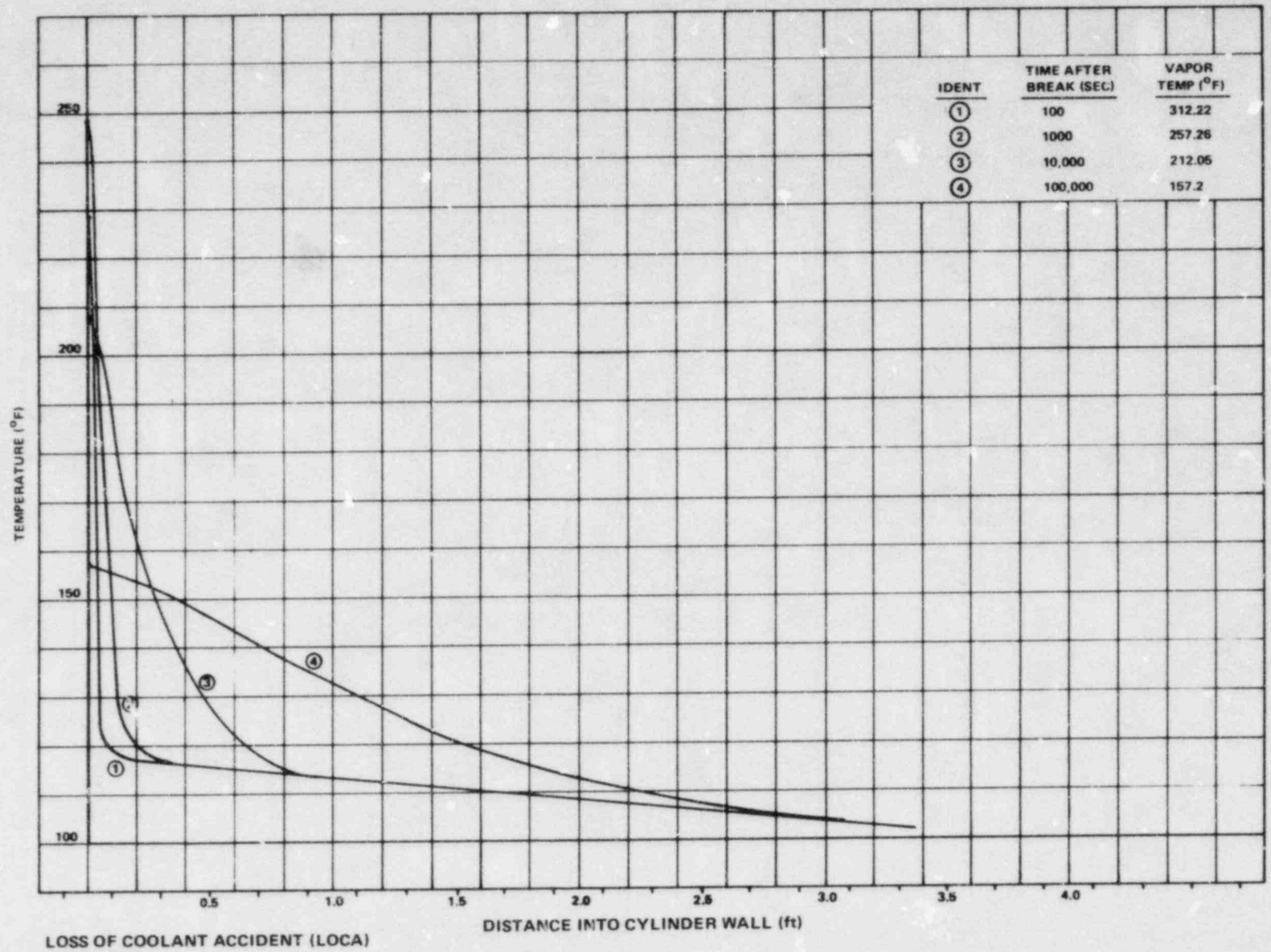

Figure 15
TEMPERATURE GRADIENTS THROUGH CONTAINMENT WALL
(Sheet 1 of 2)

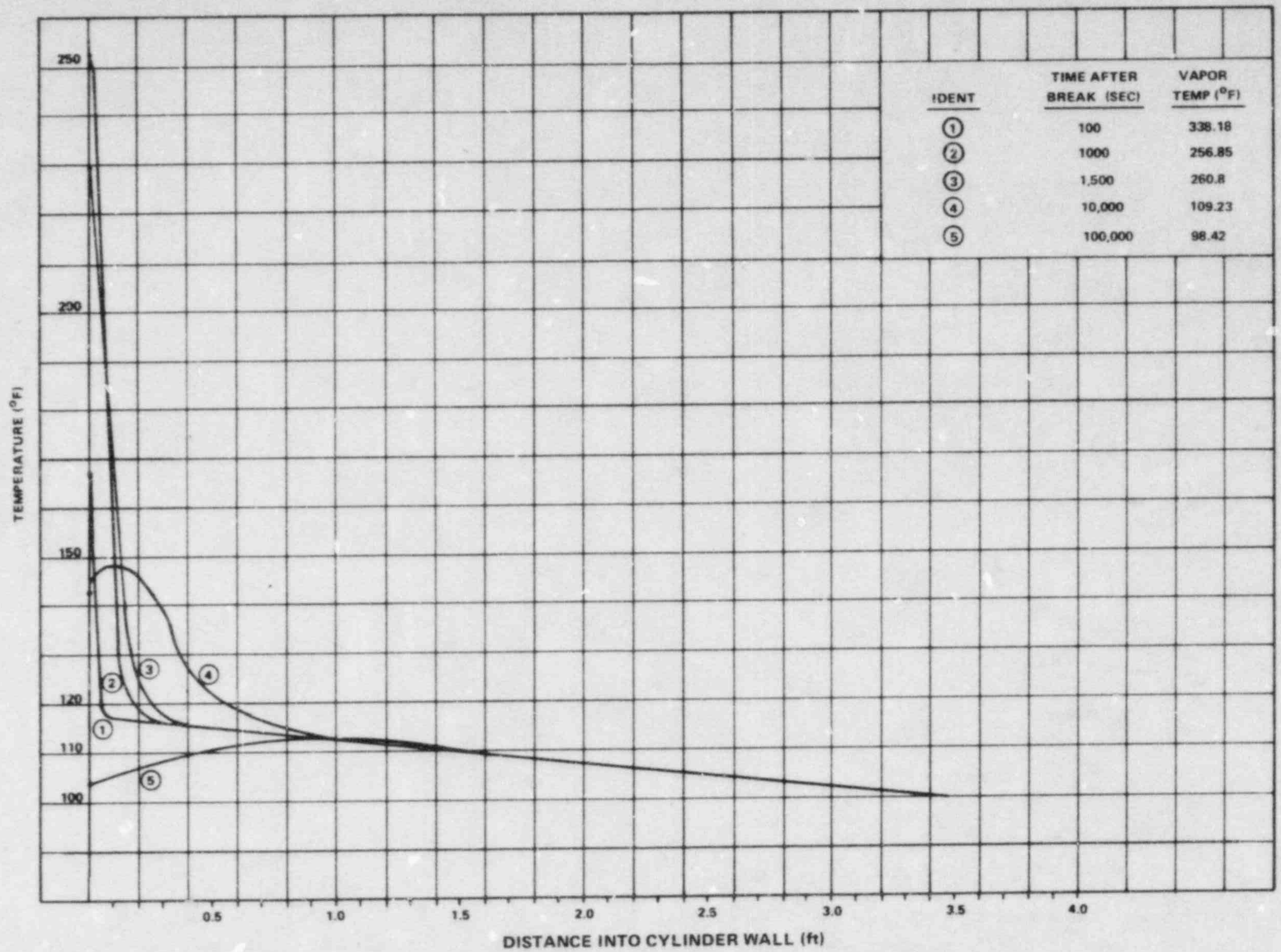

MAIN STEAM LINE BREAK (MSLB)

Figure 15
TEMPERATURE GRADIENTS THROUGH CONTAINMENT WALL
(Sheet 2 of 2)

CONTAINMENT BUILDING FINITE ELEMENT MODEL FROM BUTTRESS NUMBER 2 TO 3.

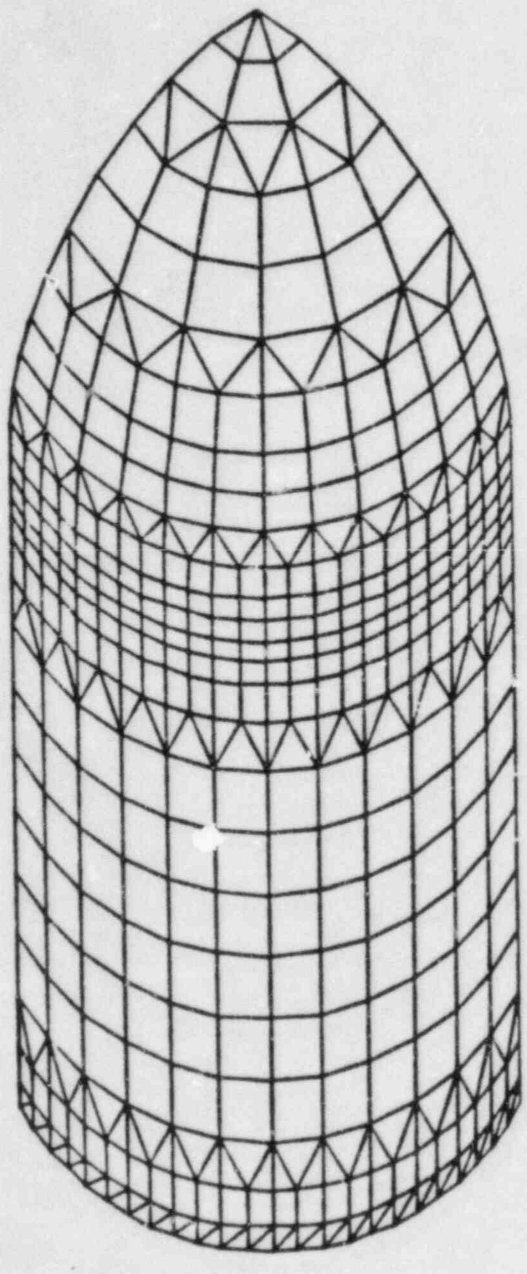

Figure 16
SHELL FINITE ELEMENT MODEL
(Sheet 1 of 4)

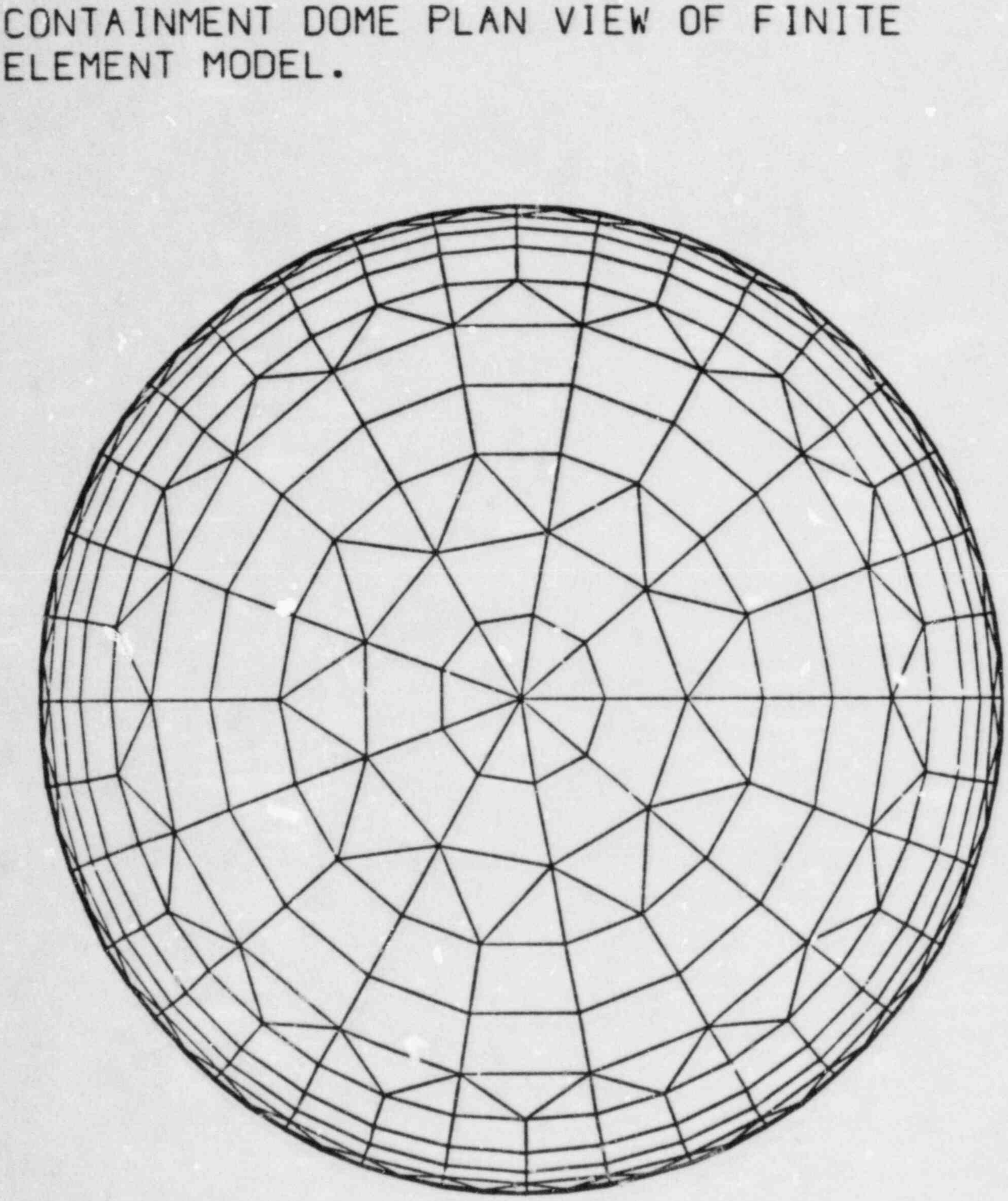

Figure 16
SHELL FINITE ELEMENT MODEL
(Sheet 2 of 4)

CONTAINMENT BASEMAT PLAN VIEW OF FINITE ELEMENT MODEL

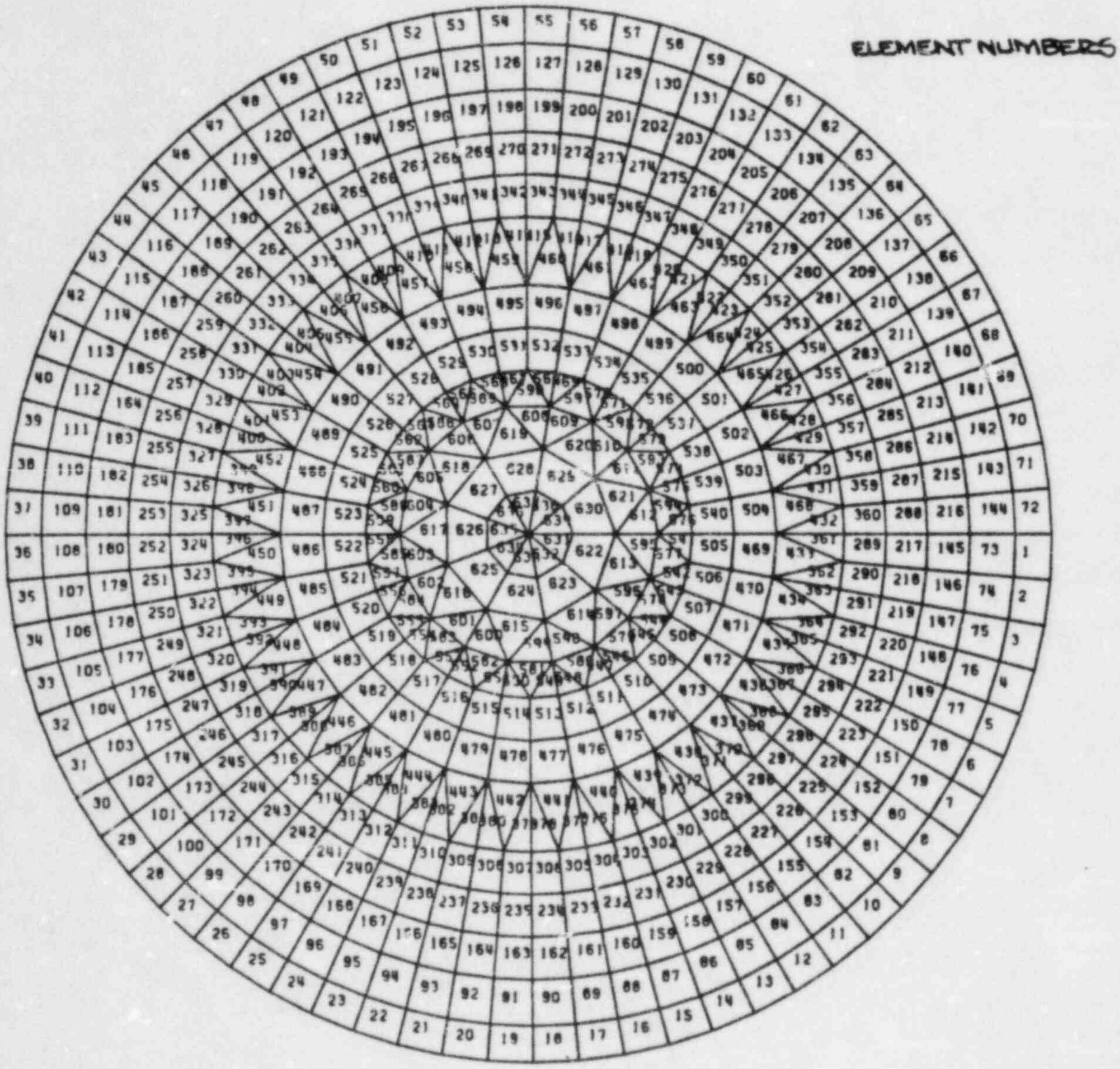

ELEMENT NUMBERS

Figure 16
SHELL FINITE ELEMENT MODEL
(Sheet 3 of 4)

A PARTIAL PLOT OF THE POLAR CRANE
BRACKET REGION OF THE CONT.BLDG.

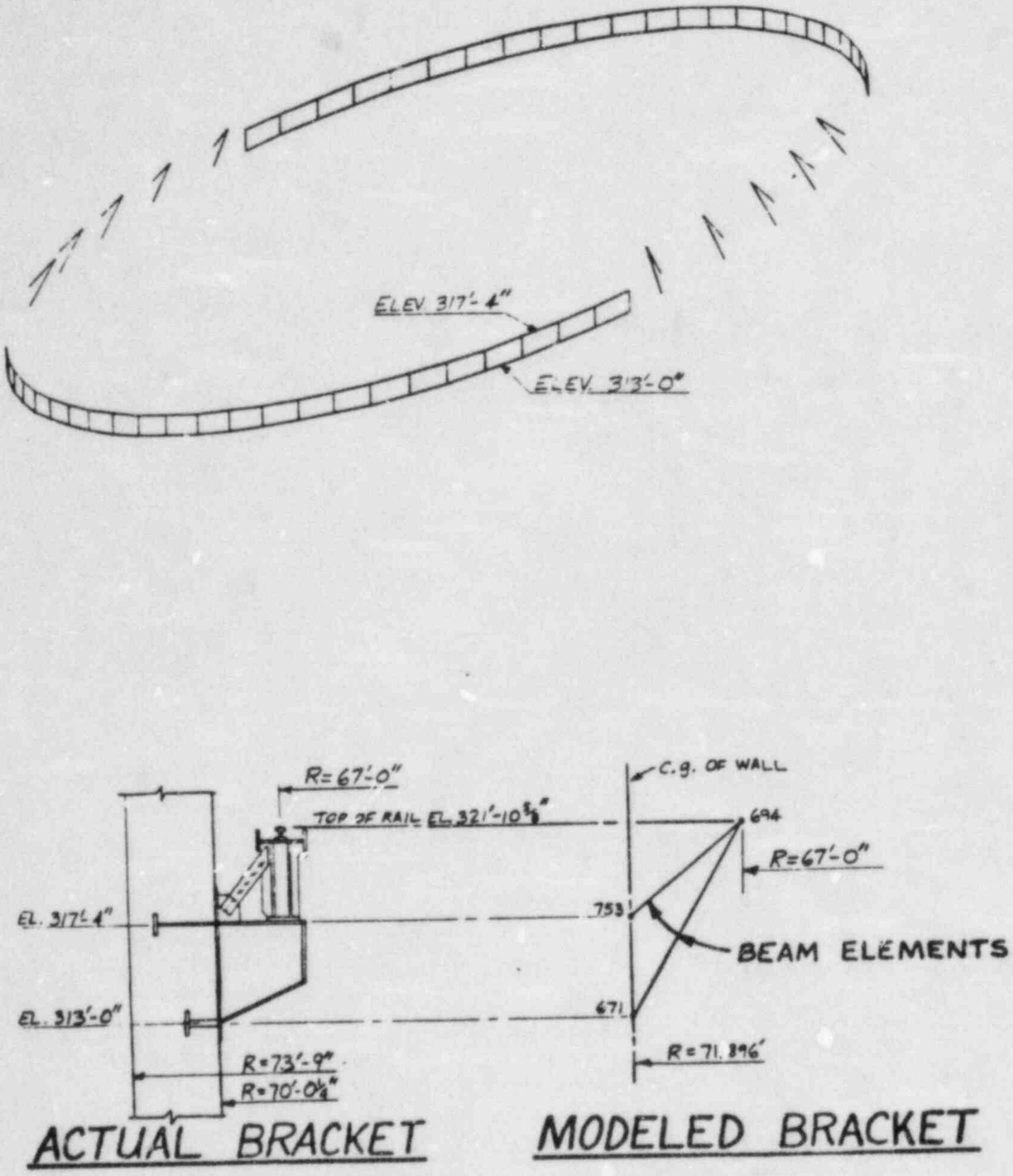

Figure 16
SHELL FINITE ELEMENT MODEL
(Sheet 4 of 4)

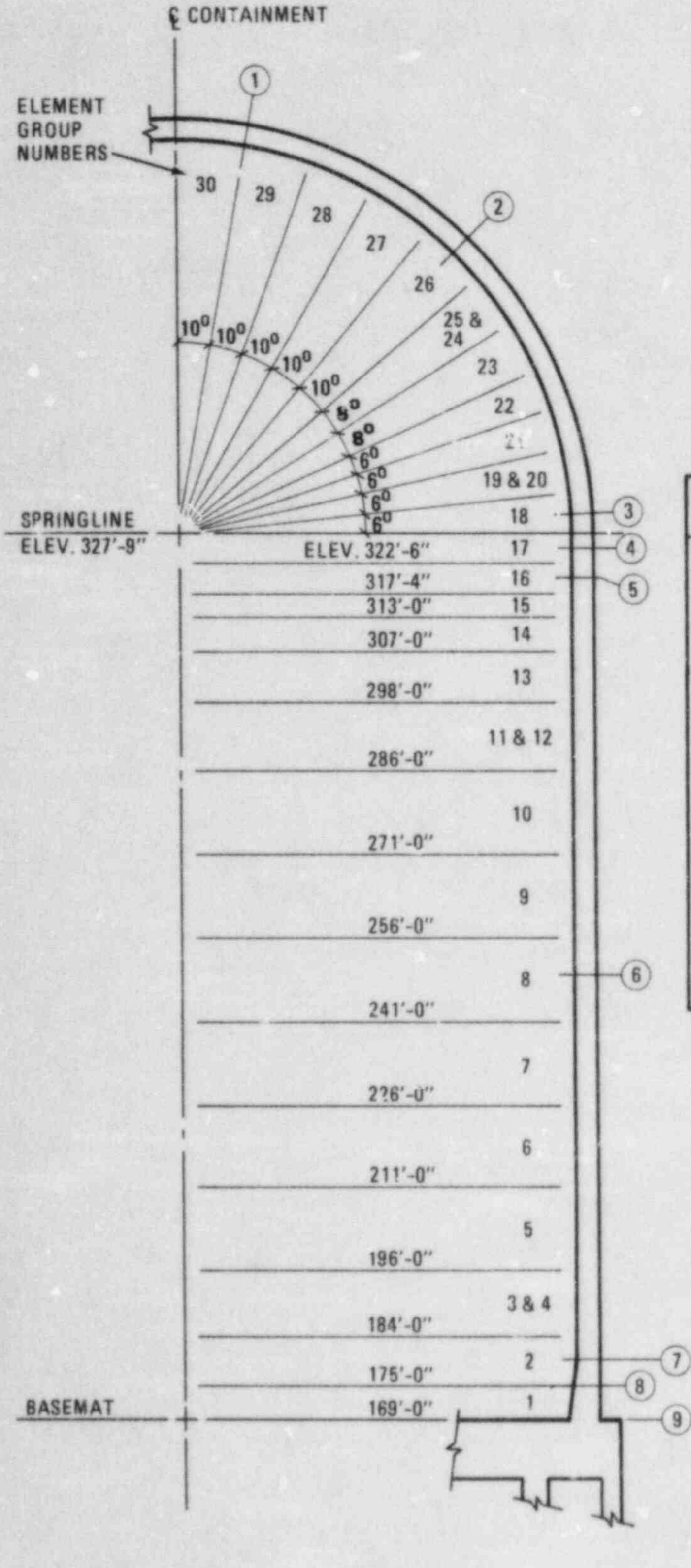

KEY LOCATIONS	DESCRIPTION	ELEV.	ELEMENT GROUP
1	10° BELOW APEX	398'-7"	30
2	45° ABOVE SPRINGLINE	378'-6"	26
3	FIRST ELEMENT ABOVE SPRINGLINE	331'-6"	18
4	FIRST ELEMENT BELOW SPRINGLINE	325'-2"	17
5	NEAR TOP OF POLAR CRANE BRACKET	319'-11"	16
6	MID-HEIGHT OF CYLINDER	248'-6"	8
7	TOP OF HAUNCH	179'-6"	2
8	ELEV. OF FIRST HOOP TENDON	175'-0"	1
9	BASEMAT/SHELL JUNCTION	169'-0"	1

Figure 17
CONTAINMENT SHELL KEY
LOCATIONS

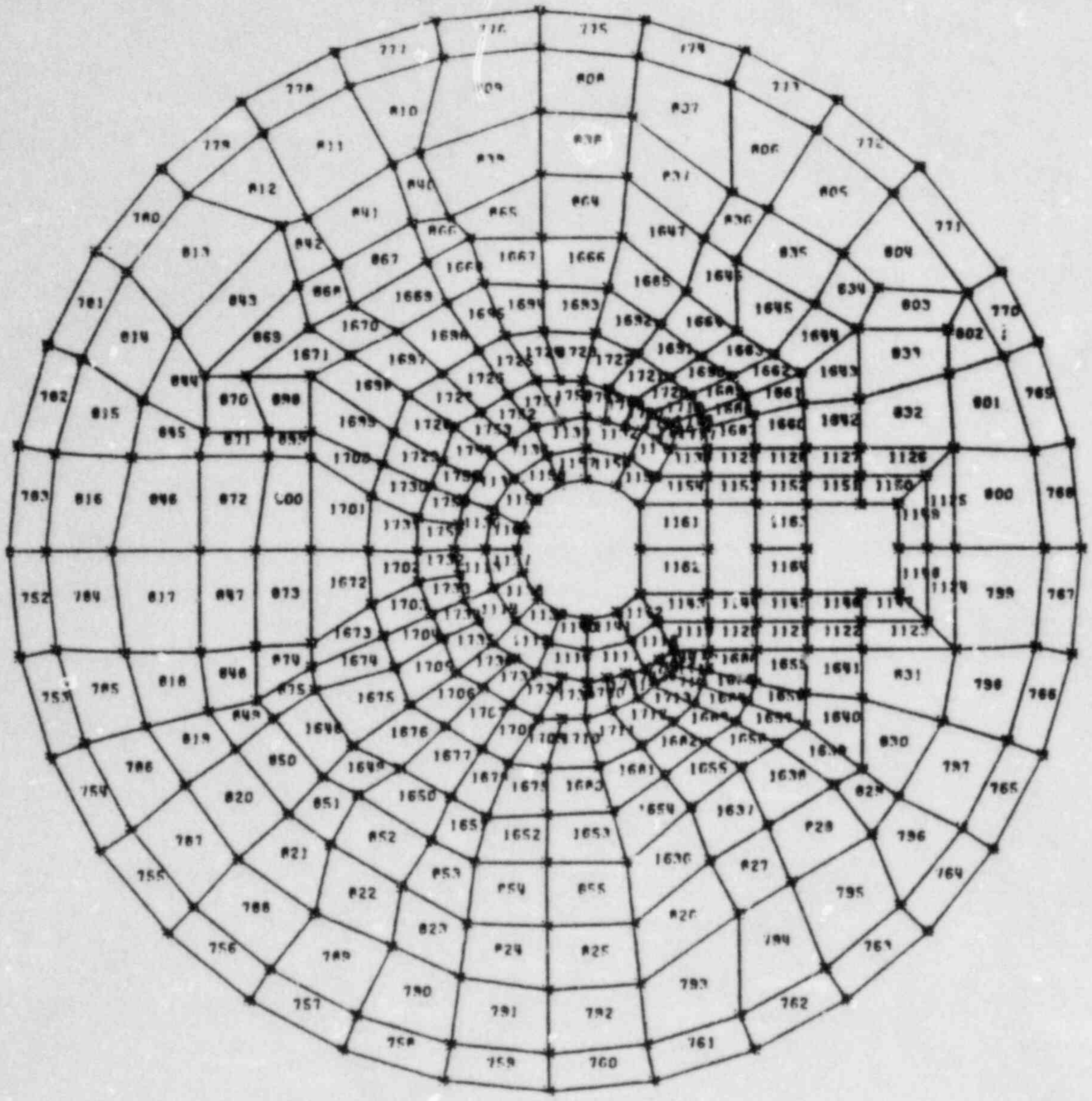

PLAN VIEW AT ELEV. 169.00

ELEMENT NUMBERS

THE TOP LAYER OF BASEMAT BRICK ELEMENTS IS SHOWN. THERE ARE THREE MORE LAYERS BELOW THIS ONE (EACH ADDITIONAL LAYER HAS A MESH IDENTICAL TO THAT OF THE TOP LAYER).

Figure 18
BASEMAT FINITE ELEMENT MODEL
(Shaet 1 of 6)

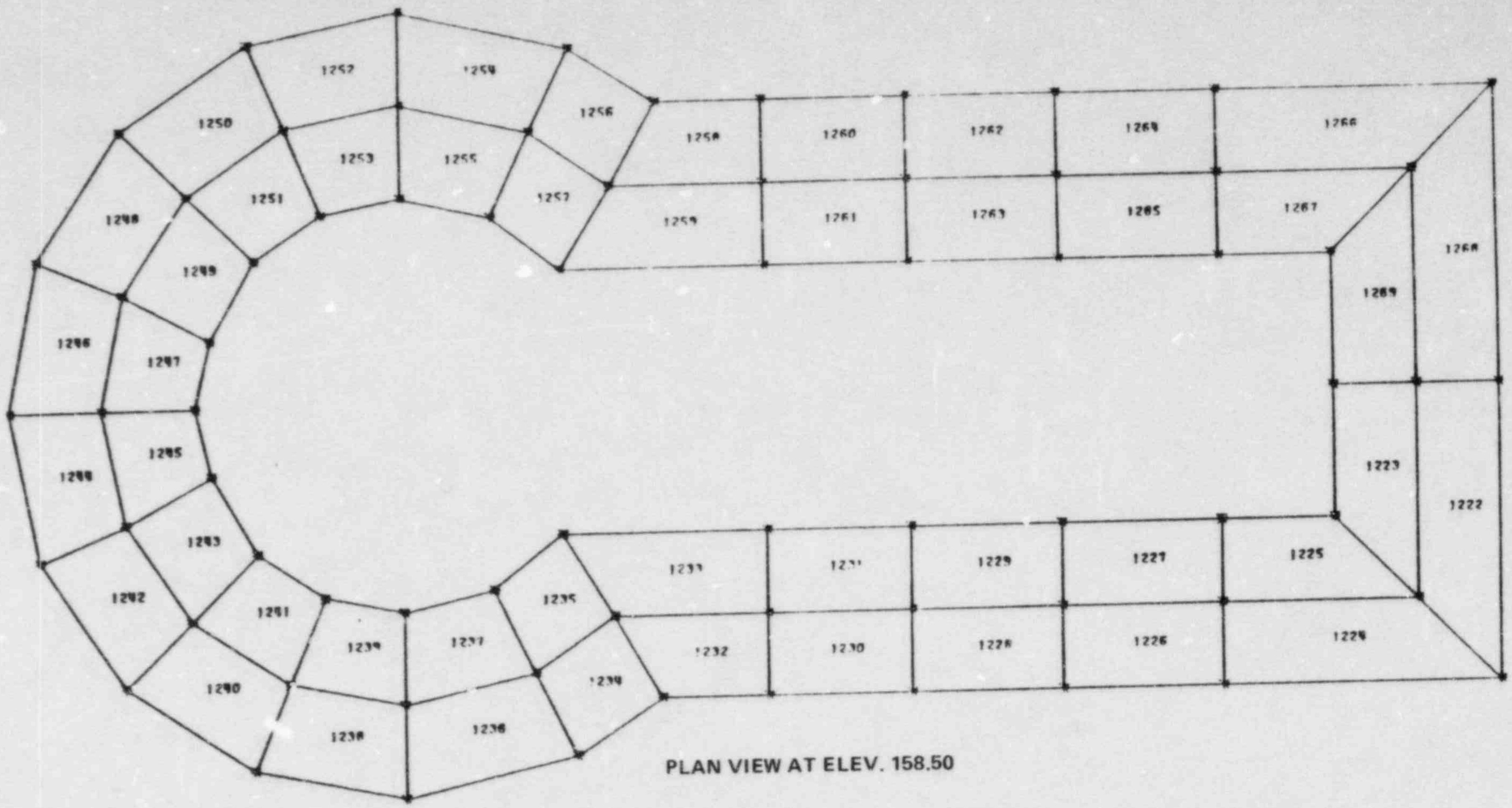

PLAN VIEW AT ELEV. 158.50

ELEMENT NUMBERS

THERE ARE TWO MORE LAYERS OF BRICK ELEMENTS BELOW THE MESH SHOWN ABOVE (EACH ADDITIONAL LAYER HAS A MESH IDENTICAL TO THAT SHOWN ABOVE) AND ABOVE THE REACTOR CAVITY BASEMAT MESH SHOWN ON SHEET 3.

Figure 18
BASEMAT FINITE ELEMENT MODEL
(Sheet 2 of 6)

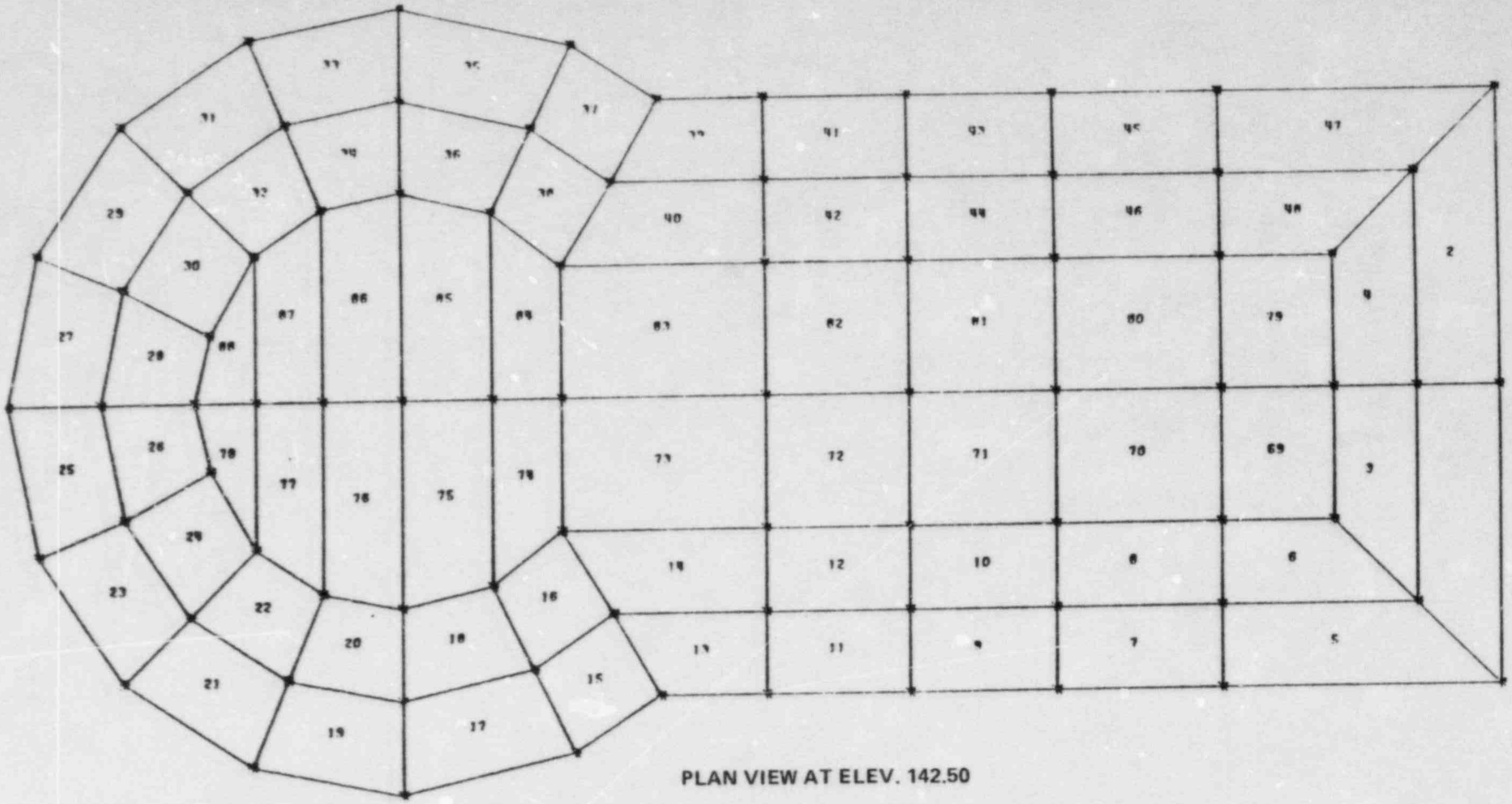

PLAN VIEW AT ELEV. 142.50

ELEMENT NUMBERS

Figure 18
BASEMAT FINITE ELEMENT MODEL
(Sheet 3 of 6)

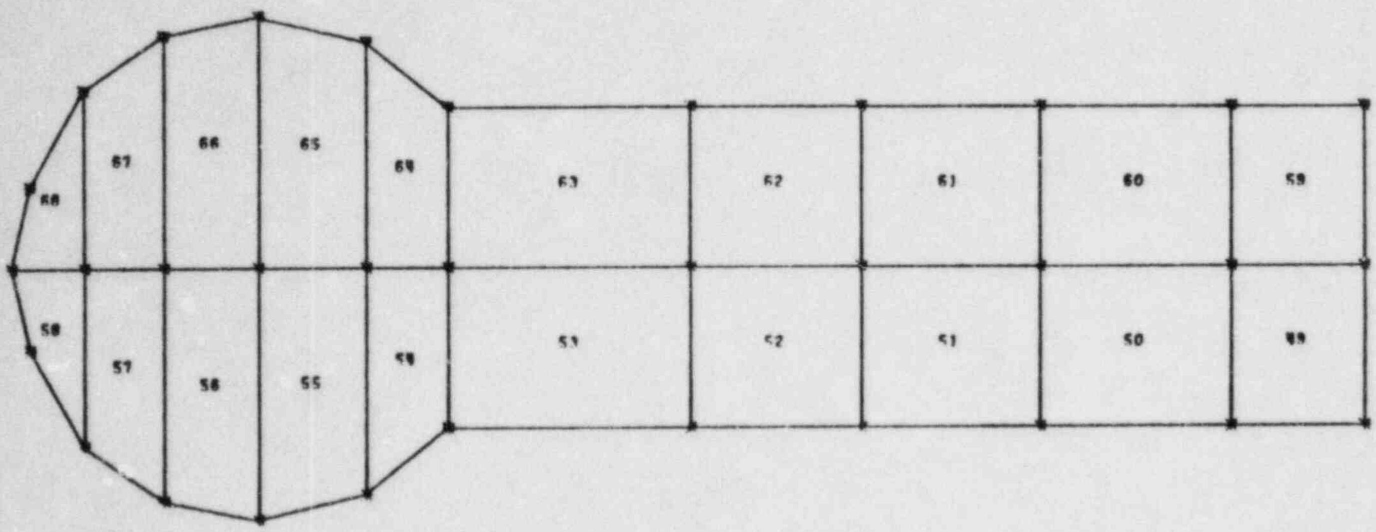

PLAN VIEW AT ELEV. 139.00

ELEMENTS NUMBERS

Figure 18
BASEMAT FINITE ELEMENT MODEL
(Sheet 4 of 6)

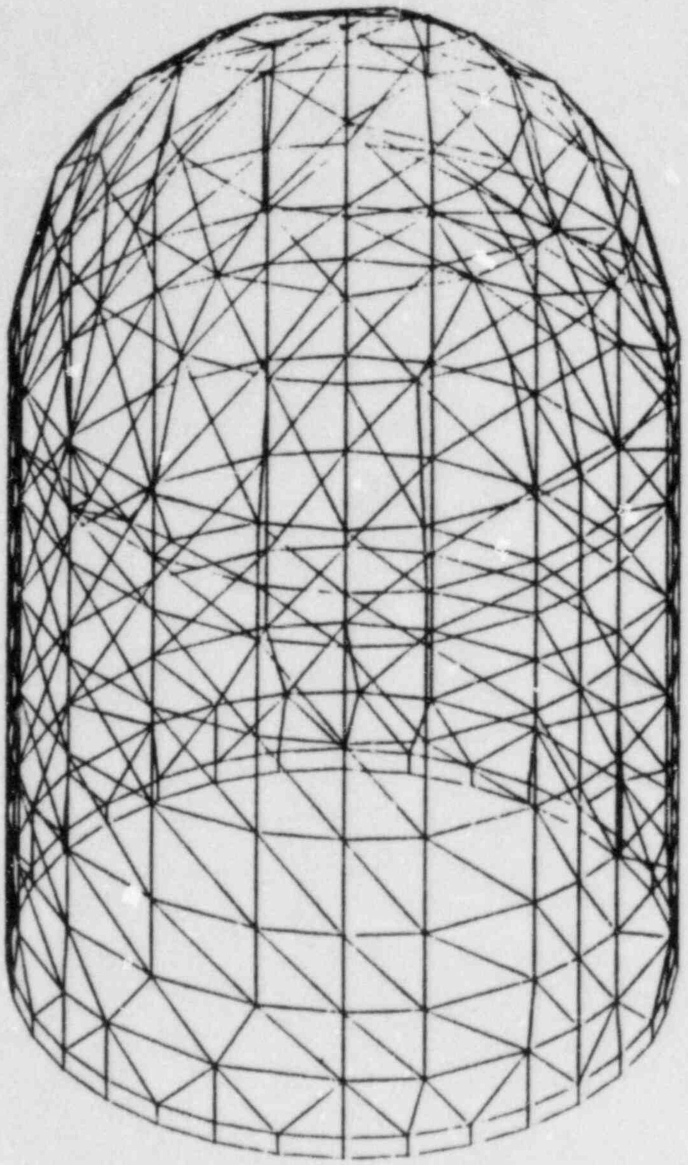

ISOMETRIC VIEW OF SHELL

Figure 18
BASEMAT FINITE ELEMENT MODEL
(Sheet 5 of 6)

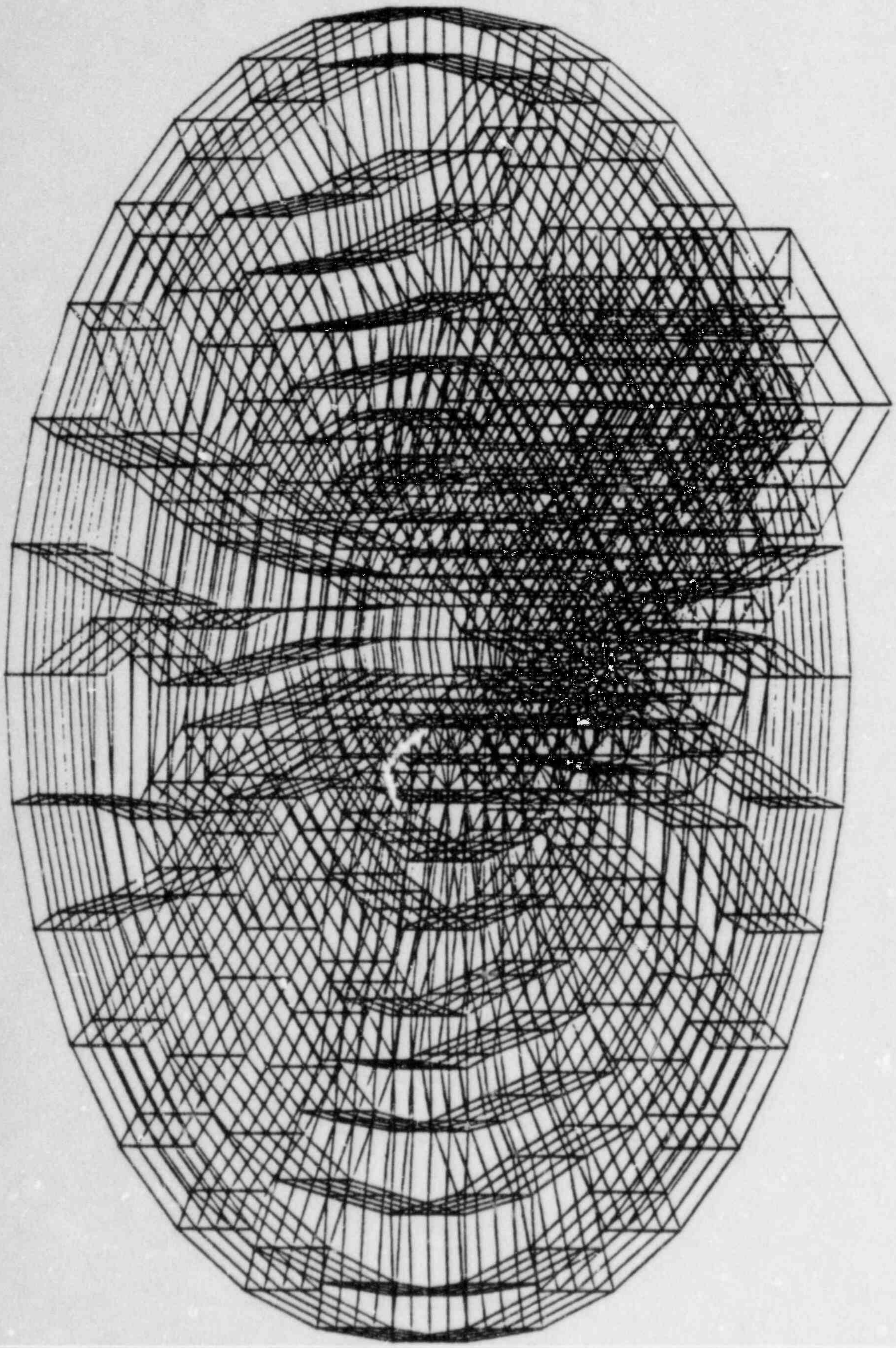

ISOMETRIC VIEW OF BASEMAT

Figure 18
BASEMAT FINITE ELEMENT MODEL
(Sheet 6 of 6)

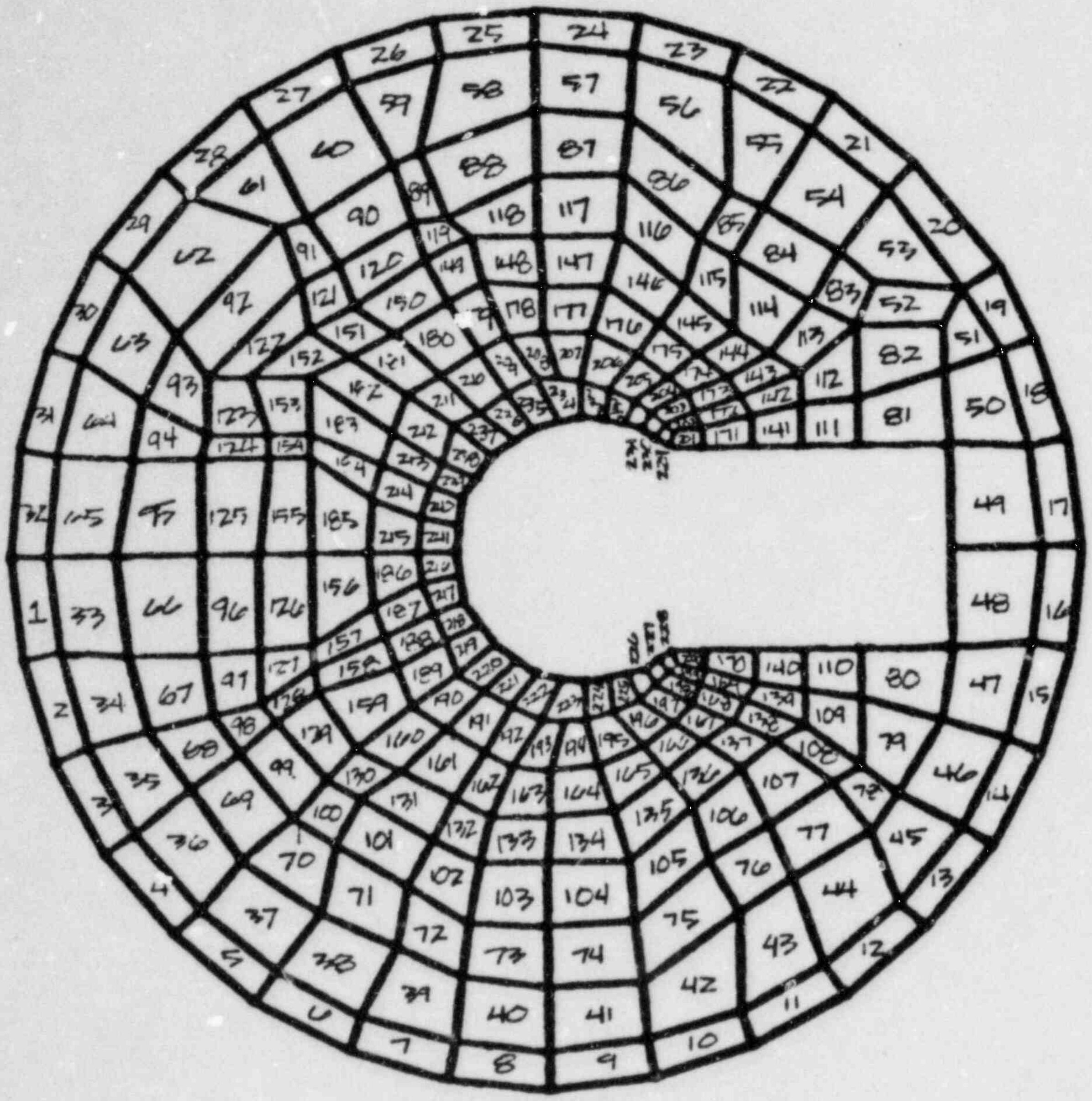

BASEMAT GRID ELEMENTS

KEY LOCATIONS	GRID ELEMENT NUMBERS	DESCRIPTION
1	96-241	INCLUDES BASEMAT AREAS WHICH HAVE A NORTH-SOUTH AND EAST-WEST REINFORCEMENT PATTERN.
2	33-65	INCLUDES THE FIRST RING OF GRID ELEMENTS INTERIOR OF THE CONTAINMENT CYLINDER. THE REINFORCEMENT PATTERN IS RADIAL AND CIRCUMFERENTIAL.

Figure 19
CONTAINMENT FOUNDATION
KEY LOCATIONS
(Sheet 1 of 3)

PLAN AT ELEVATION 153'-2" TO 158'-6"

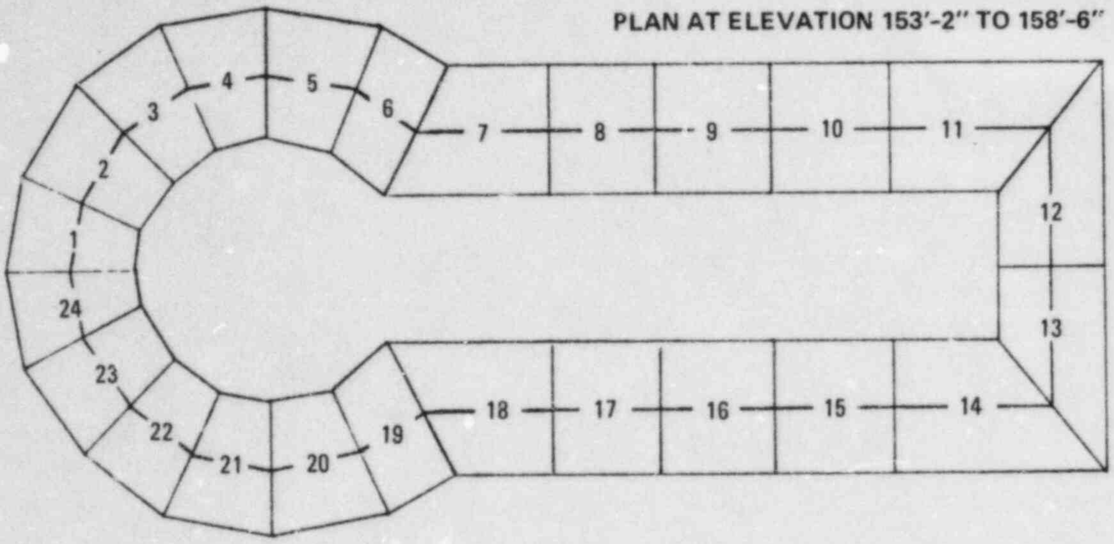

PLAN AT ELEVATION 147'-10" TO 153'-2"

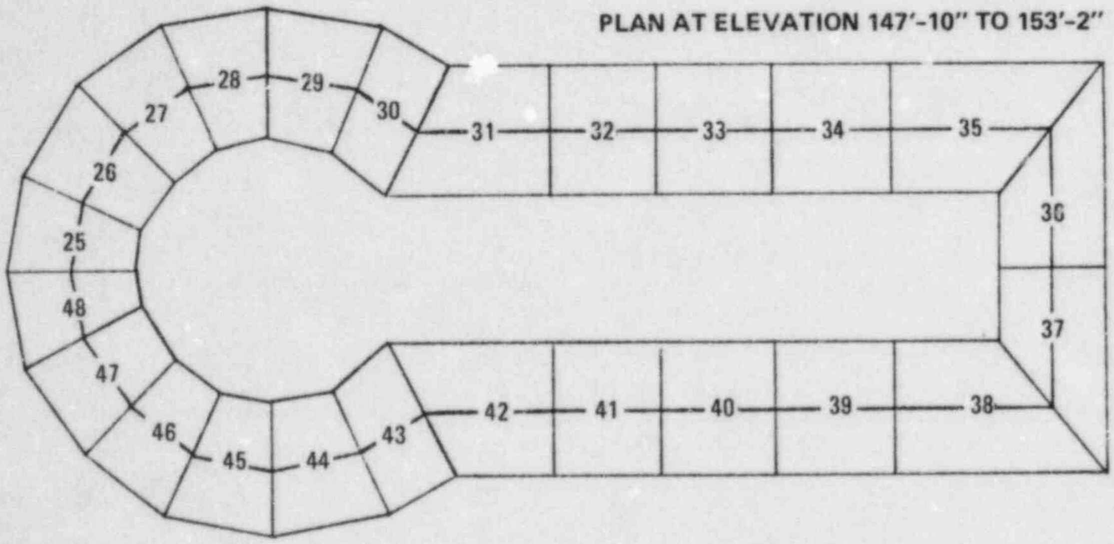

PLAN AT ELEVATION 142'-6" TO 147'-10"

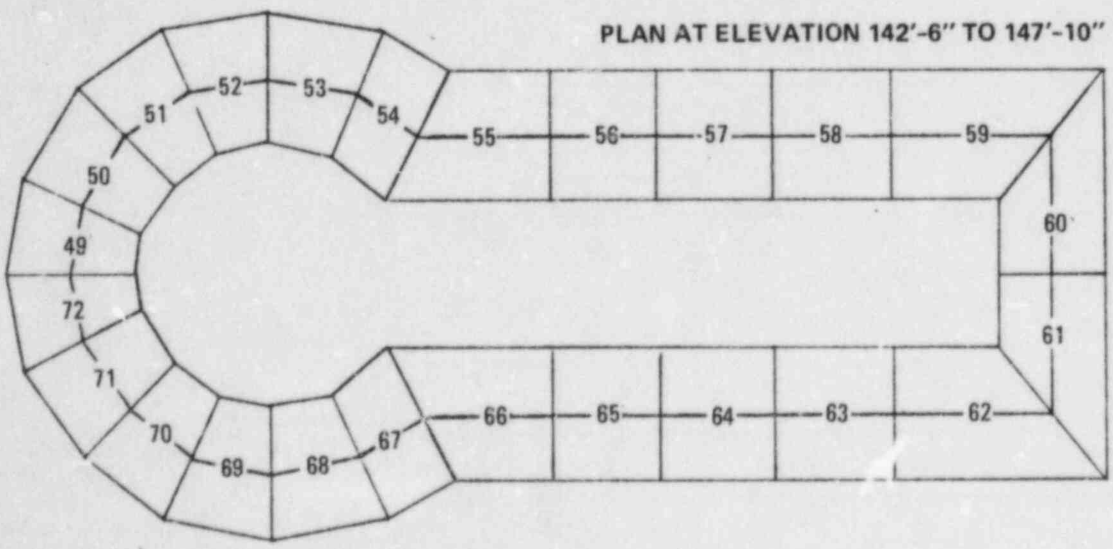

REACTOR CAVITY WALL GRID ELEMENTS (KEY LOCATION 3)

Figure 19
CONTAINMENT FOUNDATION
KEY LOCATIONS
(Sheet 2 of 3)

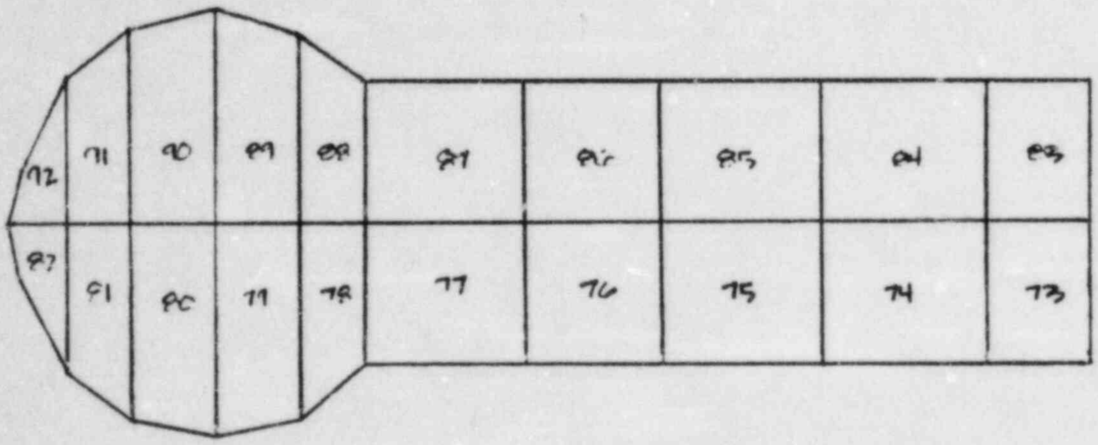

PLAN AT ELEVATION 134'-6" TO 142'-6"

REACTOR CAVITY SLAB GRID ELEMENTS (KEY LOCATION 4)

Figure 19
CONTAINMENT FOUNDATION
KEY LOCATIONS
(Sheet 3 of 3)

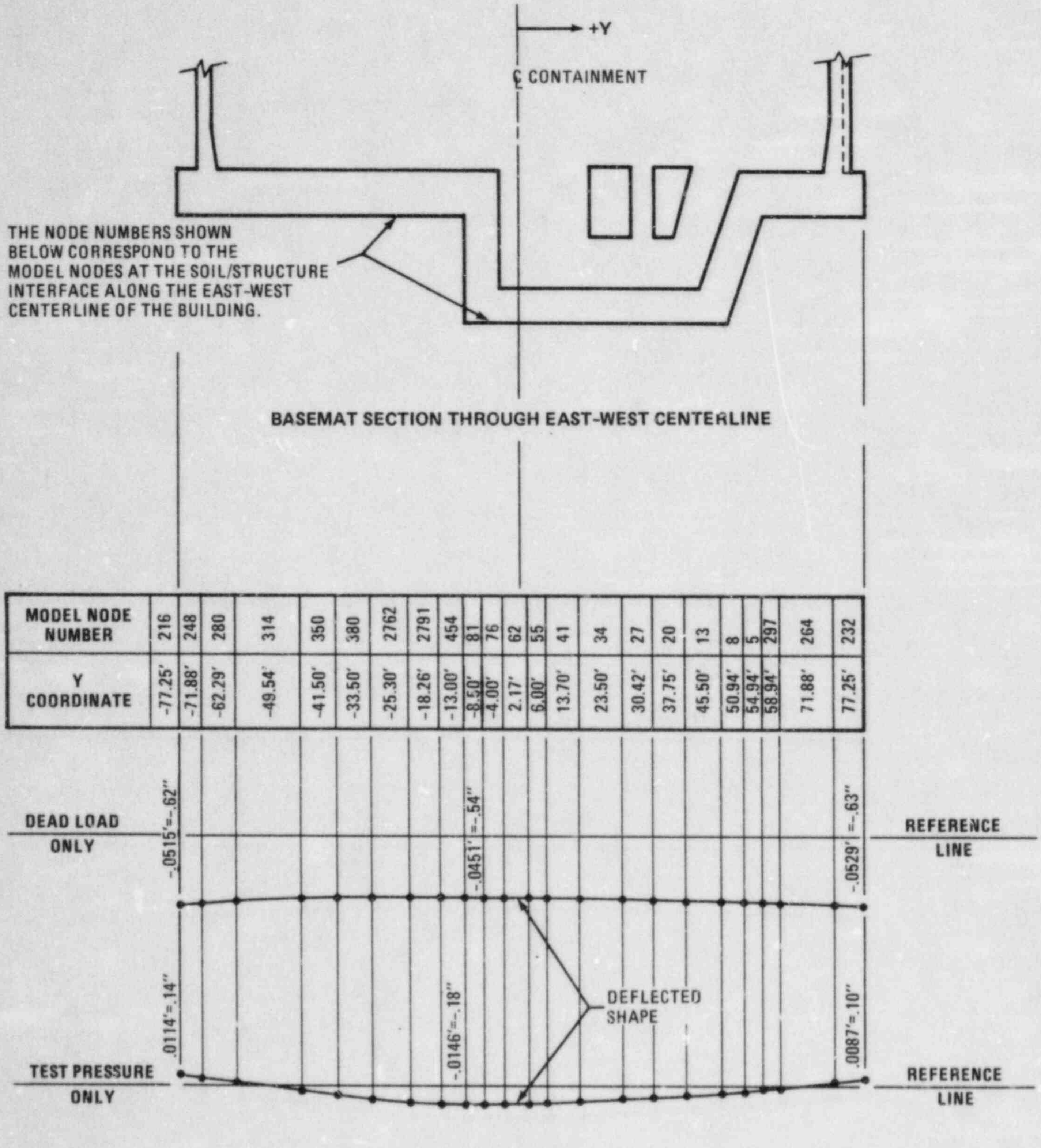

MODEL NODE NUMBER	Y COORDINATE
216	-77.25'
248	-71.88'
280	-62.29'
314	-49.54'
350	-41.50'
380	-33.50'
2762	-25.30'
2791	-18.26'
454	-13.00'
81	-8.50'
76	-4.00'
62	2.17'
55	6.00'
41	13.70'
34	23.50'
27	30.42'
20	37.75'
13	45.50'
8	50.94'
5	54.94'
297	58.94'
264	71.88'
232	77.25'

ONLY MAXIMUM AND MINIMUM DISPLACEMENTS ARE SHOWN.

Figure 20
BASEMAT DISPLACEMENT
ANALYSIS RESULTS

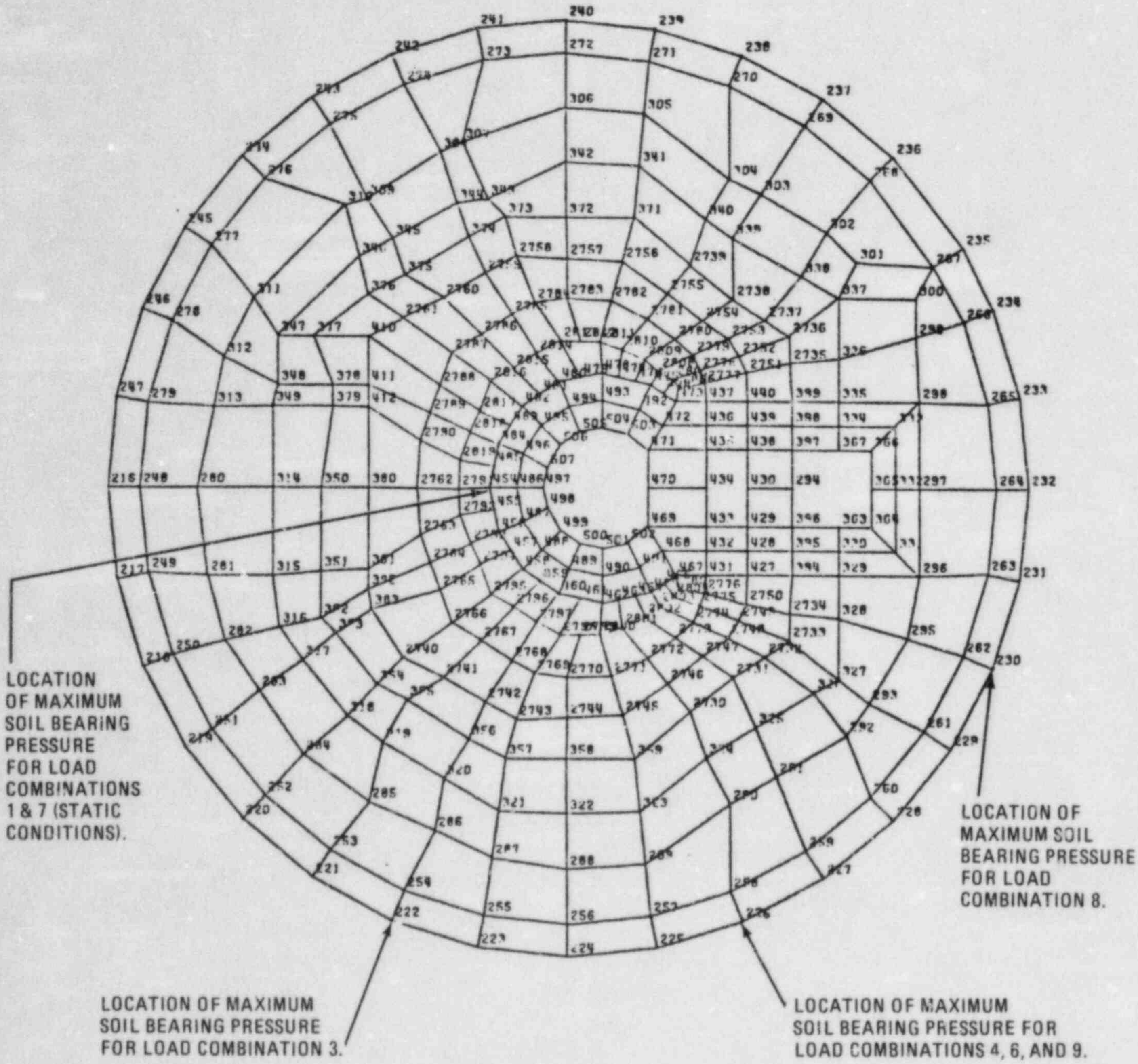

PLAN VIEW AT THE BOTTOM OF THE BASEMAT

SEE TABLE 6 FOR MAXIMUM SOIL BEARING PRESSURES.

Figure 21
LOCATIONS OF MAXIMUM
SOIL BEARING PRESSURE

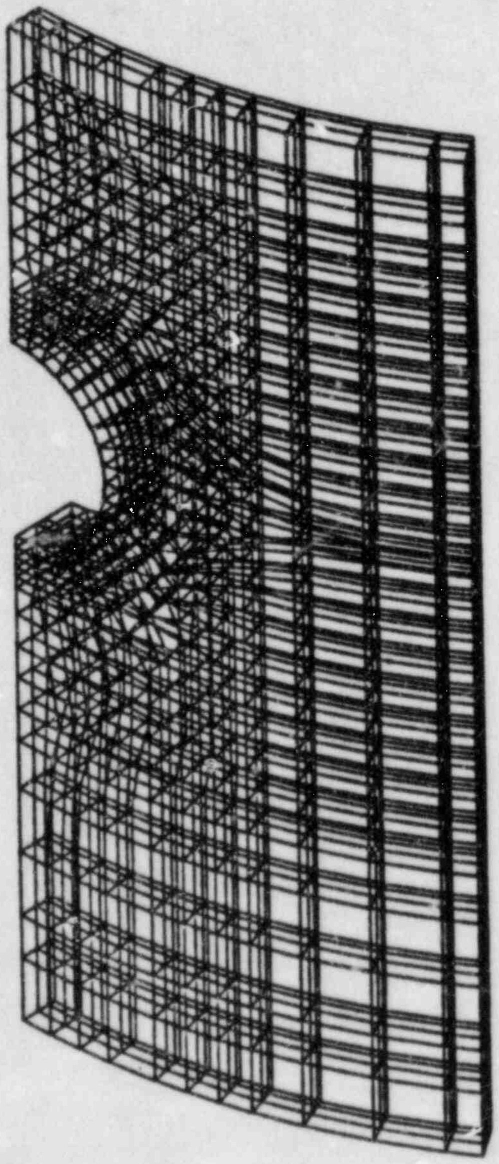

ISOMETRIC VIEW OF EQUIPMENT HATCH HALF-MODEL (BRICKS)

Figure 22
FINITE ELEMENT MODEL FOR THE THICKENED SHELL
AT THE EQUIPMENT HATCH
(Sheet 1 of 5)

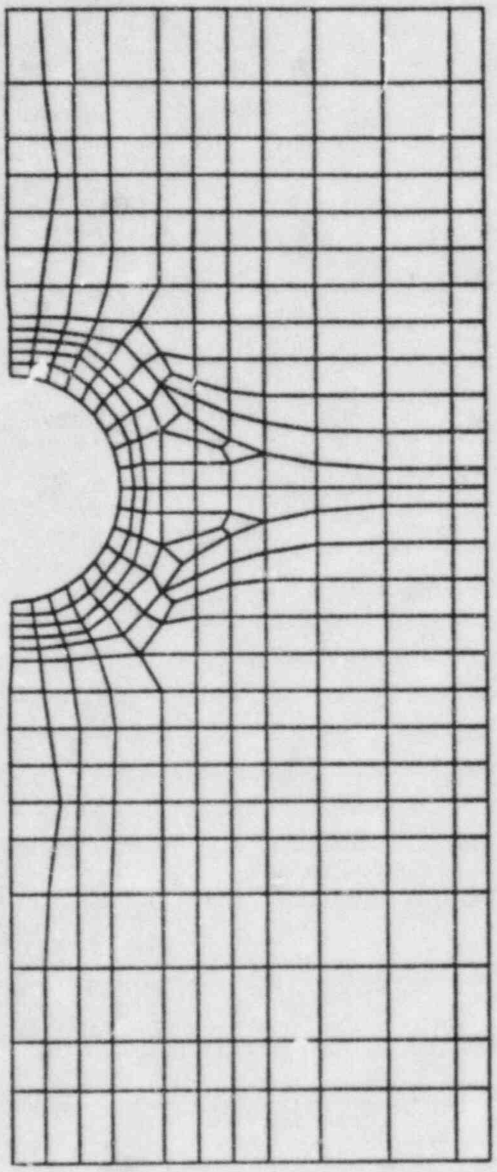

TYPICAL BRICK ELEMENT LAYER

Figure 22
FINITE ELEMENT MODEL FOR THE THICKENED SHELL
AT THE EQUIPMENT HATCH
(Sheet 2 of 5)

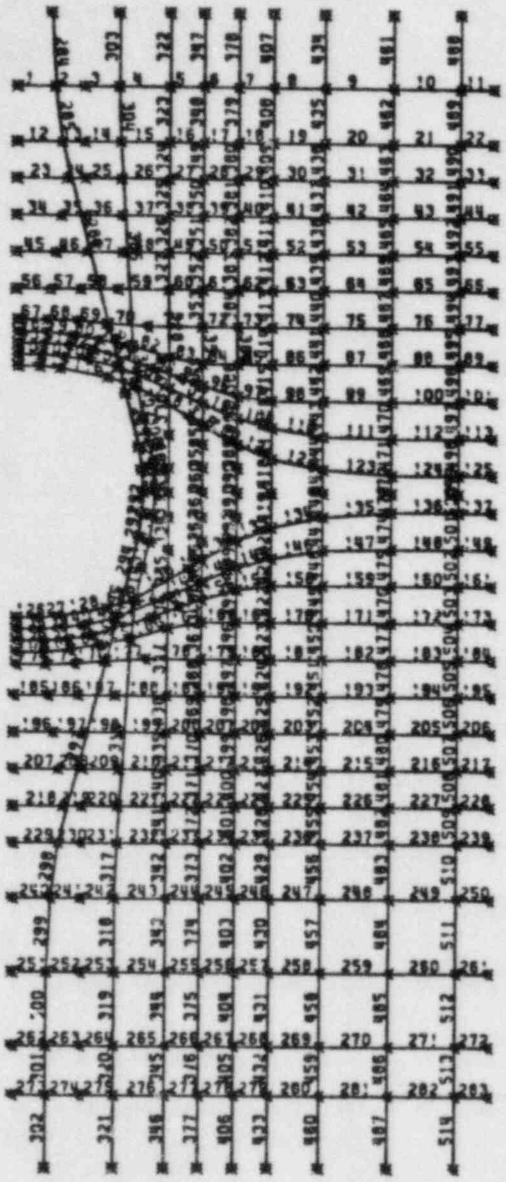

TRUSS ELEMENTS (POST-TENSIONING SYSTEM)

Figure 22
FINITE ELEMENT MODEL FOR THE THICKENED SHELL
AT THE EQUIPMENT HATCH
(Sheet 3 of 5)

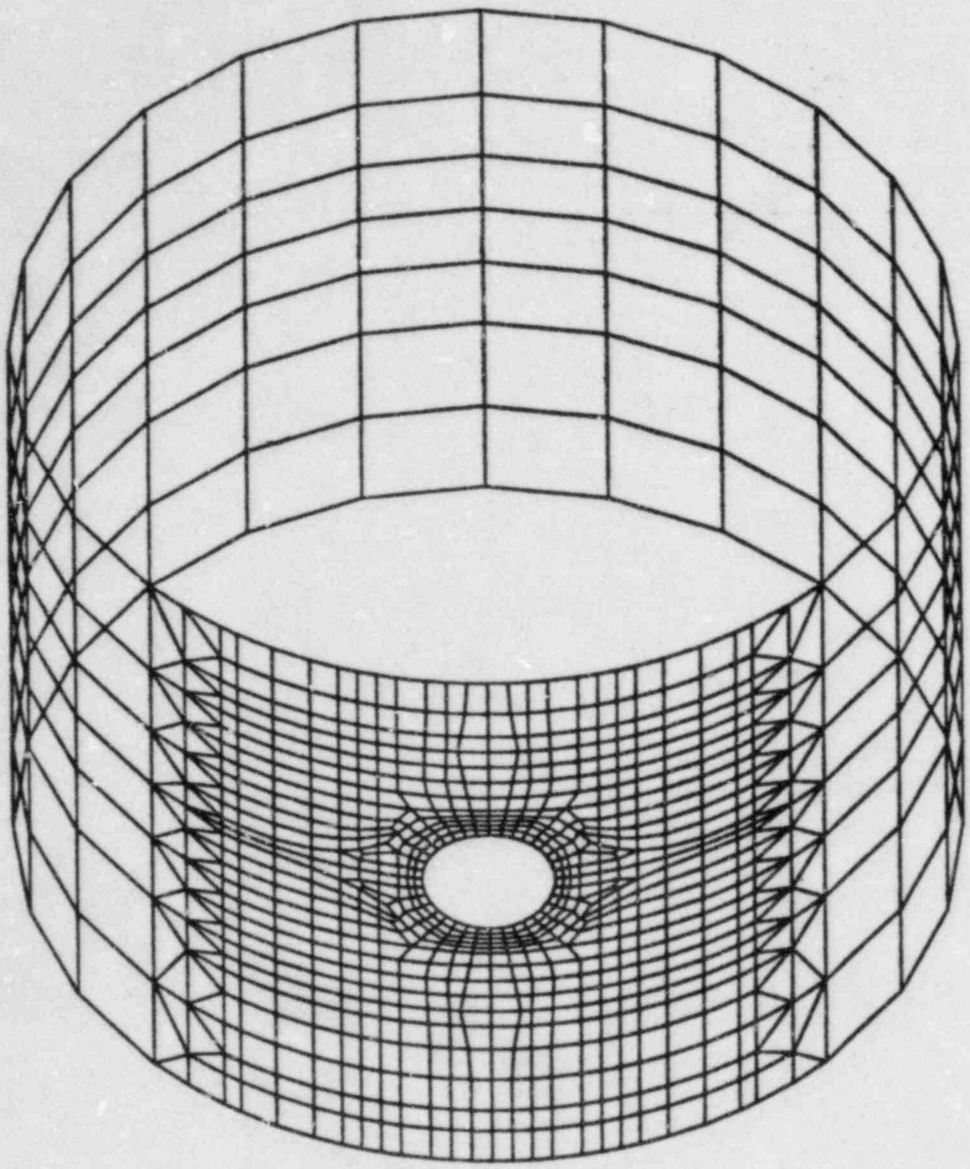

ISOMETRIC VIEW OF EQUIPMENT HATCH FULL-MODEL (LCCT9)

Figure 22
FINITE ELEMENT MODEL FOR THE THICKENED SHELL
AT THE EQUIPMENT HATCH
(Sheet 4 of 5)

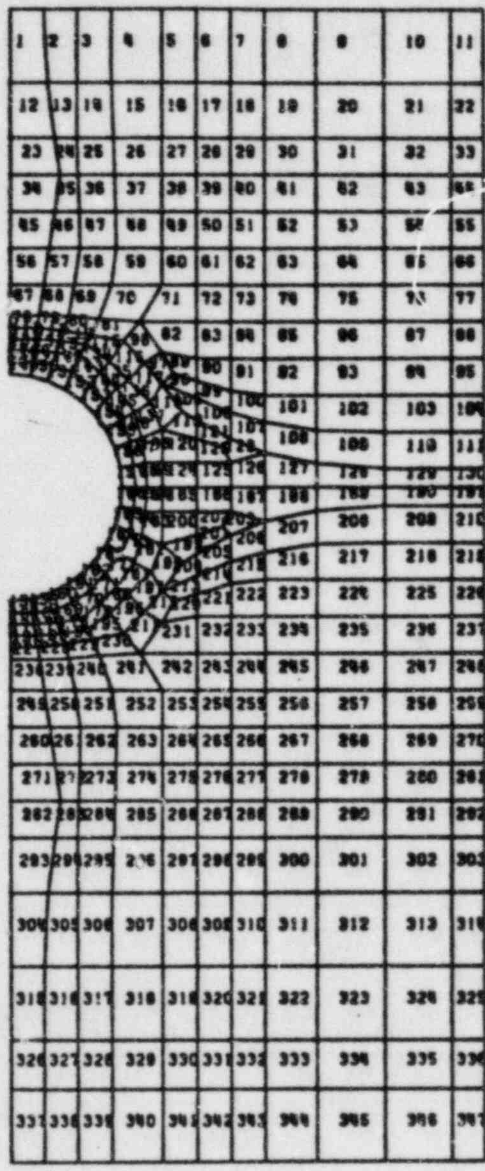

KEY LOCATION IS THE ROW OF ELEMENTS DIRECTLY BELOW THE HORIZONTAL CENTERLINE OF THE OPENING. ELEMENT NUMBERS 166, 175, AND 184 THROUGH 191.

ELEMENT NUMBERS OF ELEMENTS CORRESPONDING TO THE HALF-MODEL

PARTIAL PLOT OF FULL MODEL

NOTE: THIS PLOT AND NUMBERING SYSTEM ARE ALSO APPLICABLE TO THE GRID ELEMENTS OF THE HALF MODEL.

Figure 22
FINITE ELEMENT MODEL FOR THE THICKENED SHELL
AT THE EQUIPMENT HATCH
(Sheet 5 of 5)

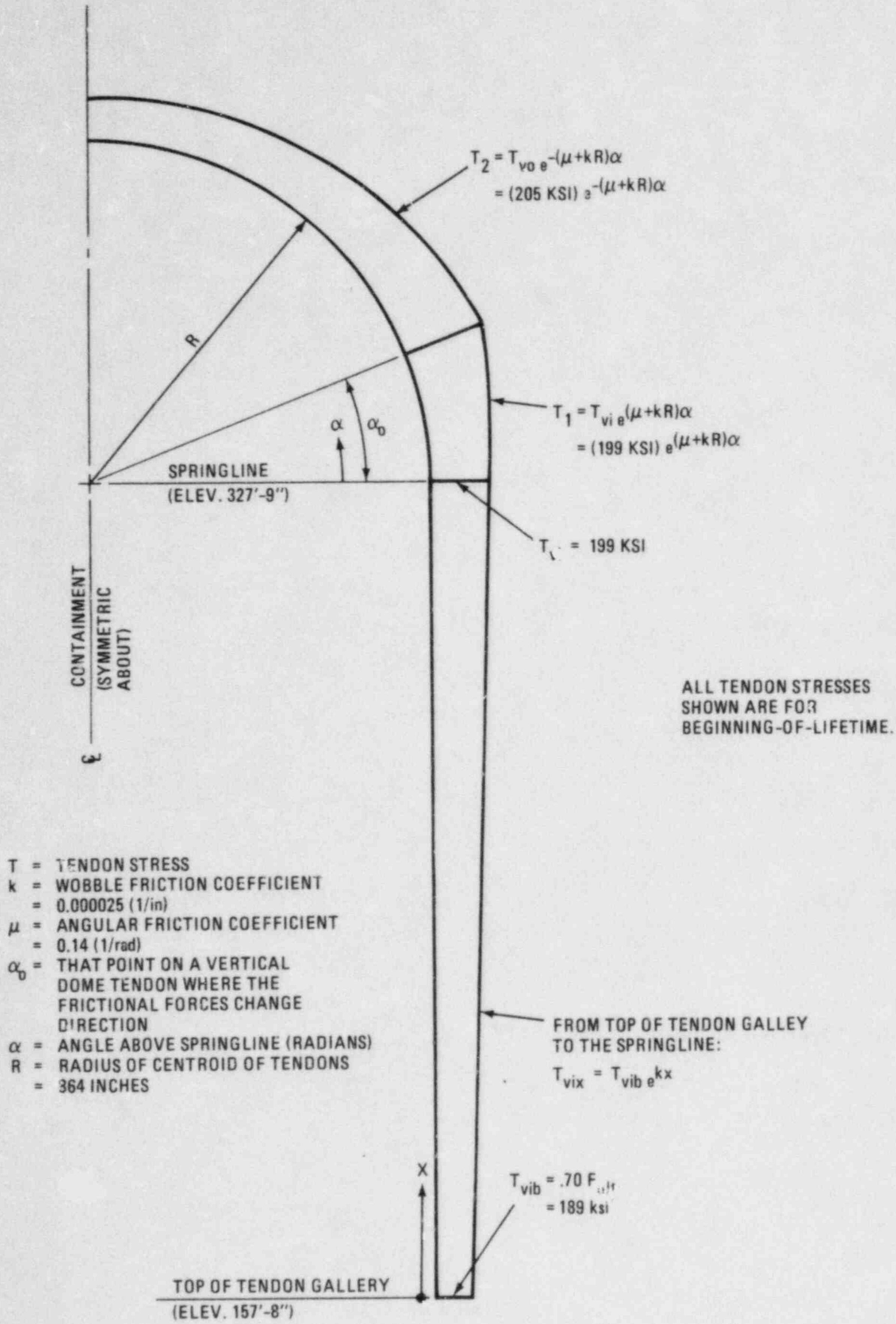

Figure 23
EFFECTIVE PRESTRESS FOR A VERTICAL
INVERTED U-SHAPED TENDON

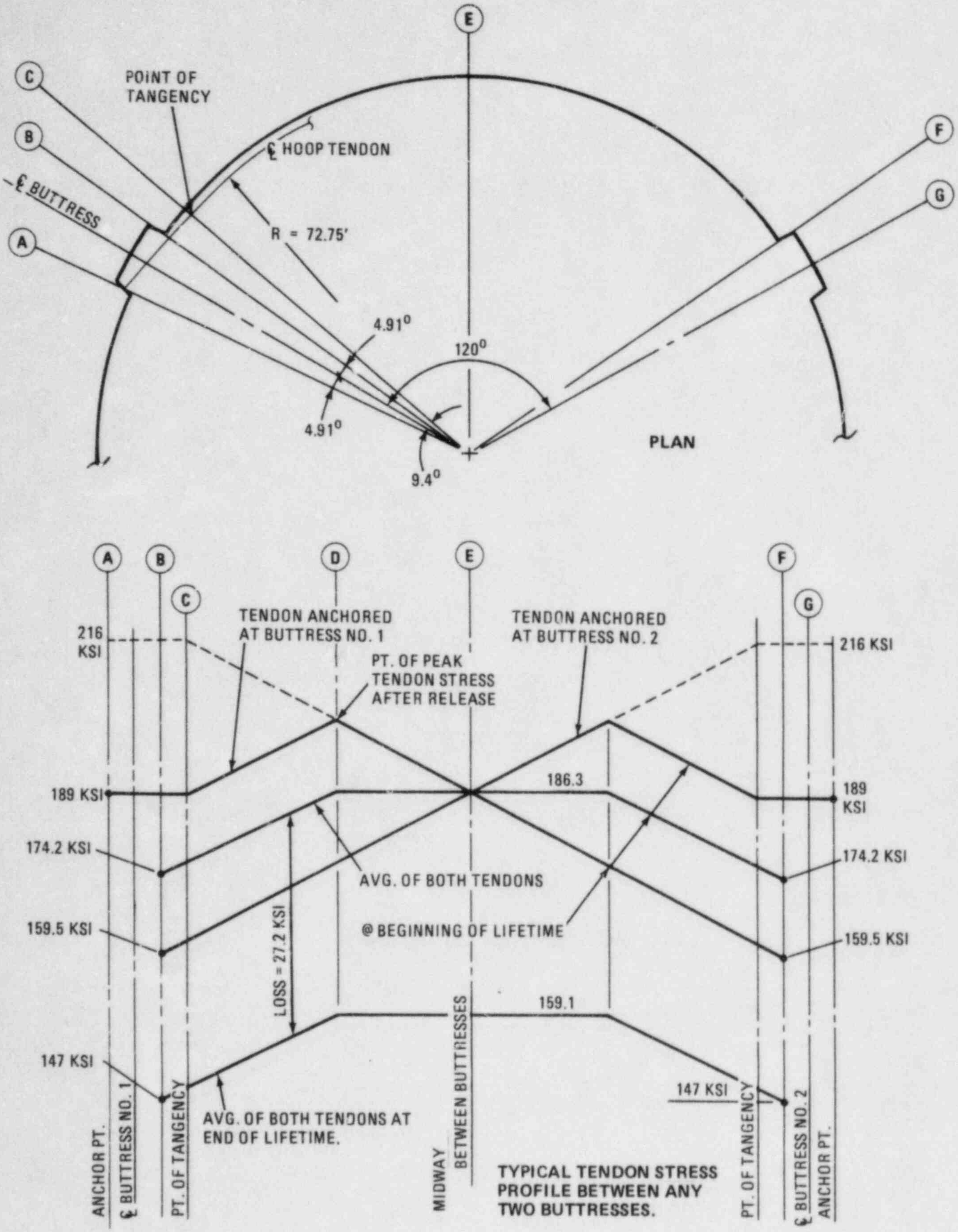

Figure 24
EFFECTIVE PRESTRESS FOR A CYLINDER HOOP TENDON

VERTICAL (MERIDONAL) REINFORCING IAD AT ELEVATION 169'-0"

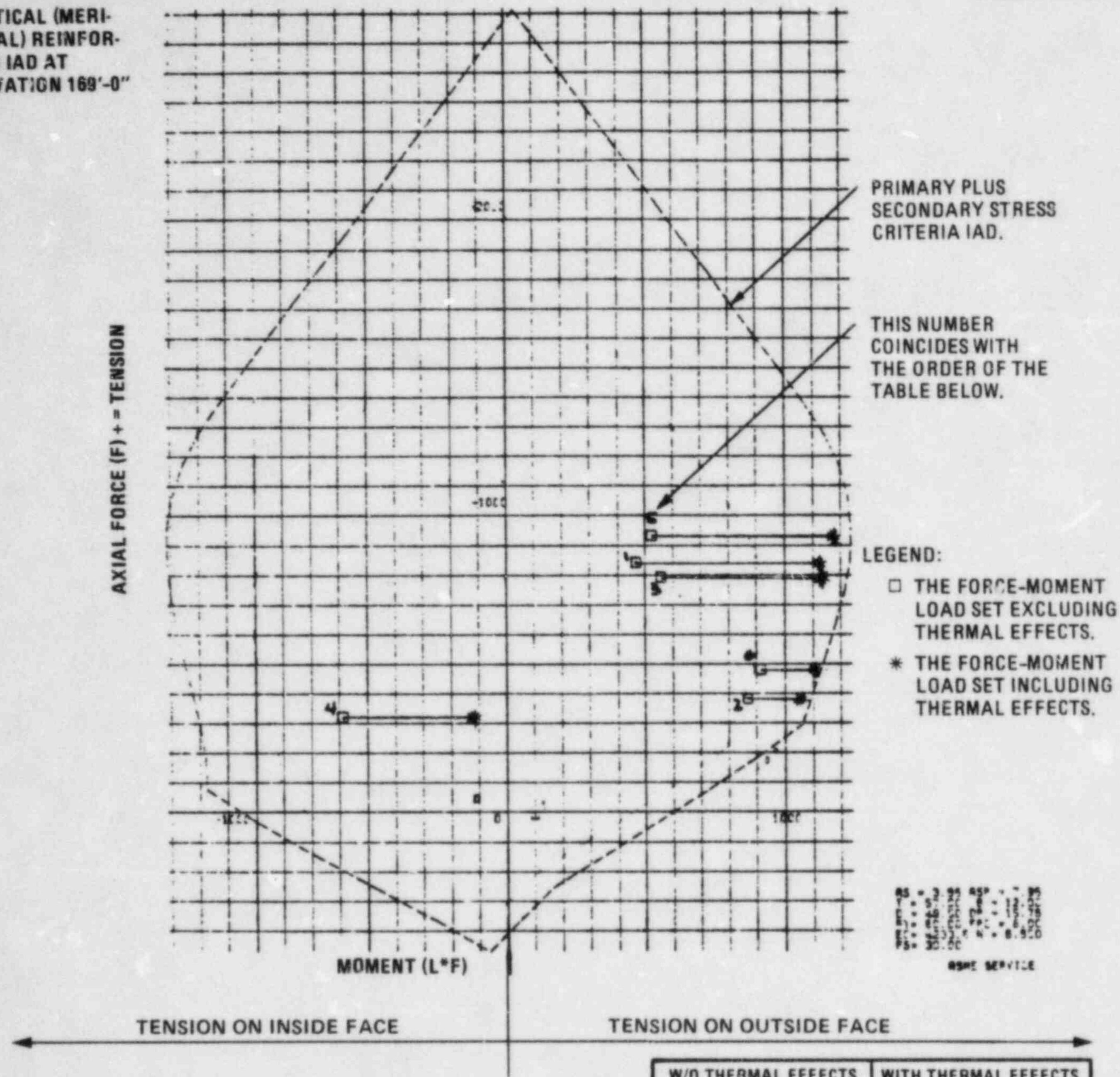

KEY LOCATION (SEE FIG. 17)	ELEMENT GROUP (SEE FIG. 17)	ELEMENT NUMBER	LOAD COMBTION (TABLE 5)	AXIAL FORCE (K/FT)	W/O THERMAL EFFECTS INITIAL MOMENT (FT-K/FT)	W/O THERMAL EFFECTS UFS % (C)	WITH THERMAL EFFECTS FINAL MOMENT (FT-K/FT)	WITH THERMAL EFFECTS UFS % (C)
9	1	10	4 (A)	-841	480	27	1119	78
9	1	55	4 (A)	-394	880	68	1065	85
9	1	55	4 (A)	-800	567	34	1132	80
9	1	10	1 (B)	-321	-577	49	-111	16
9	1	10	4 (B)	-920	525	30	1177	82
9	1	55	4 (B)	-476	930	71	1127	88

(A) PRESTRESS FORCES AT END-OF-LIFETIME.
(B) PRESTRESS FORCES AT BEGINNING-OF-LIFETIME.
(C) SEE SECTION 5.1.1 FOR A DESCRIPTION OF UTILIZATION FACTOR UFS.

Figure 25
CYLINDER INTERACTION DIAGRAMS
WITH THERMAL EFFECTS INCLUDED
(Sheet 1 of 12)

VERTICAL (MERIDONAL) REINFORCING IAD AT ELEVATION 169'-0"

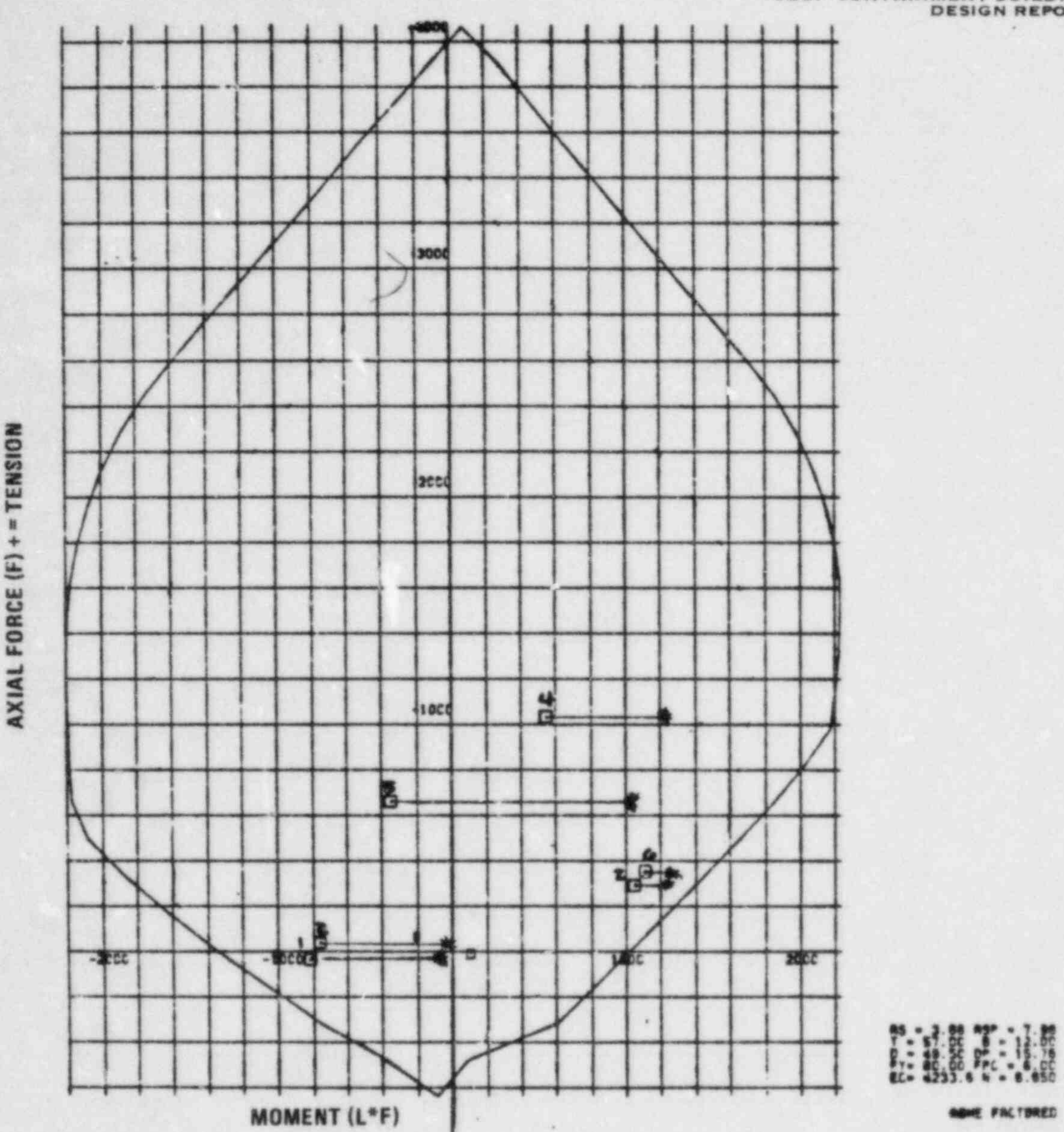

TENSION ON INSIDE FACE ← → TENSION ON OUTSIDE FACE

KEY LOCATION (SEE FIG. 17)	ELEMENT GROUP (SEE FIG. 17)	ELEMENT NUMBER	LOAD COMB'TION (TABLE 5)	AXIAL FORCE (K/FT)	W/O THERMAL EFFECTS: INITIAL MOMENT (FT-K/FT)	W/O THERMAL EFFECTS: UFS % (C)	WITH THERMAL EFFECTS: FINAL MOMENT (FT-K/FT)	WITH THERMAL EFFECTS: UFS % (C)
9	1	10	8 (A)	43	-804	56	-77	14
9	1	55	5 (A)	-292	1069	71	1236	83
9	1	10	8 (B)	-36	-758	50	-25	10
9	1	10	5 (B)	-1024	566	19	1235	50
9	1	10	9 (B)	-664	-331	20	1062	50
9	1	55	5 (B)	-374	1119	69	1287	80

(A) PRESTRESS FORCES AT END-OF-LIFETIME.
(B) PRESTRESS FORCES AT BEGINNING-OF-LIFETIME.
(C) SEE SECTION 5.1.1 FOR A DESCRIPTION OF UTILIZATION FACTOR UFS.

Figure 25
CYLINDER INTERACTION DIAGRAMS
WITH THERMAL EFFECTS INCLUDED
(Sheet 2 of 12)

HORIZONTAL (HOOP) REINFORCING IAD AT ELEVATION 169'-0"

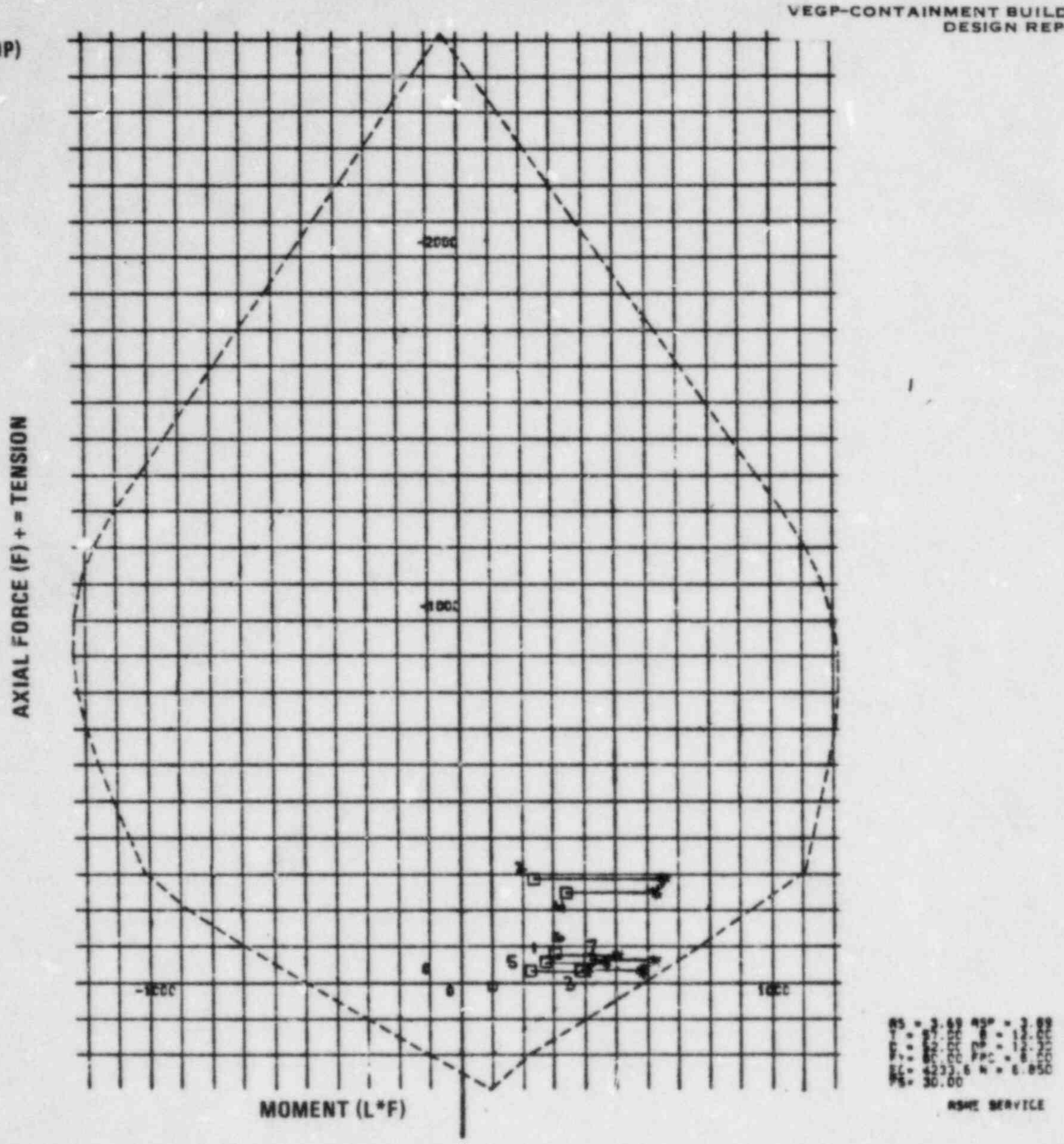

TENSION ON INSIDE FACE ⟵ ⟶ TENSION ON OUTSIDE FACE

KEY LOCATION (SEE FIG. 17)	ELEMENT GROUP (SEE FIG. 17)	ELEMENT NUMBER	LOAD COMB'TION (TABLE 5)	AXIAL FORCE (K/FT)	W/O THERMAL EFFECTS: INITIAL MOMENT (FT-K/FT)	W/O THERMAL EFFECTS: UFS % (C)	WITH THERMAL EFFECTS: FINAL MOMENT (FT-K/FT)	WITH THERMAL EFFECTS: UFS % (C)
9	1	32	4 (A)	-50	272	51	469	60
9	1	32	4 (A)	-296	244	29	648	53
9	1	56	4 (A)	-33	393	79	590	84
9	1	56	4 (A)	-247	347	42	625	55
9	1	63	4 (A)	-32	211	42	408	54
9	1	30	4 (B)	-73	305	54	502	62
9	1	56	4 (B)	-56	428	79	625	84

(A) PRESTRESS FORCES AT END-OF-LIFETIME.
(B) PRESTRESS FORCES AT BEGINNING-OF-LIFETIME.
(C) SEE SECTION 5.1.1 FOR A DESCRIPTION OF UTILIZATION FACTOR UFS.

Figure 25
CYLINDER INTERACTION DIAGRAMS
WITH THERMAL EFFECTS INCLUDED
(Sheet 3 of 12)

**HORIZONTAL (HOOP)
REINFORCING IAD
AT ELEVATION
169'-0"**

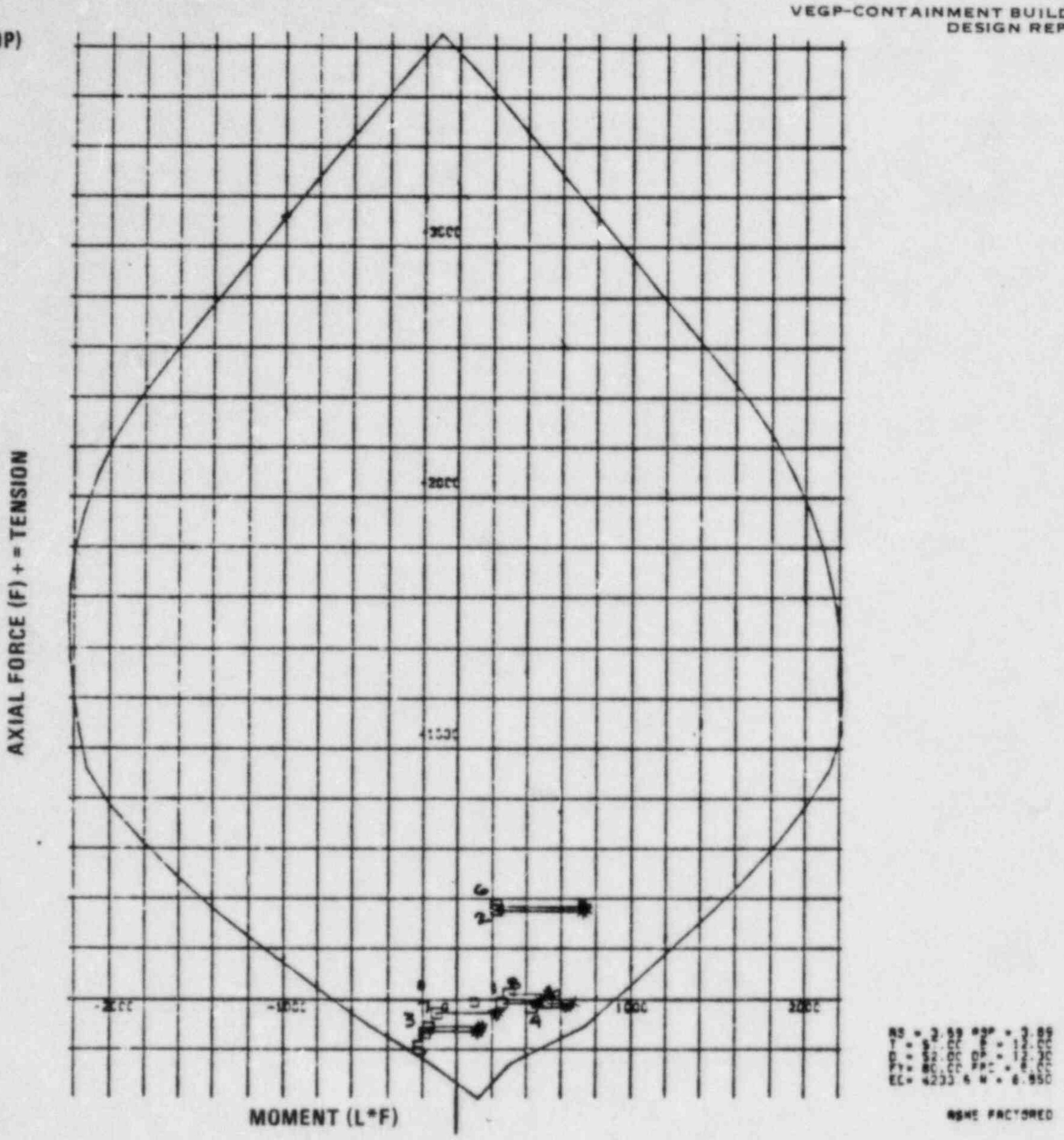

TENSION ON INSIDE FACE ⟵ ⟶ TENSION ON OUTSIDE FACE

KEY LOCATION (SEE FIG. 17)	ELEMENT GROUP (SEE FIG. 17)	ELEMENT NUMBER	LOAD COMB'TION (TABLE 5)	AXIAL FORCE (K/FT)	W/O THERMAL EFFECTS		WITH THERMAL EFFECTS	
					INITIAL MOMENT (FT-K/FT)	UFS % (C)	FINAL MOMENT (FT-K/FT)	UFS % (C)
9	1	32	5 (A)	10	280	36	479	47
9	1	32	5 (A)	-358	238	18	722	43
9	1	32	8 (A)	114	-170	42	143	1
9	1	56	5 (A)	25	445	59	644	68
9	1	63	8 (A)	128	-191	50	121	3
9	1	63	5 (A)	-366	232	17	729	43
9	1	65	9 (A)	56	-134	26	212	4
9	1	30	5 (B)	-12	311	38	511	48
9	1	56	5 (B)	3	479	61	678	68

(A) PRESTRESS FORCES AT END-OF-LIFETIME.
(B) PRESTRESS FORCES AT BEGINNING-OF-LIFETIME.
(C) SEE SECTION 5.1.1 FOR A DESCRIPTION OF UTILIZATION FACTOR UFS.

Figure 25
CYLINDER INTERACTION DIAGRAMS
WITH THERMAL EFFECTS INCLUDED
(Sheet 4 of 12)

VERTICAL (MERIDONAL) REINFORCING IAD AT ELEVATION 175'-0"

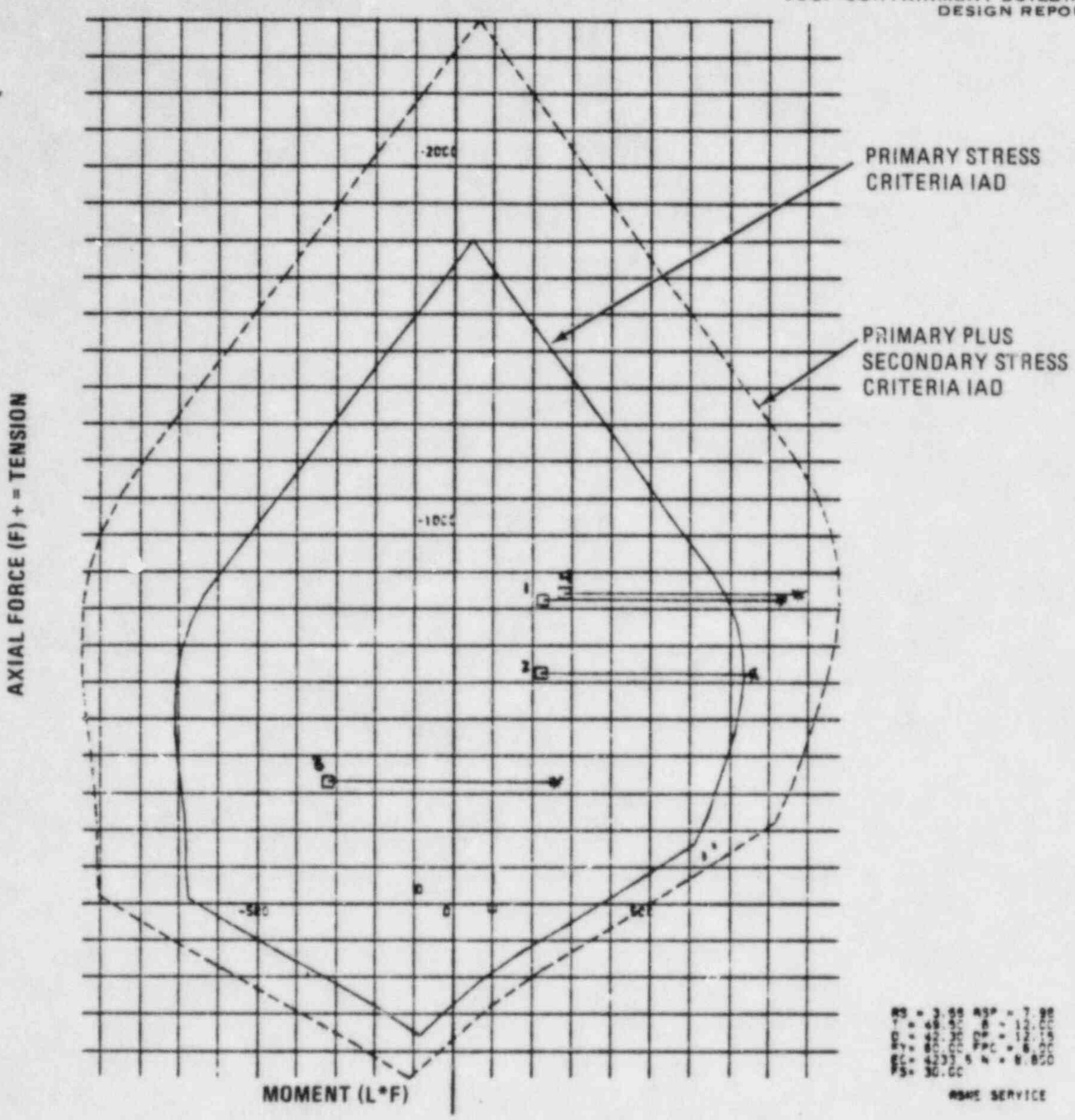

TENSION ON INSIDE FACE ⟵ | ⟶ TENSION ON OUTSIDE FACE

KEY LOCATION (SEE FIG. 17)	ELEMENT GROUP (SEE FIG. 17)	ELEMENT NUMBER	LOAD COMB'TION (TABLE 5)	AXIAL FORCE (K/FT)	W/O THERMAL EFFECTS INITIAL MOMENT (FT-K/FT)	W/O THERMAL EFFECTS UF % (C)	WITH THERMAL EFFECTS FINAL MOMENT (FT-K/FT)	WITH THERMAL EFFECTS UFS % (C)
8	1	136	4 (A)	-814	239	32	837	71
8	1	136	3 (A)	-621	234	30	762	67
8	1	136	1 (B)	-335	-321	47	263	18
8	1	136	4 (B)	-849	287	40	871	74

(A) PRESTRESS FORCES AT END-OF-LIFETIME.
(B) PRESTRESS FORCES AT BEGINNING-OF-LIFETIME.
(C) SEE SECTION 5.1.1 FOR A DESCRIPTION OF UTILIZATION FACTORS UF AND UFS

Figure 25
CYLINDER INTERACTION DIAGRAMS
WITH THERMAL EFFECTS INCLUDED
(Sheet 5 of 12)

VERTICAL (MERIDONAL) REINFORCING IAD AT ELEVATION 175'-0"

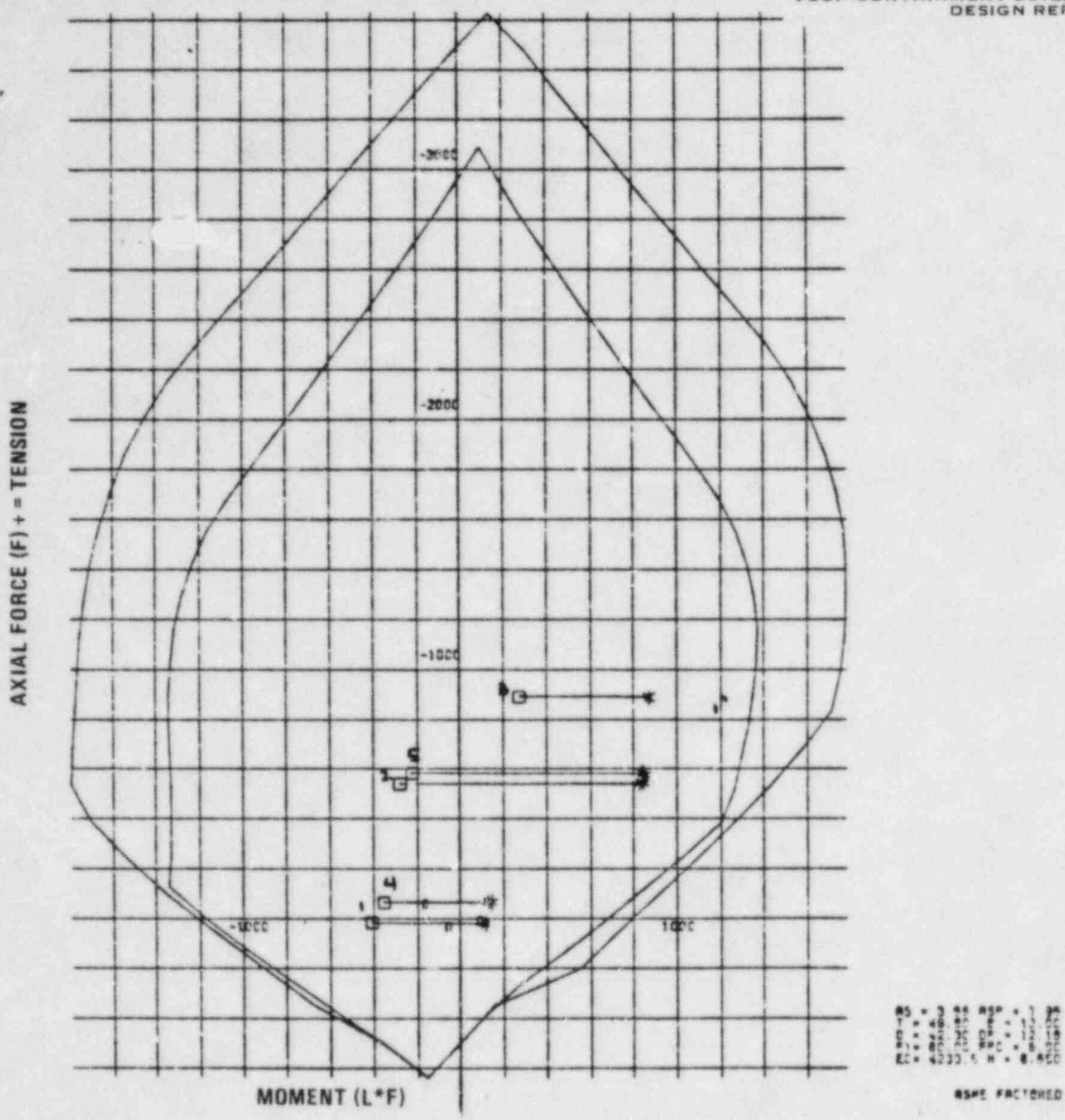

TENSION ON INSIDE FACE — TENSION ON OUTSIDE FACE

KEY LOCATION (SEE FIG. 17)	ELEMENT GROUP (SEE FIG. 17)	ELEMENT NUMBER	LOAD COMB'TION (TABLE 5)	AXIAL FORCE (K/FT)	W/O THERMAL EFFECTS: INITIAL MOMENT (FT-K/FT)	W/O THERMAL EFFECTS: UF % (C)	WITH THERMAL EFFECTS: FINAL MOMENT (FT-K/FT)	WITH THERMAL EFFECTS: UFS % (C)
8	1	136	8 (A)	17	-405	35	113	1
8	1	136	9 (A)	-579	-270	21	825	48
8	1	136	6 (A)	-900	242	17	863	42
8	1	136	8 (B)	-64	-373	30	155	1
8	1	136	9 (B)	-595	-215	17	854	49

(A) PRESTRESS FORCES AT END-OF-LIFETIME.
(B) PRESTRESS FORCES AT BEGINNING-OF-LIFETIME.
(C) SEE SECTION 5.1.1 FOR A DESCRIPTION OF UTILIZATION FACTORS UF AND UFS.

Figure 25
CYLINDER INTERACTION DIAGRAMS
WITH THERMAL EFFECTS INCLUDED
(Sheet 6 of 12)

HORIZONTAL (HOOP)
REINFORCING IAD
AT ELEVATION
175'-0"

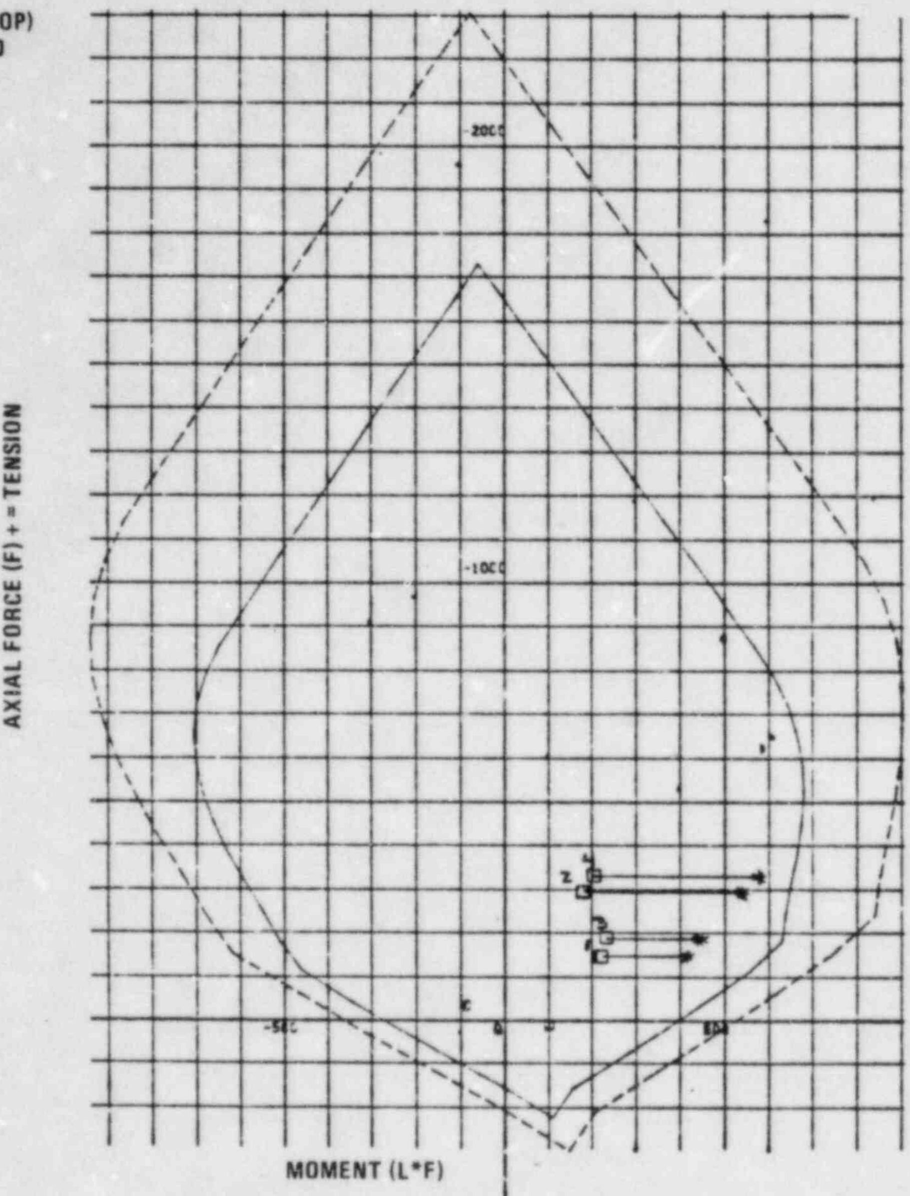

KEY LOCATION (SEE FIG. 17)	ELEMENT GROUP (SEE FIG. 17)	ELEMENT NUMBER	LOAD COMB'TION (TABLE 5)	AXIAL FORCE (K/FT)	W/O THERMAL EFFECTS		WITH THERMAL EFFECTS	
					INITIAL MOMENT (FT-K/FT)	UF % (C)	FINAL MOMENT (FT-K/FT)	UFS % (C)
8	1	127	4 (A)	-142	222	38	413	48
8	1	127	4 (A)	-296	197	32	540	51
8	1	127	4 (B)	-184	244	39	454	49
8	1	127	4 (B)	-339	219	35	582	55

(A) PRESTRESS FORCES AT END-OF-LIFETIME.
(B) PRESTRESS FORCES AT BEGINNING-OF-LIFETIME.
(C) SEE SECTION 5.1.1 FOR A DESCRIPTION OF UTILIZATION FACTORS UF AND UFS.

Figure 25
CYLINDER INTERACTION DIAGRAMS
WITH THERMAL EFFECTS INCLUDED
(Sheet 7 of 12)

HORIZONTAL (HOOP) REINFORCING IAD AT ELEVATION 175'-0"

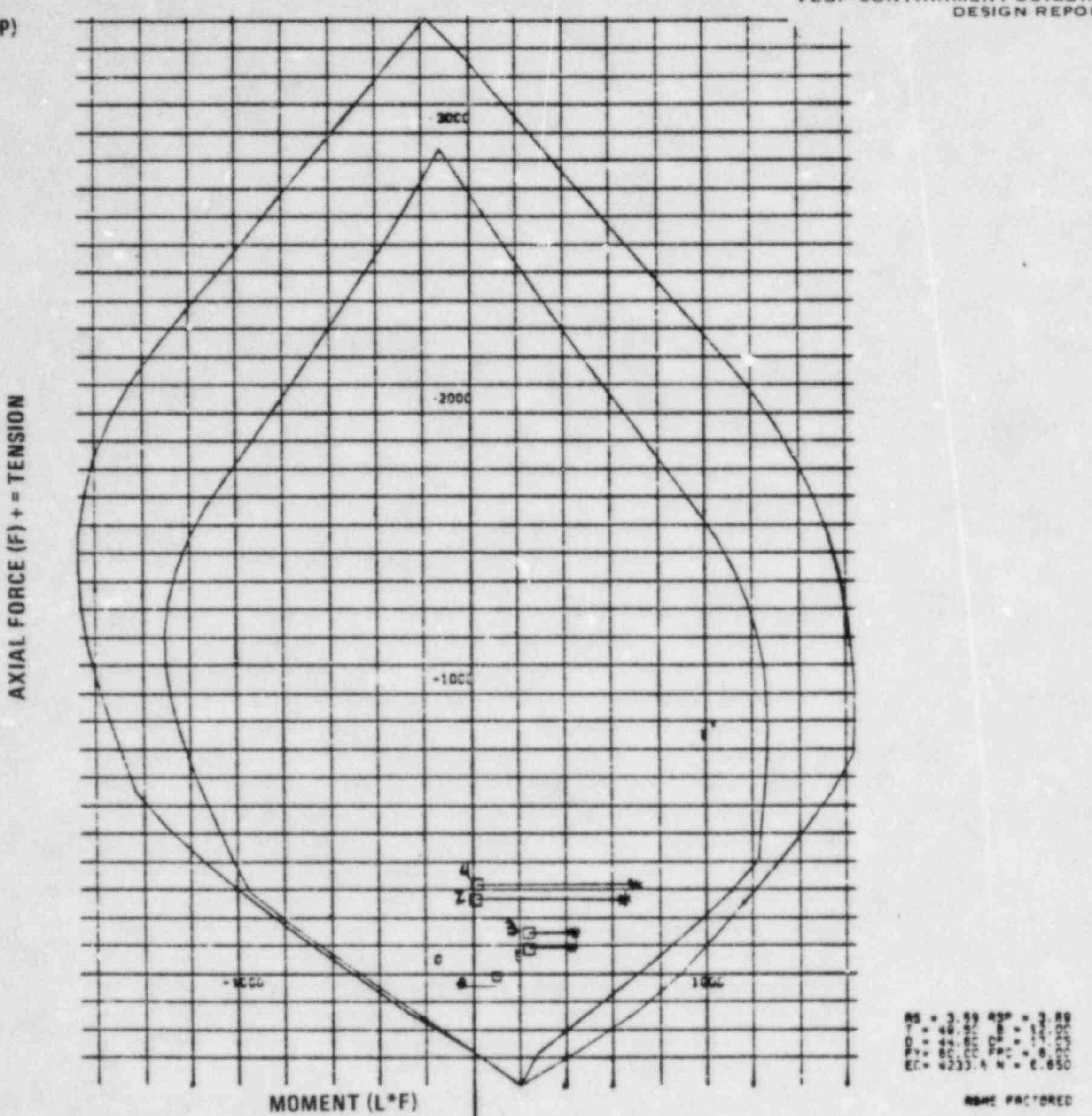

TENSION ON INSIDE FACE ⟷ TENSION ON OUTSIDE FACE

KEY LOCATION (SEE FIG. 17)	ELEMENT GROUP (SEE FIG. 17)	ELEMENT NUMBER	LOAD COMB'TION (TABLE 5)	AXIAL FORCE (K/FT)	W/O THERMAL EFFECTS: INITIAL MOMENT (FT-K/FT)	W/O THERMAL EFFECTS: UF % (C)	WITH THERMAL EFFECTS: FINAL MOMENT (FT-K/FT)	WITH THERMAL EFFECTS: UFS % (C)
8	1	127	5 (A)	-100	247	29	420	34
8	1	127	9 (A)	-265	8	1	656	46
8	1	127	5 (B)	-142	268	30	448	36
8	1	127	9 (B)	-307	30	3	703	49

(A) PRESTRESS FORCES AT END-OF-LIFETIME.
(B) PRESTRESS FORCES AT BEGINNING-OF-LIFETIME.
(C) SEE SECTION 5.1.1 FOR A DESCRIPTION OF UTILIZATION FACTORS UF AND UFS.

Figure 25
CYLINDER INTERACTION DIAGRAMS
WITH THERMAL EFFECTS INCLUDED
(Sheet 8 of 12)

VERTICAL (MERIDONAL) REINFORCING IAD ABOVE ELEVATION 179'-0"

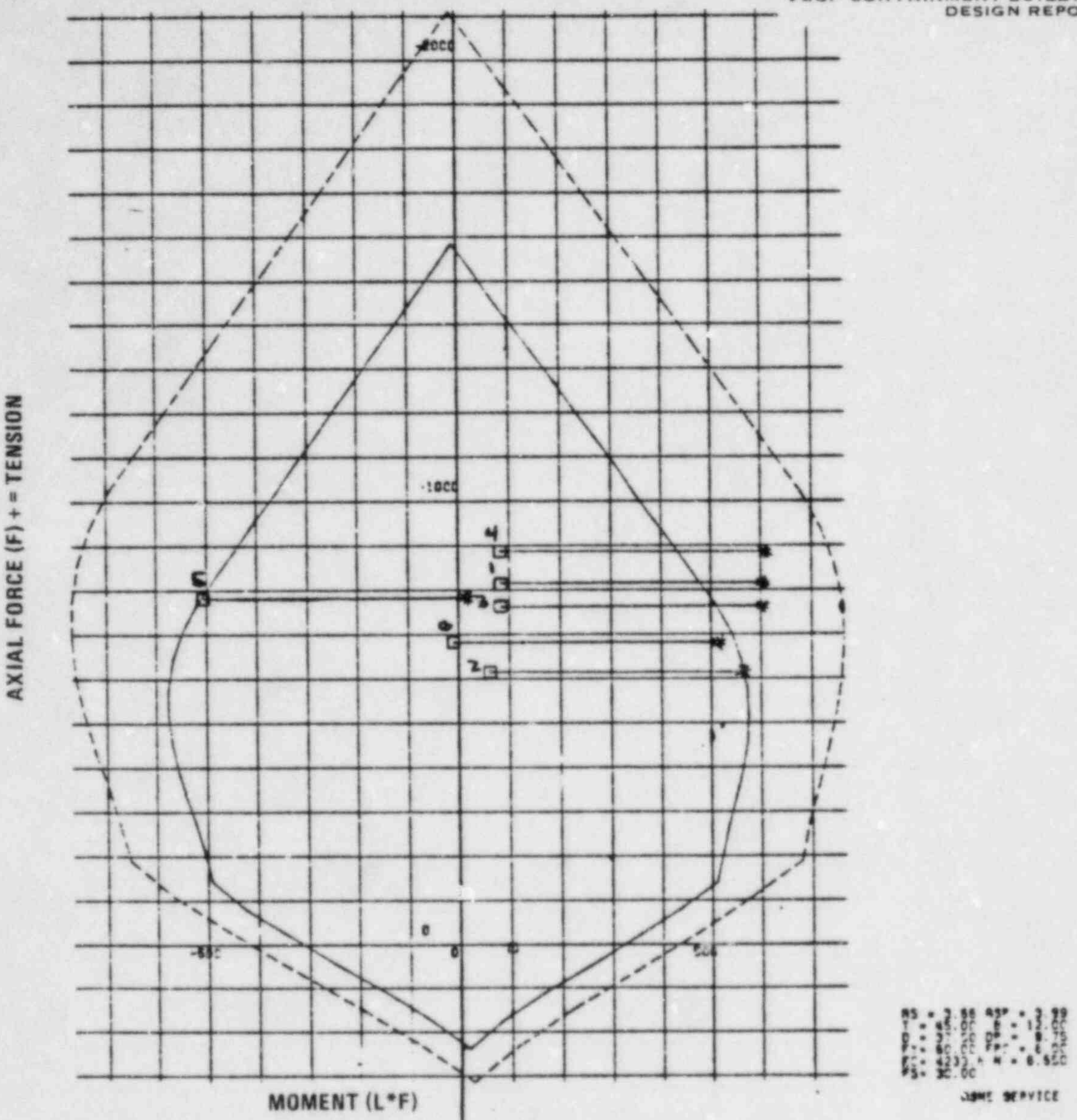

TENSION ON INSIDE FACE — TENSION ON OUTSIDE FACE

KEY LOCATION (SEE FIG. 17)	ELEMENT GROUP (SEE FIG. 17)	ELEMENT NUMBER	LOAD COMB'TION (TABLE 5)	AXIAL FORCE (K/FT)	W/O THERMAL EFFECTS INITIAL MOMENT (FT-K/FT)	W/O THERMAL EFFECTS UF % (C)	WITH THERMAL EFFECTS FINAL MOMENT (FT-K/FT)	WITH THERMAL EFFECTS UFS % (C)
7	2	45	4 (A)	-818	90	20	604	62
7	2	45	3 (A)	-616	60	11	570	60
7	2	45	4 (A)	-765	89	18	604	62
7	2	46	4 (B)	-899	92	22	601	63
5	16	51	4 (B)	-785	-507	99	28	10
5	16	51	4 (B)	-671	-9	1	522	53

(A) PRESTRESS FORCES AT END-OF-LIFETIME.
(B) PRESTRESS FORCES AT BEGINNING-OF-LIFETIME.
(C) SEE SECTION 5.1.1 FOR A DESCRIPTION OF UTILIZATION FACTORS UF AND UFS.

Figure 25
CYLINDER INTERACTION DIAGRAMS
WITH THERMAL EFFECTS INCLUDED
(Sheet 9 of 12)

VERTICAL (MERIDONAL) REINFORCING IAD ABOVE ELEVATION 179'-0"

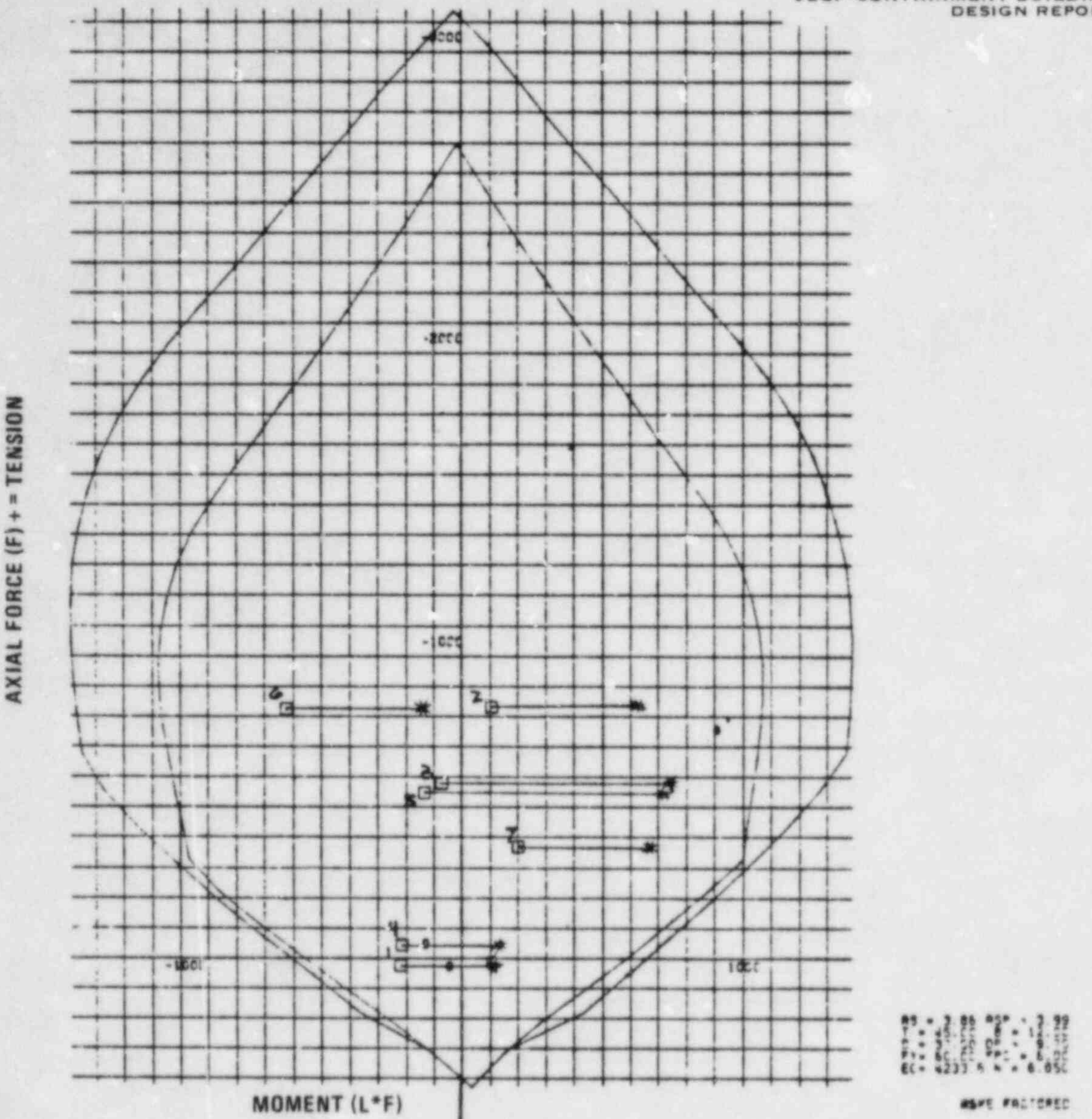

TENSION ON INSIDE FACE ⟵ ⟶ TENSION ON OUTSIDE FACE

KEY LOCATION (SEE FIG. 17)	ELEMENT GROUP (SEE FIG. 17)	ELEMENT NUMBER	LOAD COMB'TION (TABLE 5)	AXIAL FORCE (K/FT)	W/O THERMAL EFFECTS		WITH THERMAL EFFECTS	
					INITIAL MOMENT (FT-K/FT)	UF % (C)	FINAL MOMENT (FT-K/FT)	UFS % (C)
7	2	45	8 (A)	38	-214	42	116	2
7	2	45	6 (A)	-833	103	10	631	37
7	2	45	9 (A)	-582	-88	8	752	50
7	2	46	8 (B)	-41	-210	34	141	0
7	2	46	8 (B)	-557	-134	13	723	49
5	16	51	5 (B)	-814	-631	59	-144	16
5	16	51	9 (B)	-364	201	20	680	54

(A) PRESTRESS FORCES AT END-OF-LIFETIME.
(B) PRESTRESS FORCES AT BEGINNING-OF-LIFETIME.
(C) SEE SECTION 5.1.1 FOR A DESCRIPTION OF UTILIZATION FACTORS UF AND UFS.

Figure 25
CYLINDER INTERACTION DIAGRAMS
WITH THERMAL EFFECTS INCLUDED
(Sheet 10 of 12)

HORIZONTAL (HOOP)
REINFORCING IAD
ABOVE ELEVATION
179'-0"

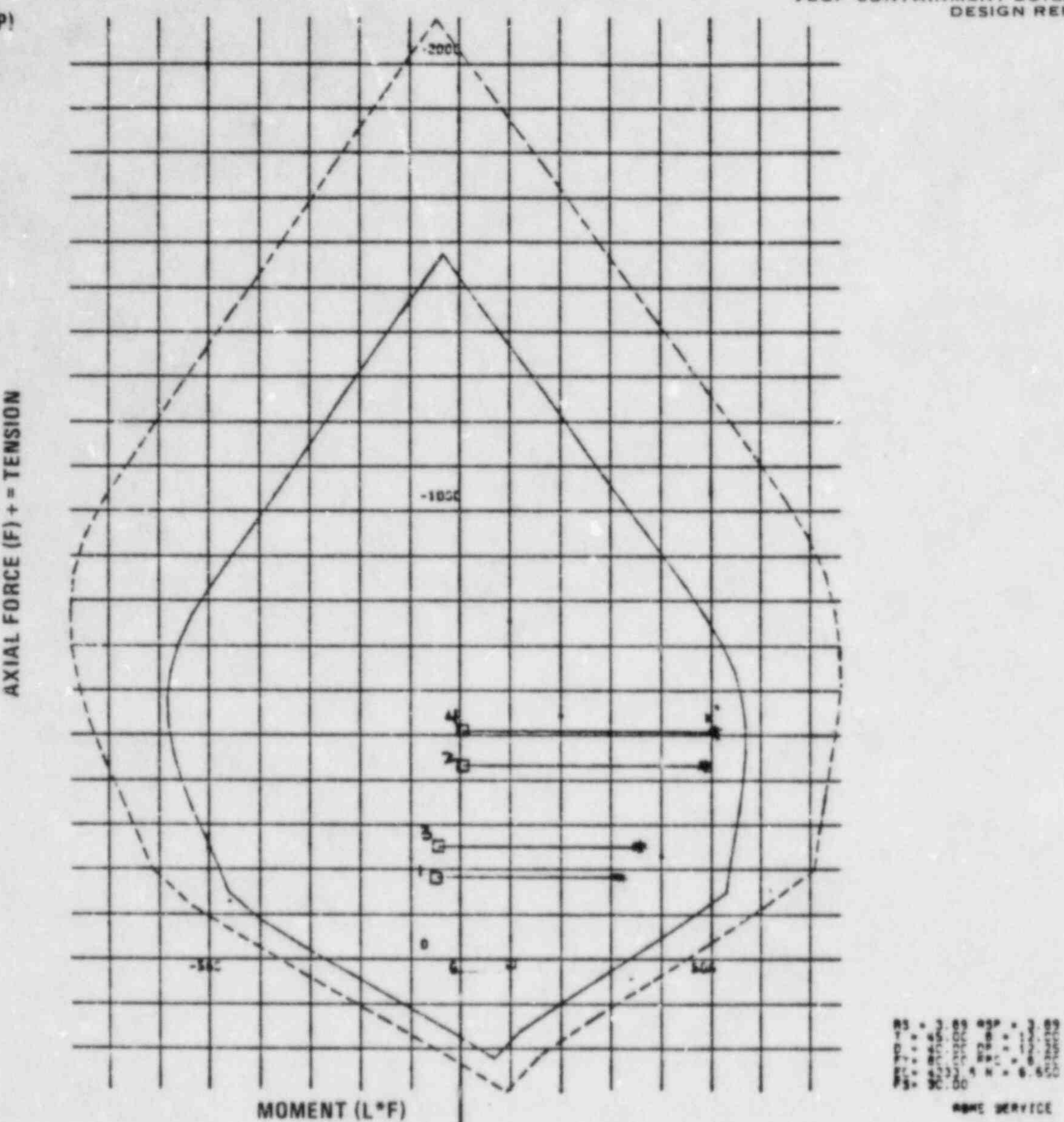

TENSION ON INSIDE FACE ←→ TENSION ON OUTSIDE FACE

KEY LOCATION (SEE FIG. 17)	ELEMENT GROUP (SEE FIG. 17)	ELEMENT NUMBER	LOAD COMB'TION (TABLE 5)	AXIAL FORCE (K/FT)	W/O THERMAL EFFECTS INITIAL MOMENT (FT-K/FT)	W/O THERMAL EFFECTS UF % (C)	WITH THERMAL EFFECTS FINAL MOMENT (FT-K/FT)	WITH THERMAL EFFECTS UFS % (C)
7	2	55	1 (A)	-184	-46	9	320	37
7	2	55	4 (A)	-440	5	3	493	52
7	2	55	1 (B)	-248	-43	8	368	39
7	2	55	4 (B)	-503	8	3	515	54

(A) PRESTRESS FORCES AT END-OF-LIFETIME.
(B) PRESTRESS FORCES AT BEGINNING-OF-LIFETIME.
(C) SEE SECTION 5.1.1 FOR A DESCRIPTION OF UTILIZATION FACTORS UF AND UFS.

Figure 25
CYLINDER INTERACTION DIAGRAMS
WITH THERMAL EFFECTS INCLUDED
(Sheet 11 of 12)

HORIZONTAL (HOOP)
REINFORCING IAD
ABOVE ELEVATION
179'-0"

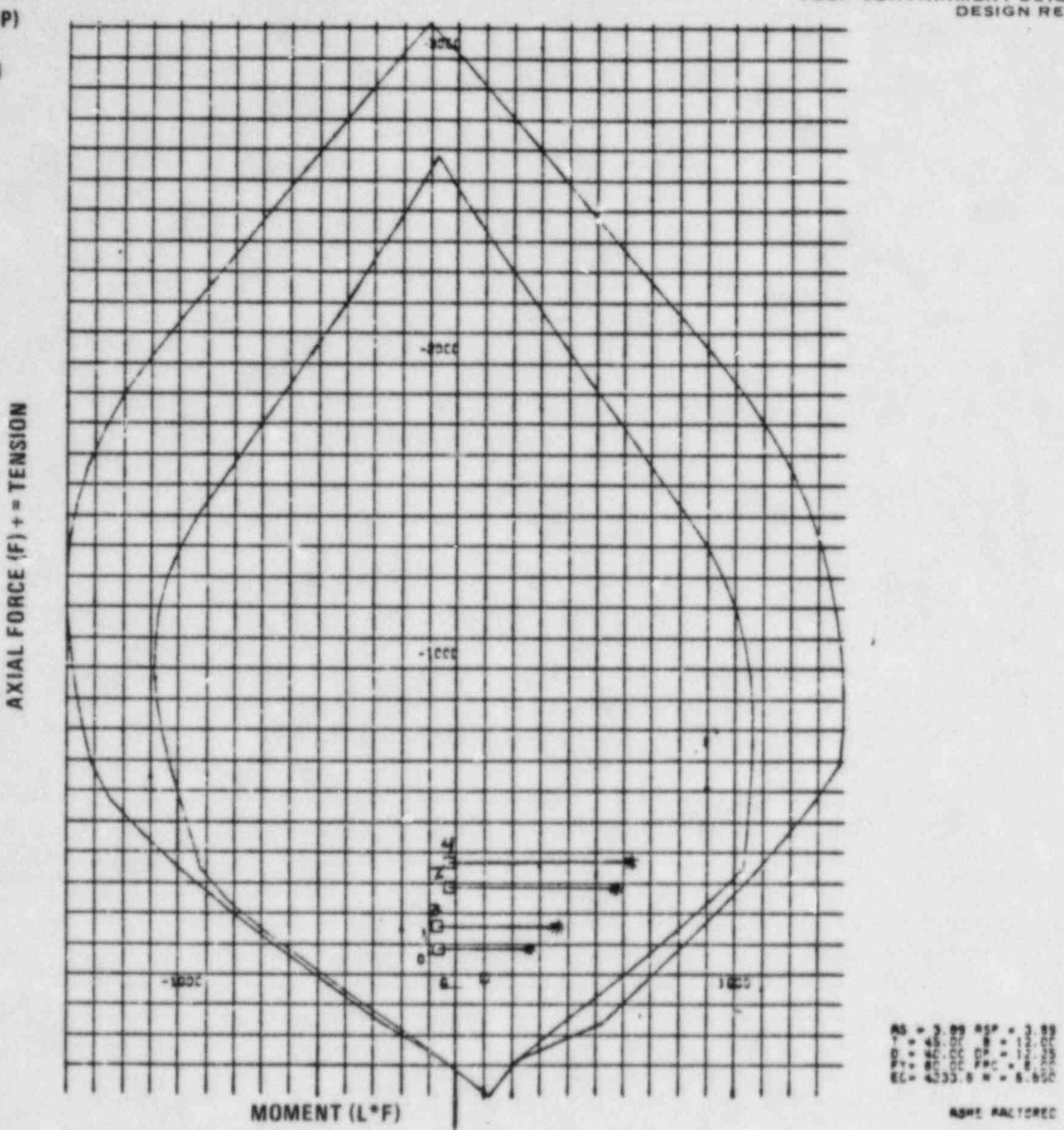

TENSION ON INSIDE FACE — TENSION ON OUTSIDE FACE

KEY LOCATION (SEE FIG. 17)	ELEMENT GROUP (SEE FIG. 17)	ELEMENT NUMBER	LOAD COMB'TION (TABLE 5)	AXIAL FORCE (K/FT)	W/O THERMAL EFFECTS INITIAL MOMENT (FT-K/FT)	W/O THERMAL EFFECTS UF % (C)	WITH THERMAL EFFECTS FINAL MOMENT (FT-K/FT)	WITH THERMAL EFFECTS UFS % (C)
7	2	55	8 (A)	-92	-58	9	264	18
7	2	55	9 (A)	-297	-30	3	588	48
7	2	55	8 (B)	-156	-55	7	360	28
7	2	55	9 (B)	-360	-27	2	638	49

(A) PRESTRESS FORCES AT END-OF-LIFETIME.
(B) PRESTRESS FORCES AT BEGINNING-OF-LIFETIME.
(C) SEE SECTION 5.1.1 FOR A DESCRIPTION OF UTILIZATION FACTORS UF AND UFS.

Figure 25
CYLINDER INTERACTION DIAGRAMS
WITH THERMAL EFFECTS INCLUDED
(Sheet 12 of 12)

BASEMAT N-S FLEXURAL REINFORCING

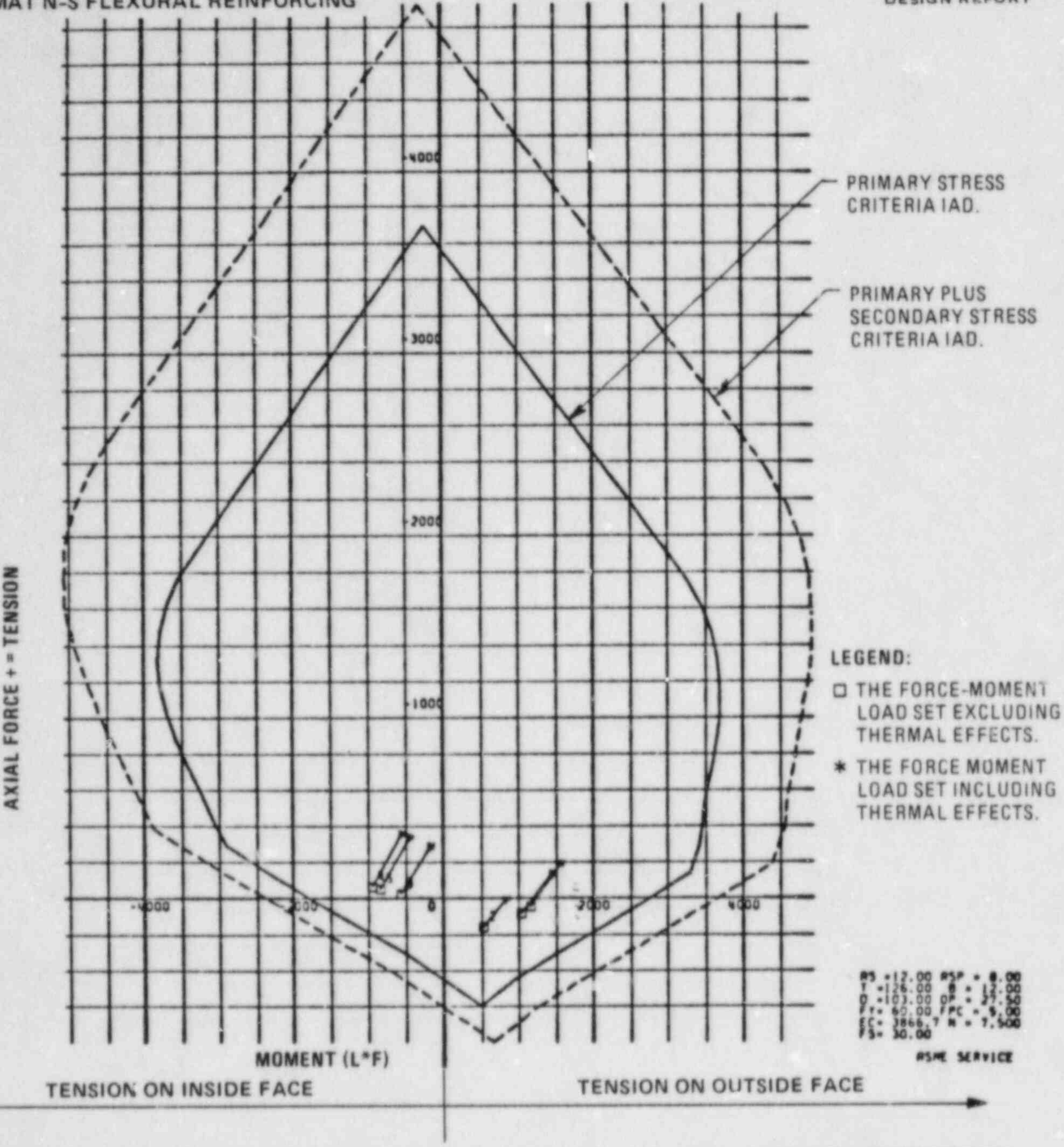

KEY LOCATION (SEE FIG. 19)	GRID ELEMENT NUMBER	LOAD COMBINATION (TABLE 5)	WITHOUT THERMAL EFFECTS			WITH THERMAL EFFECTS		
			AXIAL FORCE (K/FT)	MOMENT (FT-K/FT)	UF	AXIAL FORCE (K/FT)	MOMENT (FT-K/FT)	UFS
1	98	1	42	1144	43.5	-193	1550	35.4
1	154	1	154	526	19.8	5	831	22.7
1	130	1	83	1032	40.9	-135	1437	34.4
1	164	4	-65	-961	47.0	-360	-559	14.2
1	162	4	-54	-856	42.8	-343	-454	11.7
1	100	4	-29	-574	30.2	-294	-172	4.4

UF = UTILIZATION FACTOR FOR ASME PRIMARY STRESS ALLOWABLES.
UFS = UTILIZATION FACTOR FOR ASME PRIMARY PLUS SECONDARY STRESS ALLOWABLES.

Figure 26
FOUNDATION INTERACTION DIAGRAMS
WITH THERMAL EFFECTS INCLUDED
(Sheet 1 of 16)

BASEMAT N-S FLEXURAL REINFORCING

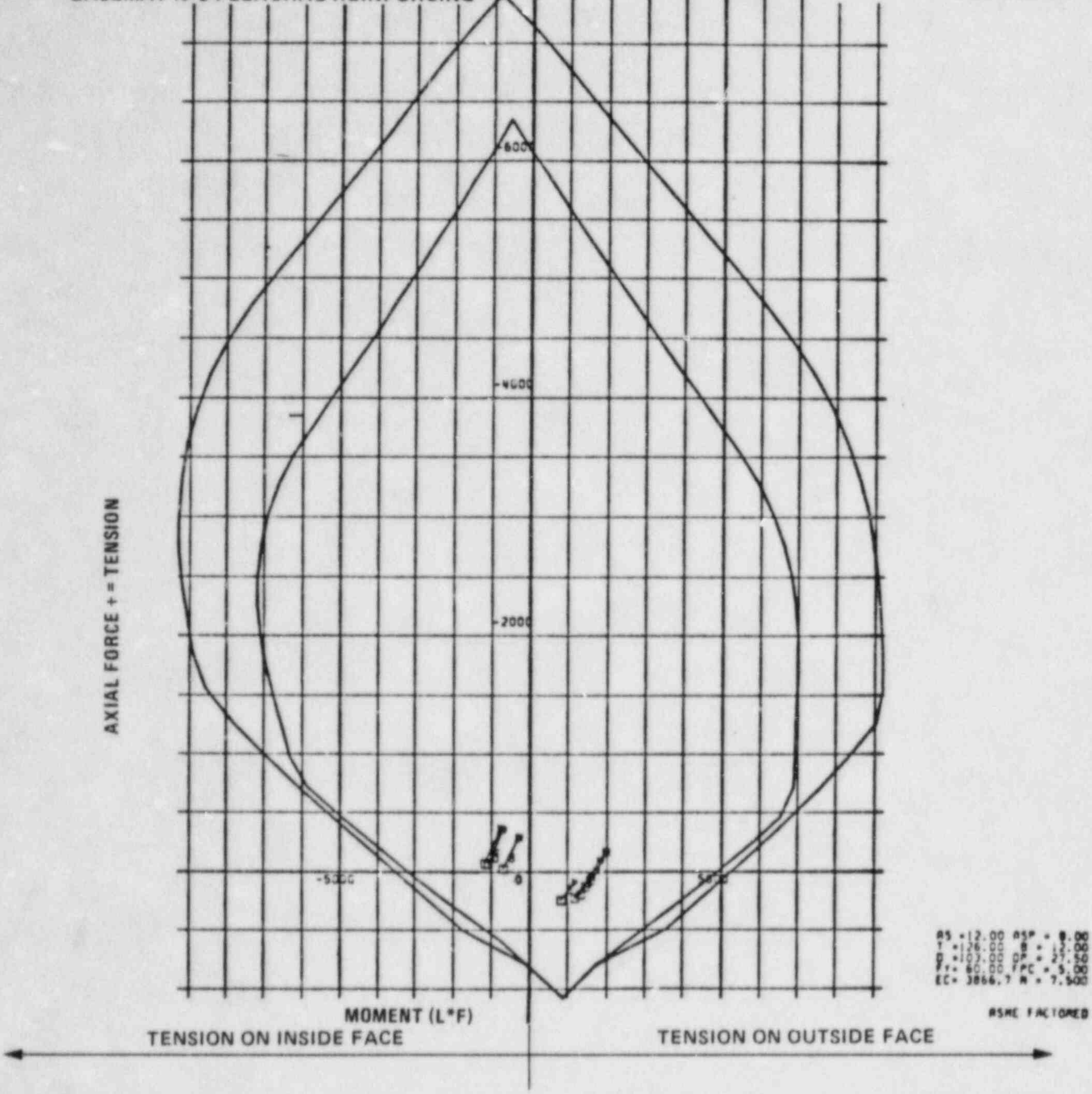

KEY LOCATION (SEE FIG. 19)	GRID ELEMENT NUMBER	LOAD COMBINATION (TABLE 5)	WITHOUT THERMAL EFFECTS			WITH THERMAL EFFECTS		
			AXIAL FORCE (K/FT)	MOMENT (FT-K/FT)	UF	AXIAL FORCE (K/FT)	MOMENT (FT-K/FT)	UFS
1	98	7	67	1571	32.9	-165	1977	33.9
1	124	8	223	1167	25.4	44	1564	30.0
1	123	8	187	1319	28.9	-7	1722	32.4
1	130	7	124	1424	30.5	-90	1830	32.8
1	154	8	237	818	16.4	87	1177	22.5
1	164	6	-78	-1173	33.5	-369	-770	15.4
1	163	6	-68	-1098	31.7	-355	-694	14.0
1	100	6	-29	-699	21.1	-289	-293	6.0

Figure 26
FOUNDATION INTERACTION DIAGRAMS
WITH THERMAL EFFECTS INCLUDED
(Sheet 2 of 16)

BASEMAT E-W FLEXURAL REINFORCING

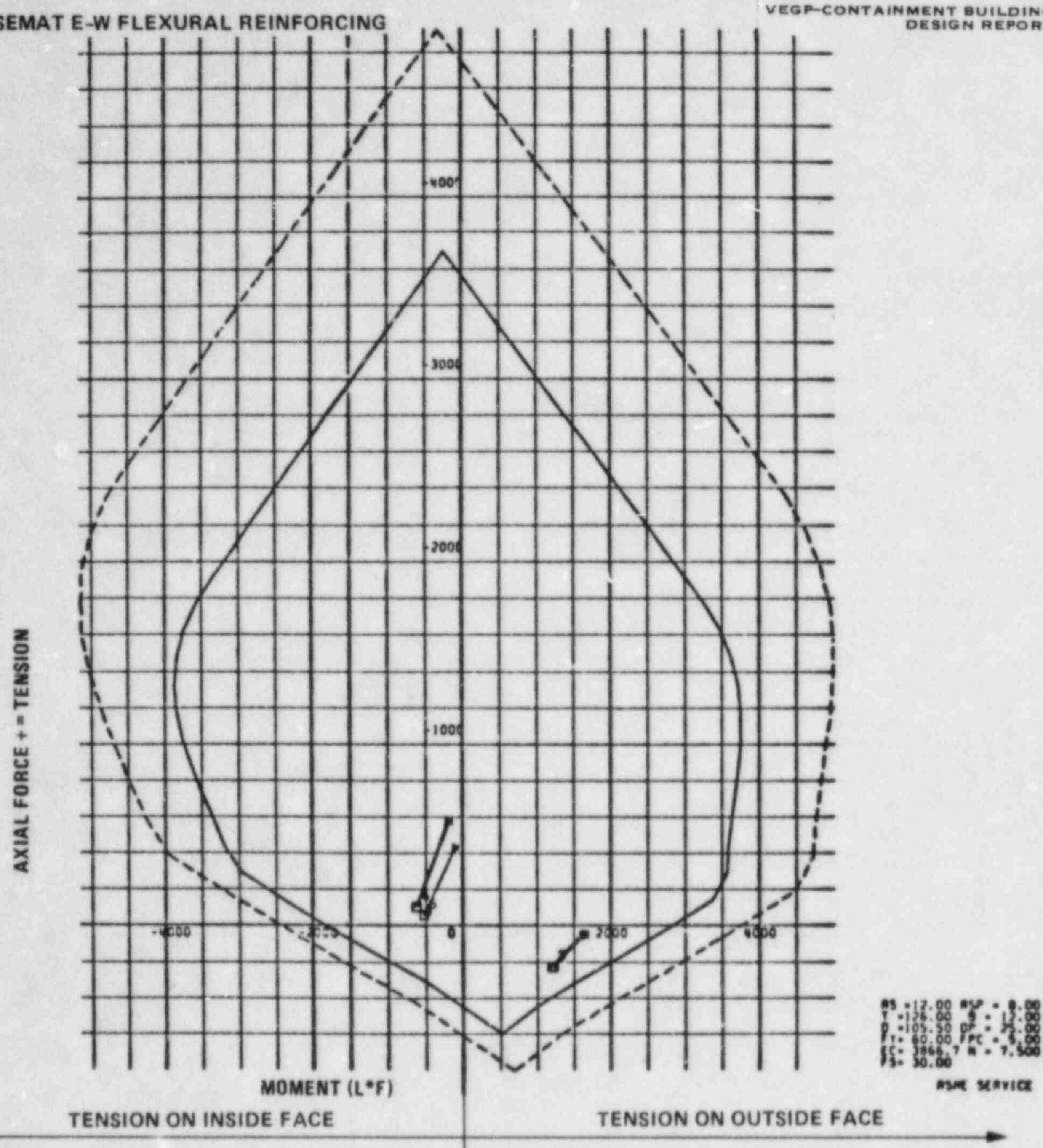

KEY LOCATION (SEE FIG. 19)	GRID ELEMENT NUMBER	LOAD COMBINATION (TABLE 5)	WITHOUT THERMAL EFFECTS			WITH THERMAL EFFECTS		
			AXIAL FORCE (K/FT)	MOMENT (FT-K/FT)	UF	AXIAL FORCE (K/FT)	MOMENT (FT-K/FT)	UFS
1	216	1	227	1214	59.5	48	1628	45.0
1	217	1	228	1186	58.1	50	1599	44.2
1	241	1	222	1215	59.1	42	1630	44.8
1	189	4	-106	-649	28.6	-580	-212	4.1
1	137	4	-61	-528	25.3	-430	-108	1.9
1	162	4	-102	-628	27.9	-577	-191	3.6

Figure 26
FOUNDATION INTERACTION DIAGRAMS
WITH THERMAL EFFECTS INCLUDED
(Sheet 3 of 16)

BASEMAT E-W FLEXURAL REINFORCING

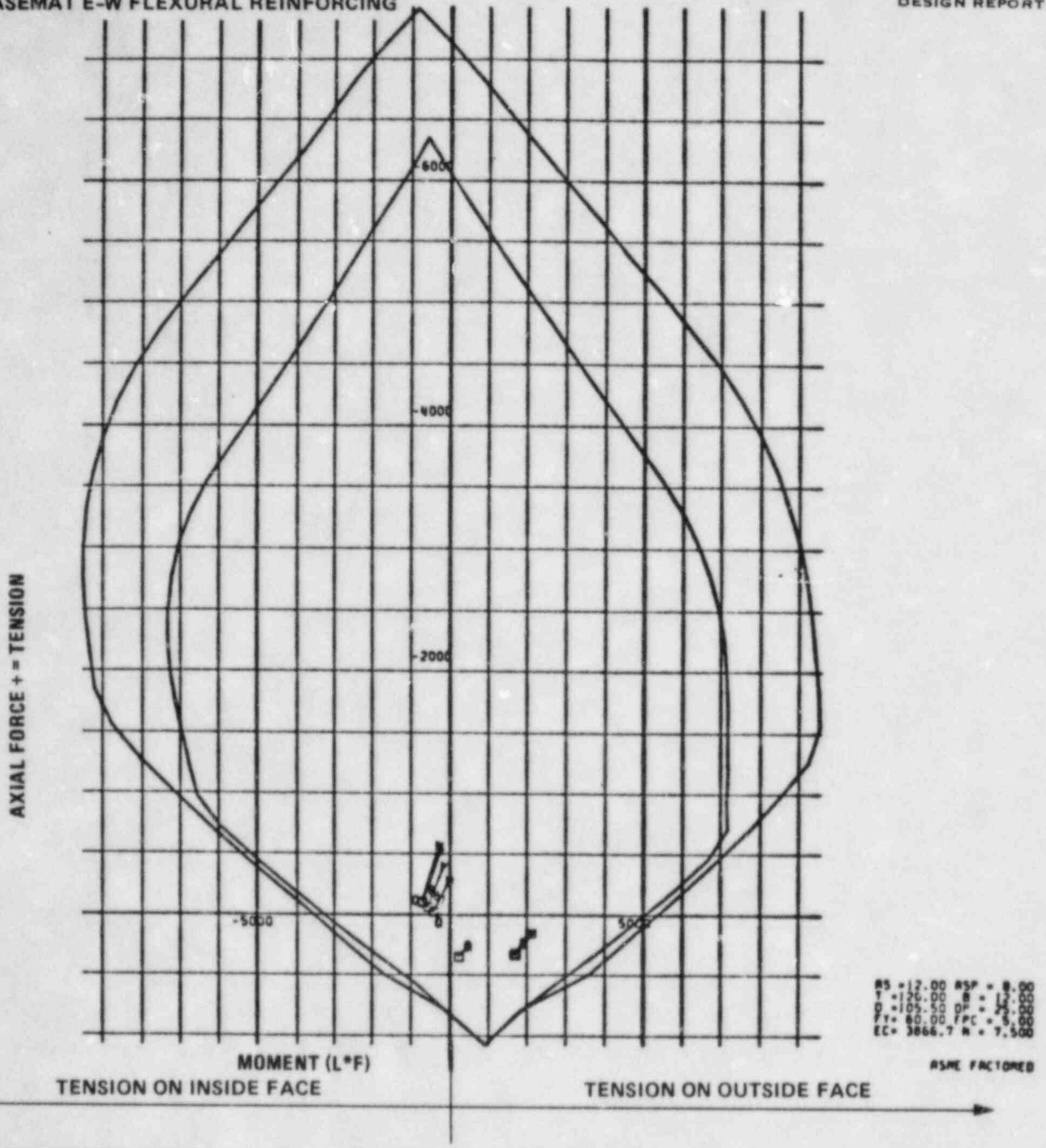

KEY LOCATION (SEE FIG. 19)	GRID ELEMENT NUMBER	LOAD COMBINATION (TABLE 5)	WITHOUT THERMAL EFFECTS			WITH THERMAL EFFECTS		
			AXIAL FORCE (K/FT)	MOMENT (FT-K/FT)	UF	AXIAL FORCE (K/FT)	MOMENT (FT-K/FT)	UFS
1	216	7	324	1692	40.5	151	2109	42.1
1	241	7	319	1693	40.4	144	2111	42.0
1	96	7	342	225	3.2	266	452	5.3
1	217	7	325	1654	39.5	153	2070	41.3
1	162	6	-117	-725	19.3	-565	-284	4.4
1	136	6	-104	-701	18.9	-522	-267	4.3
1	239	6	-28	-451	13.3	-287	-28	0.2
1	138	6	-64	-590	16.6	-410	-165	2.7

Figure 26
FOUNDATION INTERACTION DIAGRAMS
WITH THERMAL EFFECTS INCLUDED
(Sheet 4 of 16)

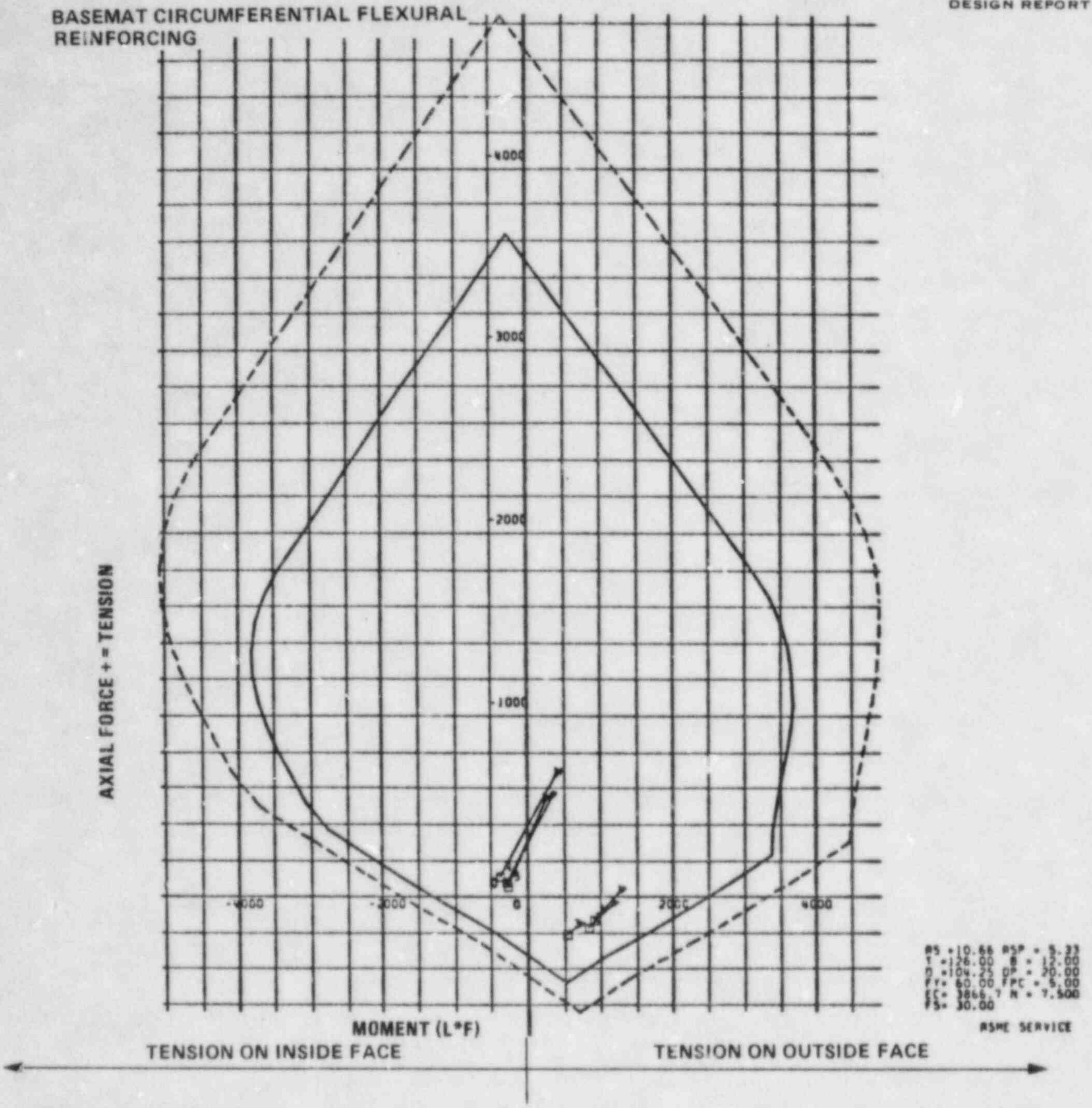

KEY LOCATION (SEE FIG. 19)	GRID ELEMENT NUMBER	LOAD COMBINATION (TABLE 5)	WITHOUT THERMAL EFFECTS			WITH THERMAL EFFECTS		
			AXIAL FORCE (K/FT)	MOMENT (FT-K/FT)	UF	AXIAL FORCE (K/FT)	MOMENT (FT-K/FT)	UFS
2 (A)	67	1	126	907	41.9	-43	1282	36.7
2 (A)	66	1	172	830	40.3	27	1187	36.3
2 (A)	1	1	209	533	21.8	149	733	22.3
2 (A)	76	4	-113	-381	21.2	-693	418	10.1
2 (A)	69	4	-59	-270	17.3	-556	266	6.7
2 (A)	73	4	-81	-296	17.8	-570	359	8.7

Figure 26
FOUNDATION INTERACTION DIAGRAMS
WITH THERMAL EFFECTS INCLUDED
(Sheet 5 of 16)

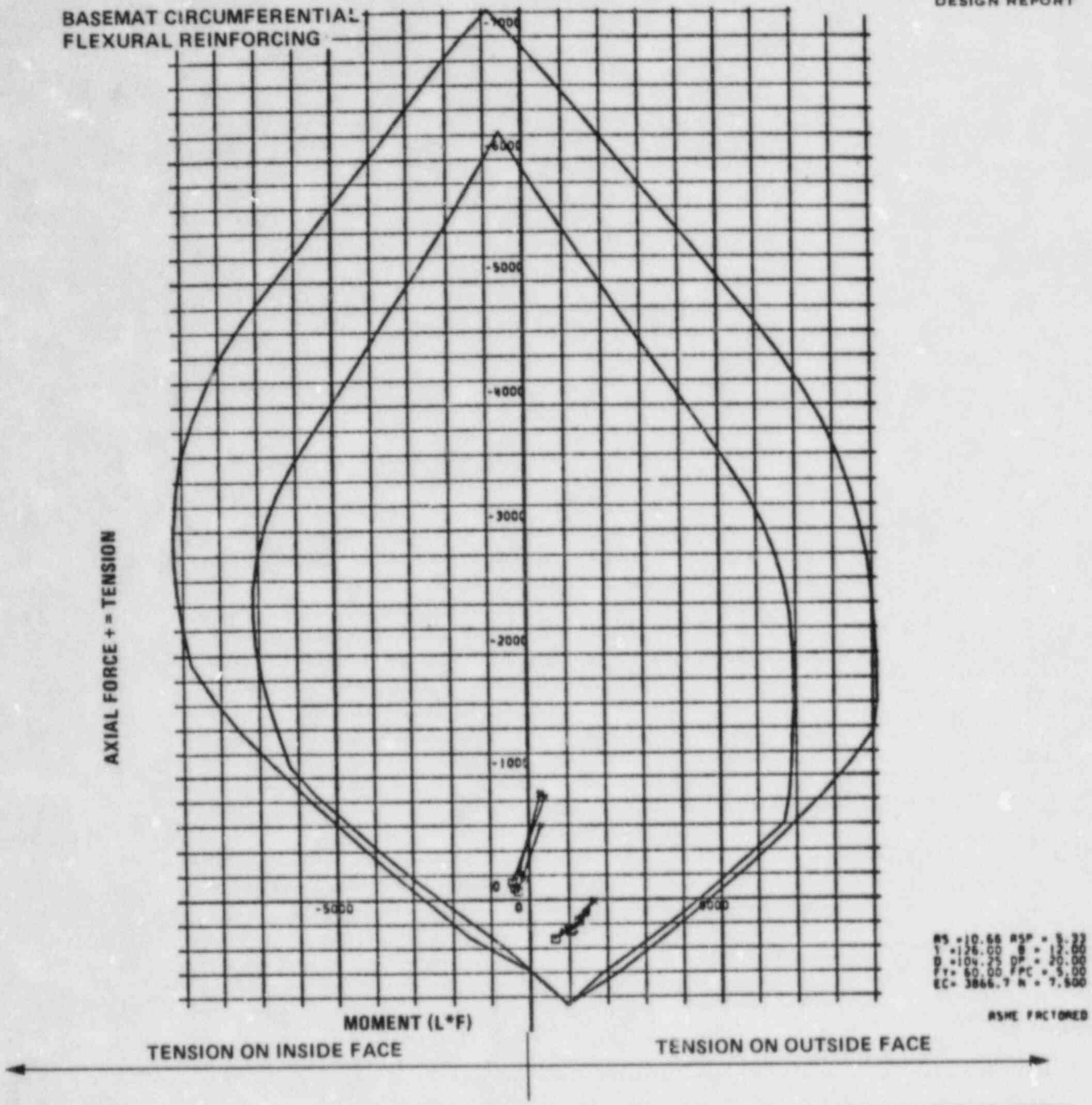

KEY LOCATION (SEE FIG. 19)	GRID ELEMENT NUMBER	LOAD COMBINATION (TABLE 5)	WITHOUT THERMAL EFFECTS			WITH THERMAL EFFECTS		
			AXIAL FORCE (K/FT)	MOMENT (FT-K/FT)	UF	AXIAL FORCE (K/FT)	MOMENT (FT-K/FT)	UFS
2 (A)	91	8	173	1232	29.1	7	1610	34.2
2 (A)	66	8	251	1030	23.8	122	1376	30.3
2 (A)	1	8	320	630	10.0	259	830	16.0
2 (A)	66	7	236	1098	25.8	97	1462	32.1
2 (A)	76	6	-141	-475	16.1	-842	420	6.1
2 (A)	72	6	-99	-402	14.4	-863	295	4.5
2 (A)	69	6	-70	-306	11.5	-604	294	4.8

Figure 26
FOUNDATION INTERACTION DIAGRAMS
WITH THERMAL EFFECTS INCLUDED
(Sheet 6 of 16)

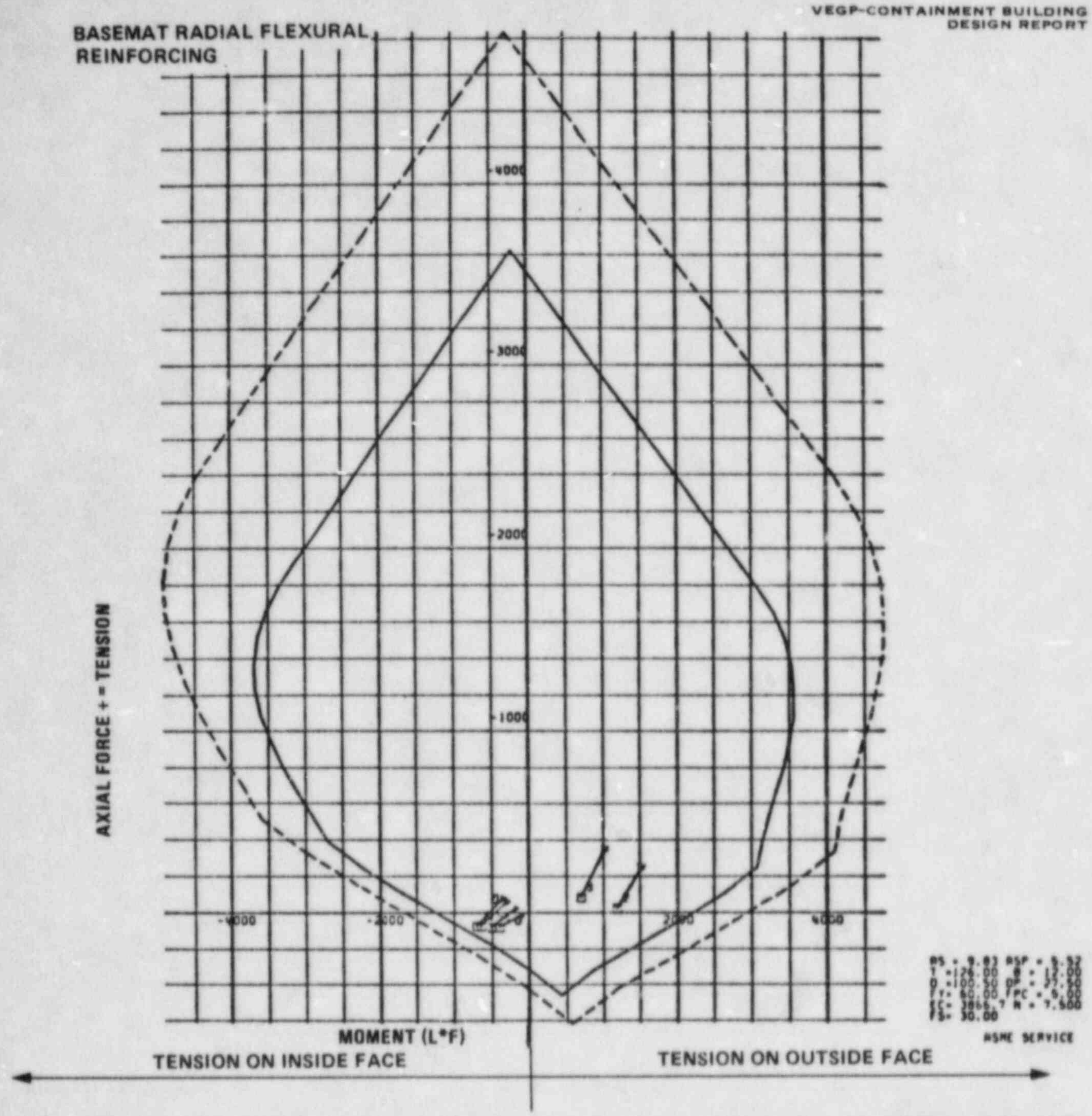

KEY LOCATION (SEE FIG. 19)	GRID ELEMENT NUMBER	LOAD COMBINATION (TABLE 5)	WITHOUT THERMAL EFFECTS			WITH THERMAL EFFECTS		
			AXIAL FORCE (K/FT)	MOMENT (FT-K/FT)	UF	AXIAL FORCE (K/FT)	MOMENT (FT-K/FT)	UFS
2	41	1	73	-700	74.5	-76	-363	18.0
2	41	4	-24	1177	50.8	-250	1507	38.4
2	48	4	-85	697	27.4	-352	1028	25.5
2	57	1	76	-638	69.5	-60	-303	15.6
2	64	1	82	-511	58.8	-20	-187	10.6
2	35	1	81	-410	48.5	23	-114	8.4

Figure 26
FOUNDATION INTERACTION DIAGRAMS
WITH THERMAL EFFECTS INCLUDED
(Sheet 7 of 16)

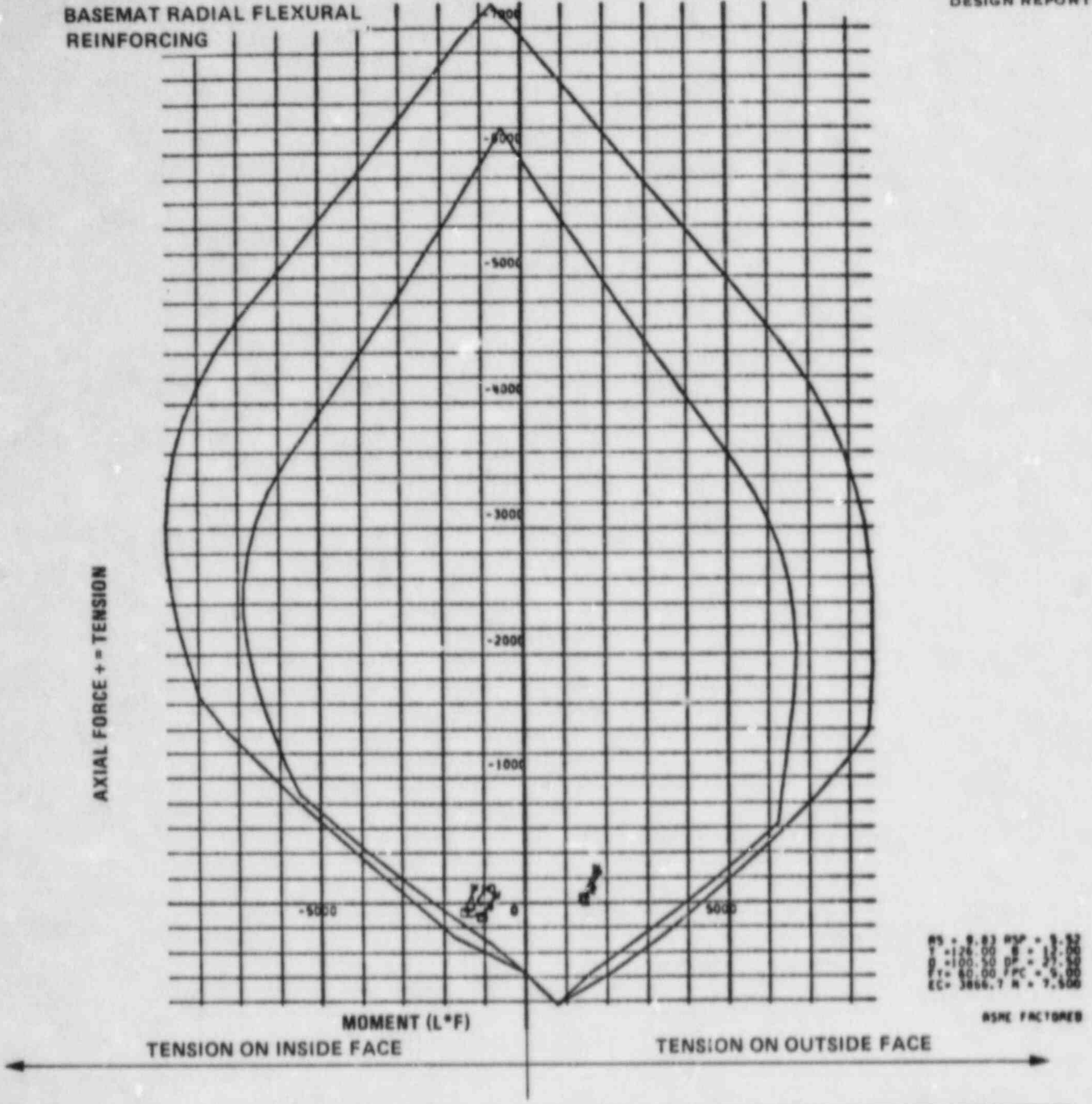

KEY LOCATION (SEE FIG. 19)	GRID ELEMENT NUMBER	LOAD COMBINATION (TABLE 5)	WITHOUT THERMAL EFFECTS			WITH THERMAL EFFECTS		
			AXIAL FORCE (K/FT)	MOMENT (FT-K/FT)	UF	AXIAL FORCE (K/FT)	MOMENT (FT-K/FT)	UFS
2	57	8	68	-1509	76.5	-127	-1244	38.9
2	41	6	-19	1461	36.1	-241	1790	34.6
2	40	6	-46	1407	33.9	-277	1737	32.8
2	40	7	104	-1078	60.5	-60	-737	24.9
2	41	7	104	-1074	60.4	-58	-734	24.8
2	64	8	72	-1348	69.2	-116	-1006	31.8

Figure 26
FOUNDATION INTERACTION DIAGRAMS
WITH THERMAL EFFECTS INCLUDED
(Sheet 8 of 16)

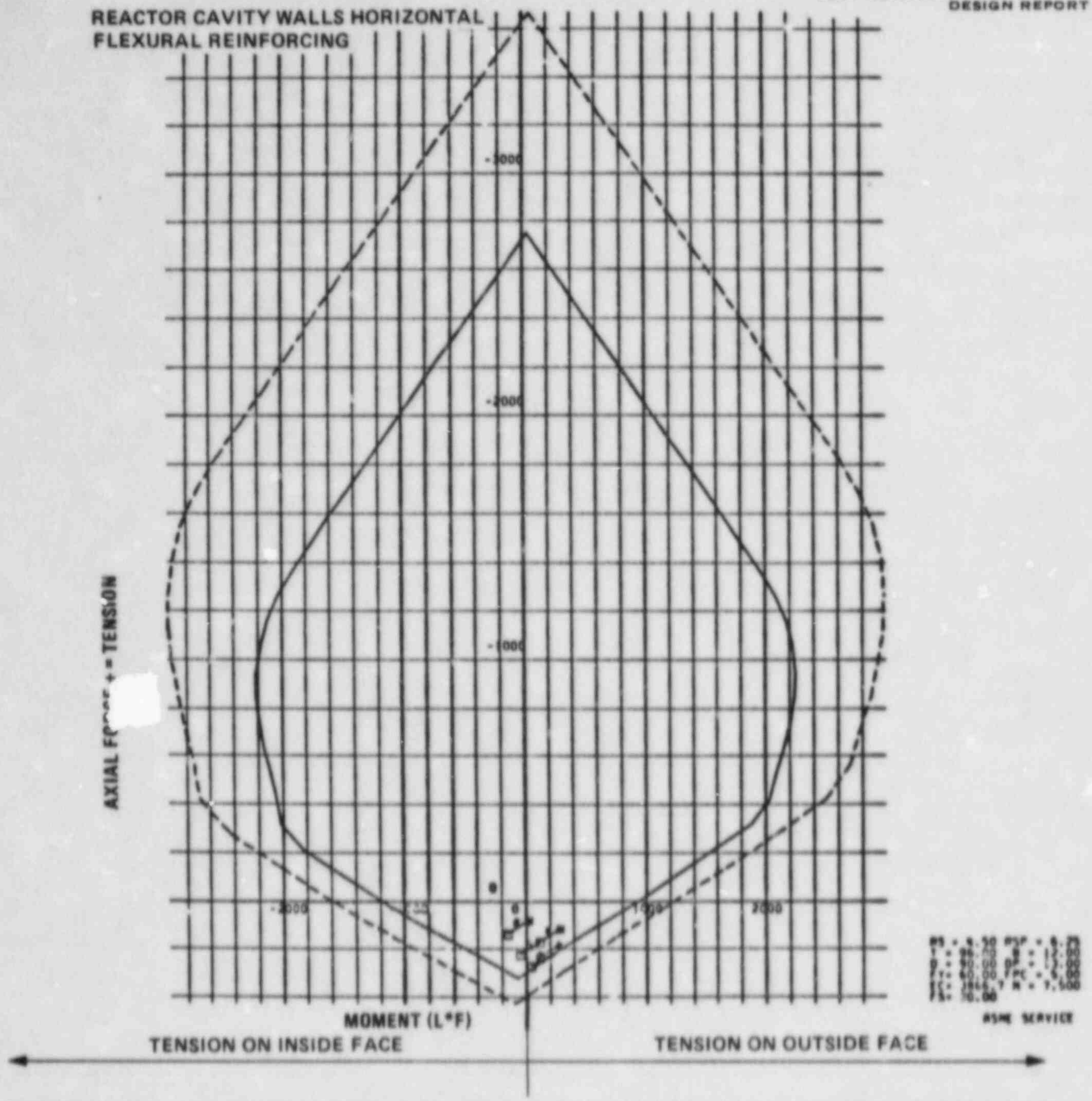

KEY LOCATION (SEE FIG. 19)	GRID ELEMENT NUMBER	LOAD COMBINATION (TABLE 5)	WITHOUT THERMAL EFFECTS			WITH THERMAL EFFECTS		
			AXIAL FORCE (K/FT)	MOMENT (FT-K/FT)	UF	AXIAL FORCE (K/FT)	MOMENT (FT-K/FT)	UFS
3	1	1	169	108	35.8	118	277	34.4
3	11	1	274	34	74.9	223	203	45.7
3	13	1	234	107	67.6	183	276	46.8
3	24	1	170	110	36.3	118	279	34.6
3	4	1	220	-55	1.0	169	114	21.2
3	28	1	133	-154	17.2	82	15	3.4
3	45	1	138	-156	17.8	86	13	3.4

Figure 26
FOUNDATION INTERACTION DIAGRAMS
WITH THERMAL EFFECTS INCLUDED
(Sheet 9 of 16)

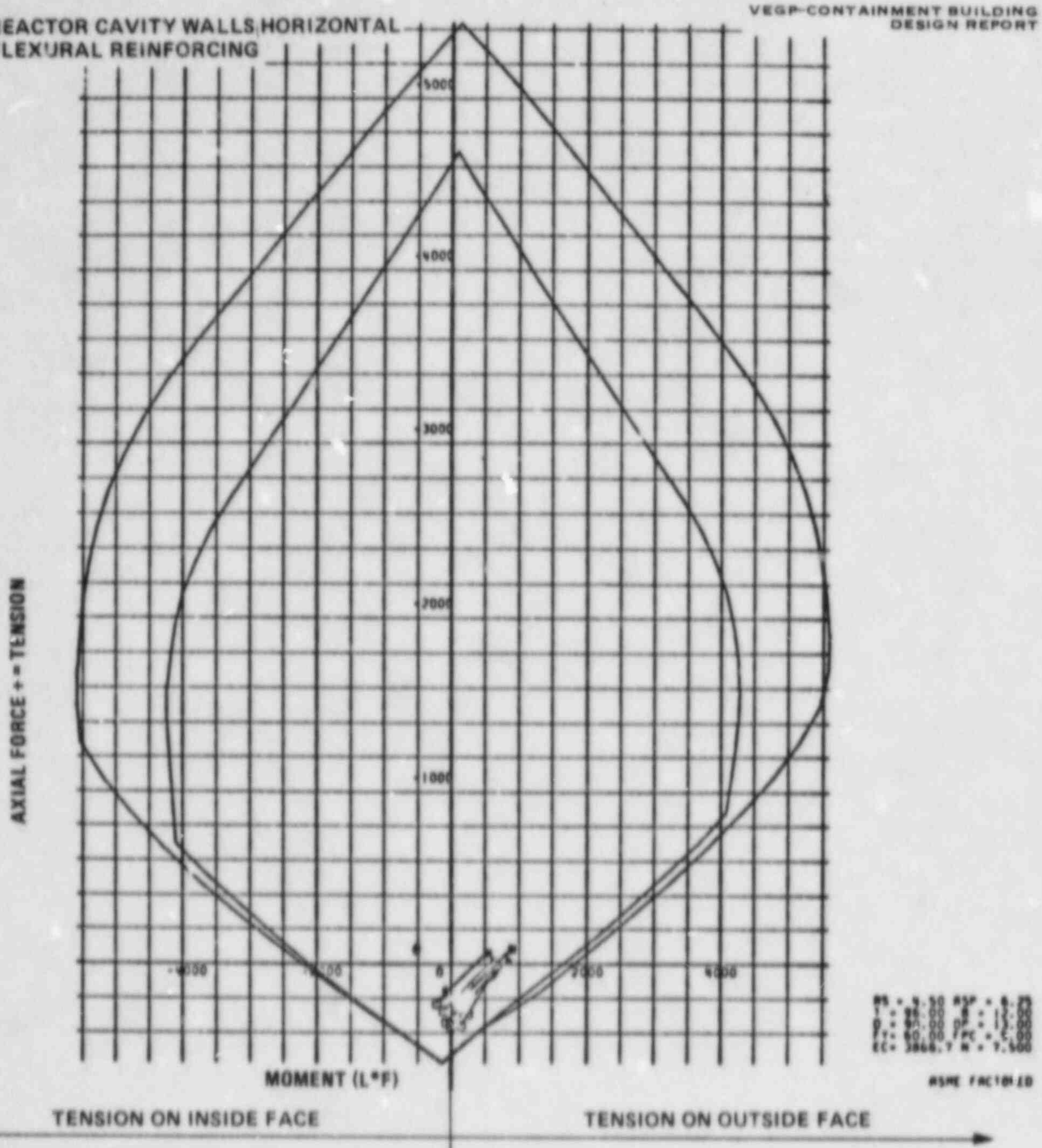

KEY LOCATION (SEE FIG. 19)	GRID ELEMENT NUMBER	LOAD COMBINATION (TABLE 5)	WITHOUT THERMAL EFFECTS			WITH THERMAL EFFECTS		
			AXIAL FORCE (K/FT)	MOMENT (FT-K/FT)	UF	AXIAL FORCE (K/FT)	MOMENT (FT-K/FT)	UFS
3	1	7	263	140	23.3	-28	835	43.7
3	10	7	195	153	18.3	-97	883	41.6
3	13	7	352	133	35.0	61	604	37.5
3	15	7	211	159	20.1	-81	889	42.8
3	45	7	229	-220	12.6	-63	532	26.3
3	28	7	223	-217	12.3	-68	532	26.1
3	38	7	265	-126	5.5	-26	625	32.8
3	21	7	336	-91	1.4	45	628	37.7
3	22	7	362	-20	10.8	71	566	35.9

Figure 26
FOUNDATION INTERACTION DIAGRAMS
WITH THERMAL EFFECTS INCLUDED
(Sheet 10 of 16)

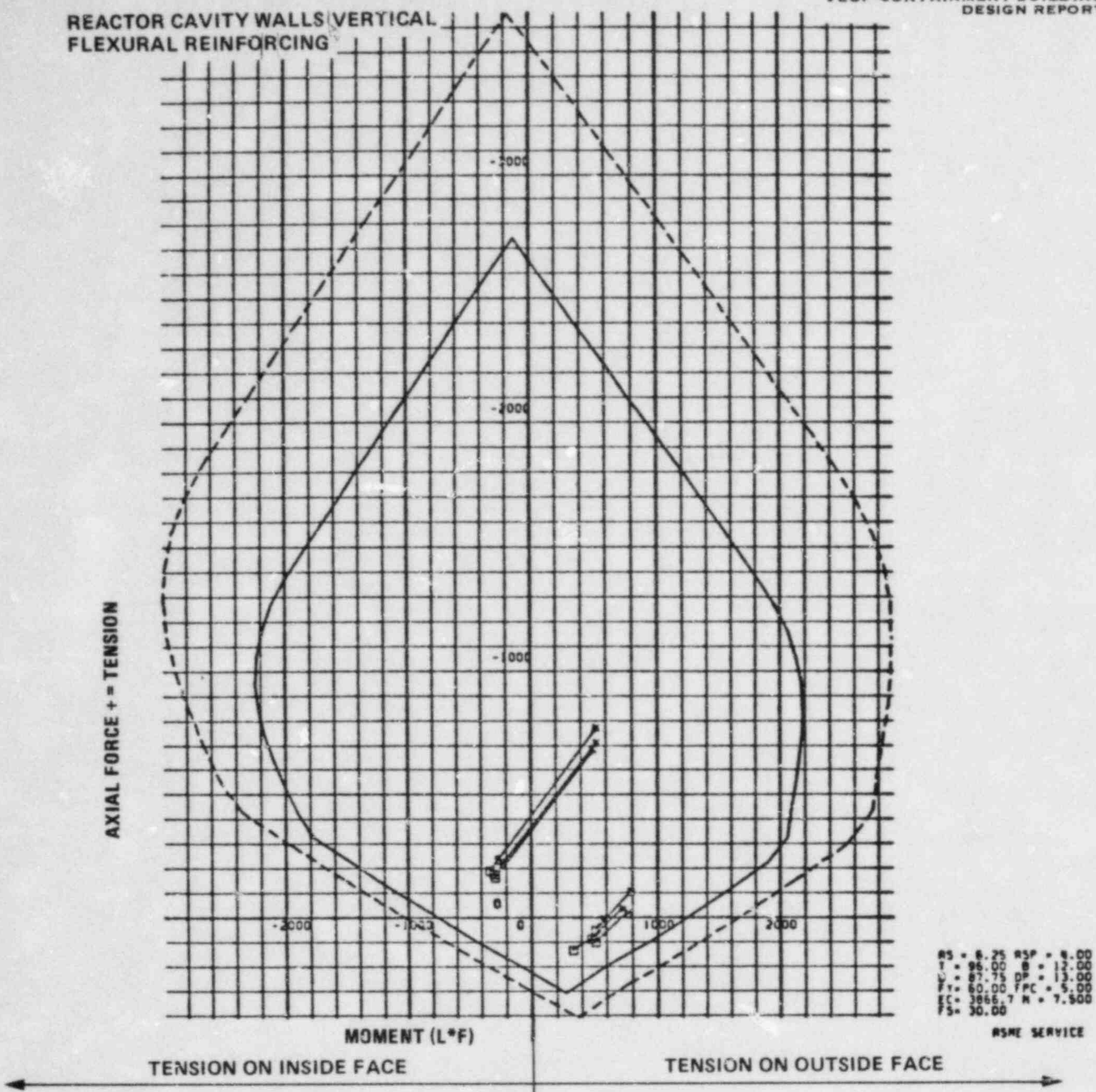

KEY LOCATION (SEE FIG. 19)	GRID ELEMENT NUMBER	LOAD COMBINATION (TABLE 5)	WITHOUT THERMAL EFFECTS			WITH THERMAL EFFECTS		
			AXIAL FORCE (K/FT)	MOMENT (FT-K/FT)	UF	AXIAL FORCE (K/FT)	MOMENT (FT-K/FT)	UFS
3	11	1	129	320	28.7	80	500	31.9
3	12	1	85	469	43.5	-39	727	40.7
3	13	1	99	504	49.3	-19	757	43.9
3	24	1	48	504	43.6	-104	784	39.7
3	13	4	-192	-341	24.2	-769	512	19.1
3	13	4	-178	-306	22.4	-709	516	19.2
3	12	4	-163	-292	22.2	-679	487	18.3

Figure 26
FOUNDATION INTERACTION DIAGRAMS
WITH THERMAL EFFECTS INCLUDED
(Sheet 11 of 16)

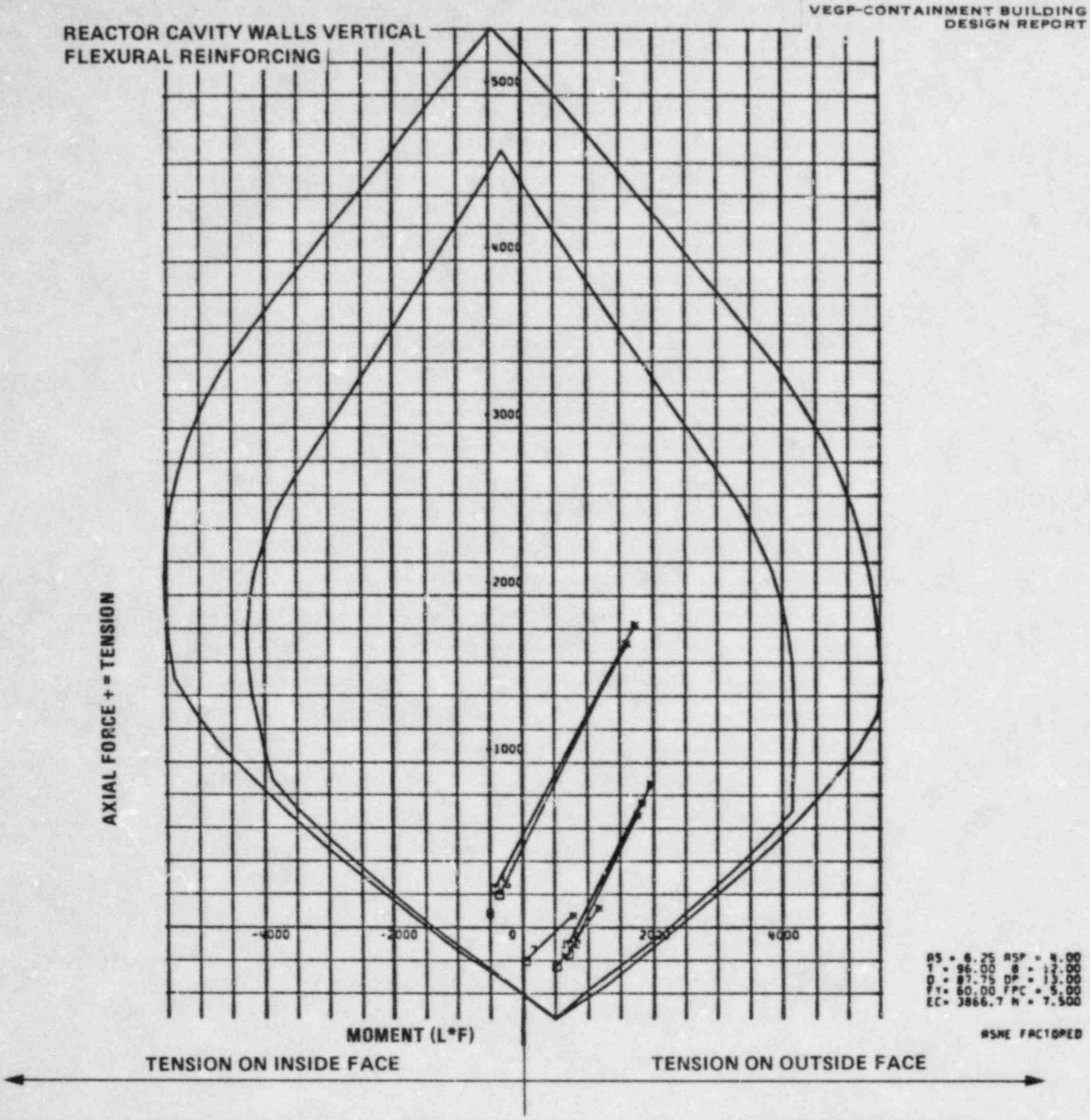

KEY LOCATION (SEE FIG. 19)	GRID ELEMENT NUMBER	LOAD COMBINATION (TABLE 5)	WITHOUT THERMAL EFFECTS			WITH THERMAL EFFECTS		
			AXIAL FORCE (K/FT)	MOMENT (FT-K/FT)	UF	AXIAL FORCE (K/FT)	MOMENT (FT-K/FT)	UFS
3	13	6	-241	-432	19.7	-1818	1724	32.7
3	13	7	159	694	34.5	-683	1745	40.8
3	12	7	138	645	31.0	-752	1815	41.0
3	14	7	232	507	23.3	-121	1158	42.1
3	24	7	98	688	32.5	-871	1950	41.7
3	12	6	-200	-364	17.6	-1704	1598	30.2
3	35	7	199	43	15.1	-79	766	20.3

Figure 26
FOUNDATION INTERACTION DIAGRAMS
WITH THERMAL EFFECTS INCLUDED
(Sheet 12 of 16)

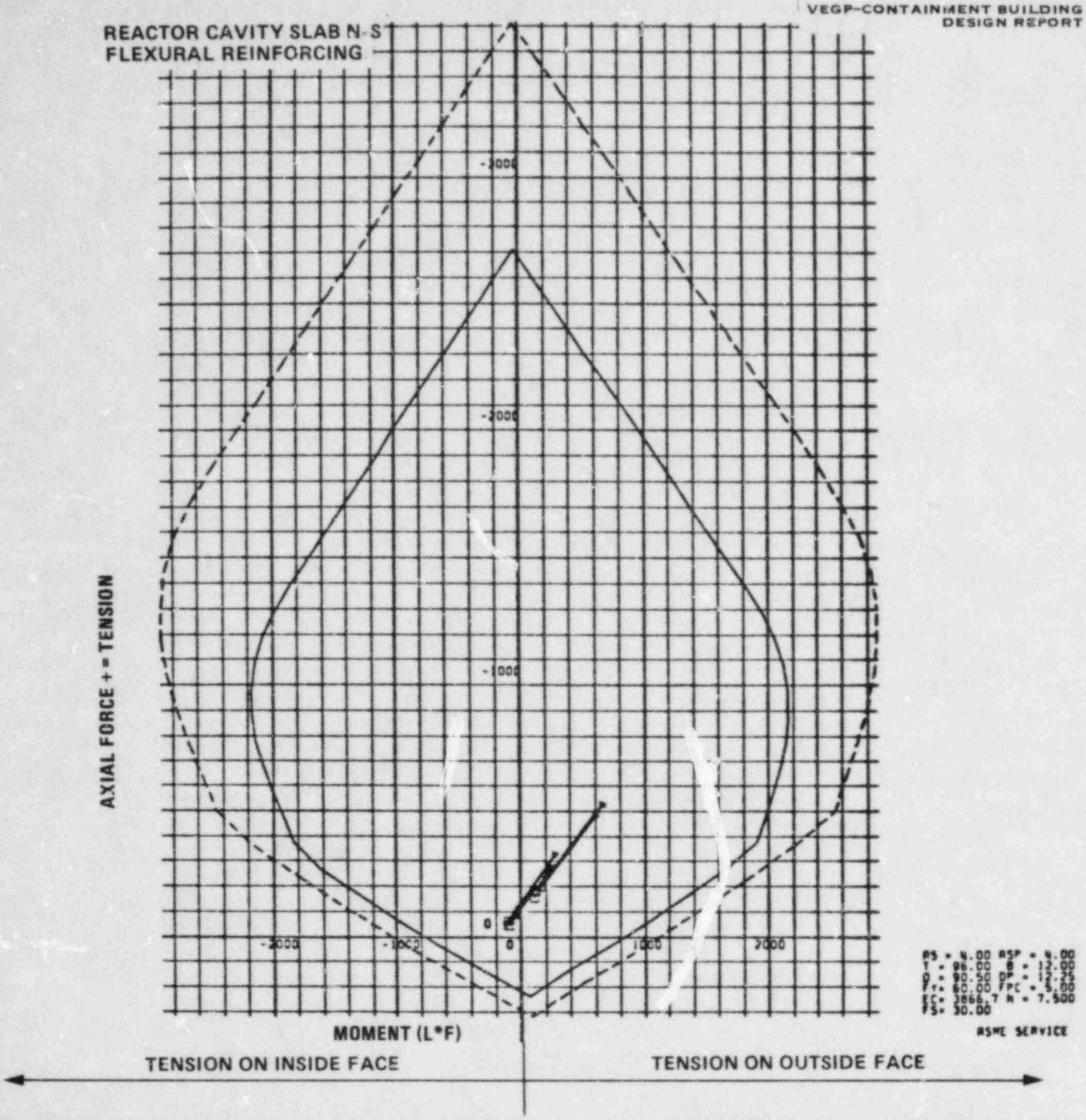

KEY LOCATION (SEE FIG. 19)	GRID ELEMENT NUMBER	LOAD COMBINATION (TABLE 5)	WITHOUT THERMAL EFFECTS			WITH THERMAL EFFECTS		
			AXIAL FORCE (K/FT)	MOMENT (FT-K/FT)	UF	AXIAL FORCE (K/FT)	MOMENT (FT-K/FT)	UFS
4	85	1	-63	-111	11.2	-328	278	13.3
4	75	4	-183	126	9.1	-527	655	25.8
4	74	4	-158	109	8.3	-481	604	24.0
4	76	1	-48	-93	9.9	-275	236	12.2
4	86	1	-47	-109	11.6	-283	221	11.3

Figure 26
FOUNDATION INTERACTION DIAGRAMS
WITH THERMAL EFFECTS INCLUDED
(Sheet 13 of 16)

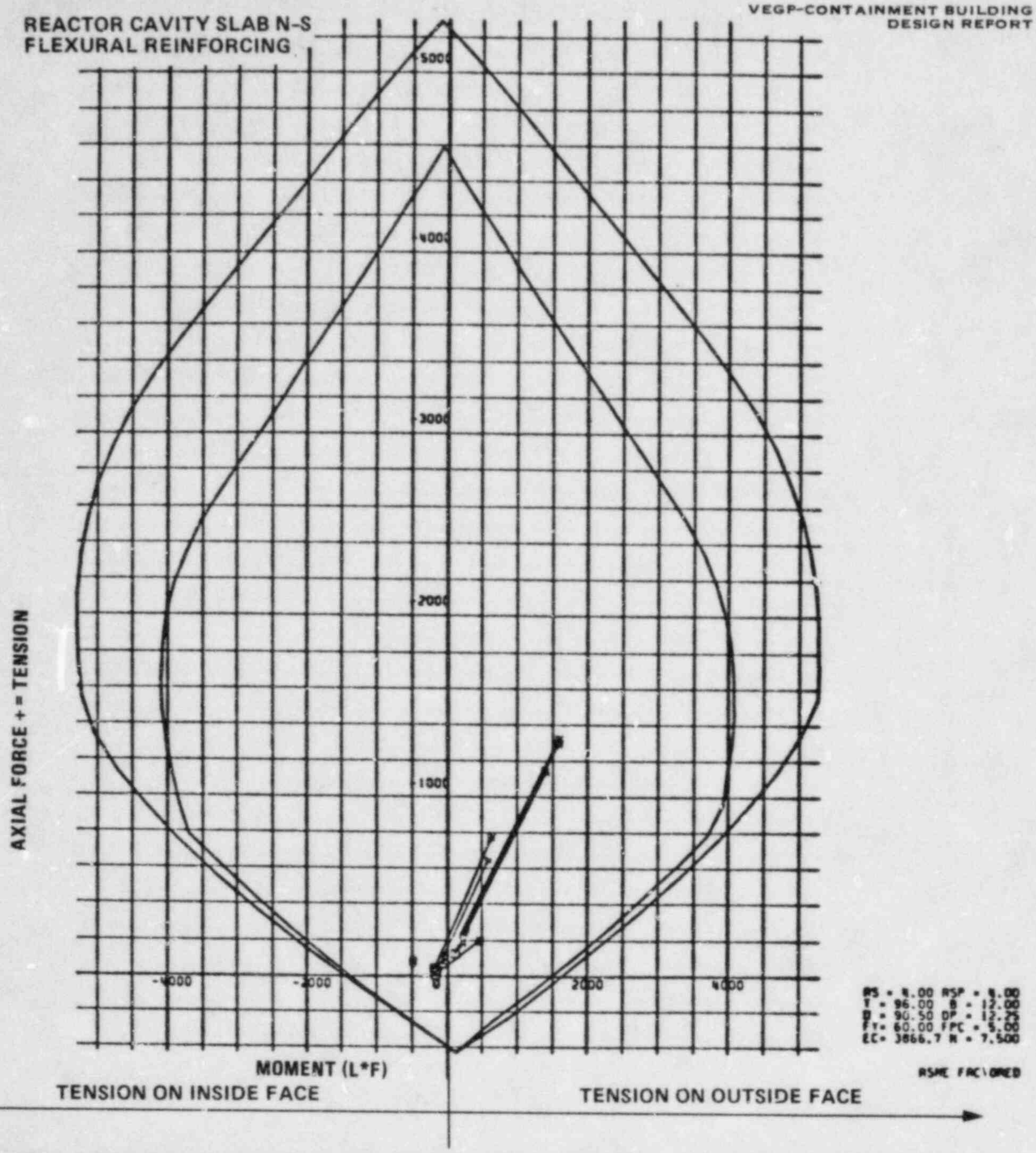

KEY LOCATION (SEE FIG. 19)	GRID ELEMENT NUMBER	LOAD COMBINATION (TABLE 5)	WITHOUT THERMAL EFFECTS			WITH THERMAL EFFECTS		
			AXIAL FORCE (K/FT)	MOMENT (FT-K/FT)	UF	AXIAL FORCE (K/FT)	MOMENT (FT-K/FT)	UFS
4	86	8	-46	-183	11.7	-777	622	16.1
4	75	6	-187	140	6.8	-1295	1562	31.8
4	76	6	-196	134	6.5	-1320	1583	32.0
4	73	6	-130	106	5.6	-1137	1391	29.9
4	86	7	-7	-169	11.8	-200	456	20.1
4	75	7	-31	-155	10.3	-647	571	16.1

Figure 26
FOUNDATION INTERACTION DIAGRAMS
WITH THERMAL EFFECTS INCLUDED
(Sheet 14 of 16)

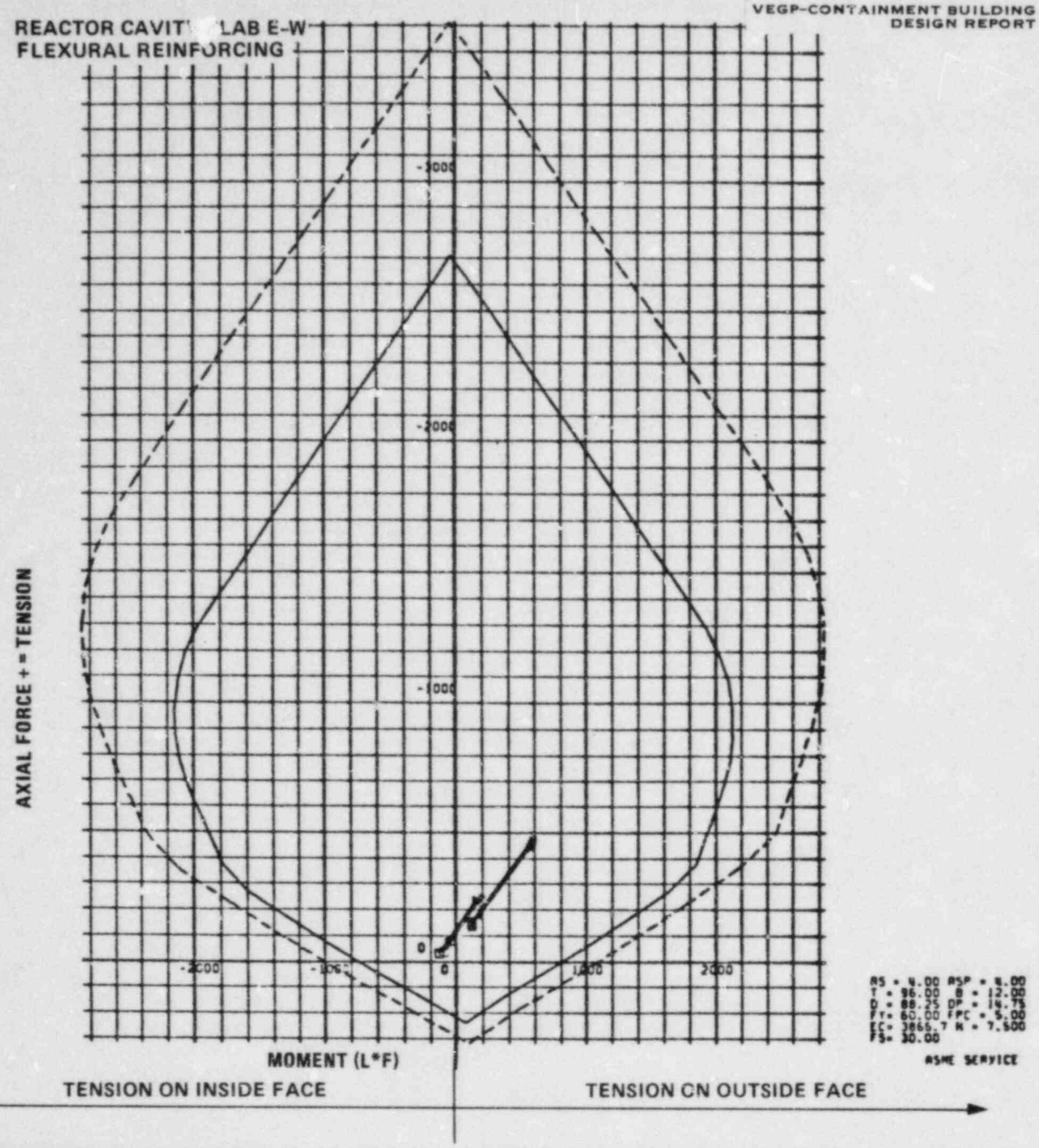

KEY LOCATION (SEE FIG. 19)	GRID ELEMENT NUMBER	LOAD COMBINATION (TABLE 5)	WITHOUT THERMAL EFFECTS			WITH THERMAL EFFECTS		
			AXIAL FORCE (K/FT)	MOMENT (FT-K/FT)	UF	AXIAL FORCE (K/FT)	MOMENT (FT-K/FT)	UFS
4	92	1	-33	-132	15.2	-239	144	8.0
4	82	4	-147	113	9.0	-458	572	23.6
4	92	4	-155	112	8.8	-473	587	24.2
4	82	3	-140	107	8.7	-444	556	23.3
4	82	1	-33	-131	15.1	-230	142	8.1
4	73	1	-40	-98	11.0	-251	194	10.6

Figure 26
FOUNDATION INTERACTION DIAGRAMS
WITH THERMAL EFFECTS INCLUDED
(Sheet 15 of 16)

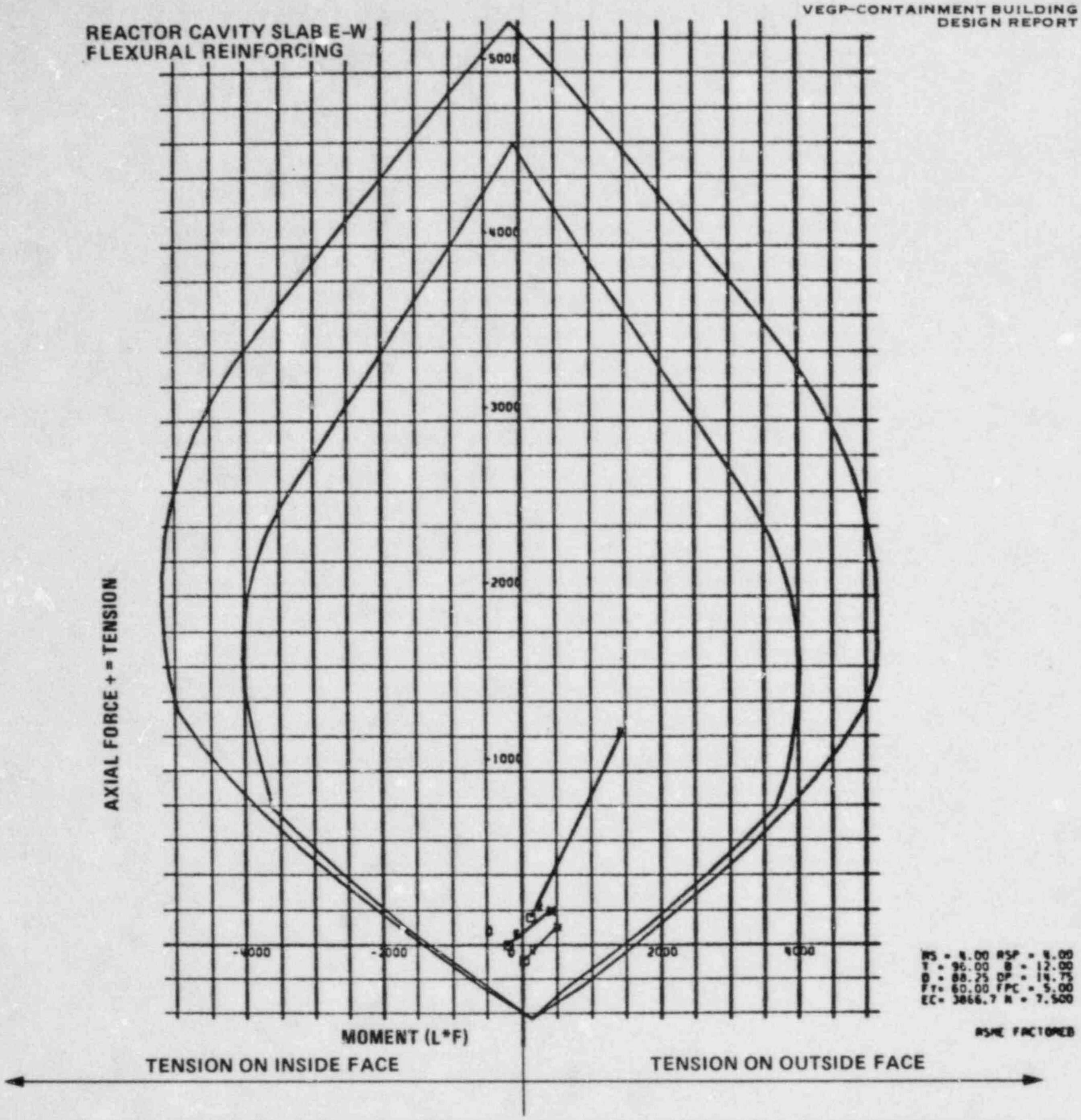

KEY LOCATION (SEE FIG. 19)	GRID ELEMENT NUMBER	LOAD COMBINATION (TABLE 5)	WITHOUT THERMAL EFFECTS			WITH THERMAL EFFECTS		
			AXIAL FORCE (K/FT)	MOMENT (FT-K/FT)	UF	AXIAL FORCE (K/FT)	MOMENT (FT-K/FT)	UFS
4	92	7	-2	-201	14.8	-195	402	18.1
4	82	6	-161	119	6.2	-1224	1439	30.5
4	92	6	-162	118	6.1	-1226	1440	30.5
4	86	7	89	20	0.5	-104	504	25.9
4	82	7	-2	-199	14.7	-194	402	18.2
4	92	7	-2	-201	14.8	-195	402	18.2

Figure 26
FOUNDATION INTERACTION DIAGRAMS
WITH THERMAL EFFECTS INCLUDED
(Sheet 16 of 16)

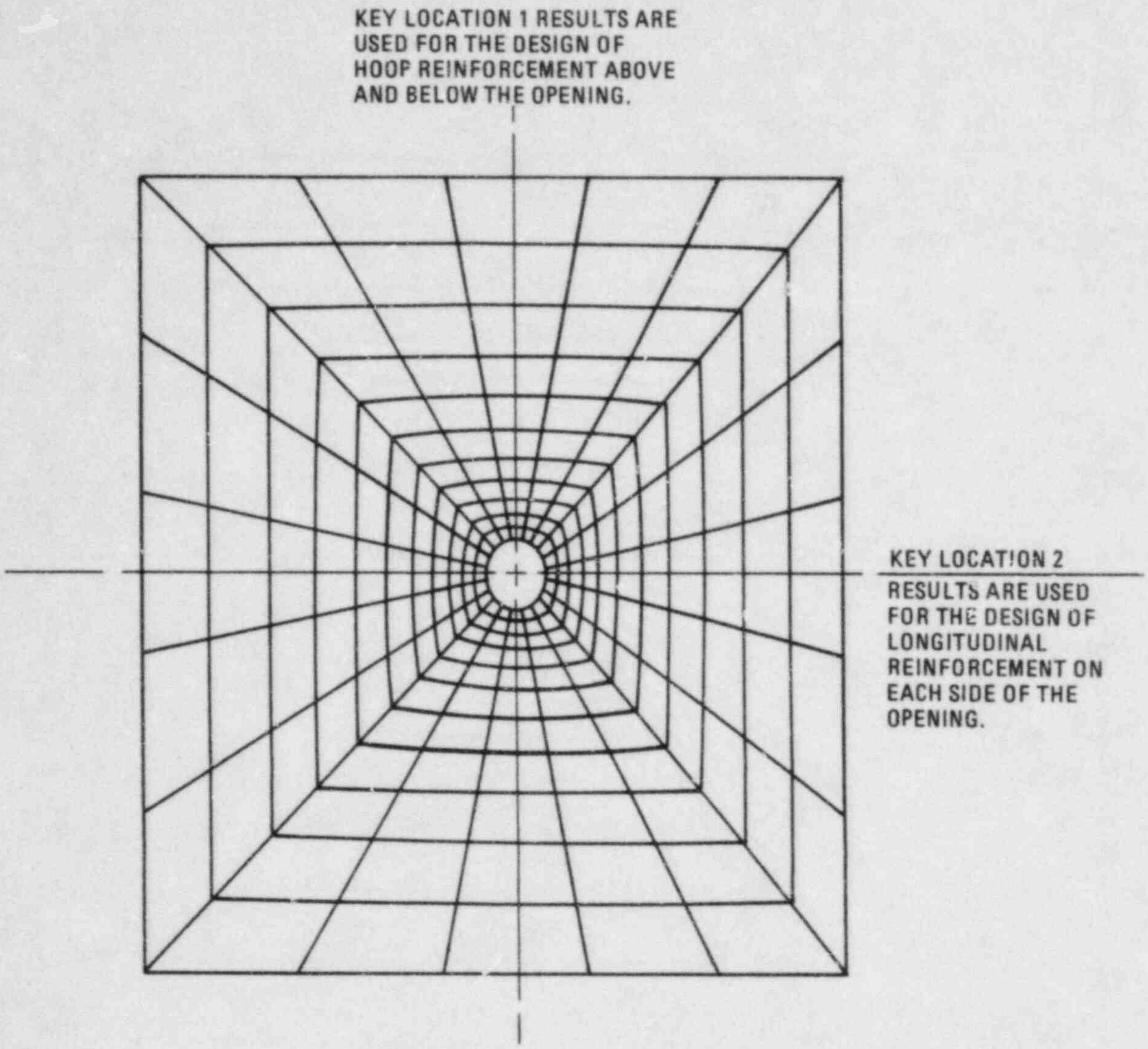

ELEVATION OF MODEL

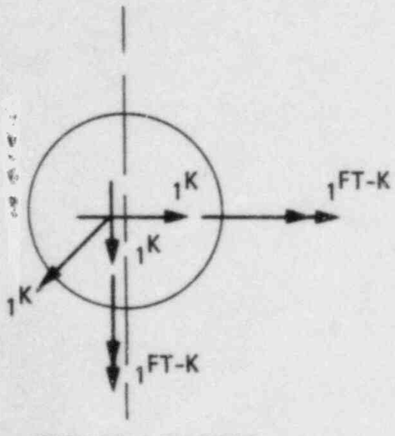

UNIT APPLIED LOADS

Figure 27
SHELL SMALL PENETRATION FINITE
ELEMENT MODEL

APPENDIX A

DEFINITION OF LOADS

APPENDIX A

DEFINITION OF LOADS

All credible loads applicable to the design of the containment building are defined as follows. The nomenclature used matches the ASME Code, Article CC-3000. The loads considered are normal loads, construction loads, test loads, severe environmental loads, extreme environmental loads, and abnormal loads.

A.1 SERVICE LOADS

The service loads are those loads which are encountered during normal plant operation and shutdown (normal loads), various construction stages (construction loads), and test conditions (test loads).

A.1.1 Normal Loads

D = dead loads, including hydrostatic and permanent equipment loads

L = live loads, including any movable equipment loads and other loads which vary with intensity and occurrence, such as soil pressures

F = loads resulting from the application of prestress

T_o = thermal effects and loads during normal operating or shutdown conditions, based on the most critical transient or steady state condition

R_o = pipe reactions during normal operating or shutdown conditions, based on the most critical transient or steady state condition

P_v = external pressure loads resulting from pressure variation either inside or outside the containment

A.1.2 Construction Loads

These loads are encountered from the start to completion of construction. The definitions for D, L, F, and T_o given for normal loads are applicable but are based on construction conditions.

A.1.3 Test Loads

These loads are applied during structural integrity or leak rate testing. The definitions for D, L, and F given for normal loads are applicable but are based on test conditions. Additionally, the following loads are considered.

P_t Pressure during the structural integrity and leak rate tests

T_t thermal effects and loads during the test

A.2 FACTORED LOADS

The factored loads include severe environmental loads, extreme environmental loads, and abnormal loads.

A.2.1 Severe Environmental Loads

These loads could infrequently be encountered during the plant life.

W = loads generated by the design wind specified for the plant site

E_o = loads generated by the operating basis earthquake. Only the actual dead load and existing live load weights need be considered in evaluating seismic response forces.

A.2.2 Extreme Environmental Loads

These loads are credible but highly improbable.

E_{ss} = loads generated by the safe shutdown earthquake. Weights considered shall be the same as for E_o.

W_t = tornado loading including the effects of missile impact. Included in W_t are the following:

W_{tq} = the loads due to tornado wind pressure

W_{tp} = the differential pressure loads due to rapid atmospheric pressure change

W_{tm} = the tornado generated missile impact effects. The type of impact, such as plastic or elastic, together with the ability of the structure to deform beyond yield shall be considered in establishing the structural capacity necessary to resist the impact.

B = loads generated by postulated blast along transportation routes.

A.2.3 Abnormal Loads

These loads are generated by a postulated high energy pipe break accident within a building and/or compartment thereof.

P_a = design pressure load within the containment generated by the postulated high energy line break.

T_a = thermal effects and loads generated by the postulated high energy line break including T_o.

R_a = pipe reaction from thermal conditions generated by the postulated high energy line break including R_o.

R_r = the local effects on the containment due to the postulated high-energy line break. The local effects include R_{rr}, R_{rj}, and R_{rm} as defined below.

R_{rr} = load on the containment generated by the reaction of a ruptured high energy pipe during a postulated line break.

R_{rj} = load on the containment generated by jet impingement from a ruptured high energy pipe during a postulated line break.

R_{rm} = load on the containment resulting from the impact of a ruptured high energy pipe during a postulated line break.

APPENDIX B

LOAD COMBINATIONS

APPENDIX B

LOAD COMBINATIONS

The load combination tables shown on the following three pages cover three codes applicable to structural elements covered in this design report.

TABLE B.1

This table is in accordance with the ASME Code, Article CC-3000. The containment building shell and basemat are designed in accordance with this table.

TABLE B.2

This table is in accordance with ACI 318-71 including the 1974 supplement. The tendon gallery, access shaft number one, and equipment hatch missile shield are designed in accordance with this table.

TABLE B.3

This table is in accordance with the 1969 AISC Specification for the Design, Fabrication, and Erection of Structural Steel for Buildings, including Supplements 1, 2, and 3. The polar crane brackets and equipment hatch missile shield support frame are designed in accordance with this table.

TABLE B.1

LOAD COMBINATIONS AND LOAD FACTORS FOR CONTAINMENT BUILDING
ELEMENTS DESIGNED IN ACCORDANCE WITH THE ASME CODE, ARTICLE CC-3000

Category	D	L	F	P_t	P_a	T_t	T_o	T_a	E_o	E_{ss}	W	W_t	R_o	R_a	R_r	P_v	B
Service																	
Test	1.0	1.0	1.0	1.0	--	1.0	--	--	--	--	--	--	--	--	--	--	--
Construction	1.0	1.0	1.0	--	--	--	1.0	--	--	--	1.0	--	--	--	--	--	--
Normal	1.0	1.0	1.0	--	--	--	1.0	--	--	--	--	--	1.0	--	--	1.0	--
Severe environmental	1.0	1.0	1.0	--	--	--	1.0	--	1.0	--	--	--	1.0	--	--	1.0	--
	1.0	1.0	1.0	--	--	--	1.0	--	--	--	1.0	--	1.0	--	--	1.0	--
Factored																	
Severe environmental	1.0	1.3	1.0	--	--	--	1.0	--	1.5	--	--	--	1.0	--	--	1.0	--
	1.0	1.3	1.0	--	--	--	1.0	--	--	--	1.5	--	1.0	--	--	1.0	--
Extreme environmental	1.0	1.0	1.0	--	--	--	1.0	--	--	1.0	--	--	1.0	--	--	1.0	--
	1.0	1.0	1.0	--	--	--	1.0	--	--	--	--	1.0	1.0	--	--	1.0	--
	1.0	1.0	1.0	--	--	--	1.0	--	--	--	--	--	1.0	--	--	1.0	1.0
Abnormal	1.0	1.0	1.0	--	1.5	--	--	1.0	--	--	--	--	--	1.0	--	--	--
	1.0	1.0	1.0	--	1.0	--	--	1.0	--	--	--	--	--	1.25	--	--	--
Abnormal/severe environmental	1.0	1.0	1.0	--	1.25	--	--	1.0	1.25	--	-	--	--	1.0	--	--	--
	1.0	1.0	1.0	--	1.25	--	--	1.0	--	--	1.25	--	--	1.0	--	--	--
	1.0	1.0	1.0	--	--	--	1.0	--	1.0	or	1.0	--	--	--	--	--	--
Abnormal/extreme environmental	1.0	1.0	1.0	--	1.0	--	--	1.0	--	1.0	--	--	--	1.0	1.0	--	--

See appendix A for definition of load symbols.

TABLE B.2[(a)(f)]

CONCRETE DESIGN LOAD COMBINATIONS STRENGTH METHOD

	EQN	D	L	P_s	T_o	T_a	E	E'	W	W_t	R_o	R_a	Y_j	Y_r	Y_m	N	B	Strength Limit
Service Load Conditions																		
	1	1.4	1.7															U
(See note b.)	2	1.4	1.7						1.7									U
(See note c.)	3	1.4	1.7				1.9											U
	4	1.05	1.275		1.275						1.275							U
	5	1.05	1.275		1.275				1.275		1.275							U
	6	1.05	1.275		1.275		1.425				1.275							U
Factored Load Conditions																		
	7	1.0	1.0		1.0			1.0			1.0							U
(See note d.)	8	1.0	1.0		1.0					1.0	1.0							U
	9	1.0	1.0	1.5		1.0						1.0						U
(See note e.)	10	1.0	1.0	1.25		1.0	1.25					1.0	1.0	1.0	1.0			U
(See note e.)	11	1.0	1.0	1.0		1.0		1.0				1.0	1.0	1.0	1.0			U
	12	1.0	1.0		1.0						1.0						1.0	U
	13	1.0	1.0		1.0						1.0					1.0		

---

a. See appendix A for definition of load symbols. U is the required strength based on strength method per ACI 318-71.
b. Unless this equation is more severe, the load combination 1.2D+1.7W is also to be considered.
c. Unless this equation is more severe, the load combination 1.2D+1.9E is also to be considered.
d. When considering tornado missile load, local section strength may be exceeded provided there will be no loss of function of any safety-related system. In such cases, this load combination without the tornado missile load is also to be considered.
e. When considering Y_j, Y_r, and Y_m loads, local section strength may be exceeded provided there will be no loss of function of any safety-related system. In such cases, this load combination without Y_j, Y_r, and Y_m is also to be considered.
f. Actual load factors used in design may have exceeded those shown in this table.

TABLE B.3[(a)]

STEEL DESIGN LOAD COMBINATIONS
ELASTIC METHOD

	EQN	D	L	P_a	T_o	T_a	E	E'	W	W_t	R_o	R_a	Y_j	Y_r	Y_m	N	B	Strength Limit(f_s)
Service Load Conditions																		
	1	1.0	1.0															1.0
	2	1.0	1.0				1.0											1.0
	3	1.0	1.0						1.0									1.0
	4	1.0	1.0		1.0						1.0							1.5
	5	1.0	1.0		1.0		1.0				1.0							1.5
	6	1.0	1.0		1.0				1.0		1.0							1.5
Factored Load																		
	7	1.0	1.0		1.0			1.0			1.0							1.6
(See note b.)	8	1.0	1.0		1.0					1.0	1.0							1.6
	9	1.0	1.0	1.0		1.0						1.0						1.6
(See notes c and d.)	10	1.0	1.0	1.0		1.0	1.0					1.0	1.0	1.0	1.0			1.6
(See notes c and d.)	11	1.0	1.0	1.0		1.0		1.0				1.0	1.0	1.0	1.0			1.7
	12	1.0	1.0		1.0						1.0						1.0	1.6
	13	1.0	1.0		1.0						1.0					1.0		1.6

a. See appendix A for definition of load symbols. f_s is the allowable stress for the elastic design method defined in Part 1 of the AISC, "Specification for the Design, Fabrication, and Erection of Structural Steel for Buildings." The one-third increase in allowable stresses permitted for seismic or wind loadings is not considered.

b. When considering tornado missile load, local section strength may be exceeded provided there will be no loss of function of any safety-related system. In such cases, this load combination without the tornado missile load is also to be considered.

c. When considering Y, Y_r and Y_m loads, local section strength may be exceeded provided there will be no loss of function of any safety-related system. In such cases, this load combination without Y_j, Y_r, and Y_m is also to be considered.

d. For this load combination, in computing the required section strength, the plastic section modulus of steel shapes, except for those which do not meet the AISC criteria for compact sections, may be used.

APPENDIX C

DESIGN OF STRUCTURES FOR TORNADO MISSILE IMPACT

APPENDIX C

DESIGN OF STRUCTURES FOR TORNADO MISSILE IMPACT

C.1 INTRODUCTION

This appendix contains methods and procedures for analysis and design of steel and reinforced concrete structures and structural elements subject to tornado-generated missile impact effects. Postulated missiles, and other concurrent loading conditions are identified in Section 3.2 of the Design Report.

Missile impact effects are assessed in terms of local damage and structural response. Local damage (damage that occurs in the immediate vicinity of the impact area) is assessed in terms of perforation and scabbing.

Evaluation of local effects is essential to ensure that protected items would not be damaged directly by a missile perforating a protective barrier or by scab particles. Empirical formulas are used to assess local damage.

Evaluation of structural response is essential to ensure that protected items are not damaged or functionally impaired by deformation or collapse of the impacted structure.

Structural response is assessed in terms of deformation limits, strain energy capacity, structural integrity, and structural stability. Structural dynamics principles are used to predict structural response.

C.1.1 Procedures

The general procedures for analysis and design of structures or structural elements for missile impact effects include:

A. Defining the missile properties (such as type, material, deformation characteristics, geometry, mass, trajectory, strike orientation, and velocity).

B. Determining impact location, material strength, and thickness required to preclude local failure (such as perforation for steel targets and scabbing for reinforced concrete targets).

C. Defining the structure and its properties (such as geometry, section strength, deformation limits, strain energy absorption capacity, stability characteristics, and dynamic response characteristics).

D. Determining structural response considering other concurrent loading conditions.

E. Checking adequacy of structural design (stability, integrity, deformation limits, etc.) to verify that local damage and structural response (maximum deformation) will not impair the function of safety-related items.

C.2 LOCAL EFFECTS

Evaluation of local effects consists of estimating the extent of local damage and characterization of the interface force-time function used to predict structural response. Local damage is confined to the immediate vicinity of the impact location on the struck element and consists of missile deformation, penetration of the missile into the element, possible perforation of the element, and, in the case of reinforced concrete, dislodging of concrete particles from the back face of the element (scabbing).

Because of the complex physical processes associated with missile impact, local effects are evaluated primarily by application of empirical relationships based on missile impact test results. Unless otherwise noted, these formulas are applied considering a normal incidence of strike with the long axis of the missile parallel to the line of flight.

C.2.1 Reinforced Concrete Elements

The parts of the building structure that offer protection for safety-related equipment against tornado-generated missiles are provided with $f_c^{'}$ = 4000 psi minimum concrete strength, have 24-inch-minimum-thick walls, and have 21-inch-minimum-thick roofs. Therefore, the walls and roofs of these structures are resistant to perforation and scabbing by the postulated missiles discussed in Section 3.2 of the Design Report under tornado loads.

C.2.2 Steel Elements

Steel barriers subjected to missile impact are designed to preclude perforation. An estimate of the steel element thickness for threshold of perforation for nondeformable missiles is provided by equation 2-1, which is a more convenient form of the Ballistic Research Laboratory (BRL) equation for perforation of steel plates with material constant taken as unity (reference 1).

$$T_p = \frac{(E_k)^{2/3}}{672D} \qquad E_k = \frac{M_m V_s^2}{2} \qquad (2\text{-}1)$$

where:

T_p = steel plate thickness for threshold of perforation (in.).

E_k = missile kinetic energy (ft-lb).

M_m = mass of the missile ($lb\text{-}s^2/ft$).

V_s = missile striking velocity (ft/s).

D = missile diameter (in.).[a]

---

a. For irregularly shaped missiles, an equivalent diameter is used. The equivalent diameter is taken as the diameter of a circle with an area equal to the circumscribed contact, or projected frontal area, of the noncylindrical missile. For pipe missiles, D is the outside diameter of the pipe.

The design thickness to prevent perforation, t_p, must be greater than the predicted threshold value. The threshold value is increased by 25 percent to obtain the design thickness.

$$t_p = 1.25\ T_p \tag{2-2}$$

where:

t_p = design thickness to preclude perforation (in.).

C.3 STRUCTURAL RESPONSE DUE TO MISSILE IMPACT LOADING

When a missile strikes a structure, large forces develop at the missile-structure interface, which decelerate the missile and accelerate the structure. The response of the structure depends on the dynamic properties of the structure and the time-dependent nature of the applied loading (interface force-time function). The force-time function is, in turn, dependent on the type of impact (elastic or plastic) and the nature and extent of local damage.

C.3.1 General

In an elastic impact, the missile and the structure deform elastically, remain in contact for a short period of time (duration of impact), and subsequently disengage due to the action of elastic interface restoring forces.

In a plastic impact, the missile or the structure or both may deform plastically or sustain permanent deformation or damage (local damage). Elastic restoring forces are small, and the missile and the structure tend to remain in contact after impact. Plastic impact is much more common in nuclear plant design than elastic impact, which is rarely encountered. For example, test data indicate that the impact from all postulated tornado-generated missiles can be characterized as a plastic collision.

If the interface forcing function can be defined or conservatively idealized (from empirical relationships or from theoretical considerations), the structure can be modeled mathematically, and conventional analytical or numerical techniques can be used to predict structural response. If the interface forcing function cannot be defined, the same mathematical model of the structure can be used to determine structural response by application of conservation of momentum and energy balance techniques with due consideration for type of impact (elastic or plastic).

In either case, in lieu of a more rigorous analysis, a conservative estimate of structural response can be obtained by first determining the response of the impacted structural element and then applying its reaction forces to the supporting structure. The predicted structural response enables assessment of structural design adequacy in terms of strain energy capacity, deformation limits, stability, and structural integrity.

Three different procedures are given for determining structural response: the force-time solution, the response chart solution, and the energy balance solution. The force-time solution involves numerical integration of the equation(s) of motion and is the most general method applicable for any pulse shape and resistance function. The response chart solution can be used with comparable results, provided the idealized pulse shape (interface forcing function) and the resistance function are compatible with the response chart. The energy balance solution is used in cases where the interface forcing function cannot be defined or where an upper limit check on structural response is desired. This method will consistently overestimate structural response, since the resisting spring forces during impact are neglected.

In defining the mass-spring model, consideration is given to local damage that could affect the response of the element. For concrete slab elements, the beneficial effect of formation of a fracture plane which propagates from the impact zone to the back of the slab (back face fracture plane) just prior to scabbing (reference 2) is neglected. The formation of this fracture plane limits the forces transferred to the surrounding slab and significantly reduces overall structural response. Since scabbing is to be precluded in the design, the structural response check is made assuming the fracture plane is not formed. It is recognized, however, that should the missile velocity exceed that for threshold of scabbing, structural response would be limited by this mechanism.

Therefore, the structural response is conservatively evaluated ignoring formation of the fracture plane and any reduction in response.

C.3.2 Structural Assessment

The predicted structural response enables assessment of design adequacy in terms of strain energy capacity, deformation limits, stability, and structural integrity.

For structures allowed to displace beyond yield (elasto-plastic response), a check is made to ensure that deformation limits would not be exceeded, by comparing calculated displacements or required ductility ratios with allowable values (such as those contained in table C-1).

C.4 REFERENCES

1. Gwaltney, R. C., "Missile Generation and Protection in Light-Water-Cooled Power Reactor Plants," ORNL NSIC-22, Oak Ridge National Laboratory, Oak Ridge, Tennessee, for the USAEC, September 1968.

2. Rotz, J. V., "Results of Missile Impact Tests on Reinforced Concrete Panels," Vol 1A, pp 720-738, Second Specialty Conference on Structural Design of Nuclear Power Plant Facilities, New Orleans, Louisiana, December 1975.

TABLE C-1

DUCTILITY RATIOS (Sheet 1 of 2)

Member Type and Load Condition	Maximum Allowable Value of Ductility Ratio (μ)
Reinforced Concrete	
Flexure(1):	
Beams and one-way slabs(2)	$\frac{0.10}{p-p'} \leq 10$
Slabs with two-way reinforcing(2)	$\frac{0.10}{p-p'} \leq 10$ or 30 (See 3 and 4)
Axial compression(1):	
Walls and columns	1.3
Shear, concrete beams and slabs in region controlled by shear:	
Shear carried by concrete only	1.3
Shear carried by concrete and stirrups	1.6
Shear carried completely by stirrups	2.0
Shear carried by bent-up bars	3.0
Structural Steel	
Columns(5) $\ell/r \leq 20$	1.3
$\ell/r > 20$	1.0
Tension due to flexure	10
Shear	10
Axial tension and steel plates in membrane tension(6)	$0.5 \frac{e_u}{e_y}$
Compression members not required for stability of building structures	10

TABLE C-1

DUCTILITY RATIOS (Sheet 2 of 2)

Notes:

(1) The interaction diagram used to determine the allowable ductility ratio for elements subject to combined flexure and axial compression is provided in figure C-1.

(2) p and p' are the positive and negative reinforcing steel ratios, respectively.

(3) Ductility ratio up to 10 can be used without an angular rotation check.

(4) Ductility ratio up to 30 can be used provided an angular rotation check is made.

(5) ℓ/r is the member slenderness ratio. The value specified is for axial compression. For columns and beams with uniform moment the following value is used:

$$\frac{14 \times 10^4}{F_y \left(\frac{k\ell}{r}\right)^2} + \frac{1}{2} \leq 10$$

(6) e_u and e_y are the ultimate and yield strains. e_u shall be taken as the ASTM-specified minimum.

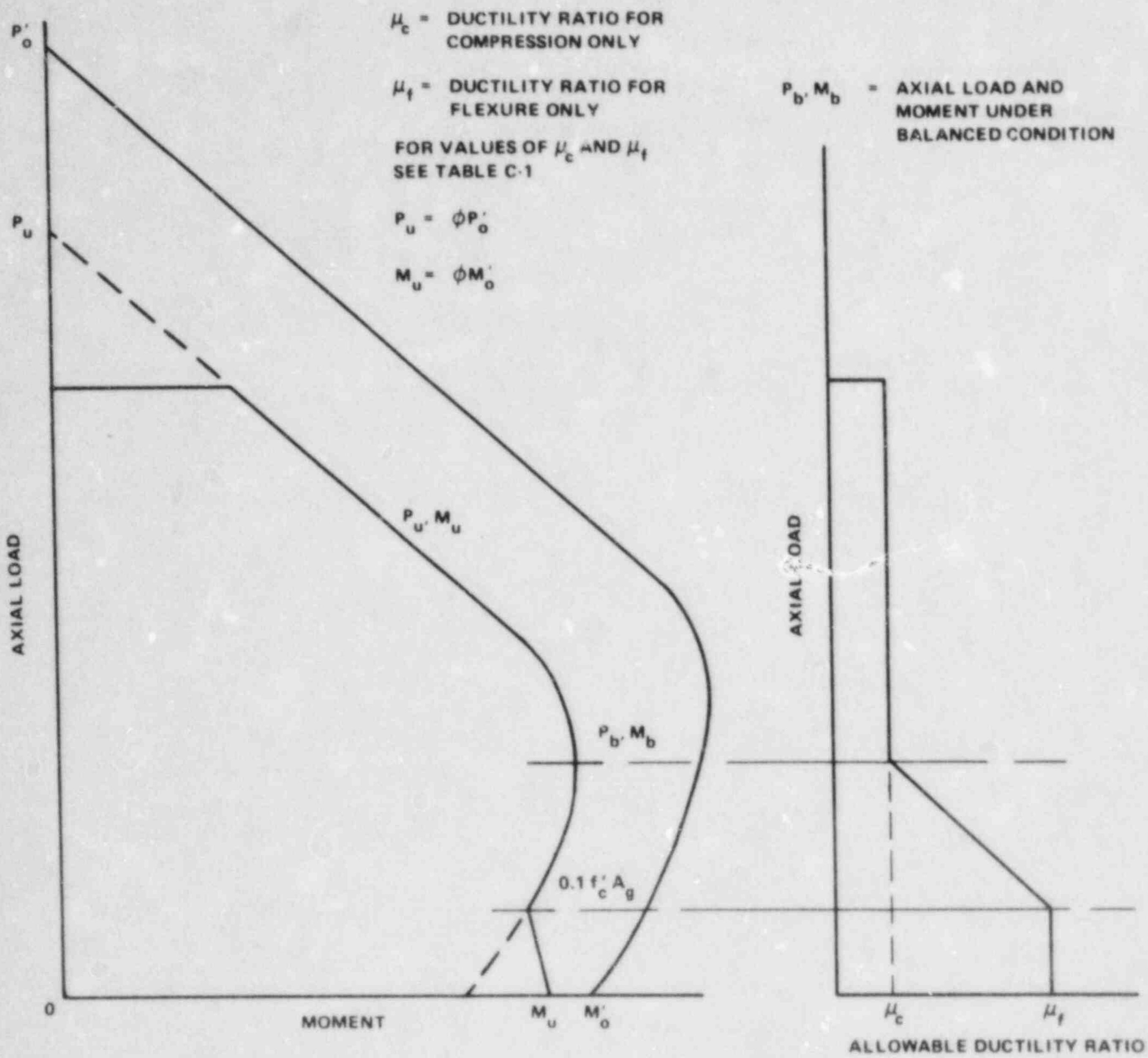

(A) REINFORCED CONCRETE INTERACTION DIAGRAM (P VS M)

(B) ALLOWABLE DUCTILITY RATIO μ VS P

Figure C–1
MAXIMUM ALLOWABLE DUCTILITY RATIO
FOR REINFORCED CONCRETE SECTION
WITH BEAM–COLUMN ACTION

APPENDIX D

CONTAINMENT ULTIMATE PRESSURE CAPACITY ANALYSIS

APPENDIX D

CONTAINMENT ULTIMATE PRESSURE CAPACITY ANALYSIS

D.1 SCOPE

An ultimate pressure capacity analysis for the containment building is performed per the requirements specified in the NRC Standard Review Plan (NUREG-0800), Section 3.8.1 acceptance criteria. The purpose of the ultimate pressure capacity analysis is to estimate the maximum internal pressure that can be achieved prior to reaching the defined failure modes. The structural integrity is based upon a peak pressure and is considered path independent. This appendix summarizes the results of this analysis in which the critical pressure at imminent failure is computed for all applicable pressure boundary elements.

Loads due to overpressurization, dead load, and prestress are incorporated into the ultimate pressure capacity analysis. Thermal stresses are not considered, although the effect of temperature on the material properties is considered. The thermal stress is determined to be self-relieving in nature, especially at high stress and strain levels. For large pressure values, the containment building shell is subjected to membrane tensile forces; with cracking of the concrete expected to occur. This state of stress will relieve any thermal stress effects.

Weld stresses are considered where applicable. In general, the welds are not critical since they are in the full penetration category. As such, the mating material governs in the component analysis.

D.2 FAILURE DEFINITION

Failure or loss of function is defined as the internal pressure at which one or both of the following occurs:

a. General structural failure - A condition where the general yielding of the structural elements (or a large segment thereof) occurs, in such a manner as to lead to the instability of the overall structure or large deformations without an increase in internal pressure.

b. Localized failure - A condition where large quantities of the containment internal atmosphere permeating through the pressure boundary is possible. As an example, failure of a penetration assembly is considered to occur (thus initiating the containment failure) if the stress level in the assembly reaches the tensile strength of the penetration material.

In the case of a general structural failure, the yield strength is the limiting factor whereas the minimum ultimate tensile strength is applicable for an evaluation of localized failure.

D.3 CRITICAL ELEMENTS

Various elements that constitute the containment pressure boundary are postulated to be contributors to potential failure modes and are analyzed to determine their individual ultimate pressure capacities. These elements include the following:

- Overall containment building
- Equipment hatch assembly
- Personnel lock assembly
- Escape lock assembly
- Fuel transfer tube housing assembly
- Encapsulation vessels
- Other penetrations (including process piping, electrical, and HVAC penetrations).

Figures 1 and 2 of the Design Report illustrate the shell configuration and the orientation of the major penetrations. References for detailed descriptions of the individual elements are furnished in the appropriate sections of the Design Report.

Table D.1 contains a summary of the ultimate pressure capacities for each of the critical elements. Element capacities are computed on the basis of minimum guaranteed yield and tensile strengths, at temperature, as specified in the appropriate American Society of Mechanical Engineers (ASME) or American Society for Testing and Materials (ASTM) standard. Since minimum values are used, the computed pressure capacities are applicable for both units.

D.3.1 <u>OVERALL CONTAINMENT BUILDING</u>

The ultimate pressure capacity determination for the overall containment building considers the following regions for potential loss of function:

- Cylinder: hoop stress consideration at cylinder midheight
- Cylinder: meridional stress consideration
- Cylinder/basemat junction
- Basemat - Refer to sections 2.3, 2.4, and figures 3, and 5 through 9 of the Design Report for a description of the shell and basemat geometry and design details.

D.3.1.1 Cylinder: Hoop Stress Consideration at Cylinder Midheight

The maximum membrane force is assumed to develop when the steel reinforcement, liner plate, and post-tensioning tendons have reached their respective yield stresses. Under the postulated increasing pressure load, the sequence of events indicates that the steel reinforcement yields first, then the liner plate, and finally the tendons. The pressure corresponding to the tendon attaining its yield stress is computed to be P_u = 169 psig.

For all practical purposes, this can be considered the ultimate pressure capacity since large deformations are expected to occur above this pressure. The behavior of the shell after the tendon has yielded is difficult to predict. This pressure represents a lower bound value since the tendon is likely to reach its ultimate strength prior to the complete failure of the shell wall. The minimum ultimate tensile strength of the tendon is 15 percent greater than the specified yield stress. Noting that the ultimate strains for the reinforcing steel and liner plate are appreciably greater than that of the tendon, it is concluded that the tendon will rupture first, followed by the failure of the liner plate and reinforcing steel.

D.3.1.2 Cylinder: Meridional Stress Consideration

Conventional membrane methods are used to determine the pressure which could be resisted by the cylinder in the meridional direction. As in the hoop stress analysis, the maximum membrane force occurs when the reinforcing steel, liner plate, and post-tensioning tendons reach their respective yield points. The ultimate pressure capacity of the shell in the meridional direction is computed to be P_u = 244 psig.

D.3.1.3 Cylinder/Basemat Junction

Due to the gross discontinuity at the cylinder/basemat junction, moments and shears are present in order to maintain equilibrium and strain compatibility. A brief description is given which outlines the methodology used in determining the ultimate pressure capacity of the cylinder/basemat junction.

D.3.1.3.1 Flexural Stress Considerations. Moment-curvature diagrams are constructed for various levels of membrane force representing the internal force relationship based upon the geometry of the section and the material properties. Considering the pressure-moment and pressure-membrane force characteristics of the shell, the yield moment and associated curvature can be obtained from the moment-curvature diagrams. Once the yield moment is reached the moment magnitude may be assumed to remain constant with increasing curvature. As such, a pinned base cylinder is used to approximate the pressure-curvature behavior beyond the yield point. Therefore the ultimate pressure capacity is the summation of the internal pressure required to attain the yield curvature and the pressure necessary to pass from the yield state to the maximum (strain limited) curvature. The ultimate pressure capacity thus calculated is 145 psig.

D.3.1.3.2 Radial Shear Stress Considerations. The radial shear at the cylinder/basemat junction is obtained by incorporating the results from the shell finite element analysis which established the moments due to dead load, prestress load and design accident pressure. The shear corresponding to these primary loads is based upon the moment gradient of the longitudinal moment diagram. The shear (V_u) associated with the ultimate pressure based on flexural capacity can be determined and compared with the ultimate shear resistance of the section (V_R).

V_u = 170 k/ft (@ P_u = 145 psig)

The total shear resistance is provided by the combined capacities of the liner plate (including stiffener angles), radial shear ties, and concrete. Temperature effects are included for the liner plate and stiffener angle material properties. The concrete capacity considers the effects of shell membrane tensile forces and shear friction in the compression region of the shell wall.

V_R = 421 k/ft > V_u

D.3.1.4 Basemat

Assuming a linear pressure-moment relationship, the basemat moment is computed at the cylinder/basemat junction for a pressure of 145 psig which is the ultimate pressure capacity of the shell at the cylinder/basemat junction. The flexural capacity of the basemat at this location is shown to be greater than the moment computed.

Additionally, at a location near the center of the basemat, the moment computed for a pressure of 145 psig is also shown to be less than the flexural capacity of the basemat at the same location.

The computed shear in the basemat for a pressure of 145 psig is shown to be less than the shear capacity of the basemat.

The basemat is therefore not a controlling failure mode in determining the ultimate pressure capacity.

D.3.2 Equipment Hatch Assembly

The following components of the equipment hatch assembly are evaluated for failure against internal pressure:

- Dished head
- Tension ring flange
- Barrel
- Welding collar insert
- Punching shear through the containment shell

Refer to section 2.4.7 and figures 8, 9, of the design report and figure D-2 of this appendix for a description of the equipment hatch assembly and design requirements.

These components are analyzed using the supplier supplied stress report as a basis for the ultimate pressure determination. The following assumptions are used to compute the individual component capacities of the assembly, with the lowest value establishing the critical pressure. These assumptions are applicable to all hatch and lock analyses.

A. The double seal, testable gaskets (personnel and escape locks), and double compression seals (equipment hatch) do not fail for the pressures under consideration.

B. The stresses in the various components of the hatch and locks are linearly proportional to the applied pressure up to the ultimate strength of the material.

C. The ultimate shear strength of a material is equal to 50 percent of the ultimate tensile strength.

D. The ultimate shear strength of a weld is equal to the ultimate shear strength of the parent material.

Incorporating the data from the equipment hatch stress report, the stresses for each of the components are linearly extrapolated to their ultimate tensile strength at 300°F. Shear stresses are proportioned to 0.5 F_y per Assumption C above. This procedure is implemented except in cases where buckling is considered to be more critical.

The punching shear capacity is determined neglecting the contribution from shear tie reinforcement. The concrete resistance includes the effects of biaxial tensile forces acting on the shell wall segment.

A summary of the individual component pressure capacities is contained in table D.3. The governing component is the dished head with a corresponding ultimate pressure capacity of P_u = 213 psig.

D.3.3 Personnel Lock Assembly

The following components of the personnel lock assembly are analyzed to determine their individual pressure capacities:

- Lock door
  - Stiffeners
  - Panels
  - Associated welds
- Lock bulkheads
  - Panels
  - Stiffeners
  - Associated welds

- Lock barrel
  - Welding collar
  - Welding ring
  - Outer sleeve
- Punching shear through shell

For a description and design details of the personnel lock assembly, refer to section 2.4.8 and figure 7 of the design report and figure D-3 of the appendix.

The vendor supplied personnel lock stress report is used to determine the pressure capacity of the various lock components. The stresses are proportioned to their respective ultimate tensile strengths in a similar manner to the equipment hatch analysis. A summary of the individual capacities is given in table D.4. The governing component pressure is the bulkhead welds with a corresponding ultimate pressure capacity P_u = 203 psig.

D.3.4 Escape Lock Assembly

The escape lock assembly is evaluated by comparison with the personnel lock assembly or by implementing a procedure similar to that performed in sections D.3.2 and D.3.3. The following components are evaluated for their pressure capacities:

- Escape lock door
- Escape lock bulkheads
  - Panels
  - Stiffeners
  - Associated welds
- Escape lock barrel
  - Welding collar
  - Welding ring
  - Outer sleeve
- Punching shear through shell

Refer to section 2.4.8 and figure 7 of the design report and figure D-3 of this appendix for a description and design details of the escape lock.

A summary of the individual component pressure capacities is contained in table D.5. The governing component is the weld of the bulkhead stiffener to the barrel with a corresponding ultimate pressure capacity conservatively determined to be P_u = 147 psig.

D.3.5 Fuel Transfer Tube Housing Assembly

One fuel transfer tube penetration per containment building is provided for refueling. Three separate sleeve assemblies, joined by four bellows act as a transfer tube housing. The penetration sleeve assemblies permit the transfer tube to penetrate the refueling canal wall, the containment shell, and the exterior wall of the fuel handling building, while maintaining a pressure boundary at each wall.

As such, the analysis methodology is similar to those performed on the equipment hatch and personnel lock. The fuel transfer tube housing stress report is used to determine the individual component pressure capacities. The following components are evaluated for their pressure capacities:

- General tube housing
  - Enclosure plate
  - End enclosure plate
  - End pipe
- Expansion bellows
- Fuel transfer tube
- Blind flange

Refer to figures 1, 2 of the design report figure and D-4 of this appendix for design details.

A summary of the individual component pressure capacities for the fuel transfer tube housing components is listed in table D.6. The governing component is the fuel transfer tube with the corresponding ultimate pressure capacity of P_u = 229 psig.

D.3.6 Encapsulation Vessel

There are two containment spray and two residual heat removal (RHR) isolation valve encapsulation vessels provided for each containment building. One set of vessels (one containment spray and one RHR) is located in both the auxiliary and fuel handling buildings. They provide a leak tight housing which function as extensions of the containment pressure boundary and thus must be evaluated as part of the ultimate capacity analysis. The various components investigated are as follows:

- Vessel cylinder
- Vessel head
- Casing flange
- Bellows
- Pipe
- Isolation valves

Refer to figure D-5 for design details.

The supplier supplied stress report for the encapsulation vessels is used as a basis for the ultimate pressure capacity determination. The assumptions provided for the equipment hatch analysis are incorporated where applicable. The stress report stresses, for the design accident pressure load case, are linearly extrapolated to the various component ultimate tensile strengths at 300°F. The stress report computes stress levels that vary depending upon the type of vessel. The vessel producing the lowest value is considered to govern.

A summary of the individual component pressure capacities is contained in table D.7. The critical component is the casing flange, with a corresponding ultimate pressure capacity of P_u = 179 psig.

D.3.7 Other Penetrations

Process piping, electrical, and HVAC (heating, ventilation, and air conditioning) penetration assemblies fall into the category of "other penetrations". They are analyzed for externally applied pressure only, neglecting the thermal stress contributions. As in sections D.3.2 and D.3.3, the stress levels given in the respective stress reports are linearly extrapolated to the ultimate tensile strength of the material where feasible. A summary of the individual pressure capacities is given in table D.8. Figure D-6 illustrates the various penetration assemblies.

D.3.7.1 Process Piping Penetration Assemblies

The ultimate capacity of a 10.75 inch diameter penetration pipe sleeve is determined to govern. The corresponding ultimate pressure capacity is P_u = 1144 psig. This value is computed using the highest operating stress as defined in the stress report but independent of faulted condition loads. The welds are determined not to govern. Refer to figure D-6, types I, II, III, V and VI for process piping penetration assembly details.

D.3.7.2 Electrical Penetration Assemblies

The following two components of the electrical penetration assembly are investigated for their pressure retaining capacity:

- Canister tube
- Header plates

The stress report for the electrical penetration assembly is used as a basis for the ultimate pressure capacity evaluation. The canister tube is determined to govern with a corresponding ultimate pressure capacity of P_u = 757 psig. Refer to figure D-6 for electrical penetration assembly details.

D.3.7.3 HVAC Penetration Assemblies

HVAC penetrations are provided for the normal process purge supply/exhaust and post-LOCA purge exhaust systems. The normal process purge penetration is a 24 inch diameter sleeve, whereas the post-LOCA penetration is a 4 inch sleeve. The following components are checked for their pressure retaining capacities:

- Sleeve
- Valve

Both systems are checked for buckling of the penetration sleeve due to an externally applied pressure. The valves for the containment building have a minimum rating of 210 psig at 300°F. A summary of the individual component capacities is contained in table D.8, with the governing ultimate pressure capacity being limited by the lower bound valve rating P_u = 210 psig.

Refer to figure D-6, type IV for HVAC penetration assembly details.

D.4 SUMMARY

The ultimate pressure capacity of the containment structures is computed as 145 psig. The failure mode associated with this pressure is the concrete crushing failure due to flexure at the cylinder/basemat junction. A summary of the individual element ultimate pressure capacities is contained in table D.1 which demonstrates that all other failure modes occur at pressures in excess of 145 psig. This ultimate pressure capacity represents a value lower than the actual value since increased section capacities based on as-built data is not utlilized in the evaluation.

TABLE D.1

SUMMARY OF ULTIMATE PRESSURE CAPACITIES

Elements	Ultimate Pressure Capacity (psig)
Shell:	
a. Hoop stress considerations	169
b. Meridional stress considerations	244
Cylinder/basemat junction:	
a. Flexural stress conditions	145
b. Radial shear considerations	>145
Basemat	>145
Equipment hatch	213
Personnel lock assembly	203
Escape lock assembly	147
Fuel transfer tube housing assembly	229
Encapsulation vessels	179
Other penetrations:	
a. Process piping	1144
b. Electrical	757
c. HVAC	210

TABLE D.2

ULTIMATE PRESSURE CAPACITIES OF THE
OVERALL CONTAINMENT STRUCTURE ELEMENTS

Elements	Ultimate Pressure Capacity (psig)
Shell wall - hoop stress considerations at cylinder mid-height	169
Shell wall - meridional stress considerations	244
Cylinder/basemat junction	145
Basemat	>145(1)

(1) By comparison with cylinder/basemat junction.

TABLE D.3

ULTIMATE PRESSURE CAPACITIES OF THE EQUIPMENT HATCH ASSEMBLY

Components	Ultimate Pressure Capacity (psig)
Dished head	213
Tension ring flange	220
Barrel	3415
Welding collar insert	1425
Punching shear through shell	582

TABLE D.4

ULTIMATE PRESSURE CAPACITIES OF THE
PERSONNEL LOCK ASSEMBLY

Components	Ultimate Pressure Capacity (psig)
Lock doors:	
a. Stiffeners	257
b. Panels	819
c. Associated welds	206
Lock bulkheads:	
a. Panels	247
b. Stiffeners	288
c. Associated welds	203
Lock barrel:	
a. Welding collar	2200
b. Welding ring	850
c. Outer sleeve	263
Punching shear through shell	582

TABLE D.5

ULTIMATE PRESSURE CAPACITIES OF THE ESCAPE LOCK ASSEMBLY

Components	Ultimate Pressure Capacity (psig)
Escape lock door:	561
Escape lock bulkheads:	
a. Panels	247[1]
b. Stiffeners	228
c. Associated welds	147
Escape lock barrel:	
a. Welding collar	$\geq$2200[1]
b. Welding ring	$\geq$850[1]
c. Outer sleeve	$\geq$263[1]
Punching shear through shell	582

(1) Comparison made with personnel lock; personnel lock pressures shown.

TABLE D.6

ULTIMATE PRESSURE CAPACITIES OF THE
FUEL TRANSFER TUBE HOUSING ASSEMBLY

Components	Ultimate Pressure Capacity (psig)
General tube housing:	
a. Enclose plate	1285
b. End enclosure plate	333
c. End pipe	2381[(1)]
Expansion bellows	677[(1)]
Fuel transfer tube	229[(3)]
Blind flange	1258

(1) Buckling failure mode.

(2) Based on allowable stress.

TABLE D.7

ULTIMATE PRESSURE CAPACITIES OF THE ENCAPSULATION VESSELS

Components	Ultimate Pressure Capacity (psig)
Vessel cylinder	498
Vessel head	282
Casing flange	179
Bellows	247
Pipe	3800
Isolation valves	200[(1)]

(1) At 250°F.

TABLE D.8

ULTIMATE PRESSURE CAPACITIES OF OTHER PENETRATION ASSEMBLIES

Components	Ultimate Pressure Capacity (psig)
Process piping penetration:	
a. Sleeve	1144
Electrical penetration:	
a. Canister tube	757
b. Header plate	996
HVAC normal process purge penetration:	
a. Sleeve	2263
b. Valve	210
HVAC post-LOCA purge exhaust penetration:	
a. Sleeve	1437
b. Valve	210

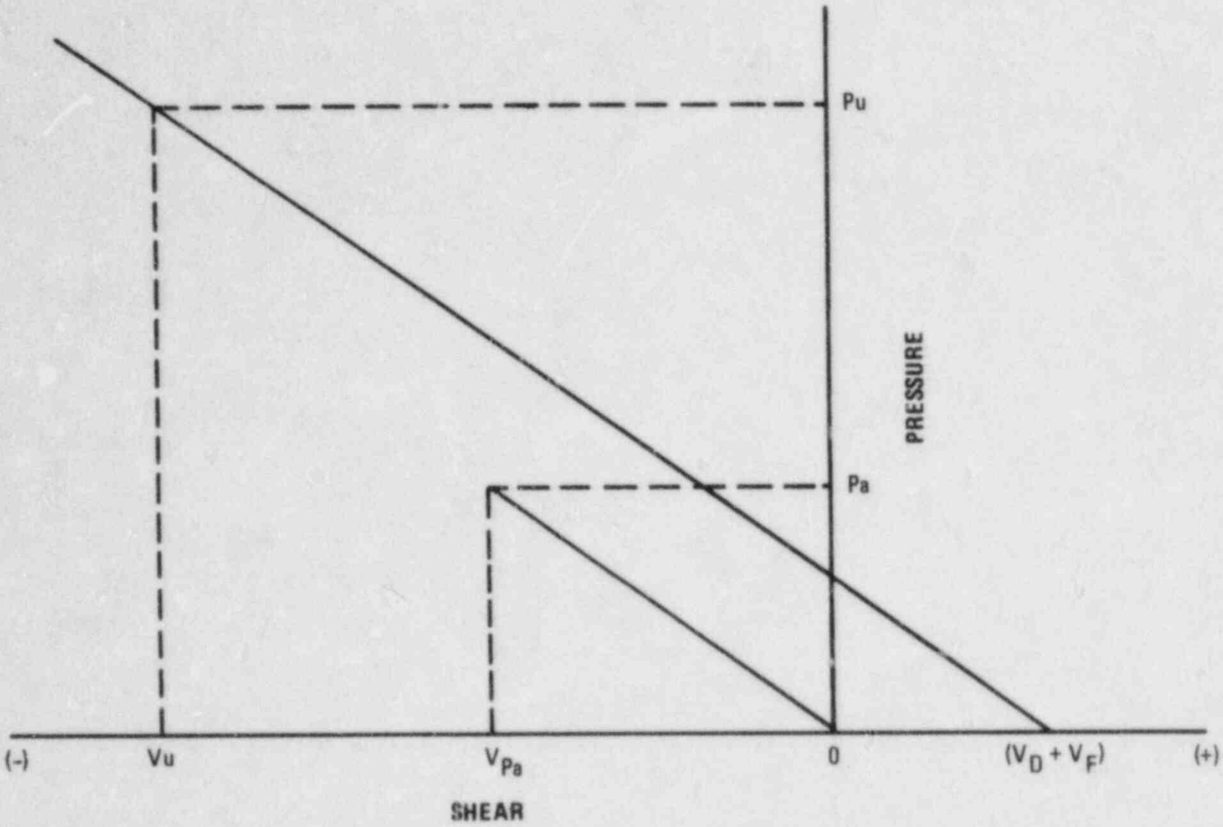

NOTE:

$(V_D + V_F)$ = SHEAR DUE TO DEAD LOAD AND PRESTRESS LOAD RESPECTIVELY. VALUES ARE OBTAINED FROM THE CONTAINMENT SHELL FINITE ELEMENT ANALYSIS.

V_{Pa} = SHEAR DUE TO THE DESIGN ACCIDENT PRESSURE (Pa) ONLY.

Vu = SHEAR CORRESPONDING TO THE ULTIMATE PRESSURE (Pu).

Pa = DESIGN ACCIDENT PRESSURE.

Pu = ULTIMATE PRESSURE AS DEFINED BY THE MOMENT CAPACITY OF THE CYLINDER/BASE MAT JUNCTION.

Figure D-1
PRESSURE – SHEAR DIAGRAM

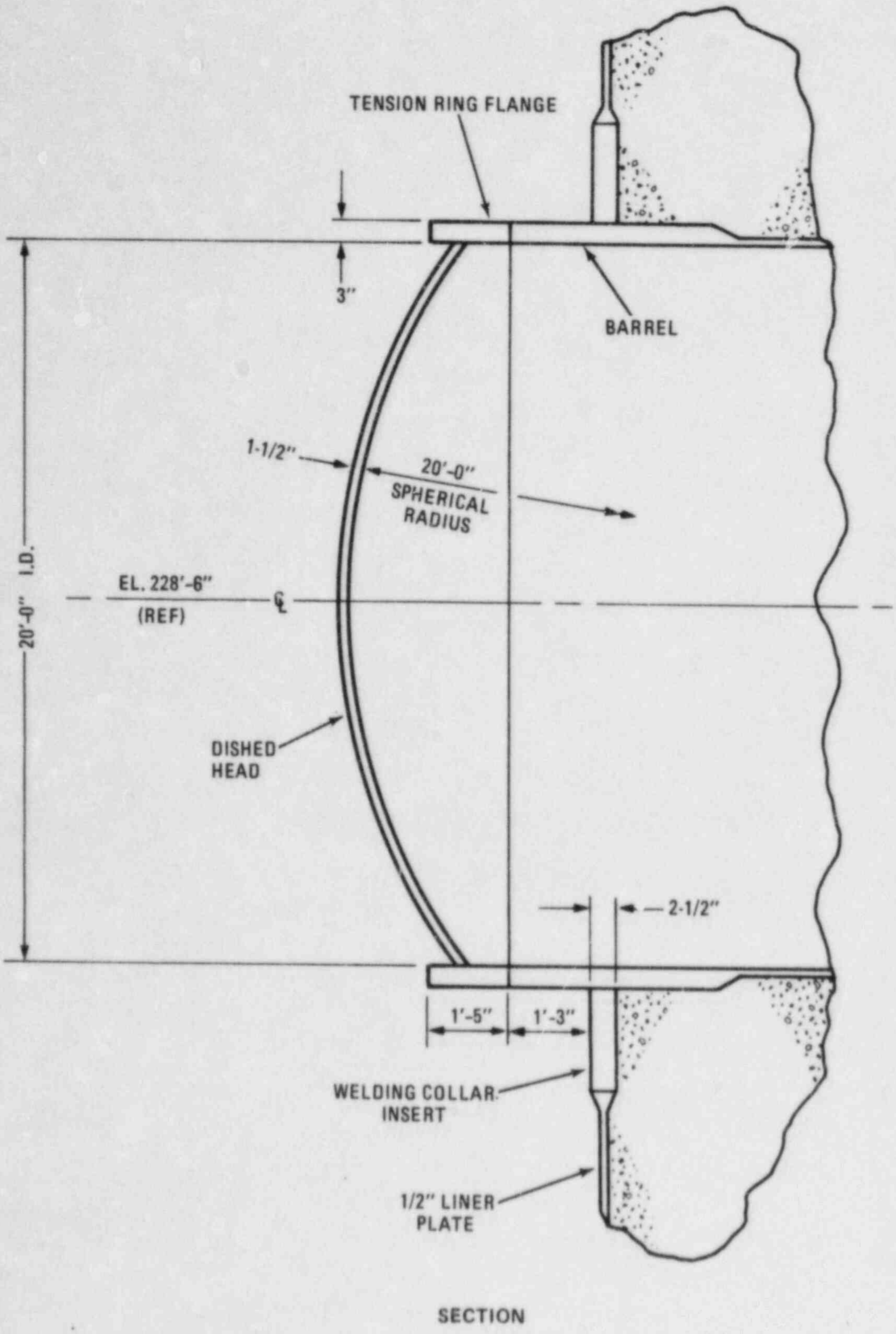

Figure D-2
EQUIPMENT HATCH ASSEMBLY

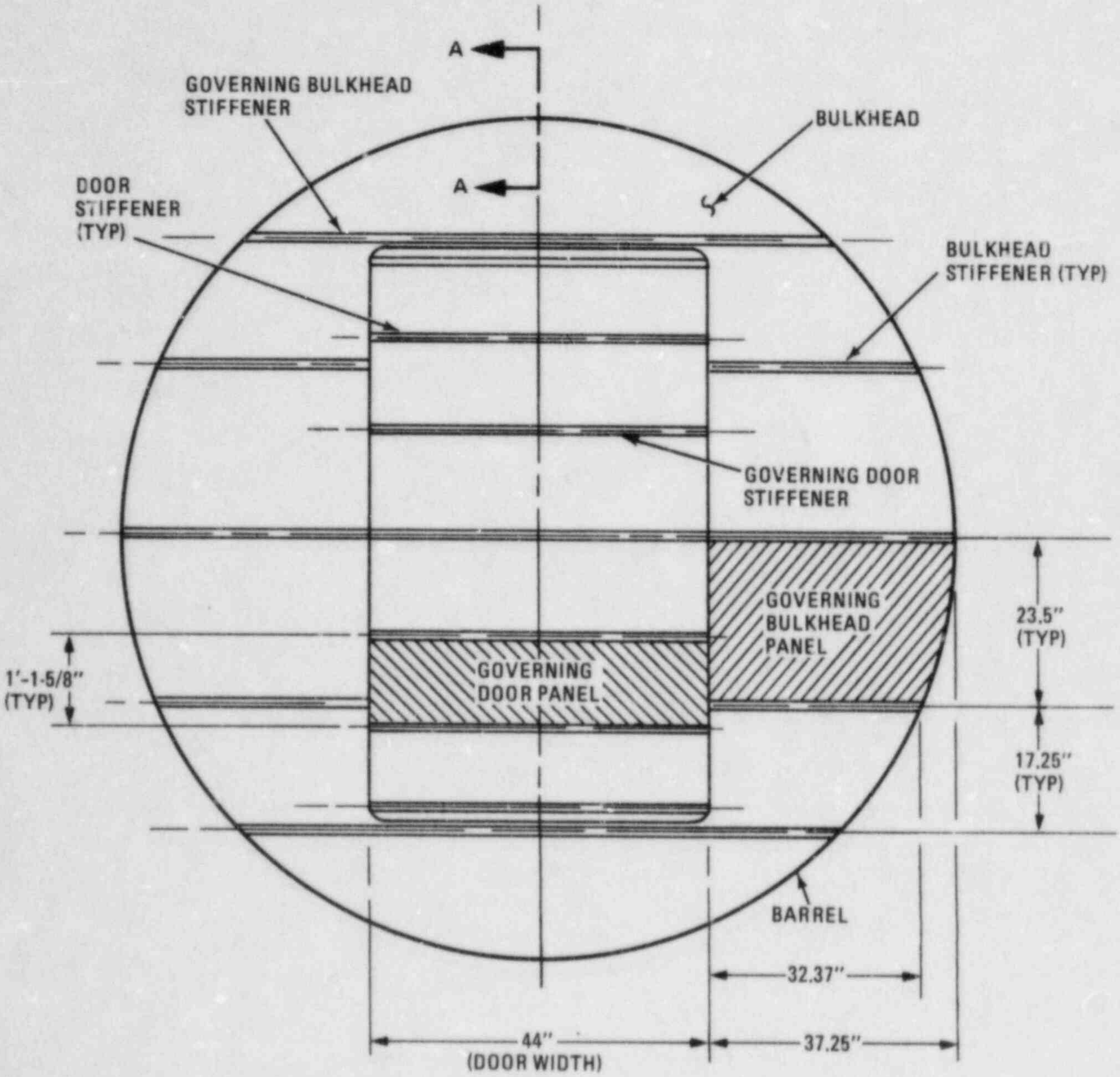

ELEVATION

PERSONNEL LOCK ASSEMBLY

Figure D-3
LOCK ASSEMBLIES
(Sheet 1 of 3)

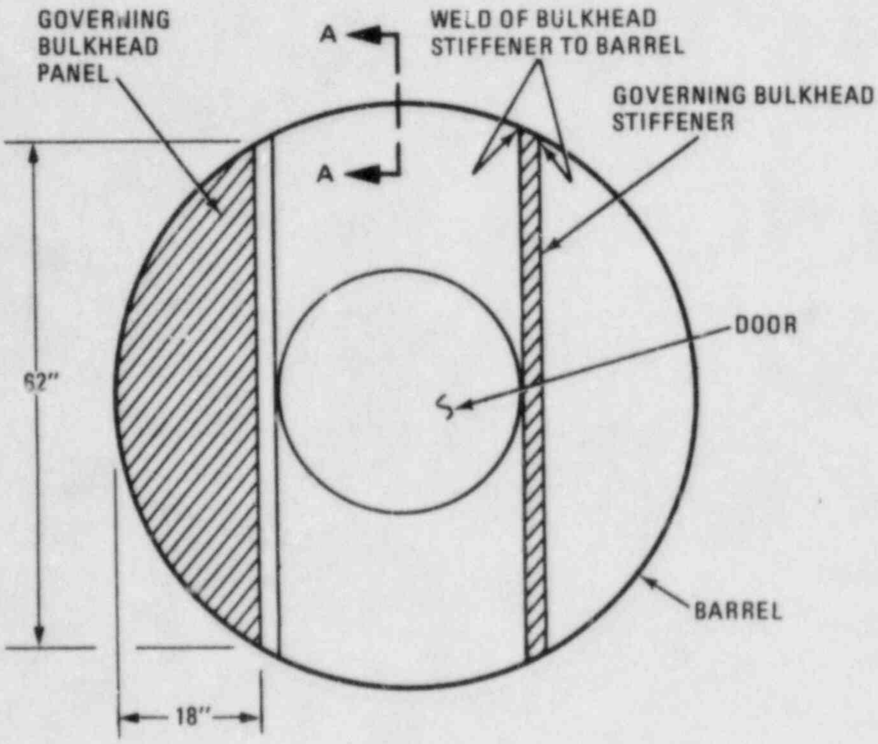

ELEVATION

ESCAPE LOCK ASSEMBLY

Figure D-3
LOCK ASSEMBLIES
(Sheet 2 of 3)

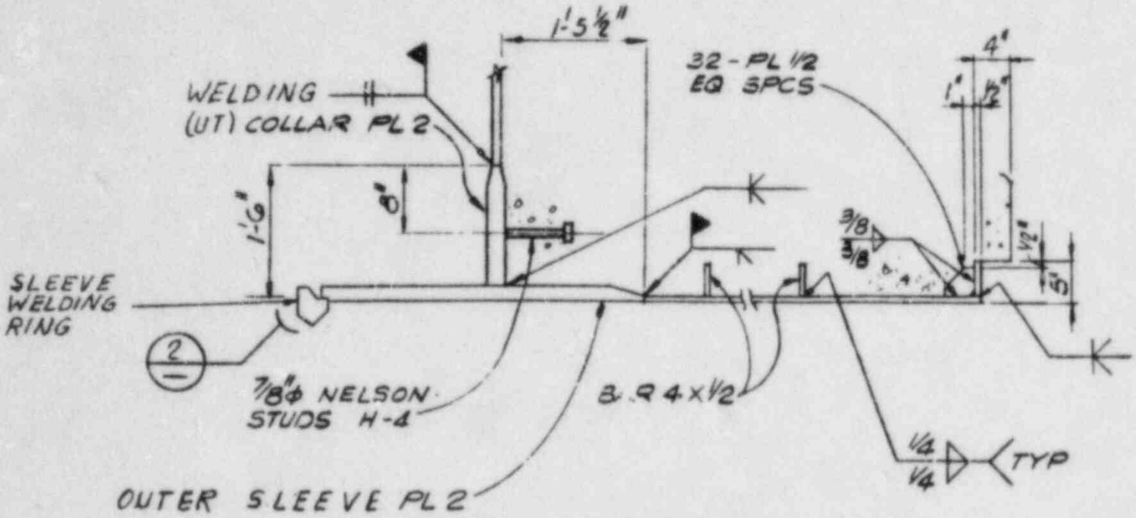

SECTION A-A

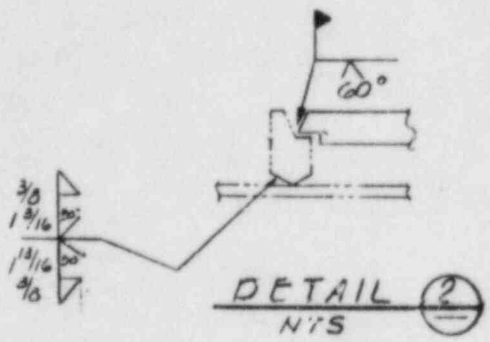

Figure D-3
LOCK ASSEMBLIES
(Sheet 3 of 3)

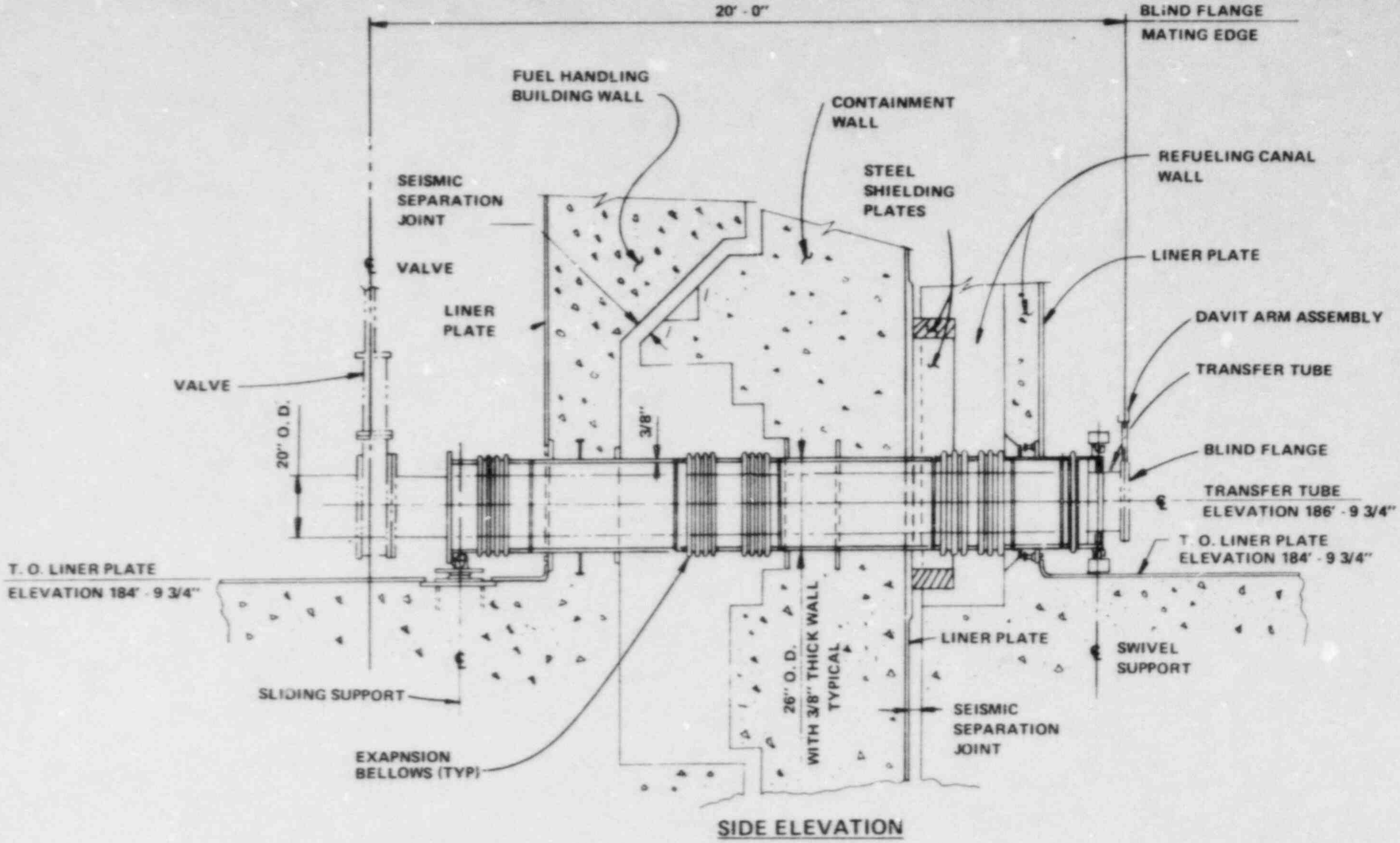

Figure D-4
FUEL TRANSFER TUBE HOUSING ASSEMBLY

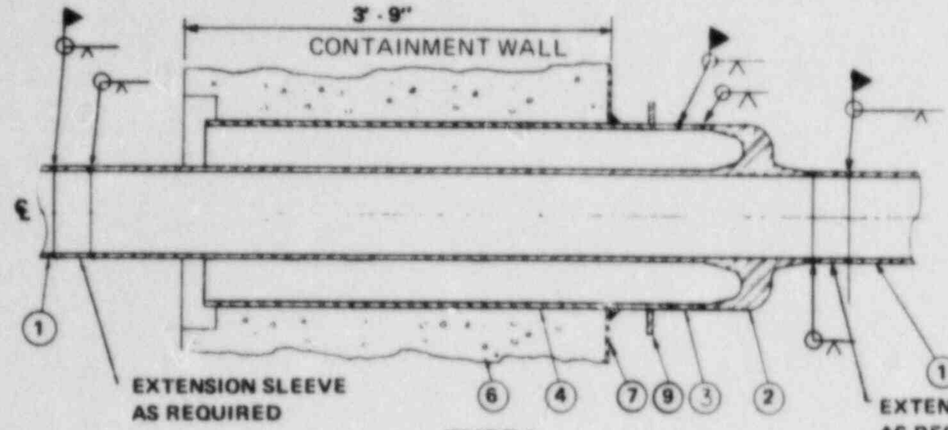

TYPE I

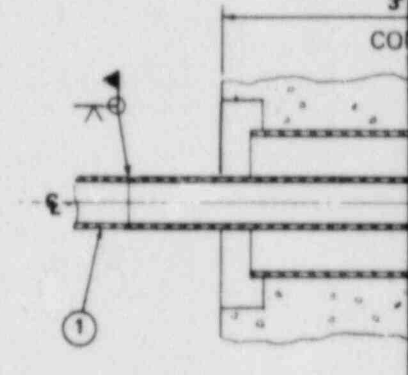

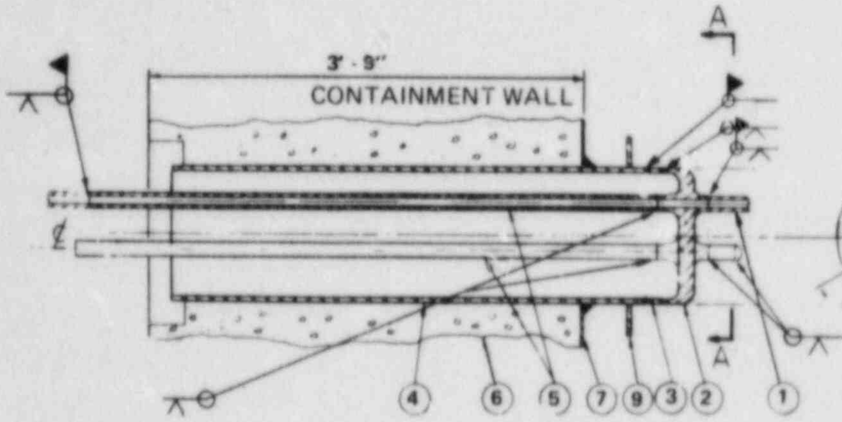

TYPE III

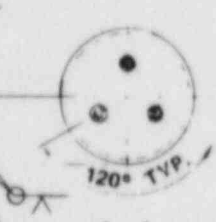

A – A

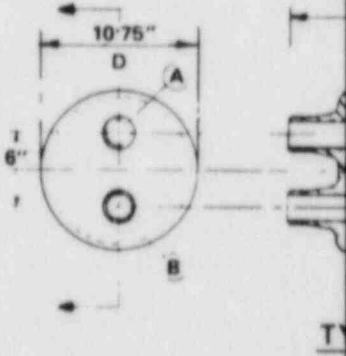

PIPING PE

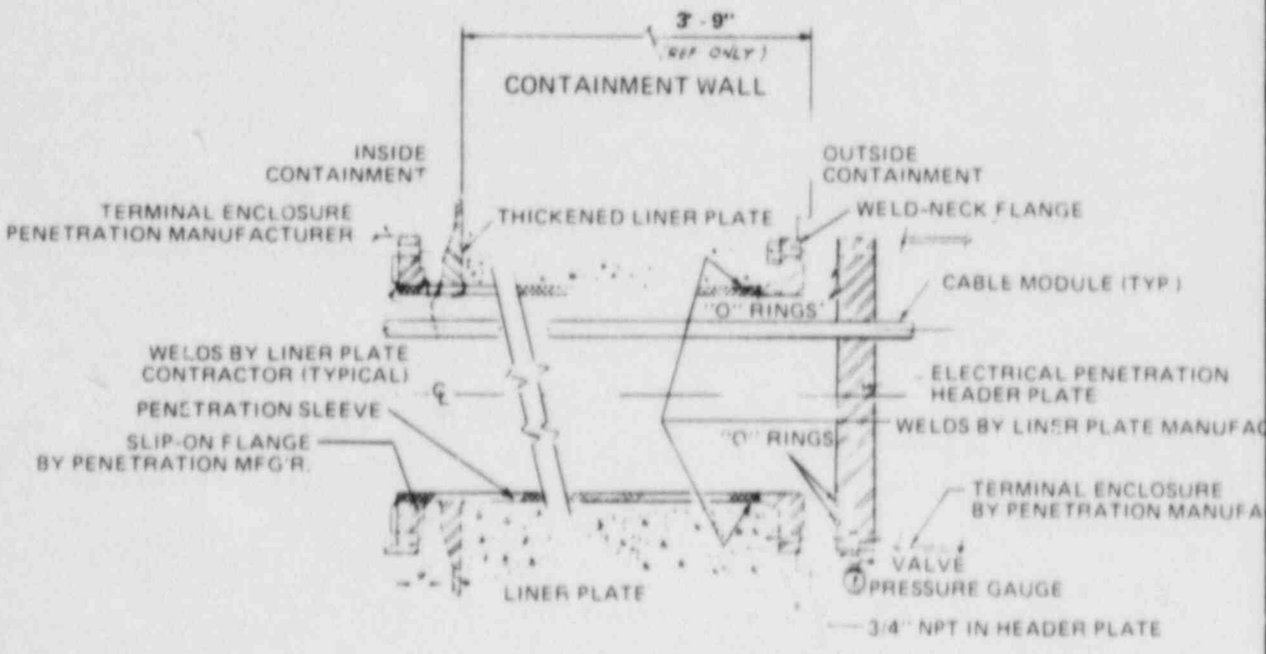

MODULAR TYPE

ELECTRICAL PENETRATION

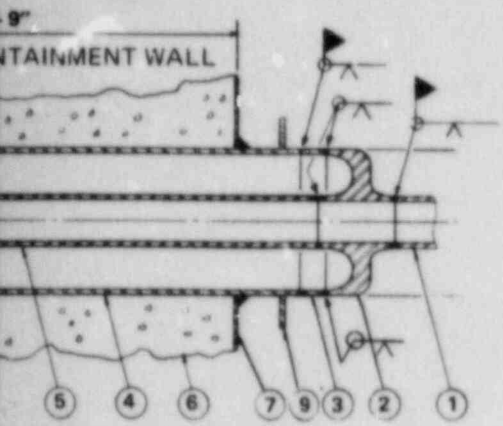

TYPE II

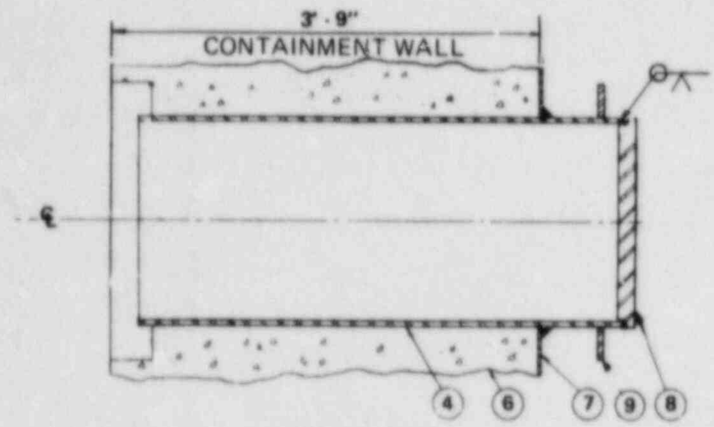

TYPE V
SPARE PENETRATION SLEEVE

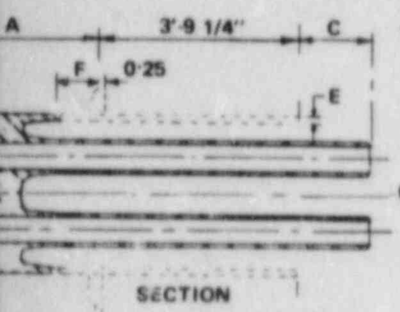

YPE VI
NETRATIONS

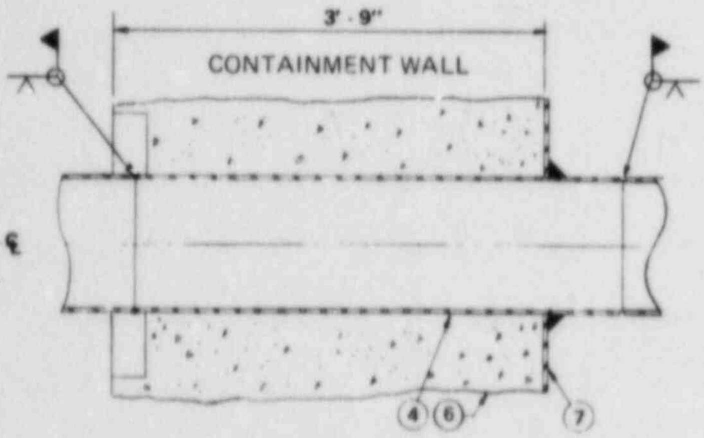

TYPE IV

LEGEND

1. CONNECTING PIPE OR COMPONENT
2. FLUED HEAD FITTING
3. INTERMEDIATE SLEEVE
4. PENETRATION SLEEVE
5. NECK EXTENSION
6. CONTAINMENT WALL
7. LINER PLATE (INSIDE CONTAINMENT WALL)
8. PERMANENT END CLOSURE
9. REINFORCING RING PLATE

TURER

TURER

NOTE: TYPE I IS FOR INSERVICE INSPECTION SERVICE AND INNER PIPE IS PART OF FLUED HEAD FORGING.

Figure D-6
OTHER PENETRATIONS

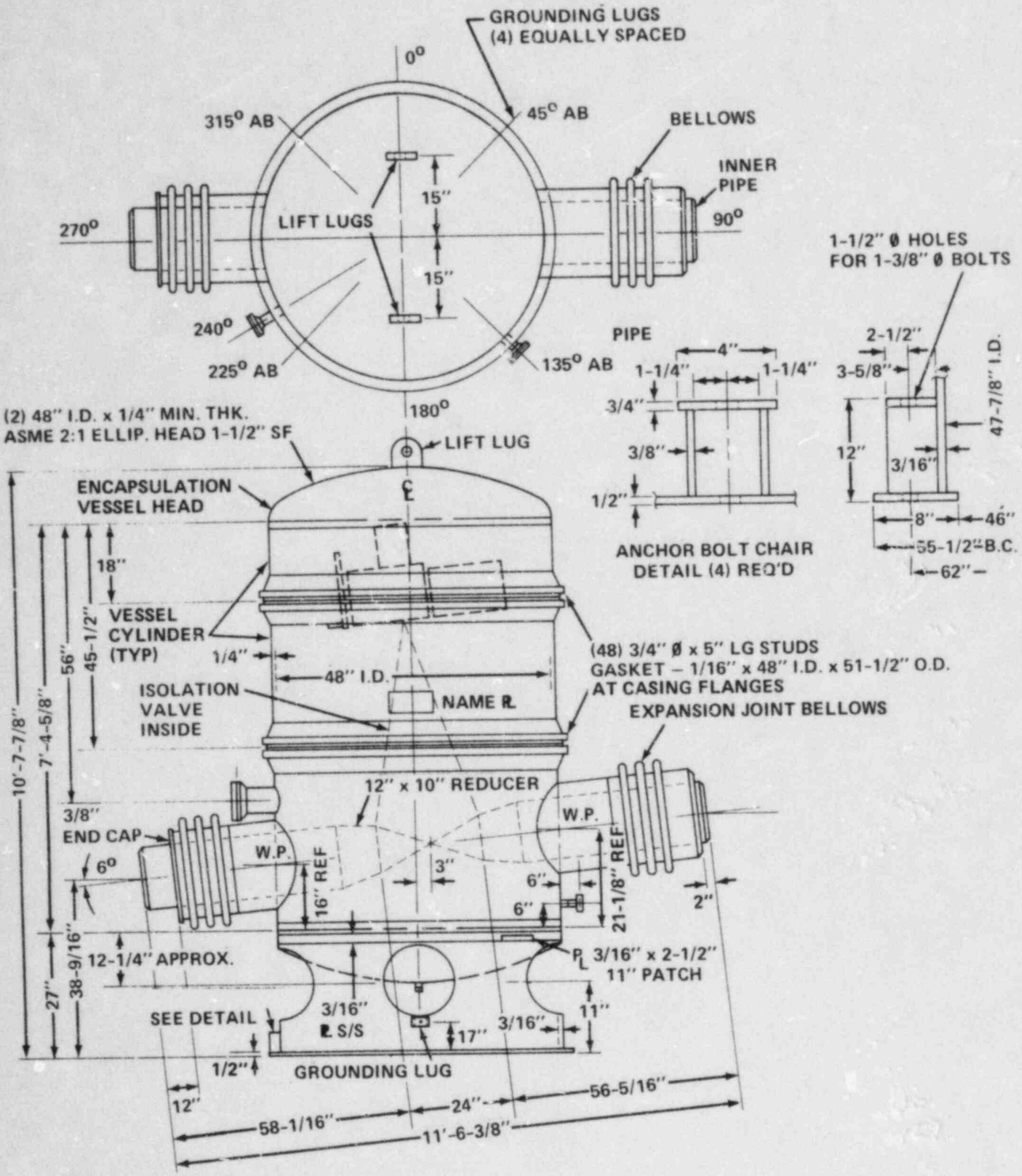

Figure D-5
ENCAPSULATION VESSEL